THE ROLE OF ZOOPLANKTON IN THE BIOLOGICAL CARBON PUMP OF THE SUBANTARCTIC SOUTHERN OCEAN

by

Svenja Halfter
M.Sc., B.Sc.

Submitted in fulfilment of the requirements
for the Degree of Doctor of Philosophy

Institute for Marine and Antarctic Studies
University of Tasmania
February, 2022

DECLARATIONS

This thesis contains no material which has been accepted for a degree or diploma by the University or any other institution, except by way of background information and duly acknowledged in the thesis, and to the best of my knowledge and belief no material previously published or written by another person except where due acknowledgement is made in the text of the thesis, nor does the thesis contain any material that infringes copyright.

Signed: _____

Svenja Halfter

Date: November 10, 2021

This thesis may be made available for loan and limited copying and communication in accordance with the *Copyright Act 1968*.

Signed: _____

Svenja Halfter

Date: November 10, 2021

The publishers of the papers comprising Chapter 2, 4 and the appendix hold the copyright for that content, and access to the material should be sought from the respective journals. The remaining non-published content of the thesis may be available for loan and limited copying in accordance with the *Copyright Act 1968*.

Signed: _____

Svenja Halfter

Date: November 10, 2021

STATEMENT ON CO-AUTHORSHIP

The following people and institutions contributed to the publication of work undertaken as part of this thesis:

Svenja Halfter - IMAS, UTAS, Australia
Charles O. Coleman - Museum für Naturkunde, Berlin, Germany
Emma L. Cavan - Imperial College London, UK
Kerrie M. Swadling - IMAS, UTAS, Australia
Ruth S. Eriksen - CSIRO, Australia
Philip W. Boyd - IMAS, UTAS, Australia
Phil Butterworth - IMAS, UTAS, Australia

Contribution of work by the co-authors for each paper:

1. Paper 1: Located in Appendix A
   Halfter, S., & Coleman, C. O. (2019). *Chevreuxiopsis franki* gen. n., sp. n. (Crustacea, Amphipoda, Thoriellidae) from the deep sea southwest of Tasmania. *Zoosystematics & Evolution*, 95(1), 125–132.
   Author contributions:
   Identified species initially: Svenja Halfter
   Confirmed species identification: Charles O. Coleman
   Created the species drawings: Svenja Halfter and Charles O. Coleman
   Wrote the manuscript: Svenja Halfter and Charles O. Coleman

2. Paper 2: Located in Chapter 2
   Halfter, S., Cavan, E. L., Swadling, K. M., Eriksen, R. S., & Boyd, P. W. (2020). The role of zooplankton in establishing carbon export regimes in the Southern Ocean – A comparison of two representative case studies in the subantarctic region. *Frontiers in Marine Science*, 7, 837.

Author contributions:
Conceived and designed review: Svenja Halfter
Analysed the data and produced infographic: Svenja Halfter
Wrote the manuscript: Svenja Halfter
Contributed with data and edited the manuscript and infographic: Svenja Halfter, Emma L. Cavan, Kerrie M. Swadling, Ruth S. Eriksen, and Philip W. Boyd

3. Paper 3: Located in Chapter 4
Halfter, S., Cavan, E.L., Butterworth, P., Swadling, K.M. & Boyd, P.W. (2021). "Sinking dead" – How zooplankton carcasses contribute to Particulate Organic Carbon flux in the subantarctic Southern Ocean. *Limnology & Oceanography*, CV, 1-13.
Author contributions:
Conceived and designed experiments: Svenja Halfter
Performed experiments: Svenja Halfter and Phil Butterworth
Analysed the data: Svenja Halfter
Contributed to the discussion of data and manuscript structure: Svenja Halfter, Emma L. Cavan, Kerrie M. Swadling and Philip W. Boyd
Wrote the manuscript: Svenja Halfter
Edited the manuscript and infographic: Svenja Halfter, Emma L. Cavan, Phil Butterworth, Kerrie M. Swadling, and Philip W. Boyd

We, the undersigned, agree with the above-stated contribution of work undertaken for each of the published and peer-reviewed manuscripts contributing to this thesis:

Signed: _____

Svenja Halfter	Philip W. Boyd	Catriona Macleod
Candidate	Primary Supervisor	Head of Centre
IMAS	IMAS	IMAS
University of Tasmania	University of Tasmania	University of Tasmania

Date: November 10, 2021

ABSTRACT

Initiatives to study the impact of climate change on carbon sequestration in the subantarctic Southern Ocean have led to regular research voyages and the establishment of long-term moorings at the Southern Ocean Time Series site (47°S, 140°E) in the region. The subantarctic zone plays an important role in the physical uptake and sequestration of carbon dioxide due to the formation and subduction of water masses. However, while extensively studied in other parts of the world's ocean, the biological production, transformation, and transport of particulate material is not well documented for the subantarctic zone.

In particular, the role of zooplankton in the biological gravitational, mesopelagic-migrant, and seasonal lipid pumps has received less attention. Current knowledge gaps extend across zooplankton species composition in subsurface waters and its seasonal development, zooplankton mortality that leads to downward carbon flux by carcasses and quantification of zooplankton respiration in the water column.

This thesis synthesises information on zooplankton and biogeochemistry in the subantarctic Southern Ocean to study the zooplankton-mediated carbon pump, including data from samples collected by deep-sea sediment traps, on field campaigns and from laboratory measurements. The thesis is composed of a general introduction (Chapter 1), a literature review (Chapter 2), three analysis chapters (Chapter 3-5) and a discussion, containing synthesis and future research priorities (Chapter 6).

The second chapter reviews the role of zooplankton in establishing characteristic carbon export regimes in the Southern Ocean. Two case studies, the Kerguelen Plateau (high productivity, relatively low export) and the High-Nutrient Low-Chlorophyll waters south of Australia (low primary productivity, relatively high downward export), illustrate the importance of the zooplankton community composition, biomass and grazing for downward carbon export. The third chapter presents a long-term time-series (>20 years) of

deep-sea zooplankton community composition data, collected as swimmers in sediment traps. Results indicate a decrease of abundance and diversity with increasing depth, low seasonality in zooplankton abundances and the absence of a long-term trend in the zooplankton community. The fourth chapter shows the importance of zooplankton carcasses for downward biological carbon export in the subantarctic zone. Estimations of the carcass flux are sensitive to alteration of mortality rates and sinking speed, but less sensitive to a change in microbial decomposition rates. Finally, a newly developed research instrument to measure zooplankton respiration in the field is presented in Chapter 5. The light trap attracts zooplankton into the main chamber of the ZOORESPIRE, which closes after a pre-set time period. During the incubation phase their respiration in-situ as a decline in oxygen concentration over time, which will enable better quantification of respiration throughout the water column and especially in the under-studied mesopelagic zone.

ACKNOWLEDGEMENTS

Almost four years ago, I started this PhD and what a ride it has been! It takes a village to raise a child and it certainly took a village of supportive and amazing people to help me to finish this PhD project plus a plethora of side adventures. As there is only limited space in this thesis to acknowledge them all, here is an incomplete selection.

First of all, I would like to thank my supervisors, Philip Boyd and Kerrie Swadling. **Philip**, I did not google you before I came to Tasmania but figured out quickly that you are the famous "Iron Man" of the Southern Ocean. While it took me at least a year to understand your emails, I thank you for your support, Boyd's Beers at Preacher's or socially distant ice cream last year during the height of the pandemic. I enjoyed sailing with you on the Investigator twice, but I swear if you offer me "Macadamia on Horseback" one more time, I'll have a meltdown. Thanks for not micro-managing me and allowing me to develop this project as I wanted. **Kerrie**, you were my rock throughout this journey! I can't thank you enough for reading all of the drafts, leading me back on the right path when I was lost and helping me with so many practical things in the lab and when organising voyages. Whenever I came to your office to ask for help or rant about things you made time for me and I appreciate that. Also, thank you for bringing me on the Umitaka voyages, it was an amazing experience to work with the Japanese. And thank you for Pizza-Wednesdays with the lab group - I had always so much fun!

Thank you, **Emma**, for your being such a great role model as an ECR and a mom in academia. Thanks for always making time to discuss data analysis and read my drafts! Too bad you went back to the UK too soon (obviously good for you) because I enjoyed working with you on land and at sea. I loved visiting you in the UK during the BIARRITZ workshop! Hopefully, I can come back once the borders are open up again. **Matthieu**, many thanks to you! Without your support and insight, the ZOORESPIRE wouldn't be where it is today. Thanks for making so many things possible. I also enjoyed sailing with

you on the Investigator and your presence and humour improved many dark (and late) hours. Thank you, **Robert**! Still waters run deep and this is certainly true for you. I love your quiet humour and your immense knowledge (is there anything you don't know???). Also, thanks for sharing cat pictures whenever I needed them - very appreciated. **Phil B.** - where can I start? How can a person be so positive and motivated even at 2 am with no sleep for days? Without your help, none of the three voyages together would have been possible or enjoyable. Thanks for all the coffee and beer you insisted on paying for. You are an amazing human, I'm glad I met you in Kerrie's course! I promise you do not have to listen to my voyage Spotify playlist ever again - that thing gave us both PTSD.

I calculated I spent almost half a year of my PhD at sea! There are too many people that made my six-and-a-half **research voyages** an amazing experience and I cannot thank them all. If you have been on any of these voyages, please feel appreciated: IN2018_V02 (Mar 2018), IN2018_V04 (Sept/Oct 2018), IN2019_V02 (Mar/Apr 2019), UM-19-06(Aug 2019), UM-19-08 (Jan 2020) and IN2020_T01 (CAPSTAN, Mar 2020). Thanks to the cooks and stewards for feeding me (too well) and thanks to the deck team to help me deploying my nets and the ZOORESPIRE. So many of the crew, support staff, and researchers became good colleagues and friends. I still see most of you around Hobart and hope to catch up with the rest soon - maybe on the next trip? In particular, I want to thank the research team on the last **SOLACE cruise** (Dec 2020 - Jan 2021). Christmas and New Year's at sea with you were just awesome! Also, thank you for coming to our regular SOLACE coffees on Wednesday! We certainly all need more solace in our lives.

The **community of colleagues, students, and friends** at IMAS and beyond brought me through my PhD. PhTea, SOLACE coffees, BOTES events, lab pizza lunches, catching up over a beer, bushwalks, planting trees, watching birds, gym sessions, outreach missions with YTS, and road trips through the state kept me sane and happy. As a person, who always had a hard time fitting in, I might have finally found my crew. I can't name you all to thank you, so I won't even try. But please feel appreciated, you truly are.

Finally, I thank **my family** for being there for me, even though we've seen each other only virtually for the past three years. Living in Australia, writing my PhD in another language, going to uni and becoming a Dr? Unimaginable even 5 years back. You taught me that hard work and dedication would bring me far and always had my back, though

you did not always know what I was working on. Here I am now, a little bit closer to becoming the person I always aspired to be. This one is for you.

TABLE OF CONTENTS

TABLE OF CONTENTS **i**

LIST OF TABLES **viii**

LIST OF FIGURES **xi**

1 Context of the thesis **1**

1.1 Introduction 1

1.2 The role of zooplankton in the oceanic carbon pumps 3

1.2.1 The biological gravitational pump 3

1.2.2 The mesopelagic-migrant pump 6

1.2.3 The seasonal lipid pump 7

1.2.4 Zooplankton respiration 8

1.3 Knowledge gaps & thesis outline 8

2 The role of zooplankton in establishing carbon export regimes in the Southern Ocean - a comparison of two representative case studies in the subantarctic region **12**

TABLE OF CONTENTS

2.1 Abstract 13

2.2 Introduction 13

2.3 Two contrasting downward export regions 15

2.4 Contributions of zooplankton to downward carbon flux in the subantarctic region 18

2.4.1 The northern Kerguelen Plateau 18

2.4.2 HNLC waters south of Australia 19

2.5 Challenges and knowledge gaps 21

2.5.1 Comparability of methods, under-sampling of small-sized zooplankton and insufficient seasonal coverage 21

2.5.2 Understudied carbon pathways – zooplankton carcass and migratory flux 22

2.5.3 The "black box": the mesopelagic zone 22

2.6 Conclusion and outlook 23

3 What >20 years of zooplankton swimmer data reveal about ecosystem variability and downward carbon export in the subantarctic Southern Ocean 24

3.1 Abstract 25

3.2 Introduction 25

3.3 Methods 27

3.3.1 Sample collection at SOTS 27

3.3.2 Sediment trap preparation and post-recovery handling 28

TABLE OF CONTENTS

3.3.3 Sample processing and swimmer identification 28

3.3.4 Data treatment and available data sets 29

3.3.5 Data analysis and statistics 30

3.4 Results 32

3.4.1 Variability in swimmer composition with depth 32

3.4.2 Seasonal variability in swimmer composition 35

3.4.3 Interannual variability in swimmer composition 38

3.4.4 Relationship of species abundance and diversity with downward particle flux parameters 39

3.5 Discussion 45

3.5.1 Copepods, amphipods, and molluscs are the most abundant taxa 45

3.5.2 Decreasing abundance and diversity with depth 47

3.5.3 Lack of seasonality and long-term trends in swimmer abundance and diversity 48

3.5.4 Relationship to flux parameters 49

3.5.5 Biases of using sediment traps to sample deep-sea zooplankton . . 50

3.5.6 Opportunities for zooplankton collection with sediment traps and outlook 53

3.6 Conclusion 55

3.7 Acknowledgments 55

3.8 Supplementary material 55

3.8.1 Dominant copepod, amphipod, and mollusc taxa 55

3.8.2 Photomicrographs of swimmer taxa 57

4 "Sinking dead" – How zooplankton carcasses contribute to Particulate Organic Carbon flux in the subantarctic Southern Ocean 64

4.1 Abstract 65

4.2 Introduction 65

4.3 Methods 67

4.3.1 Study area and environmental conditions 67

4.3.2 Zooplankton sampling and sorting 69

4.3.3 Carcass carbon and nitrogen analyses 69

4.3.4 Microbial decomposition and sinking velocities of copepod carcasses 70

4.3.5 Calculation of the downward carcass flux 71

4.3.6 Comparison to particulate matter in sediment traps 72

4.3.7 Sensitivity of downward carbon flux to controlling factors 73

4.4 Results 74

4.4.1 Environmental conditions 74

4.4.2 Epipelagic *N. tonsus* abundances 74

4.4.3 Carcass carbon content decomposition and sinking velocities . . . 75

4.4.4 Carcass sinking flux relative to downward POC flux 78

4.5 Discussion 81

4.5.1 Drivers of downward carcass flux 81

4.5.2 Knowledge gaps and limitations of this study 83

4.5.3 Future research priorities 85

4.6 Conclusion 85

4.7 Supplementary material 86

5 ZOORESPIRE (ZOOplankton RESPiration In the subsuRface ocEan) - A new tool to measure in-situ zooplankton respiration in the ocean 87

5.1 Abstract 88

5.2 Introduction 89

5.2.1 Zooplankton respiration in the oceanic carbon cycle 89

5.2.2 Previous methods to estimate zooplankton respiration 90

5.2.3 The development of the ZOORESPIRE 91

5.2.4 Aims for this chapter 93

5.3 Methods 95

5.3.1 ZOORESPIRE set-up and development 95

5.3.2 Software and mission parameters 96

5.3.3 Trials 99

5.4 Results 101

5.4.1 Gas impermeability & temperature stability 101

5.4.2 Attraction and capture efficiency 102

5.4.3 Sensitivity of respiration measurements to varying zooplankton abundances 105

5.5 Discussion 106

5.5.1 Trial results 106

5.5.2 Challenges and biases 107

5.5.3 Opportunities for future deployments & Outlook 109

5.6 Conclusion 110

5.7 Supplementary material 112

5.7.1 Prototype 2 - Images and results 112

5.7.2 Prototype 1 & 3 115

5.7.3 Prototype 4 - Results of krill attraction, capture and respiration trials 116

6 Synthesis and future directions **117**

LIST OF ACRONYMS **122**

7 Glossary **125**

A *Chevreuxiopsis franki* n. gen. n. spec (Crustacea, Amphipoda, Thoriellidae) from the deep southwest of Tasmania **127**

A.1 Abstract 127

A.2 Introduction 127

A.3 Methods 128

A.4 Systematics 129

A.5 Discussion 133

TABLE OF CONTENTS

REFERENCES **141**

LIST OF TABLES

2.1 Comparison of environmental parameters and planktonic groups between the High-Biomass Low-Export (HBLE) Kerguelen Plateau and the High-Nutrient Low-Chlorophyll (HNLC) waters south of Australia. Examples of downward carbon flux and e-ratios in the two regions are also given. The particulate organic carbon (POC) fluxes are estimated from polyacrylamide gel traps at 200 ± 10 m and 240 m depth on the Kerguelen Plateau and in the HNLC region, respectively. The e-ratio is an indicator for export efficiency and is calculated as the ratio between POC flux and primary productivity. Note that Laurenceau-Cornec et al. (2015) use net primary productivity in the euphotic zone to calculate the e-ratio, while Ebersbach et al. (2011) use gross primary productivity. 17

3.1 Total numbers of organisms identified from sediment traps at 1000, 2000 and 3800/3900 m depth between September 1997 and April 2020. UI: unidentified. 34

3.2 Biodiversity index (Shannon-Wiener, H') and Pilou's Evenness (J) based on zooplankton swimmers between depths and seasons. 35

3.3 Results of the Generalised Additive Models. Displayed are the effective degrees of freedom (edf) for the flux parameters that are significantly driving the species abundance and diversity. Non-significant results were left blank. If the relationship was proven to be linear, as shown with an edf of 1.00, the type of relationship (positiv (+) or negative (-)) was added in parentheses. 43

LIST OF TABLES

3.4 The five dominant copepod families, amphipod species, and mollusc species, summarised over all years and compared between sediment trap depths. Percentages in parentheses display contribution to total copepod, amphipod, and mollusc abundance, respectively. UI: unidentified. 56

4.1 Parameters used in the sensitivity analysis to estimate carcass downward carbon flux. Numbers in bold indicate the parameter that has been changed relative to the control experiment. The mortality rates were calculated based on an equation by Hirst and Kiørboe (2002) and measurements by Yáñez et al. (2019). The sinking velocity was either measured in this study or calculated from Table 3 in Elliott et al. (2010). The upper and lower rates of microbial decomposition represent the highest and lowest measured k during this study (0.17 and 0.02 d^{-1}). 79

4.2 Sensitivity analysis comparing carcass sinking fluxes in mg C m^{-2} d^{-1} at 1000, 2000, and 3800 m depth in comparison with POC fluxes (mg C m^{-2} d^{-1}) estimated from sediment traps at Southern Ocean Time Series (SOTS) in mid-October (midpoint date: 12 October, 2018). Ranges in parentheses consider the variability between day and night biomass and standard deviation in sinking velocity and microbial respiration. 80

4.3 Parameterisation of zooplankton mortality in the ecosystem models REcoM2, BEC and PISCES. All equations are described in more detail by (Laufkötter et al., 2016). Z is the zooplankton biomass, pzoo the quadratic mortality rate and mzoo the linear mortality rate. PISCES distinguishes between micro- and meso-zooplankton mortality and includes a factor for dissolved oxygen (f (O_2)) and temperature (Tf). 86

5.1 Mission parameters of the ZOOplankton RESPiration in the subsuRface OcEan (ZOORESPIRE) that were set with a software menu in the controller unit during the laboratory and field trials in September- November 2020. (1) Light turned off in the control trial. (2) No collection phase during this trial. 98

LIST OF TABLES

5.2 Measured lengths (TL: Total length, distance from rostrum to urosome) and wet weights of the tested krill (*Euphausia superba*). 116

6.1 Synthesis of thesis results and future research priorities. 119

6.2 Cont. 120

6.3 Cont. 121

LIST OF FIGURES

1.1 Circumpolar fronts in the Southern Ocean based on historical hydrographic data and application of water-mass criteria to define their locations (Orsi et al., 1995). The fronts are labelled from north to south: the Subtropical Front (STF), the Subantarctic Front (SAF), the Polar Front (PF), the southern Antarctic Circumpolar Front (sACCF) and the Southern Boundary front (SBdy). This thesis is focused on the subantarctic zone between the STF and SAF. Figure by Chapman et al. (2020) 2

LIST OF FIGURES

1.2 A simplified representation of the role of zooplankton in the downward carbon pumps following Boyd et al. (2019). Phytoplankton fix carbon dioxide from the seawater and are grazed upon by the upper ocean zooplankton community. As part of the biological gravitational pump (BGP), phytodetritus, i.e. dead phytoplankton cells, carcasses, and faecal pellets (FP) produced by the community sink out of the epipelagic zone (0-200 m depth). As particles sink, zooplankton at depth in the mesopelagic zone ingest, fragment, and repack particles into faecal pellets. In addition, a subset of the zooplankton community performs diel vertical migration each dusk and dawn, which actively injects particles (carcasses and faecal pellets) to deeper waters and is termed the mesopelagic-migrant pump (MMP). Zooplankton, such as polar calanoid and neocalanoid copepods, migrate seasonally and stay at depths >500 m depth for the duration of their dormancy. Individual species have different strategies; some copepods ascend to the surface in spring to complete their life cycle and reproduce or remain at depth and die. In the latter case, the mortality during and following dormancy leads to an injection of carcasses, which is termed the seasonal lipid pump (SLP). Across the various carbon export pumps, respired CO_2 and the production of dissolved inorganic carbon (DIC), represents a major carbon pathway. Depending on environmental factors and migration depth, respiration can result in a significant downward flux of inorganic carbon (Hernández-León and Ikeda, 2005b). 4

1.3 Overview of aims, study area, methodology and carbon pathways covered in chapters 2-6. Abbreviations as follows: ZOOplankton RESPiration in the subsuRface OcEan (ZOORESPIRE), Southern Ocean Time Series (SOTS), biological carbon pump (BCP), biological gravitational pump (BGP), mesopelagic-migrant pump (MMP), seasonal lipid pump (SLP). 11

LIST OF FIGURES

2.1 The zooplankton-mediated carbon cycle in summer on the naturally iron-fertilized Kerguelen Plateau (panel a) compared to the HNLC waters around SOTS (panel b). On the Kerguelen Plateau, high dissolved iron levels promote high chlorophyll *a* levels as a proxy for algal biomass at the surface. The diverse zooplankton community feeds on the sinking particle flux and acts as a "gate-keeper" to the deeper ocean by ingesting and fragmenting sinking particles and, consequently, significantly reducing the export flux out of the epipelagic. The main downward export particles are diatom resting spores, which bypass the intense grazing pressure, followed by faecal pellets. At SOTS, dissolved iron levels are lower than on the Kerguelen Plateau, but support a more diverse phytoplankton community, but with lower biomass, which, in turn, affects zooplankton community composition and biomass. The grazing pressure during summer is focused mostly on picoplankton, while larger particles are exported directly. Grazing and fragmentation of particles at both sites increases nutrient recycling in the upper water column. Challenges and knowledge gaps in aspects of the zooplankton-mediated carbon pump are highlighted. 20

3.1 (a) and (d) non-metric multi-dimensional scaling (nMDS) to display groupings of the transformed abundance data per depth (a) and season (d) using a Bray-Curtis resemblance matrix. For a better display, one major outlier was removed. (b) and (e) Canonical Analysis of Principal coordinates (CAP) that displays correspondence of flux parameters with transformed species abundance per depth (b) and season (e). (c) and (f) biodiversity (Shannon Wiener Information function) per depth and season, respectively. 37

3.2 The zooplankton swimmer community in sediment traps at SOTS. Displayed are (a) and (c) total flux (individuals m^{-2} d^{-1}) and (b) and (d) contribution to flux (% of total flux) at 1000 and 2000 m depth, respectively. Numbers above the bars indicate the sampling period (days) per respective year. Note, numbers higher than 365 are caused by using the midpoint date to determine the association with a sampling year and not the start/end date. 41

3.3 The zooplankton swimmer community in sediment traps at SOTS (cont.). Displayed are (a) total flux (individuals m^{-2} d^{-1}) and (b) contribution to flux (% of total flux) at 3800/3900 m depth, respectively. Numbers above the bars indicate the sampling period (days) per respective year. Note, numbers higher than 365 are caused by using the midpoint date to determine the association with a sampling year and not the start/end date. 42

3.4 Generalised Additive Models fitted to the standardised flux parameters as predicting factor and the total swimmer abundance (a-d), and the three dominant groups - copepods (e-h), amphipods (i-l), and molluscs (m-o), as response variables. Displayed are the significant relationships between flux parameters and species abundance ($p<0.01$). 44

3.5 Image of the recently recovered trap cup from 2000 m in 2020/2021, taken before sieving. Visible is a large, fragile object (indicated by the black arrow), that disintegrated in the sieving process afterwards. White scale bar: 1 cm. Picture: Cathryn Wynn-Edwards, AAPP, Australia. 53

3.6 Amphipods collected between 1997-2020. (a) *Pegohyperia princeps*, (b) *Pegohyperia princeps* with open abdomen and juveniles, (c) *Primno lattreillei*, (d) *Cyllopus magellanicus*, (e) *Cyphocaris richardi*, (f) *Scina* spp. (g) *Chevreuxiopsis franki*, that was is described in further detail in Chapter A, (h) *Eurythenes thurstoni*, (i) *Lanceola* sp., (j) *Parandania boecki*, (k) *Vibilia armata*, and (l) *Abyssorchomene abyssorum*. White scale bar: 1 mm. 57

3.7 Crustaceans collected between 1997-2020. (a)-(c) Unidentified decapods, (d) crustacean larvae, (e)-(f) unidentified isopods (g) ostracod *Gigantocypris* sp., (h) euphausiid *Thysanoessa macrura*, (i) euphausiid *Euphausia* sp., (j) unidentified ostracod. White scale bar: 1 mm. 58

3.8 Molluscs collected between 1997-2020. (a) *Clio recurva*, (b) *Peracle* spp., (c) *Janthina* spp., (d) *Spongibranchia australis*, (e) *Limacina helicina antarctica*, adult, (f) *Limacina helicina antarctica*, juvenile, (g) *Helicoides inflatus*, (h) heteropod *Atlanta* spp., (i) *Clio pyramidata sulcata*, (j) *Clio pyramidata lanceolata*, (k) *Clio pyramidata antarctica*, (l) juvenile squid, (m) *Limacina retroversa australis*, (n) *Cavolinia tridentata*. White scale bar: 1 mm. 59

3.9 Gelantinous communities collected between 1997-2020. (a)-(b) Chaetognath (Sagittae family), (c) Doliolid, Tunicata, (d) jellyfish medusa (Cnidaria), (e) ctenophore, (f) jellyfish medusa (Cnidaria), (g) Siphonophore (*Diphyes* spp.), (h) *Atolla* sp. (Cnidaria), (i) *Periphylla periphylla* (Cnidaria), (j) pyrosome (*Pyrosoma atlanticum*), Tunicata, (k) pyrosome (*Pyrostremma* sp.), Tunicata, (l) salp (*Salpa thompsoni*), Tunicata, (m)-(n) giant larvacean, Tunicata (trunk and feeding basket). White scale bar: 1 mm. . . 60

3.10 Polychaetes collected between 1997-2020. (a) family Alciopidae, (b)-(c) family Lopadorrhynchidae, (d) unidentified polychaete, (e) family Tomopteridae. White scale bar: 1 mm. 61

3.11 Fish collected between 1997-2020. (a) *Poromitra* sp., (b) *Stomias* sp., (c) *Cyclothones* sp., (d) family Myctophidae, (e) unidentified fish larvae. White scale bar: 1 mm. 62

3.12 Other taxa collected between 1997-2020. (a) Giant foraminiferans, (b) ophiurids, Echinodermata, (c) closest identification: Balanomorpha (barnacles). White scale bar: 1 mm. 63

4.1 (a) Mean chlorophyll *a* (in µg L^{-1}) in the subantarctic Southern Ocean south of Tasmania (green shaded land-mass) in September 2018, derived from MODIS satellite data. White areas indicate cloud cover. The sampling sites are marked in orange. (b) and (c) CTD data of temperature (°C) and salinity in the upper 1000 m at PS1 and PS2, respectively. (d) and (e) Measured particulate organic carbon (dark grey), particulate organic nitrogen (light grey), and chlorophyll *a* concentration (orange) of the upper 200 m at PS1 (left) and PS2 (right). All values are in μg L^{-1}. The lower limit of the euphotic zone is marked at 126 m (PS1) and 116 m (PS2). It was calculated as the depth of 1% of the surface photosynthetically active radiation relative to the surface radiation, measured by the CTD, following Kirk (1994) and Lee et al. (2007). The mixed layer is deeper at both stations (329 m and 199 m at PS1 and PS2, respectively) and is therefore not depicted here. 68

4.2 Size distribution of *N. tonsus* copepods (copepodites and adults) is displayed for site PS1 (a) and PS2 (b), the orange bars indicate sampling during the day, grey during the night. Dashed lines indicate approximate size boundaries for *N. tonsus* copepodite stage IV (CIV), copepodite stage V (CV) and adult (CVI), as outlined in Bradford et al. (1988). 75

4.3 Relationship between (a) copepod dry weight (μg) to carbon per individual, (b) prosome length (mm) to carbon per individual and (c) prosome length to sinking velocity (m min^{-1}). The calculated linear trend lines are added and the p and R^2 values are displayed. 76

4.4 The normalised dissolved oxygen decline in two decomposition experiments (replicates) at PS2 over 24 hours. The error bars depict the standard deviation. The linear regressions are displayed for both experiments. . . . 77

4.5 (a) The factors that impact the downward carcass flux through the water column: sinking velocity, mortality rates, and microbial decomposition. Other important factors include detritivory, turbulence and seawater density gradients in the water column. (b) The estimated carbon flux by *N. tonsus* carcasses from the surface down to 1000, 2000, and 3800 m depth in comparison to the particulate organic carbon flux in mid-October, estimated with sediment traps at SOTS. 83

5.1 Development of the prototypes of the current ZOORESPIRE. Trials were conducted either off the IMAS Wharf (42.88°S, 147.34°E), on the pier on Maria Island (42.58°S, 148.06°E), or at the Southern Ocean Time Series site (47°S, 140°E) during a research voyage in 2019. Images of the prototypes along with zooplankton counts of the successful trial of prototype 2 are displayed in the supplementary materials (Figures 5.6 and 5.7). . . . 94

5.2 Set-up of the ZOORESPIRE within the steel frame during deployment: Construction of the chamber body, including the funnel-shaped trap entrance, lid that closes the chamber, light source, oxygen optode, and sampling tap in the base plate. The sampling component is connected via cables to the controller unit, which is programmed with the mission parameters prior to deployment. The frame is attached to a cable for deployment. The total ZOORESPIRE unit weighs approximately 55 kg. 96

5.3 The ZOORESPIRE trial at the Australian Antarctic Division. (a) The ZOORESPIRE was deployed without the metal frame due to a lack of space in the krill tank. Instead, the controller and the ZOORESPIRE were suspended from the ceiling. (b) The ZOORESPIRE in the krill tank with an attached GoPro camera to document the krill behaviour. (c) An Antarctic krill during the first trial that was attracted by the light and entered the chamber afterwards. 102

5.4 The change in dissolved oxygen concentration (left panel) and temperature (right panel) during the ZOORESPIRE trials. The control outside the chamber (permeability trial) and without light (trapping efficiency trial and sensitivity trial) is depicted in purple, while the test inside the chamber or with a light source are yellow or orange. (a)-(b) The red line indicates the start and finish of the introduction of nitrogen gas into the chamber to artificially lower the dissolved oxygen concentration during the permeability trial in the IMAS laboratory. (c)-(d) and (e)-(f): The red line indicates the closing of the ZOORESPIRE after the collection phase, commencing the incubation phase. Note that the scale on the x-axis varies between trials. 104

5.5 Zooplankton abundance in the trapping efficiency trial of the ZOORESPIRE. The upper panel (a) depicts the fractions of each taxonomic group in the community, while the lower panel (b) shows the total concentration in individuals L^{-1}. The bars represent the large, medium and small zooplankton size fraction in the control trial without light (CL= control large, CM = control medium, CS= control small, respectively) and the large, medium, and small fraction in the trial with light (LL= light large, LM= light medium, LS= light small, respectively). 105

5.6 Images of the second prototype: set-up, deployment and results. The first trial was conducted off the IMAS wharf to test a light source versus an amino acid solution (Aa) in a dialysis bag to attract zooplankton (left panel): (a) Two of the three carboys, one with the dive light torch (left) and one control (right); (c) Results of the trials: light trap is visibly most successful; (e) Qualitative picture of the light sample, containing a fish larvae and many porcelain crab larvae. The second trial was conducted off the pier on Maria Island to find the best deployment time of day and duration (right panel): (b) Deployment in approximately 1.5 m water depth; (d) Zooplankton sample caught overnight; (f) Qualitative picture of the overnight sample, containing krill, polychaetes and copepods. 112

5.7 Zooplankton of the two size fractions (a) >250 μm and (b) 65-250 μm, caught overnight in prototype 2 off the IMAS Wharf. Trials were conducted with a light source (yellow), an amino acid solution in a dialysis bag (Aa, purple) and a control (dark blue). 113

5.8 Zooplankton of the two size fractions (a) - (b) >250 μm and (c)-(d) 65-250 μm, caught in prototype 2 off the pier on Maria Island, Australia, in the light treatment (left side) and control without a light source (right side). Trials were conducted over 10 hours during the day (purple), 14 hours overnight (dark blue) and over 23 hours. Note the different scales of the x-axis between the trials and size fractions. 114

5.9 (a) Images of the first prototype, a small Niskin bottle (2.5 L) that was deployed in horizontal orientation from the IMAS Wharf. A solution of amino acids was used, however, no zooplankton were caught. (b)-(d) Images of the third prototype, a large Niskin bottle (30 L) that included a light (pointing inward, d), a controller, closing mechanism and an optode (latter not pictured in c). This prototype was deployed over the side off the RV Investigator in the subantarctic Southern Ocean but did not collect any zooplankton. 115

A.1 a–d. *Chevreuxiopsis franki* n. gen. n. sp., holotype 12 mm. a) antenna 1; b) antenna 2, peduncular articles 1–2 missing; c) habitus; d) labrum and mandible, lateral view. Scale bars: a, b = 500 μm; c = 1 mm; d = 100 μm. 135

A.2 a–g. *Chevreuxiopsis franki* n. gen. n. sp., holotype 12 mm. a) right mandible; b) left mandible; c, d) maxilla 1; e) lower lip; f) mouthparts, left aspect; g) maxilla 2. Scale bars: a–e = 100 μm; f = 500 μm. 136

A.3 a–e. *Chevreuxiopsis franki* n. gen. n. sp., holotype 12 mm. a) maxilliped, opened up; b) pereopod 1, basis to dactylus; detail shows knob-like dactylus; c) pereopod 3; d) pereopod 2, without coxa; e) dactylus of pereopod 2. Scale bars: a–d = 500 μm. 137

A.4 a–c. *Chevreuxiopsis franki* n. gen. n. sp., holotype 12 mm. a) pereopod 4; b) pereopod 5; c) pereopod 7, medial aspect. Scale bars: a–c = 500 μm. 138

A.5 *Chevreuxiopsis franki* n. gen. n. sp., holotype 12 mm. a) pereopod 6; b) pleopod 1; c) coupling hooks of pleopod; d) anterior margin of propodus; e) urosome, dorsal view; f) setulated seta of pleopod. Scale bars: a, b, e = 500 μm. 139

A.6 *Chevreuxiopsis franki* n. gen. n. sp., holotype 12 mm. Photo of head, antennae, maxillipeds and anterior pereopods. Note the dark purple/black colour of the 1st pereopods. Scale bar = 500 μm. 140

Chapter 1

Context of the thesis

1.1 Introduction

Anthropogenic greenhouse gas emissions affect the oceans on a global scale. Since the Industrial Revolution in the late 18th century, humankind has emitted 440 ± 20 Pg carbon as carbon dioxide into the atmosphere (Friedlingstein et al., 2019) and approximately half (48%) is taken up by the oceans (Sabine et al., 2004; Lindsey, 2020). Two major processes are responsible for the uptake, transfer, and storage of carbon: (1) the solubility pump that transports cold, dense water masses to depth together with nutrients, carbon, and other elements, and (2) the BCP (Volk and Hoffert, 1985). The latter has been studied intensively as a regulatory mechanism of atmospheric carbon dioxide levels in the last three decades, as it is estimated to lower the CO_2 concentration by 200 ppm (Parekh et al., 2006) and store carbon for decades or centuries (Sarmiento and Gruber, 2006). The biological carbon pump (BCP) also links carbon fixation by primary producers in surface waters via carbon export through the mid-water zone to carbon storage in the ocean's interior (Boyd et al., 2019). It is estimated that organic particles transfer between 5 and 15 Pg carbon into the deep sea each year (Henson et al., 2011; Falkowski et al., 1998; Boyd et al., 2019). This downward carbon flux not only regulates atmospheric carbon dioxide but also introduces food to the deep sea fauna, which are dependent on pulses of organic material to meet their physiological demands (Turner, 2002).

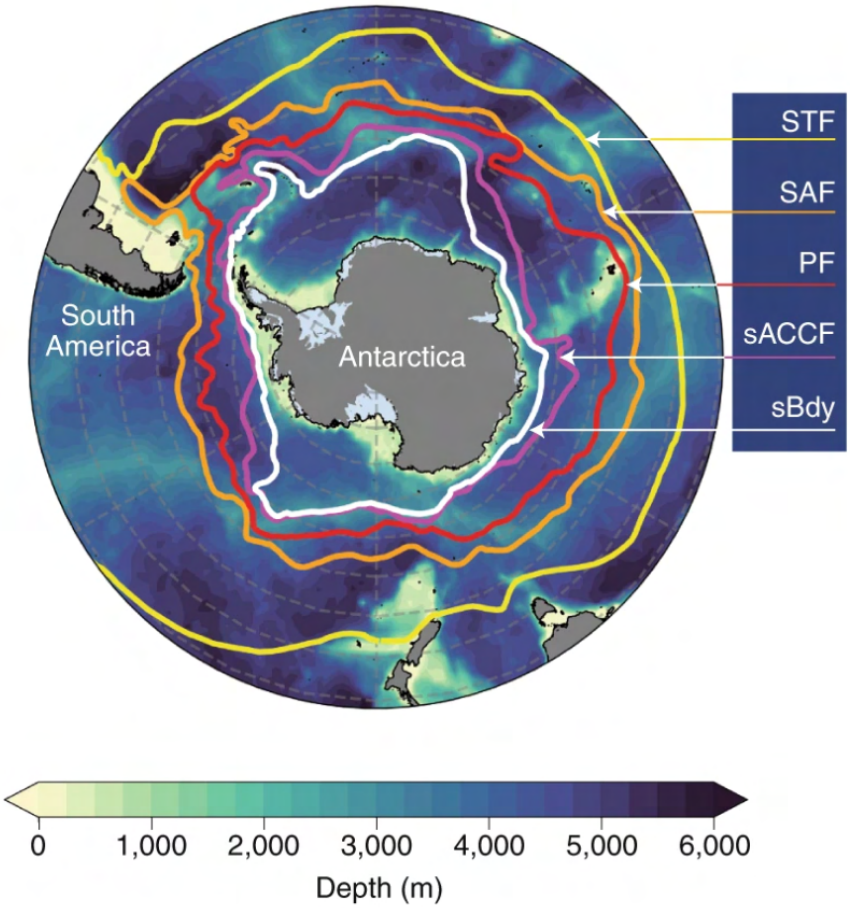

Figure 1.1: Circumpolar fronts in the Southern Ocean based on historical hydrographic data and application of water-mass criteria to define their locations (Orsi et al., 1995). The fronts are labelled from north to south: the Subtropical Front (STF), the Subantarctic Front (SAF), the Polar Front (PF), the sACCF and the Southern Boundary front (SBdy). This thesis is focused on the subantarctic zone between the STF and SAF. Figure by Chapman et al. (2020)

.

The Southern Ocean plays an important role in the Earth's climate and carbon cycle (Sabine et al., 2004). Its water masses are divided by oceanographic fronts; i.e., steep gradients in physical properties such as salinity and temperature (Orsi et al., 1995; Chapman et al., 2020, Figure 1.1). The Antarctic Circumpolar Current (ACC) connects and ventilates all oceanic basins (Bowie et al., 2011b). Along the Antarctic continental shelf, carbon dioxide is released back into the atmosphere due to upwelling of Circumpolar Deep Water (CDW); a water mass that has not been in contact with the atmosphere for cen-

turies (Bowie et al., 2011b; Frölicher et al., 2015; Khatiwala et al., 2009; Le Quéré et al., 2008; Marinov et al., 2006; Orsi et al., 1995). The physical subduction of Antarctic Intermediate Water (AAIW) by Subantarctic Mode Water (SAMW) close to the Subantarctic Front, results in the transport of large amounts of carbon dioxide into the ocean interior (Sabine et al., 2004). Consequently, while the Southern Ocean south of 30°S only occupies 30% of the Earth's surface, 43 ± 3% (42 ± 5 Pg C) of anthropogenic carbon dioxide released since 1861 has been taken up by the subantarctic Southern Ocean (Frölicher et al., 2015). The subantarctic solubility pump has been studied extensively (Marinov et al., 2006; Le Quéré et al., 2008; Bowie et al., 2011b), however, quantification of biologically-mediated carbon transport has received less attention, focusing for example on the region south of Australia in the vicinity of the Southern Ocean Time Series (SOTS) site at 47°S (Wynn-Edwards et al., 2020). Despite the focus on sites such as SOTS, the subantarctic zone is in general one of the most understudied regions globally, as it is remote and logistically challenging to sample (Trull et al., 2010). Sampling campaigns, such as the Sensitivity of the sub-Antarctic zone to environmental change (SAZ-Sense) voyage in January/February 2007 and Southern Ocean Large Scale Carbon Export (SOLACE) voyage in December 2020 to January 2021, are usually restricted to the summer season.

1.2 The role of zooplankton in the oceanic carbon pumps

In the following section and chapters, I use the categories reported in Boyd et al. (2019) to distinguish between different types of the BCP driven by zooplankton. In addition to the biological gravitational pump (BGP), i.e. the passive sinking of particles, I also address the mesopelagic-migrant pump (MMP) and the seasonal lipid pump (SLP), and highlight the role the zooplankton community plays in each pump (Figure 1.2). Additionally, I discuss zooplankton respiration as a major pathway for dissolved inorganic carbon flux.

1.2.1 The biological gravitational pump

Zooplankton contribute to the BGP by feeding on phytoplankton and producing fast-sinking faecal pellets that transport carbon to the deep sea (Boyd et al., 2019; Steinberg

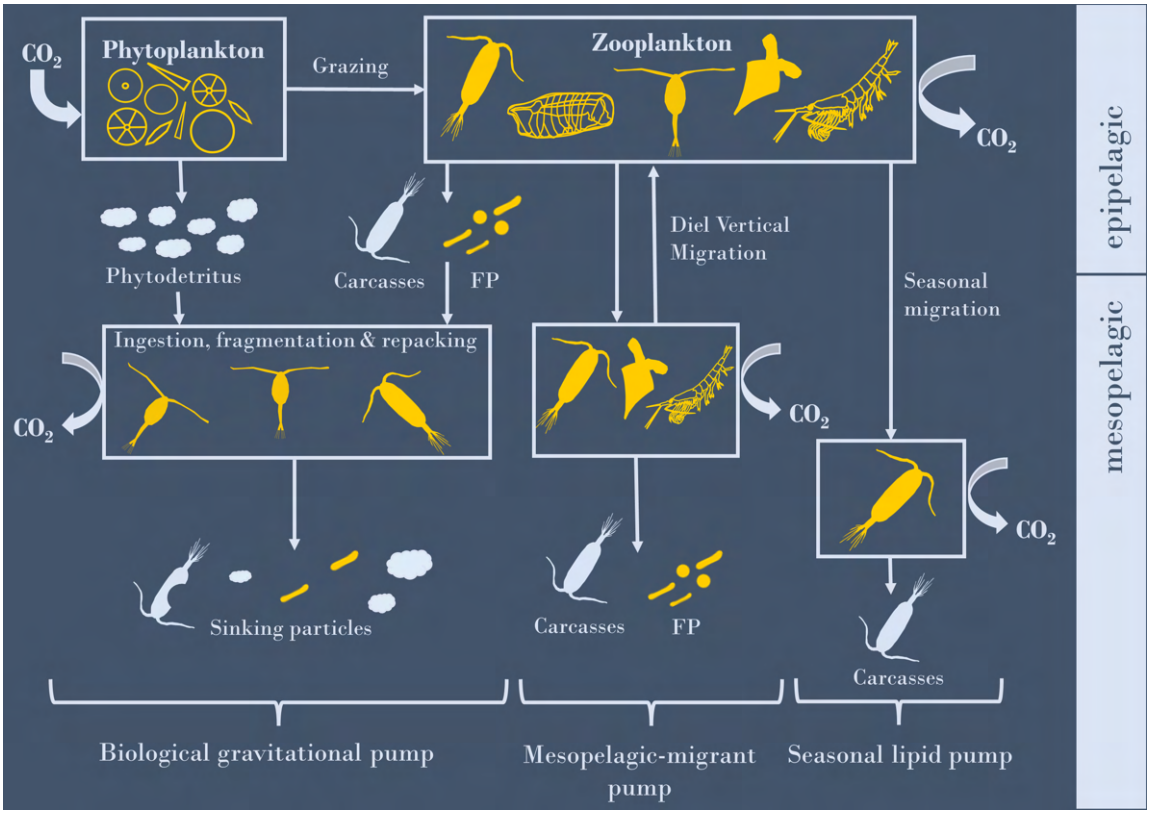

Figure 1.2: A simplified representation of the role of zooplankton in the downward carbon pumps following Boyd et al. (2019). Phytoplankton fix carbon dioxide from the seawater and are grazed upon by the upper ocean zooplankton community. As part of the BGP, phytodetritus, i.e. dead phytoplankton cells, carcasses, and faecal pellets (FP) produced by the community sink out of the epipelagic zone (0-200 m depth). As particles sink, zooplankton at depth in the mesopelagic zone ingest, fragment, and repack particles into faecal pellets. In addition, a subset of the zooplankton community performs diel vertical migration each dusk and dawn, which actively injects particles (carcasses and faecal pellets) to deeper waters and is termed the MMP. Zooplankton, such as polar calanoid and neocalanoid copepods, migrate seasonally and stay at depths >500 m depth for the duration of their dormancy. Individual species have different strategies; some copepods ascend to the surface in spring to complete their life cycle and reproduce or remain at depth and die. In the latter case, the mortality during and following dormancy leads to an injection of carcasses, which is termed the SLP. Across the various carbon export pumps, respired CO_2 and the production of dissolved inorganic carbon (DIC), represents a major carbon pathway. Depending on environmental factors and migration depth, respiration can result in a significant downward flux of inorganic carbon (Hernández-León and Ikeda, 2005b).

and Landry, 2017; Turner, 2002, 2015). In addition, non-consumptive mortality that is not caused by predation leads to a passive downward flux of zooplankton carcasses (Hirst and Kiørboe, 2002; Daase et al., 2014; Tang and Elliott, 2014).

The efficiency of the BGP mediated by zooplankton depends on several factors, such as diet, food concentration and zooplankton species composition. For example, the laboratory experiments by Hansen et al. (1996) found that faecal pellets of the copepod *Acartia tonsa* resulting from a diatom diet were more dense and slower degrading compared to animals on a flagellate diet. Sinking velocities of faecal pellets are influenced by ballasting of biominerals e.g. opal and calcium carbonate obtained from diatom and coccolithophorid diets, respectively (Turner, 2002). Consequently, downward particulate organic carbon (POC) export fluxes in the global ocean are correlated with mineral fluxes, especially for carbonate ballasting (Turner, 2015; Armstrong et al., 2009; Klaas and Archer, 2002; Francois et al., 2002). Additionally, zooplankton grazing increases silicate production in diatoms by 100% (Pondaven et al., 2007), which increases the cell wall silicification and, consequently, sinking speed and carbon export (Sanders et al., 2014).

Furthermore, phytoplankton abundance, i.e. food concentration, affects downward carbon export. For example, high feeding rates of Antarctic krill *Euphausia superba* caused by high food concentration lead to a fast gut passage time with low food absorption(Atkinson et al., 2012; Cavan et al., 2019a). In contrast, low food levels result in a fast flux of dense faecal pellets with low carbon and nitrogen content (Atkinson et al., 2012; Cavan et al., 2019a).

Similarly, the species composition of a zooplankton assemblage affects their role in the BGP. While krill egest long chains of faecal matter, copepod pellets are smaller and more compact (Cavan et al., 2017a). Consequently, krill pellets sink faster and contribute more to downward carbon export than copepod pellets, which are more likely to be biologically recycled in the upper water column (Turner, 2002, 2015; Urbin-Rich et al., 1999). In addition, fragmentation of faecal pellets by zooplankton "sloppy feeding" decreases their sinking speed and makes particles more accessible as food sources for smaller organisms and the microbial loop (Giering et al., 2014; Hosie et al., 2003; Lampitt et al., 1990; Steinberg and Landry, 2017; Turner, 2015). Half of the fast-sinking particles are ingested and fragmented by zooplankton in the mesopelagic zone and a further 30% is released as

suspended and slow-sinking material (Giering et al., 2014). The zooplankton community acts as a gatekeeper of the downward particle flux into the ocean's interior (Halfter et al., 2020; Stukel et al., 2019), however, further studies of the mesopelagic community are necessary to quantify their impact on particulate carbon export.

Zooplankton carcasses can be an important vehicle for carbon transport to the deep sea. Hirst and Kiørboe (2002) estimated that one quarter to one third of copepod mortality is due to non-predatory causes, such as starvation, environmental stressors, or infections. Other factors can be death after reproduction or incomplete consumption by predators (Daase et al., 2014). In oligotrophic regions, zooplankton carcasses may be a particularly important food source during periods of low primary production (Forest et al., 2007, 2008; Sampei et al., 2009). In addition, carcasses can contribute significantly to downward carbon flux; e.g. Sampei et al. (2009) estimated that they represent 36% of the overall downward POC flux in the Beaufort Sea in the Canadian Arctic. The contribution of zooplankton carcasses to the BGP varies between seasons and regions and is dependent on many factors, including species mortality rates, environmental conditions (e.g. turbulence or phytoplankton concentration), and migration depth as discussed below. To date, no data on zooplankton mortality rates or contribution to the downward carbon export are available for the subantarctic Southern Ocean.

1.2.2 The mesopelagic-migrant pump

Diel vertical migration (DVM), i.e. residing by the day in deeper waters and ascending to the surface to feed at night, is a predator avoidance behaviour displayed by many zooplankton species (Zaret and Suffern, 1976; Stich and Lampert, 1981; Hays, 2003). DVM leads to carbon respired, excreted, or egested in deeper water that then escapes remineralisation in the euphotic zone (Giering et al., 2014; Lampitt et al., 1990; Steinberg and Landry, 2017). The magnitude of this MMP and its importance relative to the BGP varies spatially and temporally and is dependent on the biomass and species composition of the migrating community (Steinberg and Landry, 2017). On average, carbon transported by the MMP is between 15-20% of the BGP, but during periods of high primary productivity or in areas with high zooplankton biomass, the active MMP flux is equal to or exceeds the passive BGP flux (Robinson et al., 2010, and references therein).

Migration patterns also differ with zooplankton developmental stage and changes in response to predation, food concentration, temperature, dissolved oxygen and endogenous rhythm (Folt and Burns, 1999; Dagg et al., 1997). As a result of zooplankton migration, predators such as fish also migrate within the mesopelagic zone to feed on zooplankton. The gut passage in fish takes longer and their residence depth is usually deeper, hence, their migration adds to the magnitude of the MMP (Davison et al., 2013; Klevjer et al., 2016).

1.2.3 The seasonal lipid pump

On seasonal time scales, many zooplankton species perform vertical migrations below the permanent thermocline ($\sim$ 850 m in the northern Subantarctic Zone (SAZ), Jansen et al., 2020) as part of their life cycle (Jónasdóttir et al., 2015). For example, copepods, in the families Calanidae and Eucalanidae enter diapause in their late copepodite or adult stage to avoid unfavourable conditions, such as low temperatures, lack of food and/or abundant predators (Baumgartner and Tarrant, 2017). Although individuals go into dormancy with low metabolic rates and, hence, low faecal pellet production, mortality across the community results in an injection of carbon in the form of carcasses into deeper waters (Bradford-Grieve et al., 2001; Jónasdóttir et al., 2015). In addition, the stored lipids, such as wax esters, that have been accumulated during summer are catabolised and respired to provide energy during dormancy (Baumgartner and Tarrant, 2017). In contrast to the BGP, the SLP directly transfers carbon in the form of lipids ("lipid shunt"), but not nitrogen below the permanent thermocline (Jónasdóttir et al., 2015). The magnitude of POC transported seasonally is dependent on mesopelagic temperatures and zooplankton population structure (Jónasdóttir et al., 2015). However, global estimates of the downward carbon flux via the SLP are limited due to difficulties in sampling and regional patchiness (Boyd et al., 2019; Jónasdóttir et al., 2015). Warming oceans resulting from climate change are not only increasing diapause metabolic rates, but also decreasing diapause duration, which could significantly reduce carbon sequestration by seasonally-migrating zooplankton (Baumgartner and Tarrant, 2017).

1.2.4 Zooplankton respiration

Zooplankton respiration is a transformation of POC into CO_2 and then into DIC (Figure 1.2). Depending on the migration depth of zooplankton, respiration has the potential to sequester carbon for longer than one year and longer if carbon is injected below the pycnocline beneath the wintertime mixed layer, e.g. at >500 m at SOTS (Trull et al., 2019; Boyd et al., 2019). In the Southern Ocean, zooplankton respire up to 0.6 Gt C per year, which is 22-31% of the region's primary production (Mayzaud and Pakhomov, 2014a). Usually, 50% of the ingested carbon is respired by zooplankton, but this ratio is dependent on several factors, such as body size or water temperature (Steinberg and Landry, 2017). For example, tropical and subtropical zooplankton have higher weight-specific respiration rates than larger-sized polar species (Hernández-León and Ikeda, 2005a). In addition, zooplankton diversity and abundance play an important role: e.g., Mayzaud and Pakhomov (2014a) measured the highest respiration rates at highest diversity and medium population density. Furthermore, mesopelagic copepods may have lower rates than epipelagic as a function of lower temperatures and food concentration (Nishibe and Ikeda, 2008) and daily migrating and actively feeding zooplankton have higher respiratory activities, than deeper-living, non-migrating plankton (Minutoli et al., 2014). As zooplankton species biodiversity and physiology are still poorly understood, especially in subsurface waters, the downward flux of DIC through the mesopelagic and below is not well quantified in the subantarctic zone. Another issue for measuring respiration is the indirect methodologies used. Either zooplankton are collected and the oxygen consumption is measured in laboratory-based incubation experiments (e.g. Ikeda et al., 2006; Hernández-León and Ikeda, 2005b) or their respiration rates are derived from enzyme assays from the Electron Transfer System (ETS) (Hernández-León and Ikeda, 2005a). Collection and handling of the animals can induce stress (Elliott and Tang, 2009) and, hence, impact the respiration rates. To our knowledge, there is currently no tool available to measure zooplankton respiration in-situ over a longer time period.

1.3 Knowledge gaps & thesis outline

In conclusion, while the biological carbon pump and the role that zooplankton play in carbon export have been studied for several decades, knowledge gaps remain, in particular

for the subantarctic zone. I identified the following aspects that require further research:

- Beyond species surface distribution data from Continuous Plankton Recorder (CPR) deployments (e.g. Hunt and Hosie, 2003, 2006), little is known about the sub-surface community in terms of ecology and biogeochemistry, particularly outside the main sampling season in summer. Consequently, estimations of the downward carbon export that is driven by zooplankton are restricted, as necessary information on species biodiversity, abundance and ecology is lacking.
- While research on the zooplankton mediated BGP focuses on faecal pellets as conduits for carbon export, carcasses remain understudied. We lack both mortality rates and quantification of the downward carbon flux by zooplankton carcasses in the subantarctic zone.
- Zooplankton respiration during vertical migrations has the potential to contribute significantly to the flux of inorganic carbon. However, respiration rates are rarely quantified below the accessible epipelagic zone. Although methods are available to measure zooplankton respiration in the laboratory, for example by incubating organisms or performing enzyme assays, no tool currently measures respiration in-situ, e.g. in the mesopelagic, and over an extended amount of time.

Consequently, this thesis is structured as follows (Figure 1.3):

Chapter 2 reviews the role of zooplankton in shaping downward POC export regimes by comparing two case studies in the Southern Ocean and carbon export regimes: the High-Biomass Low-Export (HBLE) region on the Kerguelen Plateau and the subantarctic High-Nutrient Low-Chlorophyll (HNLC) region south of Australia that is characterised by relatively high export. In particular, I focus on the effect of community composition, grazing and faecal pellet production in the two carbon export regimes.

Chapter 3 presents long-term (>20 years) zooplankton data using deep-ocean sediment traps from the Southern Ocean Time Series site as a tool for continuous data collection in the lower mesopelagic and bathypelagic ocean and analyses the relationship of species abundance and composition with downward particle flux. Commencing in 1997, this time-series represents one of the longest records of zooplankton biodiversity data from the deep sea.

Chapter 4 explores the role of copepod carcasses in the downward POC flux of the subantarctic Southern Ocean and highlights the importance of species ecology, including seasonal vertical migration, for estimating carbon export.

Chapter 5 reveals the newly developed research tool ZOOplankton RESPiration in the subsuRface OcEan (ZOORESPIRE) that has been designed to attract zooplankton, using a light source, in the subsurface ocean and measure their respiration as a decline in dissolved oxygen concentration in-situ. This chapter contains the technical description of the device along with results of laboratory and field trials.

Finally, **Chapter 6** synthesises the findings and highlights possibilities for future research in the Southern Ocean carbon cycle.

Figure 1.3: Overview of aims, study area, methodology and carbon pathways covered in chapters 2-6. Abbreviations as follows: ZOOplankton RESPiration in the subsuRface OcEan (ZOORESPIRE), Southern Ocean Time Series (SOTS), biological carbon pump (BCP), biological gravitational pump (BGP), mesopelagic-migrant pump (MMP), seasonal lipid pump (SLP).

	Aims	Study area	Methodology	Carbon pathway
2	**Zooplankton and carbon export** • Comparison of zooplankton communities and carbon export in two regions of the Southern Ocean • What role do zooplankton play in establishing carbon export regimes?	SOTS Kerguelen	Not applicable	CO_2 BGP & MMP & SLP & Respiration
3	**Species composition influence on carbon flux** • Biodiversity data collected with sediment traps since 1997 • Assessment of the relationship between flux parameters and species composition/abundance	SOTS	Sediment trap Laboratory analysis	BGP
4	**The role of carcasses in carbon flux** • Carcass study measuring sinking velocity and microbial decomposition by a subantarctic copepod • How much do zooplankton carcasses contribute to the flux?	SOTS	Fieldwork Laboratory analysis	BGP
5	**Quantifying zooplankton respiration in-situ** • Presentation of the development of a novel research tool, the ZOORESPIRE, which traps zooplankton and measures their respiration in-situ • Description of technical details of the trap and experimental trials	Not applicable	Laboratory analysis Local fieldwork Krill laboratory	CO_2 Respiration
6	**Synthesis and future directions** • Which gaps in knowledge have been addressed in this thesis? • What are the next steps for research on the zooplankton-mediated BCP the Southern Ocean?	Southern Ocean	Not applicable	CO_2 BGP & MMP & SLP & Respiration

Chapter 2

The role of zooplankton in establishing carbon export regimes in the Southern Ocean - a comparison of two representative case studies in the subantarctic region

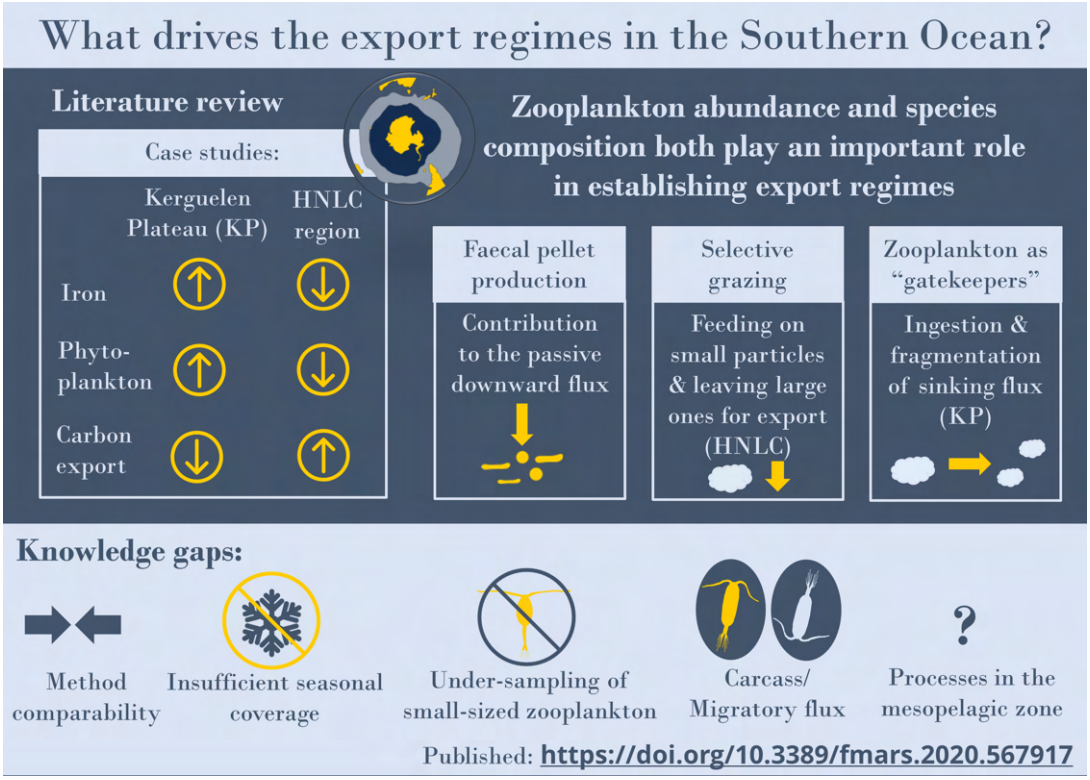

2.1 Abstract

Marine ecosystems regulate atmospheric carbon dioxide levels by transporting and storing photosynthetically fixed carbon in the ocean's interior. In particular, the subantarctic and polar frontal zones of the Southern Ocean are significant regions for physically-driven carbon uptake due to mode water formation, although it is under-studied concerning biologically-mediated uptake. Regional differences in dissolved iron concentrations lead to variable carbon export from the base of the euphotic zone. Contrary to our understanding of export globally, where high productivity often results in high export, naturally iron-fertilised regions exhibit low downward carbon export relative to their surface productivity, while High-Nutrient Low-Chlorophyll (HNLC) waters emerge as significant regions for carbon export. Zooplankton, an integral part of the oceanic food web, play an important role in establishing these main carbon export regimes. In this mini review, we explore this role further by focusing on the impact of grazing and the production of faecal pellets on the downward carbon flux. The data coverage in the subantarctic region will be assessed by comparing two case studies - the iron-replete Kerguelen Plateau and the HNLC region south of Australia. We then discuss challenges in evaluating the contributions of zooplankton to carbon flux, namely gaps in seasonal coverage of sampling campaigns, the use of non-standardized and biased methods and under-sampling of the mesopelagic zone, an important area of carbon remineralisation. More integrated approaches are necessary to improve present estimates of zooplankton-mediated carbon export in the Southern Ocean.

2.2 Introduction

The fixation of inorganic carbon through photosynthesis by phytoplankton, and subsequent export and sequestration to deeper waters, is termed the biological carbon pump (BCP). Without this process, atmospheric CO_2 levels would be 200 ppm higher than they are today (Parekh et al., 2006; Henson et al., 2019), thus the BCP is a critical component of climate regulation. Zooplankton are part of the BCP, via ingestion of lower trophic levels, faecal pellet and carcass production and respiration of CO_2 (Schnack-Schiel and Isla, 2005; Steinberg and Landry, 2017; Turner, 2015). Furthermore, they actively transport carbon below the thermocline during daily migration and seasonal descent to

overwinter at depth (Boyd et al., 2019; Jónasdóttir et al., 2015; Klevjer et al., 2016; Record et al., 2018; Steinberg and Landry, 2017). The role of zooplankton in the BCP is well-studied in some parts of the global ocean, e.g. the North Atlantic and the oxygen minimum zones in the Pacific (Cavan et al., 2017b; Jónasdóttir et al., 2015), however, is less understood in the Southern Ocean.

The Southern Ocean plays a significant role in the functioning of the Earth system (Lumpkin and Speer, 2007; Mayewski et al., 2009), and provides important ecosystem services, such as climate regulation and nutrient recycling (MEA, 2005). The region between the Subtropical Front and the Polar Front encompasses a large area of the Southern Ocean (hereafter called the "subantarctic region") and represents an important carbon sink, as the formation of intermediate and mode waters in this region contributes notably to the sequestration of atmospheric CO_2 (Eriksen et al., 2018; Sabine et al., 2004; Orsi et al., 1995). Large parts of the subantarctic region are characterised by HNLC conditions: low dissolved iron concentrations in surface waters limit the uptake of macronutrients, such as phosphate and nitrate, and hence, restrict phytoplankton growth (Bucciarelli et al., 2001; Trull et al., 2001).

In contrast, naturally iron-fertilized regions such as downstream of the Kerguelen Plateau, in the Indian sector of the Southern Ocean, are characterized by high primary production (Cavagna et al., 2015; Mosseri et al., 2008). However, high production does not always equate to high carbon export as estimated from global models (e.g. Dunne et al., 2005; Laws et al., 2011) or sediment trap data (e.g. Marsay et al., 2015). Many reported an inverse relationship between primary production and export efficiency for the Southern Ocean (e.g Cavan et al., 2015; Laurenceau-Cornec et al., 2015; Le Moigne et al., 2016; Maiti et al., 2013), which can be found at our study sites as well. While the Kerguelen Plateau is characterized as a High-Biomass Low-Export (HBLE) region, the HNLC waters exhibit a relatively high carbon export below the mixed layer (Ebersbach et al., 2011; Lam and Bishop, 2007; Rembauville et al., 2015a; Trull et al., 2001). This mini review aims to understand the role that zooplankton play in establishing the characteristic carbon export regimes in the Southern Ocean by grazing on lower trophic levels and forming and repackaging sinking particles (Lam and Bishop, 2007). After a summary of the current state of knowledge, we also list contemporary knowledge gaps and propose future research priorities.

2.3 Two contrasting downward export regions

The Kerguelen Plateau, located on the 70°E meridian, forms a naturally iron-fertilized region in the Polar Frontal Zone (PFZ) at the border of the Antarctic zone, with dissolved iron concentrations ranging from 0.45 to 0.7 nM in spring, decreasing to 0.09 nM in late summer due to phytoplankton growth (Table 2.1) (Blain et al., 2001, 2008). This review focuses on the northern Kerguelen Plateau, which is separated from the southern part by the Fawn Trough at around 56°S (Koubbi et al., 2016; Park et al., 2014). The seafloor topography forces the Antarctic Polar Front to pass above the plateau south of the Kerguelen Islands, which introduces iron from the sediments (Blain et al., 2001), and leads to intensive seasonal phytoplankton blooms downstream of the plateau, with peaks of more than 2.5 mg Chl *a* m^{-3} (Blain et al., 2007, 2013; Rembauville et al., 2015a; Schallenberg et al., 2018). Blooms over the shallow plateau last the whole summer, while the bloom period over deep waters is only observed in spring for 1 month (Schallenberg et al., 2018). The dominating phytoplankton are diatoms and dinoflagellates (Armand et al., 2008; Christaki et al., 2008, 2015; Lasbleiz et al., 2016). The zooplankton community consists of large and medium-sized calanoid copepods and small copepods in the family Oithonidae (Figure 2.1) (Carlotti et al., 2015). Non-copepod taxa account for 4-8% of the total zooplankton community, though pteropods can be abundant over the shelf (Carlotti et al., 2015, 7-12% of total abundance). Although the biomass in the pelagic ecosystem is high, the export flux is generally low (<0.5 mmol POC m^{-2} d^{-1}, 289 m depth), except for short-lived (<14 days) export pulses in summer (up to 1.6 mmol m^{-2} d^{-1}) (Rembauville et al., 2014). Hence, the Kerguelen Plateau is considered to be an HBLE environment (Lam and Bishop, 2007; Rembauville et al., 2014).

In comparison to the Kerguelen Plateau, the HNLC waters south of Australia exhibit lower dissolved iron concentrations and phytoplankton biomass, but relatively higher downward particulate organic carbon (POC) export flux (Table 2.1). We focus on the region around the Southern Ocean Time Series (SOTS) site at 142°E and 47°S, which is representative of a broad HNLC region of the Subantarctic Zone (SAZ) between 90°E

and 140°E (Sedwick et al., 1999; Shadwick et al., 2015). Phytoplankton growth is limited by low dissolved iron (0.05-0.11 nM in summer/autumn and insufficient light conditions due to high cloud cover (Cassar et al., 2011; Sedwick et al., 1999). The phytoplankton community is dominated by nanoplankton and picoplankton, coccolithophorids and other prymnesiophytes (such as *Phaeocystis antarctica*), cyanobacteria and autotrophic flagellates (Trull et al., 2001; Kopczynska et al., 2001; Odate and Fukuchi, 1995; Eriksen et al., 2018). Diatoms are mostly lightly silicified pennate diatom species rather than centric forms (de Salas et al., 2011). Phytoplankton biomass is low throughout the year, with chlorophyll *a* values generally below 0.6 mg m^{-3} (Trull et al., 2019). This has implications for zooplankton, which is dominated by the copepod *Oithona similis*, foraminiferans, and appendicularians (Hunt and Hosie, 2006), rather than a community of calanoid copepods that are not able to accumulate enough resources to complete their life cycles. During summer, a small number of species of calanoid copepods, along with the pteropods *Limacina* spp. and regionally large blooms of the salp *Salpa thompsoni*, are also observed (Figure 2.1) (Hunt and Hosie, 2006). Though primary production is low in surface waters, the total flux of POC is relatively high, e.g., 3.3 ± 1.8 mmol POC m^{-2} d^{-1} at 150 m water depth, measured with free-drifting PPS 3/3 sediment traps (Ebersbach et al., 2011).

Table 2.1: Comparison of environmental parameters and planktonic groups between the HBLE Kerguelen Plateau and the HNLC waters south of Australia. Examples of downward carbon flux and e-ratios in the two regions are also given. The POC fluxes are estimated from polyacrylamide gel traps at 200 ± 10 m and 240 m depth on the Kerguelen Plateau and in the HNLC region, respectively. The e-ratio is an indicator for export efficiency and is calculated as the ratio between POC flux and primary productivity. Note that Laurenceau-Cornec et al. (2015) use net primary productivity in the euphotic zone to calculate the e-ratio, while Ebersbach et al. (2011) use gross primary productivity.

Parameter	Kerguelen Plateau	HNLC waters
Dissolved iron levels	0.45 nM (spring), 0.09 nM (summer) (1)–(2)	0.05-0.11 nM (summer/autumn) (3)
Phytoplankton biomass	High (>2.5 mg Chl *a* m^{-3}) (4)	Low (<0.6 mg Chl *a* m^{-3}) (5)
Dominant phytoplankton	Diatoms & dinoflagellates (6)–(9)	Coccolithophorids & other prymnesiophytes, cyanobacteria, autotrophic flagellates & pennate diatoms (10)–(14)
Dominant zooplankton	Large and medium-sized calanoid copepods, Oithonidae, pteropods (15)	*Oithona similis*, foraminiferans, appendicularians, calanoid copepods, pteropods & salps (16)
POC fluxes	66 mg C m^{-2} d^{-1} (17) (*a*)	127.2 mg C m^{-2} d^{-1} (18)
e-ratio	0.03 (17) (*a*)	0.16 (18) (*b*)

(1) Blain et al. (2001), (2) Blain et al. (2008), (3) Cassar et al. (2011), (4) Blain et al. (2007), (5) Trull et al. (2019), (6) Armand et al. (2008), (7) Christaki et al. (2008), (8) Christaki et al. (2015), (9) Lasbleiz et al. (2016), (10) Trull et al. (2001), (11) Kopczynska et al. (2001), (12) Odate and Fukuchi (1995),. (13) Eriksen et al. (2018), (14) de Salas et al. (2011), (15) Carlotti et al. (2015), (16) Hunt and Hosie (2006), (17) Laurenceau-Cornec et al. (2015), (18) Ebersbach et al. (2011).
(*a*) High phytoplankton biomass site (A3-2), (*b*) SOTS site

2.4 Contributions of zooplankton to downward carbon flux in the subantarctic region

2.4.1 The northern Kerguelen Plateau

On the Kerguelen Plateau, zooplankton biomass increases 4-fold from winter (July-August) to mid-summer (February) (Carlotti et al., 2015; Razouls et al., 1996; Semelkina, 1993). This is caused by (1) seasonal ontogenetic migrations by large calanoid copepods, such as *Rhincalanus gigas* and *Calanoides acutus*, which spend winter in diapause in deeper waters and ascend to surface in spring and (2) an increase in other species, e.g. *Calanus simillimus* and the smaller *Oithona* spp., that resume their population development from survivors of previous years to start reproduction in spring following the phytoplankton bloom (Carlotti et al., 2015; Schnack-Schiel, 2001; Atkinson, 1998). Remarkably, mesozooplankton (200 μm - 20 mm) consume only a small fraction of the phytoplankton biomass directly; e.g. Sarthou et al. (2008) measured a low ingestion of 1-10% of total Chl *a* d^{-1} by copepods in summer. In contrast, they are known to control protist growth by grazing (Carlotti et al., 2008). Heterotrophic protists, such as ciliates and some dinoflagellates in turn reduce the standing stock of pico- and nanophytoplankton and diatoms through grazing (Calbet, 2008; Calbet and Landry, 2004; Peloquin et al., 2011; Quéguiner, 2013). The grazing pressure by mesozooplankton on protozooplankton releases the top-down control on diatoms and favors phytoplankton blooms dominated by large diatoms (Carlotti et al., 2015; Henjes et al., 2007).

Additionally, zooplankton ingest and fragment particles, which enhances subsequent microbial respiration and increases the recycling of nutrients, e.g. iron (Sarthou et al., 2008) and ammonium (Mosseri et al., 2008). Grazing not only affects nutrient levels in surface waters but also the efficiency of carbon transfer (Dagg et al., 2014). The omnivorous and detritivorous zooplankton community acts as a "gate-keeper" in the mesopelagic zone (Figure 2.1): They ingest and fragment phytoplankton aggregates and faecal pellets that are quickly remineralised and retained in the surface layer (Dagg et al., 2014; Iversen and Poulsen, 2007; Quéguiner, 2013). Predominantly omnivorous and detritivorous copepod species in the genera *Oithona* and *Oncaea/Triconia* link the classical food web to the microbial loop (Atkinson, 1998; Pasternak et al., 2009). This efficient transfer of carbon to

higher trophic levels or the microbial loop in surface waters leads to low export flux during most of the year and establishes the HBLE characteristics on the Kerguelen Plateau (Rembauville et al., 2015a, 2014). Despite the dominance of the downward carbon flux by faecal pellets in early spring (56 ± 19% of total carbon flux, 200 m depth Laurenceau-Cornec et al., 2015), the faecal pellet flux decreases rapidly with depth, while diatom resting spores (resistant to grazing Davis et al., 1980; Salter et al., 2012; Smetacek, 1985) and detrital aggregates dominate the deeper flux at 289 m depth (Cavan et al., 2019b). This indicates preferential reprocessing and remineralisation of faecal material over other particles in the mixed layer and upper mesopelagic, which leads to a lower faecal pellet flux similar to other iron-fertilized regions, e.g. South Georgia (Cavan et al., 2015; Rembauville et al., 2015a; Blain et al., 2013).

2.4.2 HNLC waters south of Australia

The dominance of protozooplankton, small copepods and patchy salp blooms in HNLC waters, rather than a diverse and abundant mesozooplankton community as on the northern Kerguelen Plateau, results in control of the low phytoplankton biomass by protist grazing, and efficient remineralization of carbon and nutrients in the upper water column (Figure 2.1) (Atkinson et al., 2004; Landry et al., 2002; Mayzaud et al., 2002; Pakhomov et al., 2002). Considering the omnivorous and detritivorous diet of *Oithona similis* (Takahashi et al., 2010), it would be expected that the POC export out of the epipelagic zone would be low, as ingestion and fragmentation of sinking particles increase the particle flux attenuation. However, studies such as Sensitivity of the sub-Antarctic zone to environmental change (SAZ-Sense) in January/February 2007 have shown a relatively high POC transfer efficiency out of the mixed layer in the HNLC waters around SOTS, in comparison to other sites in the Subantarctic Zone (SAZ) with higher dissolved iron levels or in the PFZ with a diatom-dominated phytoplankton community (Ebersbach et al., 2011). Even though the POC concentration was low at the surface (5.2 ± 0.9 mmol m^{-2} d^{-1}), the carbon export flux at SOTS was highest in both gel traps (8.1 mmol m^{-2} d^{-1} at 290 m water depth) and PPS 3/3 sediment traps (3.3 ± 1.8 mmol m^{-2} d^{-1} at 150 m water depth) (Ebersbach et al., 2011).

The two main differences from the Kerguelen Plateau that cause the higher relative and

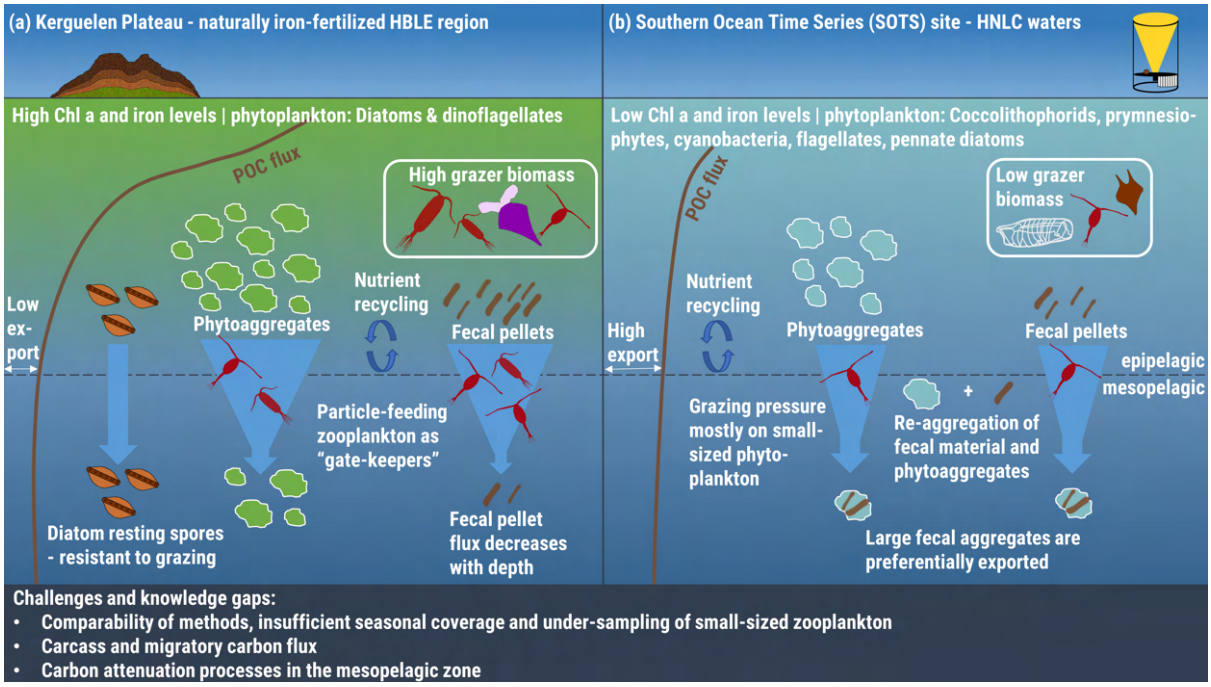

Figure 2.1: The zooplankton-mediated carbon cycle in summer on the naturally iron-fertilized Kerguelen Plateau (panel a) compared to the HNLC waters around SOTS (panel b). On the Kerguelen Plateau, high dissolved iron levels promote high chlorophyll *a* levels as a proxy for algal biomass at the surface. The diverse zooplankton community feeds on the sinking particle flux and acts as a "gate-keeper" to the deeper ocean by ingesting and fragmenting sinking particles and, consequently, significantly reducing the export flux out of the epipelagic. The main downward export particles are diatom resting spores, which bypass the intense grazing pressure, followed by faecal pellets. At SOTS, dissolved iron levels are lower than on the Kerguelen Plateau, but support a more diverse phytoplankton community, but with lower biomass, which, in turn, affects zooplankton community composition and biomass. The grazing pressure during summer is focused mostly on picoplankton, while larger particles are exported directly. Grazing and fragmentation of particles at both sites increases nutrient recycling in the upper water column. Challenges and knowledge gaps in aspects of the zooplankton-mediated carbon pump are highlighted.

total export flux in HNLC waters are the community composition and size-partitioning of zooplankton (Figure 2.1). The dominant microzooplankton (20-200 µm) and heterotrophic nanoflagellates at SOTS can consume 82% of the primary production per day in summer (Pearce et al., 2011). This is in line with Trull et al. (2019), who estimated a 10-fold higher grazing pressure in December compared to September as a function of zooplankton biomass. This grazing pressure focuses mostly on the picoplankton size fraction (0.2 - 2 μm), which leaves phytoplankton aggregates and other large particles for export

below the mixed layer (Pearce et al., 2011). Omnivorous and detritivorous copepods are not as abundant as on the Kerguelen Plateau, which limits their abilities to efficiently reduce the sinking flux. Consequently, more particles (11-53% of the primary production Jacquet et al., 2011) are exported from HNLC surface waters (Figure 2.1), predominantly as faecal aggregates (pellets and faecal material reaggregated with phytodetritus Ebersbach and Trull, 2008; Laurenceau-Cornec et al., 2015).

Our findings indicate that species composition and size-partitioning of zooplankton are important factors in modifying the downward carbon flux and establishing a regime of low biomass at the surface but with relatively high carbon transfer efficiency. Hence, zooplankton play a more important role in the export regimes in the subantarctic region than previously thought. However, common algorithms to estimate the carbon export efficiency in the Southern Ocean, such as by Arteaga et al. (2018) or Britten et al. (2017), only include temperature, net primary production or silicate concentration and do not contain a zooplankton term. In contrast, our findings show that zooplankton, while being influenced by their physical environment and food availability, also control lower trophic levels and carbon export efficiency. Future research efforts should therefore focus on including zooplankton in the algorithms, for example as size fractions or a proportion of trophic mode (e.g. ratio between zooplankton herbivory versus detritivory zooplankton), and improve our estimation of carbon uptake by the Southern Ocean.

2.5 Challenges and knowledge gaps

2.5.1 Comparability of methods, under-sampling of small-sized zooplankton and insufficient seasonal coverage

Different methodologies make it difficult to compare the zooplankton species composition and biomass between the subantarctic regions. Ship-based net deployments are temporally and spatially limited, but provide higher vertical resolution in the water column, while the Continuous Plankton Recorder (CPR) covers a large geographical area but only provides surface data and under-samples the vertical migrating community during the day (Carlotti et al., 2015, 2008; Dippner and Krause, 2013). Acoustic data provides information on distribution and biomass of certain size fractions over the whole annual

cycle, but cannot provide species composition data (Trull et al., 2019). It is also important to note that both the CPR (silk mesh size 270 μm) and standard zooplankton nets with a mesh size of >200 μm are known to under-sample smaller-sized zooplankton, e.g. Oithonidae and copepodite stages (Gallienne and Robins, 2001) that dominate the community in HNLC waters. Finally, limited access to the subantarctic region due to logistical constraints results in a lack of winter data, as the sampling campaigns by research and supply vessels are mostly focused on the summer season.

2.5.2 Understudied carbon pathways – zooplankton carcass and migratory flux

As the literature on other high latitude systems suggests, zooplankton carcass flux can be a seasonally significant contribution to total carbon flux (Daase et al., 2014; Sampei et al., 2012; Tang et al., 2014). However, data on drivers and rates of mortality and carcass flux from the Southern Ocean are currently not available. The lack of data could lead to an underestimation of downward carbon flux, especially in the HNLC waters, where fast-sinking salp blooms could significantly increase the downward carbon flux as "jelly falls", e.g. by 330% in the Tasman Sea further north (Henschke et al., 2013). Similarly, active transport of carbon by zooplankton, both by diel and seasonal vertical migrators, is not well understood. Translating the seasonal changes in the distribution of acoustic scattering layers into transported carbon is not possible without information on species composition (Trull et al., 2019).

2.5.3 The "black box": the mesopelagic zone

The transfer efficiency of organic matter through the mesopelagic (200-1000 m depth) is driven by plankton species composition in the epi- and mesopelagic (Lam et al., 2011). Studies such as Liszka et al. (2019), Manno et al. (2015) and Marsay et al. (2015) suggest that vertical distribution of zooplankton, community composition, and feeding behavior, along with temperature in the mesopelagic, are important in shaping the downward carbon flux. However, mesopelagic processes, such as respiration and remineralisation of organic material and food web interactions, are not well understood (Robinson et al., 2010). Sampling campaigns in both regions rarely include the mesopelagic: while zoo-

plankton studies on the Kerguelen Plateau focus on the upper 300 m of the water column, zooplankton data in the HNLC waters around SOTS were either collected from surface waters or from deeper, moored sediment traps. To increase our understanding of interactions between mesopelagic zooplankton, protists and bacteria, and their influence on particle formation and remineralisation, future sampling campaigns need to focus on the mesopelagic.

2.6 Conclusion and outlook

Zooplankton play an important role in the downward carbon flux of both subantarctic regions. On the Kerguelen Plateau, grazing by the mesozooplankton community limits protozooplankton growth, which releases the grazing pressure on phytoplankton. Zooplankton also fragment particles, leading to increased nutrient recycling, and contribute to the carbon flux by producing faecal pellets. High rates of omnivory and detritivory result in a low export flux and establish the HBLE conditions on the plateau. In contrast, the dominance of smaller-sized zooplankton and heterotrophic protists in HNLC waters leads to high grazing pressure on picoplankton, which leaves large aggregates and faecal pellets for export. The lower total abundance of detritus-feeders results in a larger export of faecal aggregates. Knowledge gaps, resulting from limited seasonal coverage, non-standardization and bias of methods between sampling campaigns, and under-sampling of the mesopelagic zone, impede our understanding of zooplankton-mediated carbon flux, especially of the carcass and migratory flux. To predict future changes in marine carbon storage efficiency, it is important to focus research efforts on the zooplankton-mediated carbon flux. The inclusion of, for example, zooplankton size fractions or trophic modes in algorithms can refine predictions of carbon export in the Southern Ocean. More integrated research approaches, e.g. using the network of biogeochemical Argo floats in combination with stationary moorings (e.g. Rembauville et al., 2017; Trull et al., 2019), are necessary to improve inter-seasonal and spatial data coverage of the Biological Carbon Pump in the Southern Ocean.

Chapter 3

What over 20 years of zooplankton swimmer data can tell us about ecosystem variability and carbon export in the subantarctic Southern Ocean

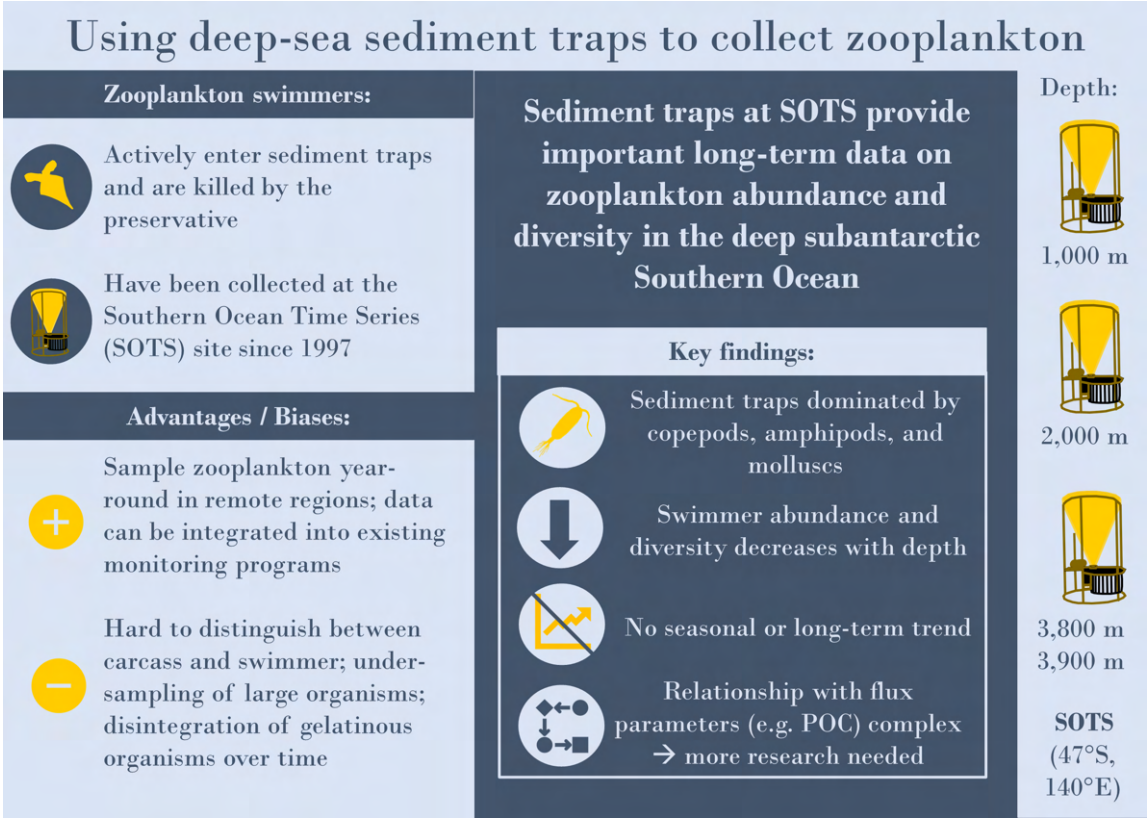

3.1 Abstract

Despite playing an important role in the food webs and carbon cycle of the Southern Ocean, zooplankton biodiversity and dynamics in subsurface waters remain largely understudied. Our understanding of temporal variability in the zooplankton community is hampered by logistical constraints that come with working in this remote oceanic region. In this chapter, I present a multi-decadal time-series of zooplankton swimmers intercepted by moored sediment traps at 1000, 2000, and 3800/3900 m depth; tools that are usually used to measure time-series in downward particle flux. In contrast to passive sinking particles, swimmers are organisms that actively enter the traps and are immediately preserved. At the Southern Ocean Time Series (SOTS) site (47°S, 140°E) in the subantarctic zone, sediment traps have been deployed in the meso- and bathypelagic zone since 1997, resulting in one of the longest time-series for deep-sea zooplankton. Analysis of the archive from 1997-2020 indicates that the zooplankton community was dominated by copepods, amphipods, and molluscs (mainly pteropods), and their abundance and diversity decreased with depth. For most taxa, no significant seasonal increase in abundance during summer was found. Generalised Additive Models showed that the relationship between species abundance and diversity and the flux parameters (PC, POC, PIC, PN, and BSi) is significant, although non-linear in most cases. Hence, additional drivers for species abundance and diversity need to be considered to explain these trends. Finally, I present biases associated with sediment traps if they are to be used to collect deep-sea zooplankton data, along with a discussion of opportunities for future integration of sediment traps into zooplankton monitoring programs and using swimmers as indicators of future ecosystem change in the subantarctic Southern Ocean.

3.2 Introduction

The Southern Ocean plays an important role in the Earth's climate system. Although it occupies 30% of the global ocean surface area, it is responsible for the uptake of 43% ± 3% of anthropogenic carbon dioxide (CO_2) and 75% ± 22% of excessive heat (Frölicher et al., 2015). The Subantarctic Zone (SAZ) encompasses >50% of the Southern Ocean (Orsi et al., 1995). It is characterised by HNLC conditions, with low year-round primary production despite high concentrations of nitrate and phosphate (Bucciarelli et al., 2001).

For the phytoplankton, this is caused by silicate and iron limitation (Blain et al., 2001) and light limitation due to deep winter mixing (Bucciarelli et al., 2001; Trull et al., 2001). However, the Subantarctic Zone (SAZ) is an important oceanic carbon sink (Shadwick et al., 2015; Wynn-Edwards et al., 2020), driven by physical dissolution, i.e. the solubility pump (Marinov et al., 2006; Wilks et al., 2017; Trull et al., 2001), and by carbon fixation by phytoplankton and subsequent downward particle export, i.e. the biological carbon pump (BCP). While the significance of the SAZ for oceanic carbon and heat storage is widely accepted, research on the efficiency of the biological pump is still limited by logistical challenges caused by the region's remoteness (Trull et al., 2010).

To overcome logistical restrictions in observations of biogenic downward flux, sediment traps have been deployed to investigate the time-series of composition and temporal variability in particle flux (Trull et al., 2001; Buesseler et al., 2007a). In other regions of the global ocean, for example in the Mediterranean Sea and Monterey Bay, they were also used as a tool to understand interseasonal and interannual changes in zooplankton species composition (Danovaro et al., 2017; Howard et al., 2011; Matsuno et al., 2015; Michaels et al., 1990). The zooplankton community performs an important role in the BCP by ingesting and fragmenting sinking particles, repacking material into fast-sinking faecal pellets, and performing vertical migrations, which actively pump carbon into the deep-sea (Steinberg and Landry, 2017; Turner, 2002, 2015). Therefore, zooplankton abundance and biodiversity affect and control processes such as POC attenuation and sequestration (Cavan et al., 2019b; Liszka et al., 2019; Steinberg and Landry, 2017; Stukel et al., 2019).

Zooplankton "swimmers", i.e. zooplankton that actively enter the sediment trap and are immediately preserved, have been largely seen as contamination, as they can increase the downward carbon flux estimation by ∼87% (Ivory et al., 2014) and are usually removed prior to particle analysis (Danovaro et al., 2017; Karl and Knauer, 1989; Knauer et al., 1979; Lee et al., 1992). In contrast, swimmer abundance and biodiversity can serve as indicators for a changing environment (Danovaro et al., 2017). Total numbers and relative species richness varies over season and between years, depending on zooplankton abundance in the water column, their behaviour and characteristics, sinking rates, hydrodynamic features, such as underwater currents (Danovaro et al., 2017; Harbison and Gilmer, 1986; Peterson and Dam, 1990), as well as general location and depth of the trap (Matsuno et al., 2015; Romano et al., 2017), trap design and preservative used

(Kraft et al., 2010). Therefore, the species composition and abundance of zooplankton swimmers provide insight into temporal dynamics and ecology in addition to changes in environmental conditions, both at the surface and at depth.

The aims of this chapter are:

- A description of **swimmer abundance and diversity** data from the deep-sea (1000, 2000, and 3800/3900 m depth) sediment trap array at SOTS as a baseline of deep-sea zooplankton diversity. In particular, I focus on copepods, amphipods, and molluscs, the most abundant groups in this region of the SAZ. In addition, I aim to establish potential indicators to detect environmental change.

- An analysis of the impact of downward **particle flux** on zooplankton species composition and abundance.

3.3 Methods

3.3.1 Sample collection at SOTS

The SOTS site is a sub-facility of the Australian Integrated Marine Observing System (IMOS). As part of SOTS, the SAZ sediment trap mooring is deployed at around 47°S and 140°E and has been serviced regularly since September 1997. The time-series spans >20 years, with partial records from the late 1990s to an almost complete coverage from 2009 until present. The McLane PARFLUX conical sediment traps are equipped with a 0.5 m^2 baffled funnel at the top and a carousel of cups (either 13 or 21) that rotates over the course of the deployment (usually 12 months). Cups are open between 4 and 60 days. The sediment traps are deployed at depths of 1000, 2000, 3800 or 3900 m, except in the year 2003 (500, 1000, and 2000 m). The moorings are also equipped with current meters to detect under-sampling due to high subsurface currents. Data gaps were caused by sediment trap failures (year 2005 - only 1000 m and 2000 m recovered), mooring loss (2001, 2004, 2006), vessel unavailability and insufficient trap material. The mooring was not deployed at SOTS in 2007, 2008, 2014 and 2017, resulting from by the lack of ship time or funding. Additional information on moorings and deployment

voyages are given in the SOTS Annual Reports, accessible on Research Data Australia (https://researchdata.edu.au/) (Wynn-Edwards et al., 2020).

3.3.2 Sediment trap preparation and post-recovery handling

Before deployment, the sediment trap cups were filled with a brine solution (0.8 μm GF/F filtered seawater and 5 g L^{-1} NaCl) to increase density and improve particle retention, as well as 2 g L^{-1} $Na_2B_4O_7$ $10H_2O$ to buffer pH and reduce carbonate dissolution, 0.22 g L^{-1} $SrCl_2$ $6H_2O$ for preservation of acantharian radiolarians and 3 g L^{-1} $HgCl_2$ as biocide. After mooring recovery, the sediment traps were washed with fresh water and material in the cups was allowed to settle for several days. Approximately 20% of supernatant was removed from each cup to reduce the risk of spillage. The cups were then closed and stored in the dark until transport to the laboratory refrigerator onshore, where material was allowed to settle for at least 3 days.

3.3.3 Sample processing and swimmer identification

Before processing, a photograph was taken to document fragile material in the cups. The supernatant was sampled for pH and salinity measurements and discarded. Then, material was resuspended and transferred onto a 1 mm nylon sieve to remove the zooplankton swimmers from the particulate fraction. Where faecal pellets were present, a photograph was taken, and they were rinsed through the sieve with buffered seawater and photographed again. Swimmers were stored in buffered filtered seawater, re-poisoned if necessary to avoid degradation during storage, and archived at 4°C. The remaining fraction (<1 mm) was analysed for particulate carbon (PC), particulate organic carbon (POC), particulate inorganic carbon (PIC), particulate nitrogen (PN), and Biogenic Silica (BSi), as described in Wynn-Edwards et al. (2020). Zooplankton swimmers were identified under a Zeiss binocular stereo-microscope (5-fold magnification) to species level (amphipods, pteropods, and euphausiids), family or species level if possible (copepods, fish), or broader taxonomic group (ostracods, peracarid decapods, chaetognaths, tunicates, cnidarians, and ctenophores). In samples from 1997-2005, fish were not stored together with the remaining swimmers, however, identifications could be made based on the cup pictures (accessible at http://imos-data.s3-website-ap-southeast-2.amazonaws.

com/?prefix=IMOS/DWM/SOTS/images/). If the copepods were intact, their prosome length was measured using a microscale. Afterwards, samples were washed back into the cups with buffered filtered seawater from SOTS and archived at 4°C. In this study, only traps from 1000 m, 2000 m and 3800/3900 m water depth were considered. Hence, 2008-2009 data were not analysed as the mooring was established at 45°S instead of at 47°S and, in 2003-2004, the shallowest trap at 500 m was excluded from the analysis.

3.3.4 Data treatment and available data sets

To account for varying opening times of the cups, the swimmer abundances were converted into swimmer flux (individuals m^{-2} d^{-1}), with the trap open surface area being 0.5 m^2 and the sampling interval as the time between the cup opening and closing (between 10-60 days, on average approx. 18 days).

$$\text{Swimmer flux } (ind.\, m^{-2} d^{-1}) = \frac{\text{Swimmer count}}{\text{Trap mouth area } (m^2) \times \text{Sampling interval } (d)} \tag{3.1}$$

Some trap content was difficult to quantify, including:

- Fragile objects, such as fragments of tunicates and other gelatinous material, faecal pellets, and degraded material. Although they potentially entered the trap intact, they disintegrated due to handling and extended storage time.
- Abundant objects that were stuck to larger marine snow particles, e.g., foraminiferans that were attached to marine snow and could not be separated by sieving even though they belonged to the <1 mm fraction.
- Parts of organisms, e.g., fish otoliths, scales, spines, or fish bones, as it was difficult to estimate total species abundance based on these objects.
- Juvenile amphipods that entered the traps inside the brood pouches of female amphipods, for example the species *Pegohyperia princeps*.
- and other objects, such as acantharian colonies.

The abundance of the above object per cup was separated into the following categories: "+" 1-2 observations, "++" 3-5 observations and "+++" >5 observations. Although these categories were only semi-quantitative, the resulting dataset gives useful background knowledge about the trap samples, e.g., presence-absence data for fragile gelatinous zooplankton. Data and code for analysis are freely accessible on GitHub (https://github.com/SvenjaHalfter/SOTSswimmer).

3.3.5 Data analysis and statistics

For analysis of the swimmer abundance and biodiversity, the midpoint date of the collection period between opening and closing date was used to display data over year and season. As the peak downward particle flux season was found to be mid-September to mid-March (Wynn-Edwards et al., 2020), the annual cycle was defined as being between June 1 until May 31 in the following year. Seasons were defined as winter (June 1 - August 31), spring (September 1 - November 30), summer (December 1 - February 28/29) and autumn (March 1 - May 30). All data were processed in R (version 4.1.0). Using the packages ncdf4 (Pierce, 2019) and lubridate (Grolemund and Wickham, 2011), the sampling periods and corresponding flux parameters (PC, POC, PIC, PN and BSi) were extracted from the netcdf files. Tidyverse (Wickham, 2017), including the tidyr, dplyr and ggplot2, ggrepel (Slowikowski, 2021), voxel (Garza et al., 2018) and reshape2 packages (Wickham, 2007) were used for data manipulation, analysis and visualisation. Cowplot (Wilke, 2019), (Auguie, 2017), and the pals colours palette (Wright, 2019) improved data visualisation. The General Additive Models (GAM) and other statistical tests, as well as the diversity and evenness indices were performed and calculated using vegan (Oksanen et al., 2020) and (Wood, 2011).

The zooplankton species diversity and evenness were calculated using the Shannon-Wiener information function (H', with log base 2) (Shannon and Weaver, 1949) and Pilou's Evenness (Pielou, 1975) in the vegan package (Oksanen et al., 2020). Both were calculated for broad taxonomic groups (e.g. "Copepods", "Amphipods", etc.). An Analysis of Similarities (ANOSIM) tested the null hypothesis that there were no differences in species abundance between water depths, seasons, and years. In addition, if the Analysis of Similarities (ANOSIM) showed significant differences, a pairwise non-

parametric Kruskal-Wallis with a Dunn's post-hoc test was performed to explore which taxa were responsible for the significant difference. Similarly, Kruskal-Wallis and Dunn's tests compared species diversity between depths, seasons, and years.

To explore whether samples could be grouped according to seasons or depth, an ordination was produced via non-metric multi-dimensional scaling (nMDS). Prior to analysis, the species abundance data were square-root transformed to avoid highly abundant species dominating the results. A Bray-Curtis resemblance matrix was then produced (Bray and Curtis, 1957; Clarke, 1993). Bray-Curtis is preferred when working with ecological data with many absent (0) species per sample (Bray and Curtis, 1957). As comparison, a Permutational Multivariate Analysis of Variance (PERMANOVA) was performed on both the transformed and un-transformed species abundance. The PERMANOVA included depth (fixed factor, 3 levels) and season (random factor, 4 levels) and sampling years (fixed factor, 18 levels) and was carried out using a Bray-Curtis resemblance matrix as above, with 999 permutations. To explore the relationship between species abundance and biodiversity, and flux parameters, the environmental parameters were normalised by their standard deviations. Then, a Canonical Analysis of Principal coordinates (CAP) was applied, again, with a Bray-Curtis resemblance matrix and using season and depth as factors. In addition, GAM were fitted (family=Gaussian, link=identity) with each taxon separately to identify environmental drivers of taxon abundances and diversity. Other distributions were tested as well (i.e., Poisson and negative binomial), however, as the R^2 and the percentage of deviance explained were lower compared to the Gaussian and, hence, the results from other distributions are not shown here. The GAM were fitted using smoothing terms. If the GAM results indicated a linear relationship between a parameter and either species abundance or diversity as the response variable, the smooth function was removed to explore if the relationship was positive or negative. Moreover, GAM without smoothing functions were fitted (family=Gaussian, link=identity), which are essentially Generalised Linear Models (GLM) to find the model that explained most deviance.

3.4 Results

3.4.1 Variability in swimmer composition with depth

Overall, 25,769 individual zooplankton swimmers were collected in the sediment traps at SOTS between September 1997 and April 2020. Total abundance decreased with depth: while 17,569 individuals were counted at 1000 m (68%), approximately 24% (6164 individuals) and 8% (2036 individuals) were collected at 2000 m and at 3800/3900 m, respectively. Consequently, the swimmer flux was highest at 1000 m (0-39.4 ind. m^{-2} d^{-1}, mean 7.0 ± 6.3 ind. m^{-2} d^{-1}), decreased at 2000 m (0-10.1 ind. m^{-2} d^{-1}, mean 2.7 ± 1.5 ind. m^{-2} d^{-1}) and was lowest in the deepest trap (0-3.6 ind. m^{-2} d^{-1}, mean 0.9 ± 0.6 ind. m^{-2} d^{-1}).

Additionally, the species composition changed with depth (Table 3.1). The shallowest trap was dominated by copepods in the families Calanidae, Scolecitrichidae, Metridinidae and Eucalanidae followed by amphipods, molluscs (mainly pteropods of the species *Limacina helicina antarctica* and *Clio* spp.), ostracods, and chaetognaths (see Table 3.4 for the dominating families and species). In the traps at 2000 m, amphipods decreased in importance, while copepods, especially the families Calanidae, Eucalanidae, Aeteideae and Oncaeidae, remained the dominant taxon. At 3800/3900 m, molluscs (mainly *L. helicina antarctica*) dominated the species abundance, followed by copepods, amphipods, ostracods, and ctenophores. Most of the groups decrease in abundance with depth, except brittle stars (Ophiuridea, Echinodermata), which were collected in slightly higher numbers at 2000 m (22 ind. in total) compared to 1000 (12 ind.) and the deepest depth (11 ind.). The ANOSIM on square-root transformed abundance data revealed a significant difference in species abundance between 1000 and 3800/3900 m, 2000 and 3800/3900 m, and between 1000 and 2000 m (global R= 0.44, R= 0.32, and 0.20, $p<0.01$). This was supported by nMDS, where there was a clear distinction between the different depth groups despite some overlap (Figure 3.1) and the PERMANOVA, which showed depth was the most important factor explaining variability in species abundance (R^2 0.30, $p<0.01$). The Kruskal-Wallis tests, performed for each taxon separately, showed that only the taxa ophiurids, fish, euphausiids, decapods, and ctenophores did not significantly differ in abundances between depths ($p<0.01$), while all other taxa, including the total sum of swimmers in each trap, varied significantly between depths.

The species diversity changed significantly between sediment trap depths (Figure 3.1e and Table 3.2). The pairwise Kruskal-Wallis tests with Dunn's post-hoc test indicated that diversity was similar at 1000 and 2000 m (1.93 ± 0.89 and 1.94 ± 0.67, respectively), but decreased significantly in the deepest trap (1.30 ±0.59). Moreover, the species evenness slightly increased with depth from 0.79±0.23 at 1000 m to 0.87±0.18 at 3800/3900 m (Table 3.2). Both species diversity and evenness were highly variable between samples, years, and season in each trap.

Table 3.1: Total numbers of organisms identified from sediment traps at 1000, 2000 and 3800/3900 m depth between September 1997 and April 2020. UI: unidentified.

1000 m	**Total**	**2000 m**	**Total**	**3800/3900 m**	**Total**
Copepoda	7978 (45.4%)	Copepoda	3406 (55.3%)	Mollusca	983 (48.3%)
Amphipoda	5855 (33.3%)	Mollusca	1179 (19.1%)	Copepoda	474 (23.3%)
Mollusca	1888 (10.7%)	Amphipoda	595 (9.7%)	Amphipoda	155 (7.6%)
Ostracoda	507 (2.9%)	Ostracoda	196 (3.2%)	Ostracoda	138 (6.8%)
Chaetognatha	364 (2.0%)	Polychaeta	188 (3.0%)	Ctenophora	80 (3.9%)
Crustacean larvae	217 (1.2%)	Cnidaria	171 (2.8%)	Polychaeta	77 (3.8%)
Polychaeta	197 (1.1%)	Tunicata	148 (2.4%)	Cnidaria	46 (2.3%)
Euphausiacea	178 (1.0%)	Euphausiacea	73 (1.2%)	Isopoda	25 (1.2%)
Pisces	165 (0.9%)	Isopoda	54 (0.9%)	Tunicata	22 (1.1%)
Cnidaria	60 (0.3%)	Chaetognatha	42 (0.7%)	Crustacean larvae	13 (0.6%)
Decapoda	52 (0.3%)	Crustacean larvae	41 (0.7%)	Echinodermata	11 (0.5%)
Tunicata	50 (0.3%)	Ctenophora	39 (0.6%)	Euphausiacea	4 (<0.1%)
Isopoda	17 (<0.1%)	Echinodermata	22 (0.4%)	Chaetognatha	3 (<0.1%)
Ctenophora	15 (<0.1%)	Decapoda	5 (<0.1%)	Decapoda	3 (<0.1%)
Echinodermata	12 (<0.1%)	UI Crustacean	3 (<0.1%)	Pisces	1 (<0.1%)
Balanomorpha	4 (<0.1%)	Pisces	2 (<0.1%)	UI Crustacean	1 (<0.1%)
UI Crustacean	2 (<0.1%)	Balanomorpha	0 (0%)	Balanomorpha	0 (0%)

Table 3.2: Biodiversity index (Shannon-Wiener, H') and Pilou's Evenness (J) based on zooplankton swimmers between depths and seasons.

Depth	Parameter	Range	Mean ± SD
1000 m	H'	0 - 3.04	1.93 ± 0.80
	J	0 - 1	0.79 ± 0.23
2000 m	H'	0 - 2.83	1.94 ± 0.67
	J	0 - 1	0.86 ± 0.20
Deep	H'	0 - 2.33	1.30 ± 0.59
	J	0 - 1	0.87 ± 0.18
Season	**Parameter**	**Range**	**Mean ± SD**
Spring	H'	0 - 3.04	1.68 ± 0.79
	J	0 - 1	0.85 ± 0.21
Summer	H'	0 - 2.95	1.63 ± 0.80
	J	0 - 1	0.81 ± 0.25
Autumn	H'	0 - 2.98	1.95 ± 0.70
	J	0 - 1	0.86 ± 0.17
Winter	H'	0 - 2.92	1.85 ± 0.64
	J	0 - 1	0.85 ± 0.18

3.4.2 Seasonal variability in swimmer composition

The swimmer abundance exhibited low seasonality (ANOSIM, Global R:<0.15), which was caused by low seasonal dynamics by the following taxa: ctenophores, isopods, cnidaria, decapods, euphausiids, barnacles, crustacean larvae and chaetognaths, including the dominant copepods and amphipods (Kruskal-Wallis-test, $p<0.01$). Hence, their contribution to the swimmer flux was consistent throughout the year. In contrast, numbers of molluscs, ostracods, fish, tunicates, polychaetes, and ophiurids exhibited seasonal changes, mostly with significantly higher abundances in summer/autumn (Kruskal-Wallis-test and Dunn-test, $p<0.01$). The low overall seasonality of species abundance was confirmed in the nMDS that showed overlapping samples and the absence of clear groups (Figure 3.1). In contrast to ANOSIM and nMDS, the PERMANOVA showed a significant relationship between species abundance and season, though the factor season explained a low proportion of the variance in species abundance ($R^2=0.02$, $p<0.01$).

Species diversity shows significant differences between seasons (Figure 3.1f, Kruskal-Wallis-test, $p<0.01$) despite high standard variation. The Dunn's test indicated that the diversity index in autumn was significantly higher than during spring and summer,

but not significantly different to winter (Table 3.2). In contrast, the species evenness did not exhibit significant seasonal differences (Kruskal-Wallis-test, $p>0.01$).

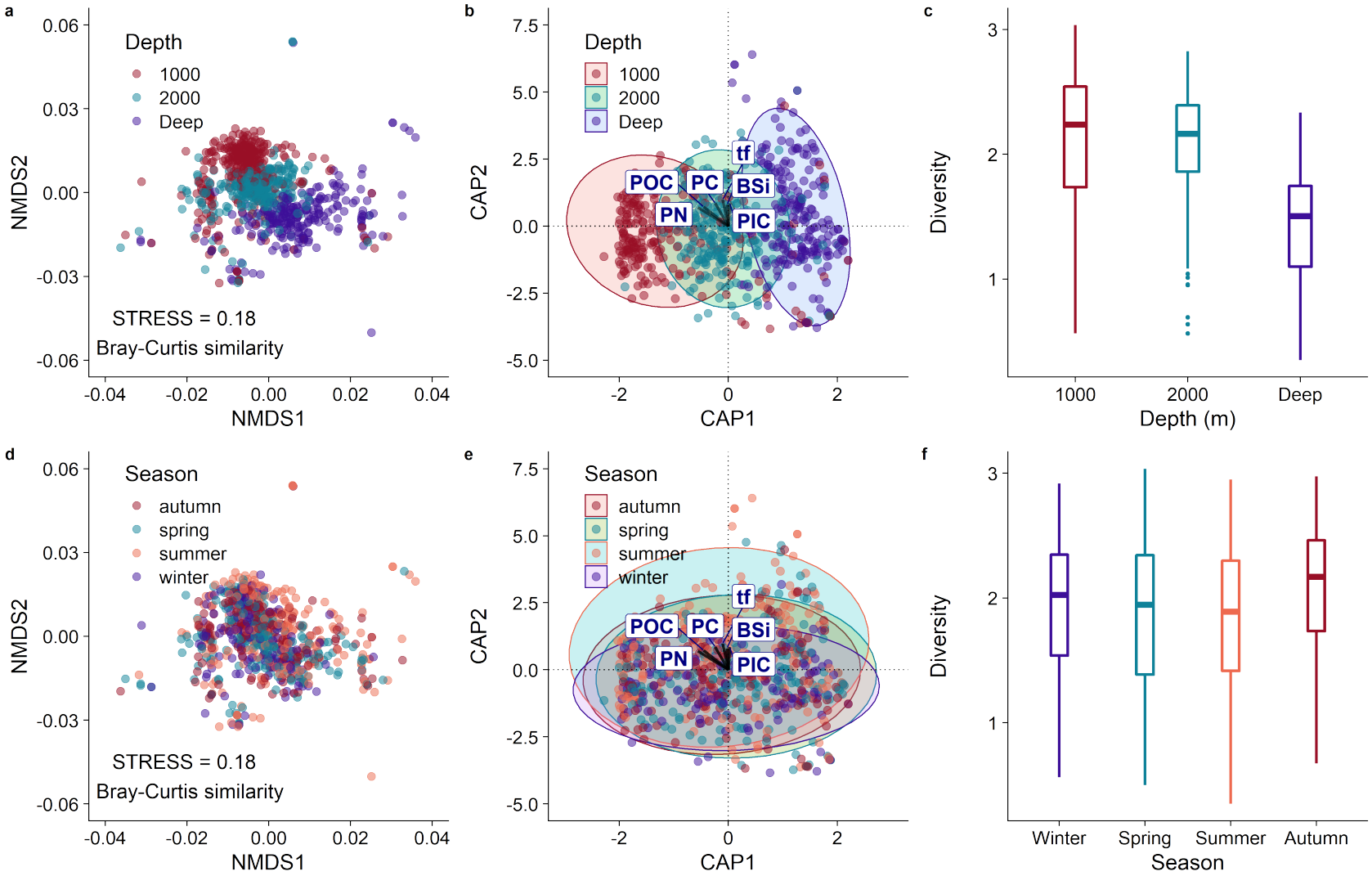

Figure 3.1: (a) and (d) nMDS to display groupings of the transformed abundance data per depth (a) and season (d) using a Bray-Curtis resemblance matrix. For a better display, one major outlier was removed. (b) and (e) CAP that displays correspondence of flux parameters with transformed species abundance per depth (b) and season (e). (c) and (f) biodiversity (Shannon Wiener Information function) per depth and season, respectively.

3.4.3 Interannual variability in swimmer composition

The zooplankton swimmer community was highly variable between years. In the PERMANOVA, the factor sampling year was significant but explained less variance in swimmer abundance relative to depth (R^2= 0.06, p<0.01). Copepods, amphipods, and molluscs dominated the swimmer community at 1000 m depth on inter-annual scales, though their contribution and total abundances varied between years (Figure 3.2a). The total flux of swimmers was highly variable, ranging between 0.5 and 15 individuals m^{-2} d^{-1} on average per sampling year (June-May). The contribution of copepods to the swimmer community typically ranged between $\sim$ 25% and 55%, however, low flux years, such as 2003/2004 were distinguished by a higher proportion of copepods ($\sim$ 75%) relative to other taxa (Figure 3.2a, b). The years 1999/2000 and 2018/2019 were characterised by large influxes of amphipods, which significantly increased the total swimmer flux compared to the other years. In these years, amphipods represented $\sim$ 50% of the swimmer community. The interannual variability in amphipod abundance at 1000 m depth was driven by swarms of three dominant amphipods *Primno latreillei*, *Eurythenes thurstoni* and orchomenids, such as *Abyssorchomene spp.*. Over all of the years analysed, these species made up 51%, 24% and 10%, respectively, of the whole amphipod community at 1000 m (Supplementary material, Table 3.4). Higher average percentages of molluscs ($\sim$ 25%) were collected in 2009/2010 and 2012/2013. When comparing swimmer community composition between years, gaps in the time-series caused by sediment trap failure and other deployment issues, have to be taken into consideration, especially in the earlier years of the mooring (e.g. in 2001/2002, 2004/2005, 2005/2006, and 2014/15). For example, the high contribution of ostracods to the community in 2005/06 was a result of both high influxes of the taxon and incomplete coverage of sampling during the winter season at SOTS.

At 2000 m depth, no large amphipod swarms were collected. The total swimmer flux was therefore more even between years and largely dominated by copepods ($\sim$ 50%, Figure 3.2b). Total swimmer flux typically ranged between 0.5 and 3.9 ind. m^{-2} d^{-1} per year (Figure 3.2c and d). When comparing years with full or close to full coverage (>300 days of sampling period per year), the years 2012/2013 - 2013/2014 were relatively high flux years (>3.5 ind. m^{-2} d^{-1}), 1999/2000 and 2016/2017-2018/2019 medium flux (2-3.5 ind. m^{-2} d^{-1}) and 2015/2016 and 2019/2020 low flux years (<2 ind. m^{-2} d^{-1}).

In the deepest trap (3800/3900 m), total swimmer abundances were low, ranging between 0.45 and 1.4 m^{-2} d^{-1} per year on average. Molluscs dominated the flux (30-60% of the total flux), followed by copepods, amphipods, and ostracods, while other taxa only played minor roles. In general, a higher influx of swimmers was estimated for recent years (since 2012/2013, except 2015/2016), even when taking the varying opening times into account. Ostracods were present in all years except 2010/2011, 2016/2016 and 2018/2019-2019/2020. Additionally, a notably higher number of ctenophores were counted in deep traps from recent years (since 2013/2014) and in the samples from 1997/1998.

3.4.4 Relationship of species abundance and diversity with downward particle flux parameters

The relationship between species abundance and flux parameters is more complex than previously assumed. First, the CAP indicated the flux parameters only played a minor role driving the total species abundance (Figure 3.1). When fitting GAM without smoothing functions, i.e., assuming a linear relationship, only a low percentage of deviance could be explained (max. 29%, total swimmer abundance). However, when fitting GAM with smoothing terms which allowed for non-linearity in the environmental driver-response variable relationship, the explained deviance rose to 47.3% (Table 3.3). Species abundance was mostly dependent on changes in POC, PIC, PN, and BSi and rarely related to changes in total downward flux or PC. Effective degrees of freedom (edf) of 1.00 indicated a linear negative response of total swimmers and amphipods to increasing BSi levels, as well as a negative response of chaetognaths and crustacean larvae to increasing POC content in the trap and cnidarians to increasing PC concentrations. A positive relationship was seen between cnidarians and increasing PIC. All other relationships were non-linear. The abundance of isopods, ctenophores, ophiurids and barnacles could not be explained by any of the tested parameters. For a better visualisation, abundances of total swimmers and the three dominant taxa, i.e. copepods, amphipods, and molluscs were displayed in relationship to significant flux parameters (Figure 3.4). Generally, zooplankton swimmer abundances related negatively with increasing POC, and positively with increasing particulate organic nitrogen (PON), though there was large variability at high flux conditions. In addition, species abundances decreased slightly with increasing

PIC and BSi. Given that the R^2 and explained deviance by the fitted models were generally low, it suggests that other drivers potentially affect species abundance that have not been accounted for in the present analysis. The species diversity is driven by POC, PN, BSi and total flux (tf), but, similarly, a low R^2 and explained deviance (0.28 and 30.3%, respectively) indicated that other environmental parameters drive the differences in species diversity.

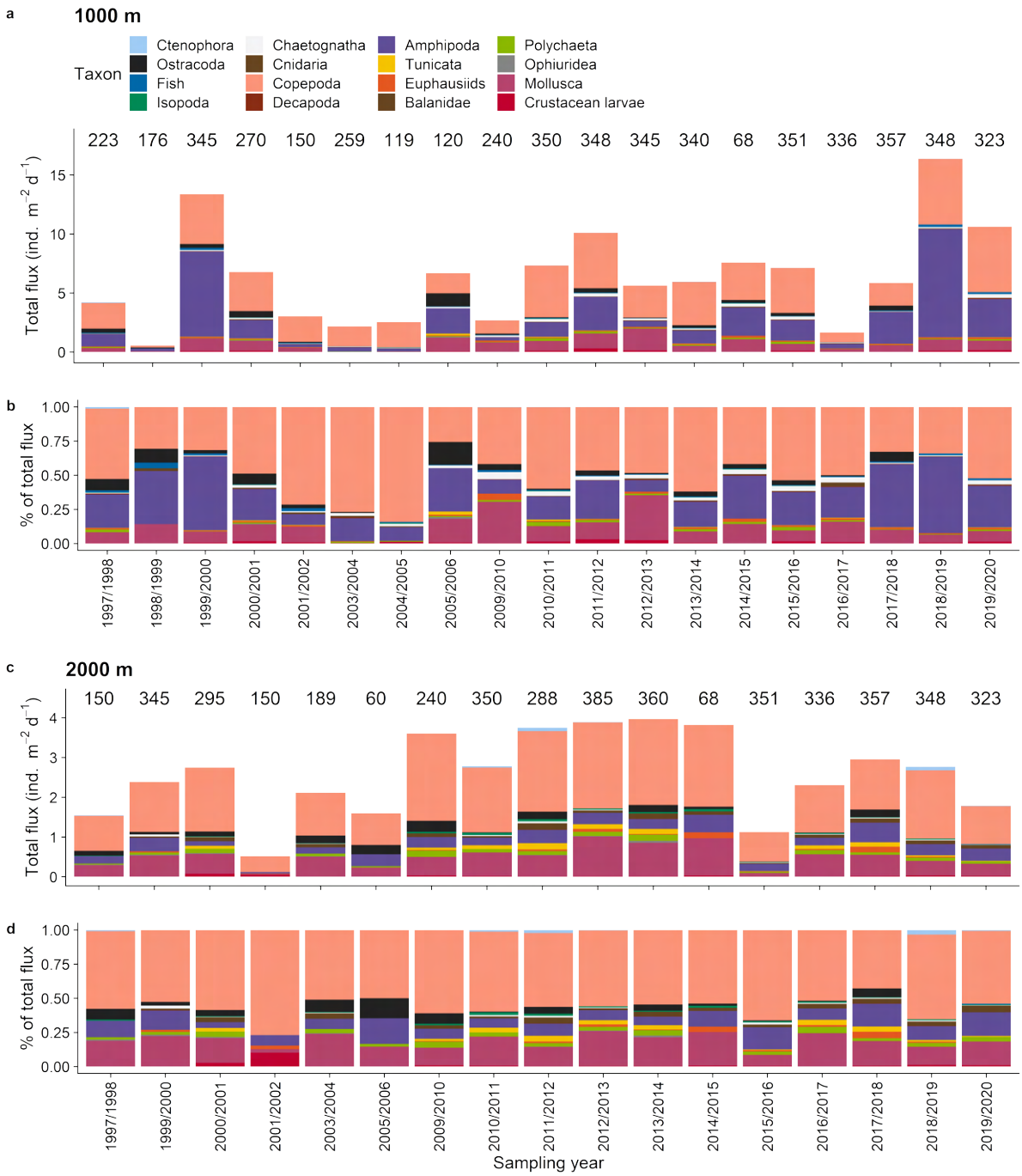

Figure 3.2: The zooplankton swimmer community in sediment traps at SOTS. Displayed are (a) and (c) total flux (individuals m^{-2} d^{-1}) and (b) and (d) contribution to flux (% of total flux) at 1000 and 2000 m depth, respectively. Numbers above the bars indicate the sampling period (days) per respective year. Note, numbers higher than 365 are caused by using the midpoint date to determine the association with a sampling year and not the start/end date.

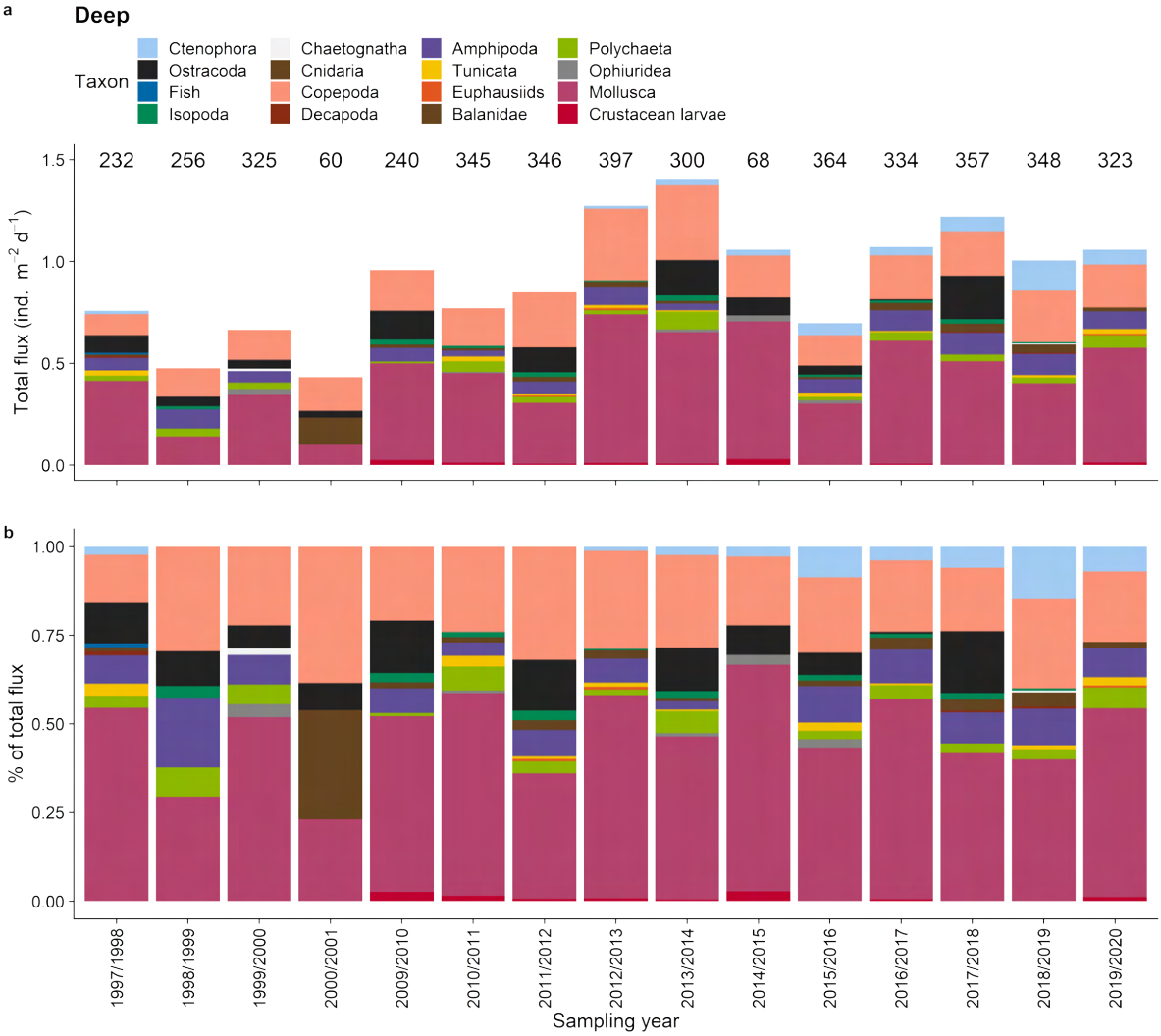

Figure 3.3: The zooplankton swimmer community in sediment traps at SOTS (cont.). Displayed are (a) total flux (individuals m^{-2} d^{-1}) and (b) contribution to flux (% of total flux) at 3800/3900 m depth, respectively. Numbers above the bars indicate the sampling period (days) per respective year. Note, numbers higher than 365 are caused by using the midpoint date to determine the association with a sampling year and not the start/end date.

Table 3.3: Results of the Generalised Additive Models. Displayed are the effective degrees of freedom (edf) for the flux parameters that are significantly driving the species abundance and diversity. Non-significant results were left blank. If the relationship was proven to be linear, as shown with an edf of 1.00, the type of relationship (positiv (+) or negative (-)) was added in parentheses.

GAM	**tf**	**PC**	**POC**	**PIC**	**PN**	**BSi**	**R^2 (adj.)**	**Deviance explained (%)**
Abundance:								
Total			5.67	3.94	5.00	1.00 (-)	0.45	47.3
Copepoda			5.65	2.72	4.73	6.21	0.38	39.7
Amphipoda			7.42	5.02	7.24	1.00 (-)	0.36	38.4
Ostracoda	2.62		7.39		7.10		0.23	25.5
Chaetognatha	2.87		1.00 (-)	2.32	5.90	1.66	0.21	22.7
Euphausiids				2.17	6.56	3.14	0.20	21.5
Fish			8.31	3.66	7.91	1.83	0.18	21.0
Mollusca			1.88		5.01	1.10	0.14	15.0
Crustacean larvae			1.00 (-)	4.01	5.21		0.12	13.8
Polychaeta				7.93	5.51		0.08	10.0
Tunicata						8.10	0.07	9.2
Decapoda					4.42	6.87	0.06	8.0
Cnidaria		1.00 (-)		1.00 (+)			0.02	4.0
Isopoda							0.01	2.9
Ctenophora							0.02	2.8
Ophiuridea							<0.01	2.8
Balanomorpha							<0.01	0.6
Diversity:								
Shannon-Wiener	2.12		3.38		8.26	6.25	0.28	30.3

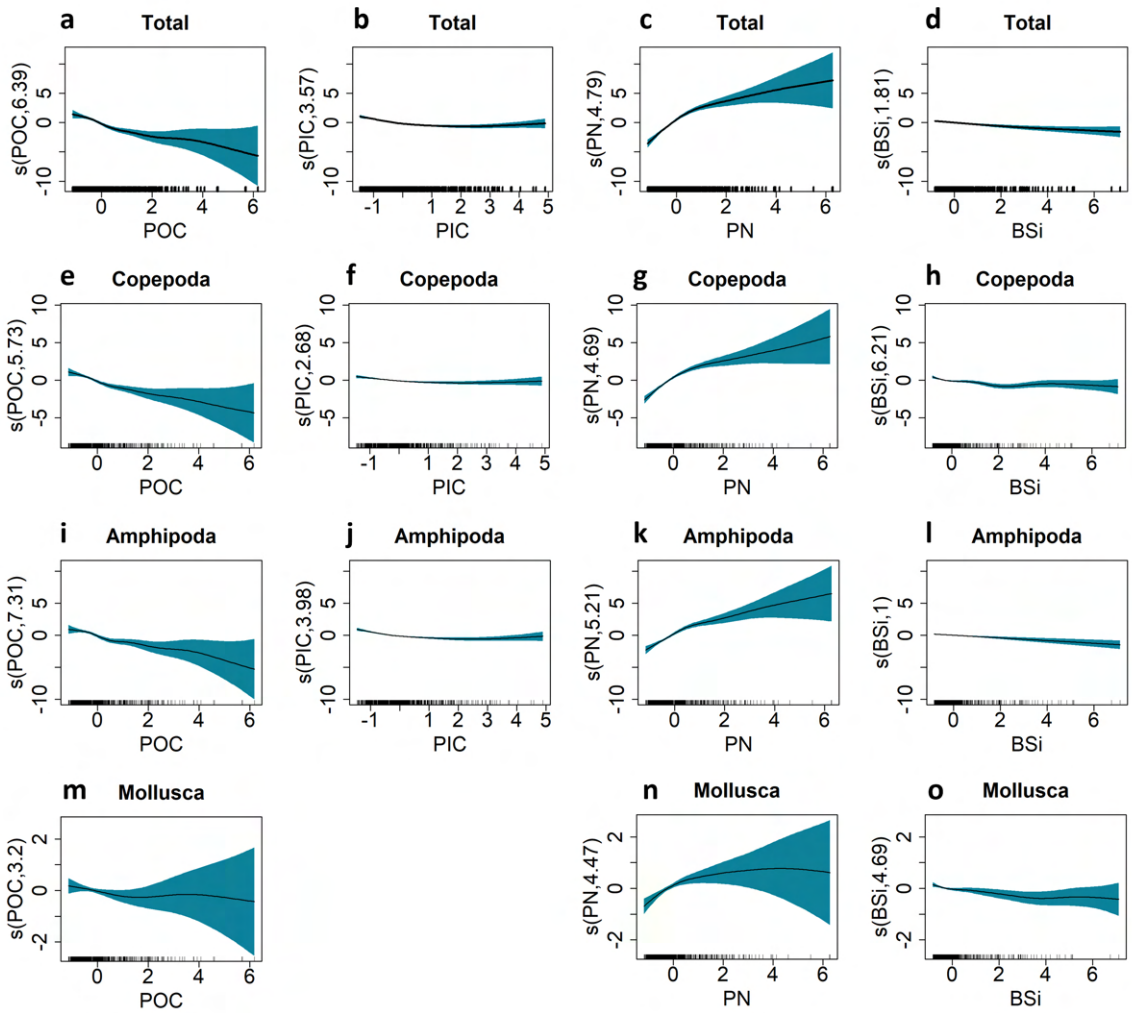

Figure 3.4: Generalised Additive Models fitted to the standardised flux parameters as predicting factor and the total swimmer abundance (a-d), and the three dominant groups - copepods (e-h), amphipods (i-l), and molluscs (m-o), as response variables. Displayed are the significant relationships between flux parameters and species abundance ($p<0.01$).

3.5 Discussion

3.5.1 Copepods, amphipods, and molluscs are the most abundant taxa

Copepods, amphipods, and molluscs dominated the swimmer community between 1997 and 2020. This pattern was only partly reflected in the surface zooplankton community sampled by Continuous Plankton Recorder (CPR) deployed off ships of opportunity (Hunt and Hosie, 2006). In addition to foraminiferans, the copepod species *Oithona similis*, and appendicularians, the surface zooplankton community was shown to be dominated by pteropods (*Limacina* spp.), various copepod species in the families Calanidae, Clausocalanidae, and Eucalanidae, and chaetognaths during summer. While some taxa, notably calanoid copepods and pteropods, were dominant in both surface and deep-sea communities when comparing both methods, others are rarely collected by sediment traps in the >1 mm fraction (chaetognaths, appendicularia, or foraminifera) or by surface ocean CPR tows (amphipods). As the collection capability varies between methodologies, e.g. as discussed for the CPR by (Dippner and Krause, 2013) or for sediment traps in this chapter (see section 3.1.5), it is unclear if the differences were caused by a different deep-sea community compared to surface or a difference in the collection methods. However, the results are consistent with other studies using sediment traps as opportunistic tools of collecting zooplankton and micronekton. For example, Steinberg et al. (1998) found that calanoid copepods and hyperiid amphipods constituted the majority of swimmer biomass at 450 m depth in Monterey Bay, USA. In addition, Matsuno et al. (2014) found calanoid copepods to be the dominating swimmer in sediment traps at 181-218 m depth in the western Arctic Ocean, followed by amphipods. Seasonally, they recorded high numbers of the amphipod *Themisto libellula*. Finally, Danovaro et al. (2017) found sediment traps in the Adriatic Sea (150 and 1050 m depth) to be dominated by copepods, while ostracods and polychaetes were the major contributor in other basins of the Mediterranean Sea.

As in other studies, many scavenging copepod families were collected in the SOTS traps. For example, the copepod species *Triconia antarctica* (Oncaeidae) was highly abundant in the 2000 m trap and many of them were females carrying eggs. This family is known for its close association with detritus (e.g., at 450 m depth in Monterey Bay, Steinberg et al., 1998). Similarly, Matsuno et al. (2015) collected *Oncaea parila* with egg sacs through-

out the year, and suggested they were captured with the sinking detritus due to their poor swimming abilities. The copepod community at 184–260 m depth in the western Arctic was dominated by Calanidae and scavenging copepods in the families Metridiae, Euchaetidae, and Heterorhabdidae (Matsuno et al., 2015). Another important component of the scavenging community at SOTS are amphipods. In addition to the swarms of *Eurythenes thurstoni*, *Primno latreillei* and Orchomenids, such as *Abyssorchomene* spp., many common pelagic species were collected in the SOTS sediment traps that are common in the pelagic Southern Ocean, e.g. *Cyphocaris richardi*, *Scina* spp. or *Lanceola* spp. Because of their good swimming abilities, amphipods are typically under-sampled with net tows (Kraft et al., 2012). Hence, baited traps have been previously used for analysis of the species inventory (e.g. Horton et al., 2013; Duffy et al., 2012), mostly on the seafloor in different regions of the global ocean, but rarely in the pelagic Southern Ocean. Consequently, sediment traps can be used in addition to baited traps to increase the temporal coverage of biodiversity studies of deep-sea amphipods.

As shown by the SOTS results, molluscs are an integral part of the swimmer community, in particular the pteropods *Limacina helicina antarctica* and *Clio* spp. *L. helicina antarctica* is broadly distributed in surface waters between the Subantarctic Front and the Antarctic Coast (Van der Spoel and Dadon, 1999). Especially at 2000 m and in the deepest SOTS trap, this species represents the majority of collected molluscs, while *Clio* spp. were the second most abundant mollusc at 1000 m depth. Overall, the diversity of collected molluscs at SOTS reflected the surface community, though the abundance varied between the collection methods as described in Howard et al. (2011). For example, during the SAZ-Sense voyage to the subantarctic Southern Ocean in summer 2007, mainly *Limacina retroversa australis*, *Clio pyramidata sulcata*, *Limacina helicina antarctica*, and *Clio recurva* were collected from surface waters in the region around SOTS (Howard et al., 2011). Sampling the deep-sea mollusc community at different water depths with sediment traps will enable an early detection of ecosystem changes in the subantarctic zone.

Thecosome pteropods, such as *L. helicina antarctica* and *Clio* spp., produce aragonite shells, which increase their vulnerability to ocean acidification (Orr et al., 2005; Roberts et al., 2008). When the Southern Ocean becomes under-saturated in respect to aragonite within the next 50 years (Howard et al., 2011; Orr et al., 2005), pteropods and other

calcifying organisms will be affected first, especially in the deep Southern Ocean. At present, the aragonite saturation horizon (ASH) is at 1,200 m depth with a shoaling trend (Howard et al., 2011), hence, shells of dead pteropods are sinking through undersaturated waters that promote their dissolution, before they are collected in the 2000 and 3800/3900 m traps. In future, with a further shallowing of the ASH, changes in abundances and distribution ranges are possible, with implications for marine ecosystem and carbon cycle. Species, such as *Clio recurva*, that live in deep waters of the Southern Ocean (200-1000 m, Van der Spoel and Dadon, 1999) close to the ASH are predominantly affected.

3.5.2 Decreasing abundance and diversity with depth

The "swimmer problem", i.e. swimmers being reported as artefacts in sediment traps, decreases with depth as zooplankton and micronekton biomass is lower in the deep-sea (Buesseler, 1998; Lee et al., 1988; Michaels et al., 1990; Silver, 1991; Steinberg et al., 1998). Both in this SOTS study and others from various oceanographic regions, such as the Mediterranean Sea and the western Arctic, the abundance and diversity show a decreasing trend with depth (Romano et al., 2017; Danovaro et al., 2017; Matsuno et al., 2014). The estimated swimmer flux at SOTS (0-39.4 ind. m^{-2} d^{-1}) is within the range of previous studies, despite the different deployment depths which limit the comparison of total numbers between studies and regions. For example, Danovaro et al. (2017) recorded a 100-times higher flux at 150 m (225-5175 ind. m^{-2} d^{-1}) than at 1050 m (1-34 ind. m^{-2} d^{-1}, near-bottom) in the Adriatic Sea. In the Ionian Sea, at 2250 m, they measured 4-14 ind. m^{-2} d^{-1} in the near-bottom trap at 2250 m and also found a decreasing biodiversity with depth throughout their study. In the western Arctic, Matsuno et al. (2014) estimated a swimmer flux to be between 5 and 44 ind. m^{-2} d^{-1} at 184 and 1300 m.

As observed for swimmer abundance, the species diversity is within the same range as comparable literature. For example, our results indicate a higher zooplankton diversity in the deep subantarctic Southern Ocean than in the Adriatic Sea (both at 150 and 1050 m water depth) or in the deep Ionian Sea (2250 m) (Danovaro et al., 2017) but lower diversity compared to Mediterranean deep-sea canyons (Romano et al., 2017). Similar to the present study at SOTS, the evenness increased with depth in the Mediterranean

Sea, which suggests a more equitable zooplankton and micronekton community in both the bathypelagic Mediterranean Sea as well as in the subantarctic zone. Sediment traps as tools for continuous and long-term monitoring of the deep-sea diversity enable studying changes in the meso- and bathypelagic community composition following e.g. ocean warming of surface waters as projected for the subantarctic zone (Herraiz-Borreguero and Rintoul, 2011).

3.5.3 Lack of seasonality and long-term trends in swimmer abundance and diversity

Neither a seasonal trend nor a long-term trend in species abundance could be observed at SOTS, probably due in part to high variability between samples. Other studies from different oceanic regions have reported a peak or increase in spring or summer, e.g. in the western Arctic at 184 m depth (Matsuno et al., 2014), in the Mediterranean Sea between 270 and 1870 m (Romano et al., 2017), or on the Kerguelen Plateau at 289 m (Rembauville et al., 2015b). It was also noted that seasonality can vary between sites and depths (Danovaro et al., 2017; Romano et al., 2017). Steinberg et al. (1998) found no obvious seasonal pattern in total swimmer abundance at 450-650 m depth, but did observe seasonal species succession within the swimmer assemblage.

The low seasonality in swimmer abundance at SOTS can be a reflection of the low seasonality at the surface. Due to a deep mixing layer and low dissolved iron supply, the phytoplankton production at SOTS is relatively low (Eriksen et al., 2018; Trull et al., 2019, 2001). Rather than a typical spring bloom, the phytoplankton abundance increases moderately with a successive development of different species of diatoms, flagellates, haptophytes, and cyanobacteria during spring and summer (Eriksen et al., 2018). In addition, the timing of primary production and particle flux down to the sediment traps might be decoupled because of water column processes, such as active feeding and repacking of sinking material by the zooplankton at the surface, i.e. detritivorous copepods, appendicularia, and foraminifera (Hunt and Hosie, 2006), and by the mid-water community, that either retain particles in the water column or promote their downward export (Koski et al., 2020; Mayor et al., 2014; Steinberg and Landry, 2017; Turner, 2002, 2015). Many of these processes in the water column and the resulting ecological implications (e.g. trophic

cascades and successions) in the SAZ are understudied and require future research efforts. Remarkably, despite the evenness of the zooplankton community being similar between seasons, the species diversity is highest in autumn and lower in spring and summer. Potentially, the ontogenetic downward migration of some copepods, e.g. *Neocalanus tonsus*, leads to an increased species diversity in the deep-sea zooplankton. Local oceanographic phenomena, e.g. eddies that introduce subtropical water and organisms from the north, can lead to this difference as well. The drivers for this pattern remain unclear and the understanding of what drives deep-sea biodiversity at SOTS should be the aim for future research.

Overall, long-term trends over seasons or years were not detected in this SOTS study. As there are no other swimmer time-series data collected in sediment traps over an extended period of time, a comparison is limited to carbon flux studies. For example, Wynn-Edwards et al. (2020) did not find a long-term trend in the POC or mass flux beyond natural variability since the establishment of SOTS. The same trend was reported for the North Atlantic from the deep (3200 m) Bermuda Atlantic Time Series (BATS) (Conte et al., 2001). Deep-sea organisms that rely on the sinking particle flux for food (Danovaro et al., 1999; Gambi and Danovaro, 2006), are therefore unlikely to change in species composition or diversity with time. In addition, drawing conclusions from a dataset with temporal gaps, especially in earlier years, due to the absence or failure of deployments, is limited. However, the collected swimmer community provides important baseline data for understanding future changes in ecology and downward carbon flux at the SOTS site caused by environmental changes.

3.5.4 Relationship to flux parameters

Many meso- and bathypelagic zooplankton are detritivorous and feed on sinking particles (Danovaro et al., 1999; Steinberg et al., 1998; Steinberg and Landry, 2017; Turner, 2015). Hence, it is remarkable that the GAM showed that the relationship between species abundance and diversity and the flux parameters was not very strong and only explained between 15-40% of the variability in the dominant taxa, the copepods, amphipods and molluscs. In addition, most relationships are non-linear with high complexity (high numbers of edf). The negative relationship between POC and swimmer abundances is re-

markable as well, i.e. the higher the POC concentration in the cups the less swimmers were collected, and vice versa. In contrast, swimmer abundances are positively related to PN concentrations. It is not well understand, why increasing levels of these two parameters cause opposite response patterns by the swimmer community. Many factors dictate whether organisms swim into the sediment trap (as discussed in the next section). Hence, the relationship between flux driving swimmer abundance and diversity is not simple, as it is reflected both in this study and in the literature. For example, Rembauville et al. (2015b) analysed the swimmer numbers in sediment traps (289 m) on the Kerguelen Plateau and found pronounced seasonality, but no correlation between mass flux, POC and PON fluxes. They suggested that the low correlation indicated that the swimmer presence did not systematically affect particulate fluxes inside the trap, but also noted that swimmers potentially feed on sinking particles in the trap funnel, modifying particle flux collection. Danovaro et al. (2017) found that total nitrogen and organic carbon only played a minor role in explaining variance in swimmer abundance and taxonomic composition in the Mediterranean Sea, relative to depth and latitude. However, when focusing on specific sampling sites, the importance of flux parameters as drivers of variability increased. For future research into drivers of swimmer abundance and diversity, other parameters should be considered as well. Net Primary Productivity (NPP) was originally to be included in the GAM however, Wynn-Edwards et al. (2020) did not find any correlation between satellite-derived NPP and POC flux magnitude at depth. Therefore, it was not included in this study, but can be considered in future research. In addition large-scale phenomena, such as El Niño–Southern Oscillation (ENSO), can impact the phyto- and zooplankton community and should therefore be analysed (e.g. Loeb et al., 2009).

3.5.5 Biases of using sediment traps to sample deep-sea zooplankton

As for any other methodology, collecting zooplankton and micronekton with sediment traps creates biases caused by the difficulty in distinguishing between the passive sinking of carcasses and active swimmers, the design of the trap itself, and the sampling protocol. First, it remains difficult to distinguish between carcasses as part of the passive downward carbon flux and active swimmers in the trap (Ivory et al., 2014). This problem

has been discussed for many years, as carcasses need to be included when calculating the downward particle flux, whereas swimmers can make up to 14-90% of the POC of the trap material and have to be removed (Buesseler et al., 2007a). To avoid this issue, all organisms >1 mm are typically removed, such as in this and other studies (Buesseler et al., 2007a; Wynn-Edwards et al., 2020). Consequently, this removal potentially underestimates the overall carbon flux. Moreover, the difficulty of separation of carcasses from swimmers differs from case to case. For example, finding fragments of tunicate colonies or mollusc shells likely means that they sunk into the trap when dead, while the distinction between swimmer and carcasses for copepods and other crustaceans is more difficult. Amphipods are good swimmers and are known to scavenge on sinking detritus (De Broyer and Jazdzewski, 1996; Dauby et al., 2003; Zeidler and De Broyer, 2009). Hence, most of the amphipods collected by sediment traps are likely swimmers. Ophiurids, on the other hand are typically attached to larger aggregates and can be considered part of the passive flux (Steinberg et al., 1998). Small juvenile amphipods (<1 mm) could emerge from the marsupium of female amphipods (part of the active flux, Steinberg et al., 1998) or are associated with detritus (passive downward flux). Herbivorous copepods that are collected in the deep-sea will likely be carcasses, however, deep ontogenetic migration may lead them down to 1000 m depth and deeper (Bradford-Grieve et al., 2001; Jónasdóttir et al., 2015; Atkinson and Sinclair, 2000). In addition, many species feed opportunistically, for example *Rhincalanus gigas* (Graeve et al., 1994), which impedes decisions on swimmer definition based on feeding type. Related to this issue is the uncertainty in the source of the organisms collected by sediment traps. As the SOTS traps are deployed for a year, and the cups collect particles and swimmers over several days, the resolution is not high enough to give information on potential daily and annual migration. Based on the sediment trap records, it is unknown if the zooplankton/micronekton died in surface waters and sank down into the trap, if they died at depth just above the mooring or if they actively swam into the trap.

Moreover, the design of the sediment trap itself leads to a biased sampling of organisms. The baffle on top of the funnel, which is necessary to avoid system clogging by organisms and particles, also leads to the undersampling of larger animals, such as pyrosomes and larvacean houses. Steinberg et al. (1998) found many giant larvaceans in their samples in Monterey Bay, but noted that many were not collected as the baffle gives larvaceans the opportunity to escape before aggregates descends into the trap. Mostly, only the

feeding basket was caught, while the house was too big to enter. Appendicularians are a major component of the surface zooplankton community (Hunt and Hosie, 2006), and considering they are infrequently found in traps, an undersampling caused by the baffled funnel is likely. In addition, pyrosomes and other gelatinous plankton can reach higher colony and body sizes than would fit through the baffle or in the cup, which means only small colonies/individuals or fragments are collected. Another issue is the attraction of scavengers, e.g. amphipods, by particles along the inner edges of the funnel-shaped trap (Buesseler et al., 2007a; Rembauville et al., 2015b). Feeding on particles before they enter the cup as well as releasing faecal pellets, changes the quantity and chemical composition of caught material, which biases flux estimates. (Buesseler et al., 2007a). In addition, the preservation method affects the swimmer abundance, with implications for the effectiveness of the treatments (Lee et al., 1992). Mercuric chloride is known to attract more gammarid amphipods compared to other treatments (Lee et al., 1992). Moreover, high swimmer numbers can lower the effectiveness of the treatment with potential implications for later species identification and carbon flux estimates (Buesseler et al., 2007a).

Finally, the sampling protocol creates biases, e.g. the time period between collection and identification, and the mechanical handling during sieving. The degradation of organisms in the trap during long-term deployments hampers the detailed species identification following recovery (Michaels et al., 1990). In addition, the delay between recovery and identification produces artefacts, such as the increased occurrence of ctenophores in recent years in the deepest sediment trap (see Figure 3.3). The samples of 1997/1998 were analysed soon after recovery of the traps by John Kitchener (AAD, Australia) and contained ctenophores as well, while in the samples between 1998-2011 this taxon was absent. Consequently, the disintegration of ctenophores during the storage period rather than an overarching temporal pattern is likely responsible for their absence in the earlier years. In general, fragile specimens disintegrate during sieving. For example, the picture of the recently recovered 2020/2021 trap from 2000 m shows a large object that disappeared during sieving (Figure 3.5). Due to the opportunistic nature of studying zooplankton from sediment traps, these specimens, called "cryptic swimmers" (Buesseler et al., 2007a), remain unidentified and sometimes undetected, leading to an underestimation of the fragile gelatinous part of the food web.

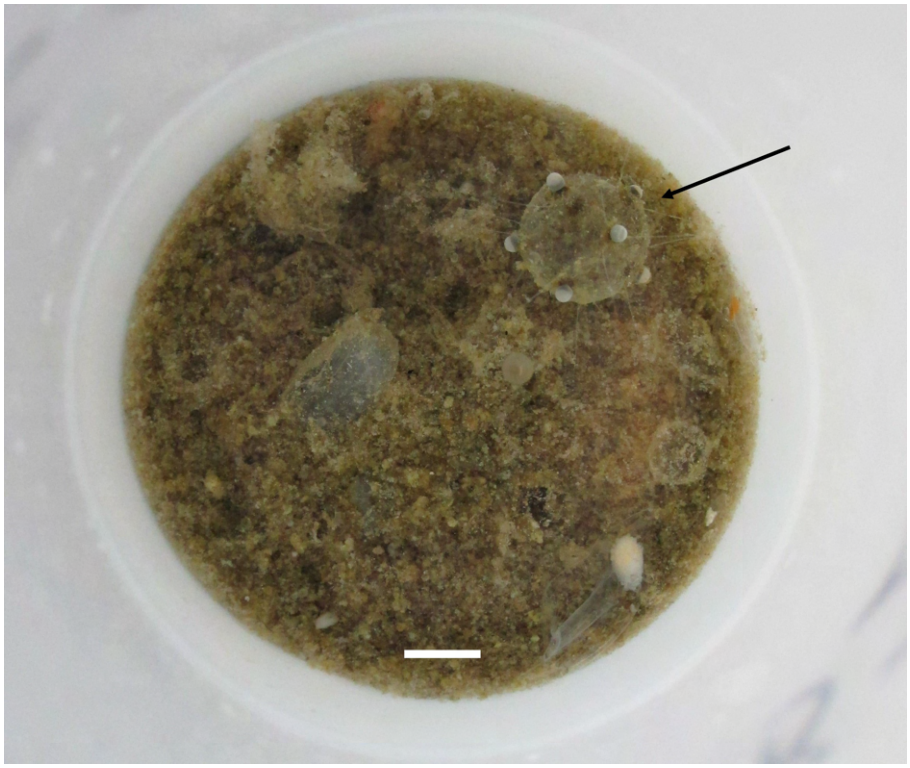

Figure 3.5: Image of the recently recovered trap cup from 2000 m in 2020/2021, taken before sieving. Visible is a large, fragile object (indicated by the black arrow), that disintegrated in the sieving process afterwards. White scale bar: 1 cm. Picture: Cathryn Wynn-Edwards, AAPP, Australia.

3.5.6 Opportunities for zooplankton collection with sediment traps and outlook

Despite the discussed biases, swimmer community data collected in sediment traps offer many opportunities to improve our understanding of deep-sea ecosystems and carbon flux. They are useful tools to sample the zooplankton community year-round in regions difficult to access (Makabe et al., 2016; Romano et al., 2017). The subantarctic zone is remote and logistically challenging to sample (Trull et al., 2010) and most of the information on subantarctic zooplankton dynamics comes from CPR deployments and net tows in surface waters during the summer season (Hunt and Hosie, 2006; McLeod et al., 2010; Takahashi et al., 2020). Consequently, sediment traps provide complementary insights into deep-sea zooplankton abundance, diversity, and variability over a long sampling period, especially outside the well-studied summer season. Also, sediment traps can be

used to increase the knowledge on deep-sea biodiversity. As part of this study, a new amphipod species was described (Appendix A) and a further three await classification. Although gelatinous material disintegrates over time, the traps are a gentler alternative to trawls, because organisms either sink or swim into the traps undamaged. Fragile taxa, which are often damaged during the net collection process, are more efficiently collected by sediment traps in comparison (Michaels et al., 1995).

For future research on the biological carbon pump and biodiversity in the subantarctic zone, an integration of sediment traps with other methods to collect zooplankton, i.e. CPR and net trawls, is necessary. While sediment traps provide species abundance and diversity information on a larger horizontal and temporal extent, net trawls and CPR deployments provide higher spatial surface coverage. For an integration of sediment traps into existing zooplankton monitoring programs, the qualitative and quantitative differences between surface and deep-sea collection methods need to be studied. Species that are associated with warm water and are relatively unaffected by disintegration in the trap over time, e.g. the pyrosome *Pyrosoma atlanticum*, can be used as an indicator for an intrusion of subtropical waters from East Australian Current (EAC) extensions. This will enable a tracking of the projected intensification of the EAC with increased ocean warming, especially because the sub-surface influx of warm water masses (e.g. during the SOLACE voyage to the SAZ and PFZ in summer 2020/2021) that is not always detectable as a change in sea surface temperature via remote-sensing. Not only will this aid in understanding the oceanographic impact of climate change, but also the consequences for the subantarctic ecosystem dominated by pyrosome blooms. The integration of camera systems will be a useful addition to sediment traps, as cameras allow observations of zooplankton behaviour around the traps and the under-sampling of larger taxa, e.g. pyrosomes and larvacean houses. In addition, observing the feeding of amphipods and other scavenging organisms in the trap funnel, will enable the quantification of the bias of downward carbon flux estimates in the region both on seasonal and annual scales. Currently, the BCP in the subantarctic Southern Ocean transports considerable amounts of carbon to the deep sea, despite its HNLC condition, with inter-annual flux variations higher than estimated from satellite observations (Wynn-Edwards et al., 2020). Understanding the influence of carbon flux on the deep-sea community and vice versa will further advance the understanding of deep-sea biogeochemical and ecological processes.

3.6 Conclusion

This study presents the multi-decadal time-series of abundance and diversity of zooplankton swimmers, collected by sediment traps at the Southern Ocean Time Series site. Using sediment traps as opportunistic sampling methods allowed the coverage of long time-scales in the otherwise logistically challenging to access subantarctic zone. The deep-sea communities were dominated by copepods, amphipods, and molluscs (mainly pteropods), with decreasing species abundance and diversity, but increasing species evenness with depth. GAM showed a complex relationship with the flux parameters (PC, POC, PIC, PN, and BSi), that, however, did not explain all of the variability in swimmer abundances. Neither strong seasonality or a long-term trend in zooplankton abundance and biodiversity since the beginning of the time-series in 1997 was observed. While the method introduces biases in quantifying deep-sea biodiversity and dynamics, i.e. caused by the distinction between active swimmers and passive sinking carcasses, the trap design, and the sampling protocol, sediment traps enable a year-round long-term observational tool that provides insight into ecology and carbon cycle in meso- and bathypelagic Southern Ocean.

3.7 Acknowledgments

Australia's IMOS is enabled by the National Collaborative Research Infrastructure Strategy (NCRIS). It is operated by a consortium of institutions as an unincorporated joint venture, with the University of Tasmania as Lead Agent.

3.8 Supplementary material

3.8.1 Dominant copepod, amphipod, and mollusc taxa

Table 3.4: The five dominant copepod families, amphipod species, and mollusc species, summarised over all years and compared between sediment trap depths. Percentages in parentheses display contribution to total copepod, amphipod, and mollusc abundance, respectively. UI: unidentified.

Copepod family	**Total**	**Amphipod species**	**Total**	**Mollusc species**	**Total**
		1000 m			
Calanidae	1613 (20.2%)	*Primno latreillei*	3000 (51.2%)	*Limacina helicina antarctica*	665 (35.2%)
Calanoidea (UI)	1546 (19.4%)	*Eurythenes thurstoni*	1387 (23.7%)	*Clio* spp.	647 (34.3%)
Scolecitrichidae	1458 (18.3%)	Orchomenids	577 (9.9%)	*Clio recurva*	103 (5.5%)
Metridinidae	850 (10.6%)	*Scina incerta*	150 (2.6%)	*Peracle* spp.	89 (4.7%)
Eucalanidae	813 (10.2%)	*Cyllopus magellanicus*	101 (1.7%)	*Clio pyramidata*	85 (4.5%)
		2000 m			
Calanidae	903 (26.5%)	Orchomenids	222 (37.3%)	*Limacina helicina antarctica*	688 (58.4%)
Eucalanidae	731 (21.5%)	*Cyllopus magellanicus*	65 (10.9%)	*Atlanta* spp.	79 (6.7%)
Aeteideae	366 (10.7%)	*Halice macronyx*	37 (6.2%)	*Clio pyramidata*	58 (4.9%)
Oncaeidae	297 (8.7%)	*Themisto gaudichaudii*	27 (4.5%)	*Peracle* spp.	54 (4.6%)
Calanoidea (UI)	281 (8.2%)	UI Hyperiids	23 (3.8%)	*Heliconoides inflatus*	52 (4.4%)
		3800/3900 m			
Aeteideae	146 (30.8%)	Orchomenids	22 (14.2%)	*Limacina helicina antarctica*	624 (63.5%)
Metridinidae	100 (21.1%)	*Cyphocaris richardi*	19 (12.2%)	*Clio pyramidata antarctica*	50 (5.1%)
Calanoidea (UI)	65 (13.7%)	UI Hyperiids	13 (8.4%)	*Heliconoides inflatus*	47 (4.8%)
Calanidae	57 (12.0%)	*Lanceola loveni*	11 (7.1%)	*Limacina retroversa australis*	45 (4.6%)
Scolecitrichidae	43 (9.1%)	*Lanceola pacifica*	8 (5.2%)	*Clio* spp.	41 (4.2%)

3.8.2 Photomicrographs of swimmer taxa

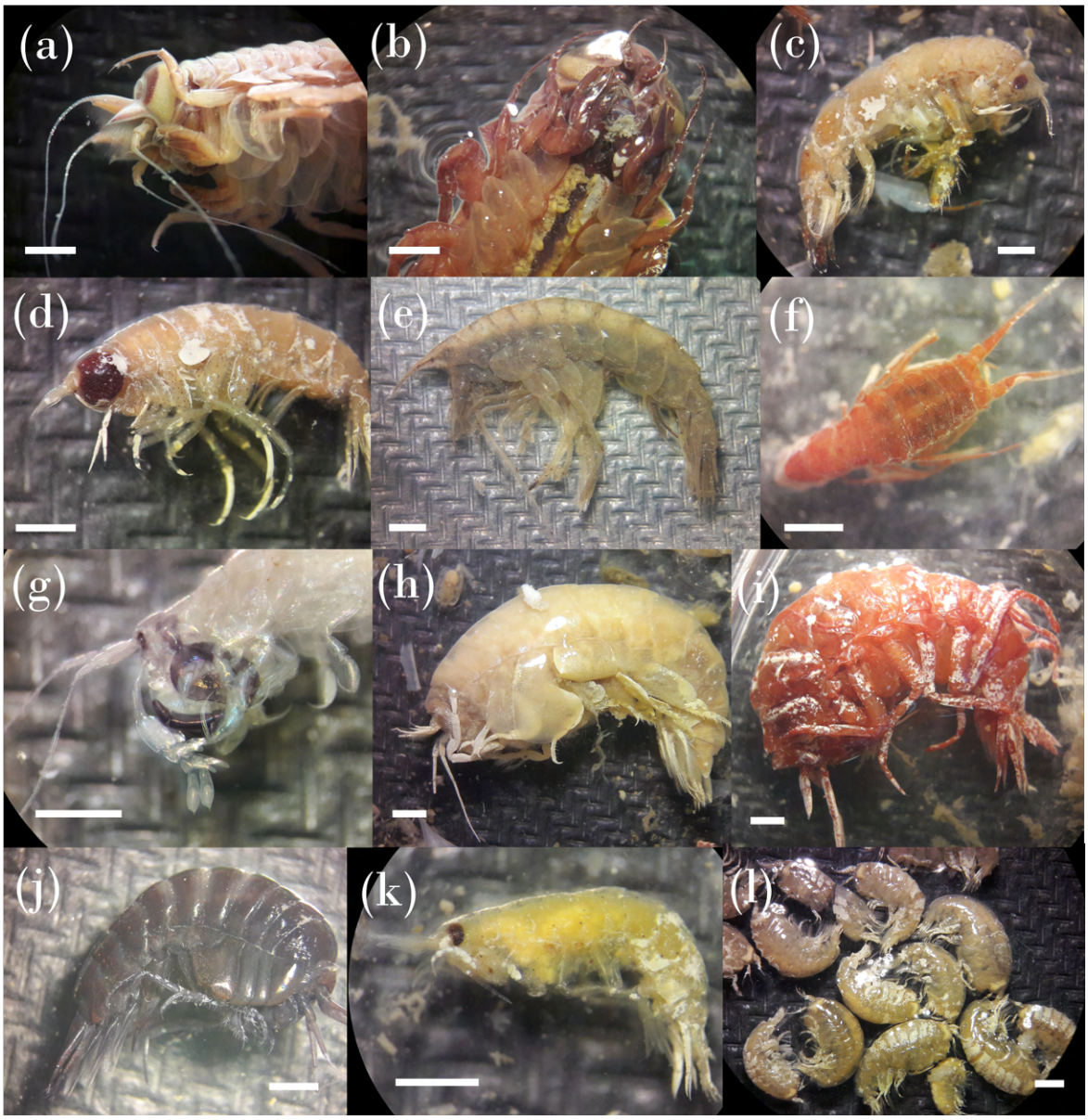

Figure 3.6: Amphipods collected between 1997-2020. (a) *Pegohyperia princeps*, (b) *Pegohyperia princeps* with open abdomen and juveniles, (c) *Primno lattreillei*, (d) *Cyllopus magellanicus*, (e) *Cyphocaris richardi*, (f) *Scina* spp. (g) *Chevreuxiopsis franki*, that was is described in further detail in Chapter A, (h) *Eurythenes thurstoni*, (i) *Lanceola* sp., (j) *Parandania boecki*, (k) *Vibilia armata*, and (l) *Abyssorchomene abyssorum*. White scale bar: 1 mm.

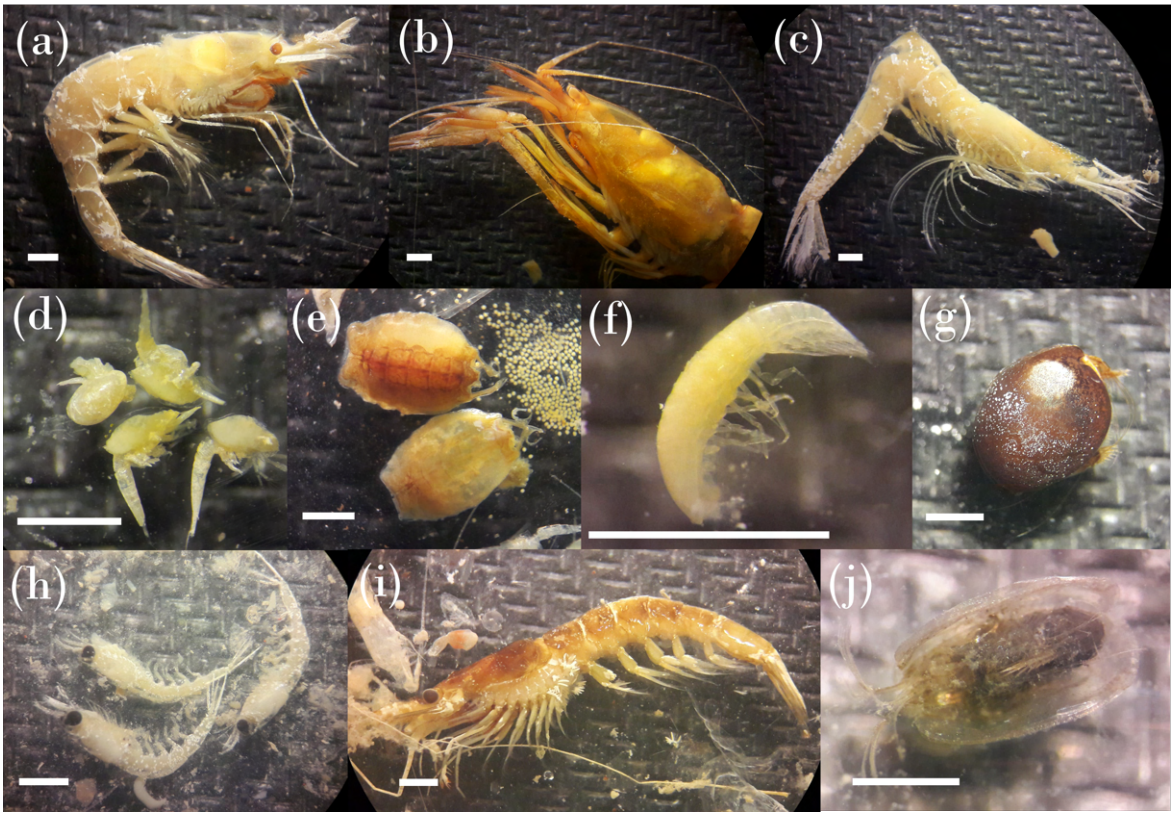

Figure 3.7: Crustaceans collected between 1997-2020. (a)-(c) Unidentified decapods, (d) crustacean larvae, (e)-(f) unidentified isopods (g) ostracod *Gigantocypris* sp., (h) euphausiid *Thysanoessa macrura*, (i) euphausiid *Euphausia* sp., (j) unidentified ostracod. White scale bar: 1 mm.

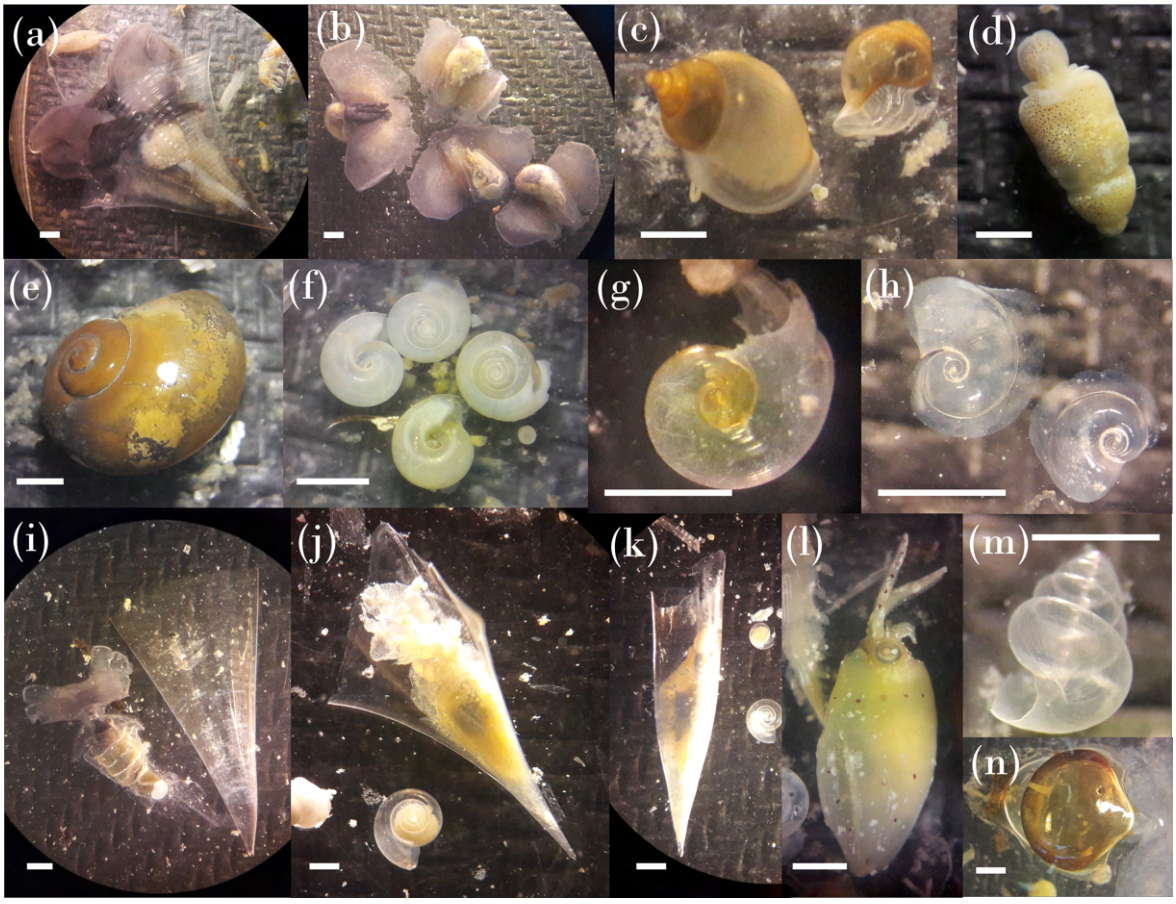

Figure 3.8: Molluscs collected between 1997-2020. (a) *Clio recurva*, (b) *Peracle* spp., (c) *Janthina* spp., (d) *Spongibranchia australis*, (e) *Limacina helicina antarctica*, adult, (f) *Limacina helicina antarctica*, juvenile, (g) *Helicoides inflatus*, (h) heteropod *Atlanta* spp., (i) *Clio pyramidata sulcata*, (j) *Clio pyramidata lanceolata*, (k) *Clio pyramidata antarctica*, (l) juvenile squid, (m) *Limacina retroversa australis*, (n) *Cavolinia tridentata*. White scale bar: 1 mm.

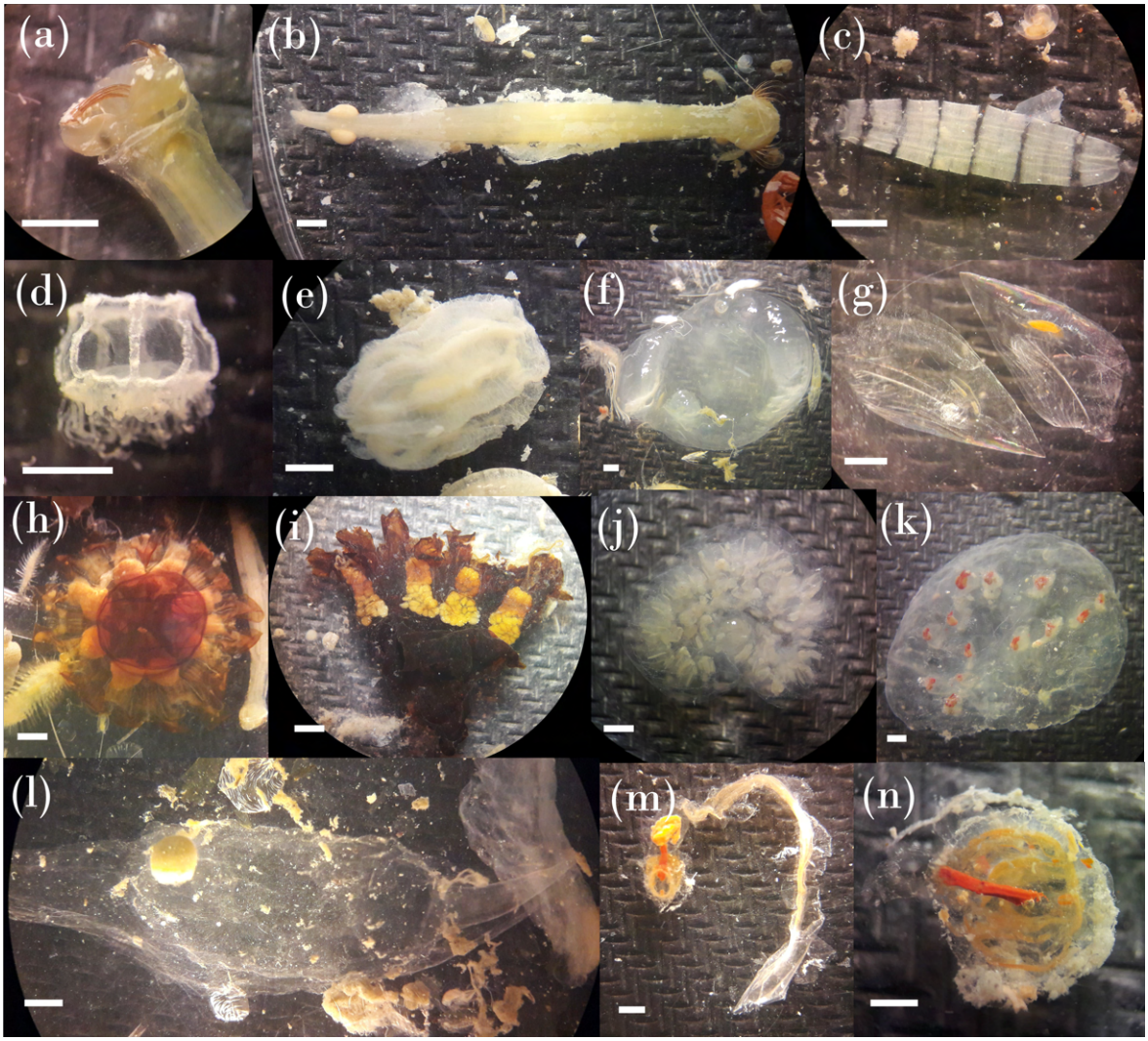

Figure 3.9: Gelantinous communities collected between 1997-2020. (a)-(b) Chaetognath (Sagittae family), (c) Doliolid, Tunicata, (d) jellyfish medusa (Cnidaria), (e) ctenophore, (f) jellyfish medusa (Cnidaria), (g) Siphonophore (*Diphyes* spp.), (h) *Atolla* sp. (Cnidaria), (i) *Periphylla periphylla* (Cnidaria), (j) pyrosome (*Pyrosoma atlanticum*), Tunicata, (k) pyrosome (*Pyrostremma* sp.), Tunicata, (l) salp (*Salpa thompsoni*), Tunicata, (m)-(n) giant larvacean, Tunicata (trunk and feeding basket). White scale bar: 1 mm.

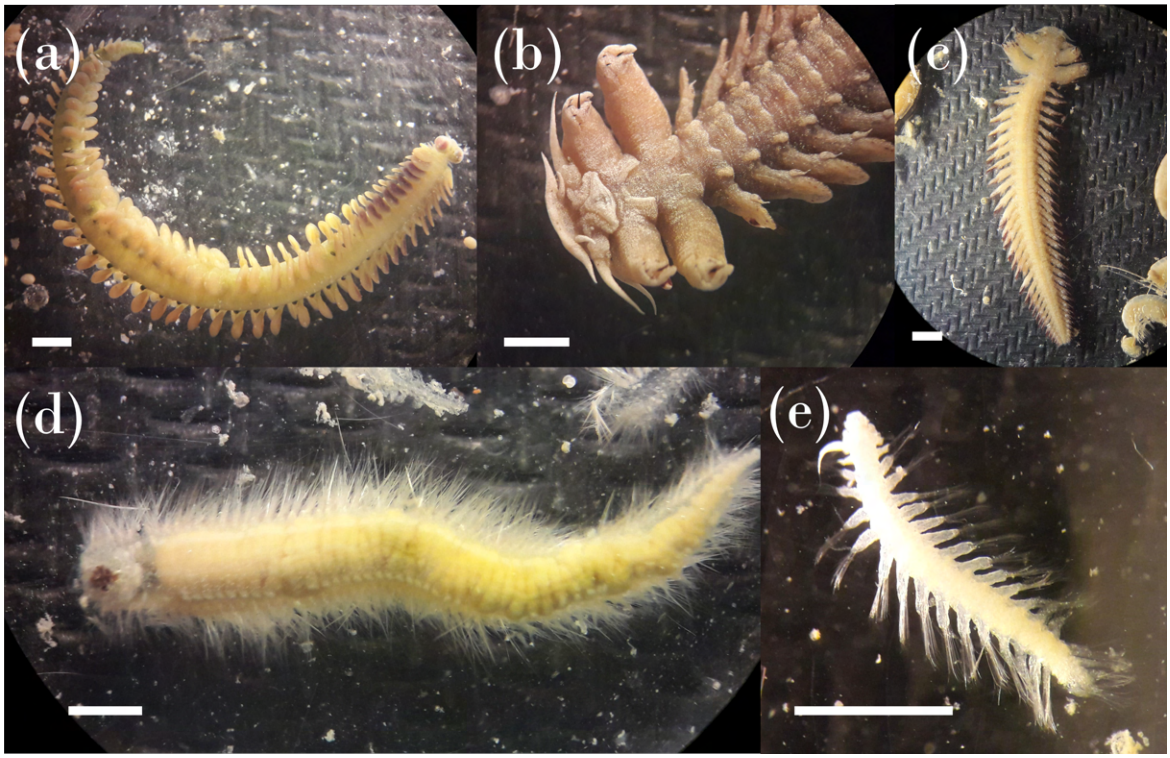

Figure 3.10: Polychaetes collected between 1997-2020. (a) family Alciopidae, (b)-(c) family Lopadorrhynchidae, (d) unidentified polychaete, (e) family Tomopteridae. White scale bar: 1 mm.

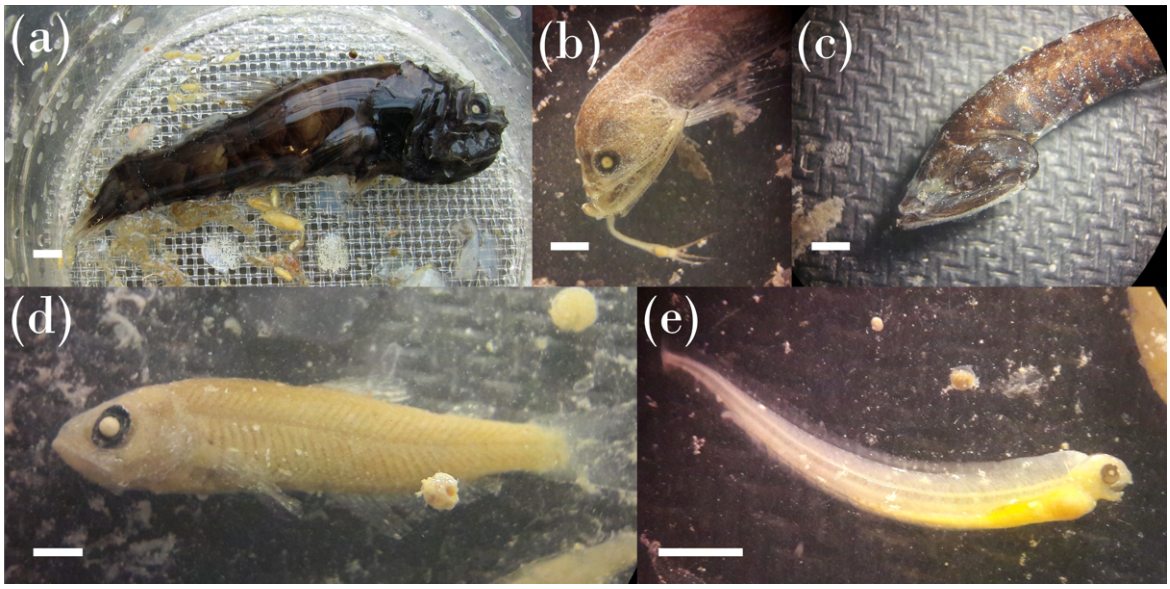

Figure 3.11: Fish collected between 1997-2020. (a) *Poromitra* sp., (b) *Stomias* sp., (c) *Cyclothones* sp., (d) family Myctophidae, (e) unidentified fish larvae. White scale bar: 1 mm.

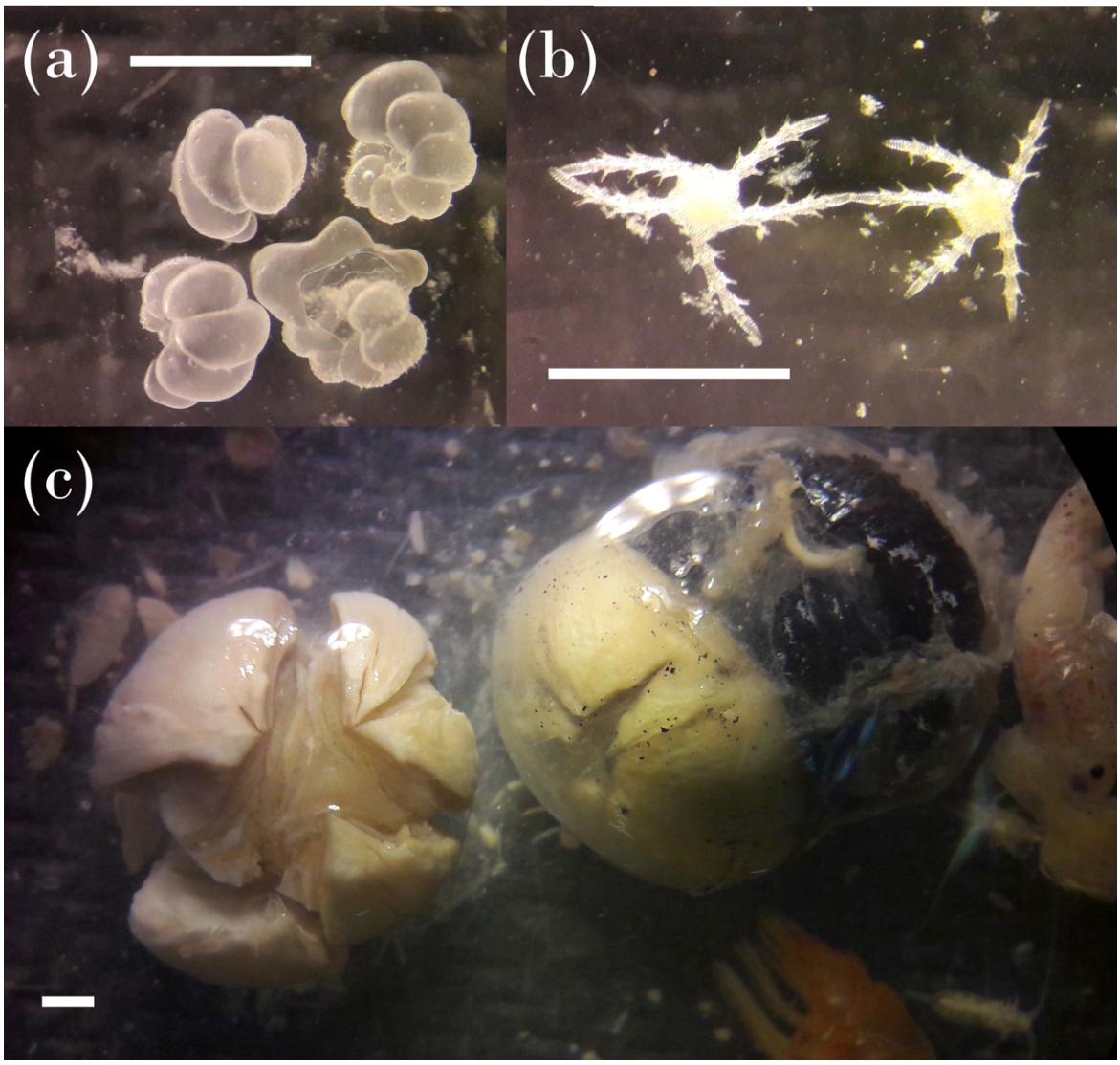

Figure 3.12: Other taxa collected between 1997-2020. (a) Giant foraminiferans, (b) ophiurids, Echinodermata, (c) closest identification: Balanomorpha (barnacles). White scale bar: 1 mm.

Chapter 4

"Sinking dead" – How zooplankton carcasses contribute to Particulate Organic Carbon flux in the subantarctic Southern Ocean

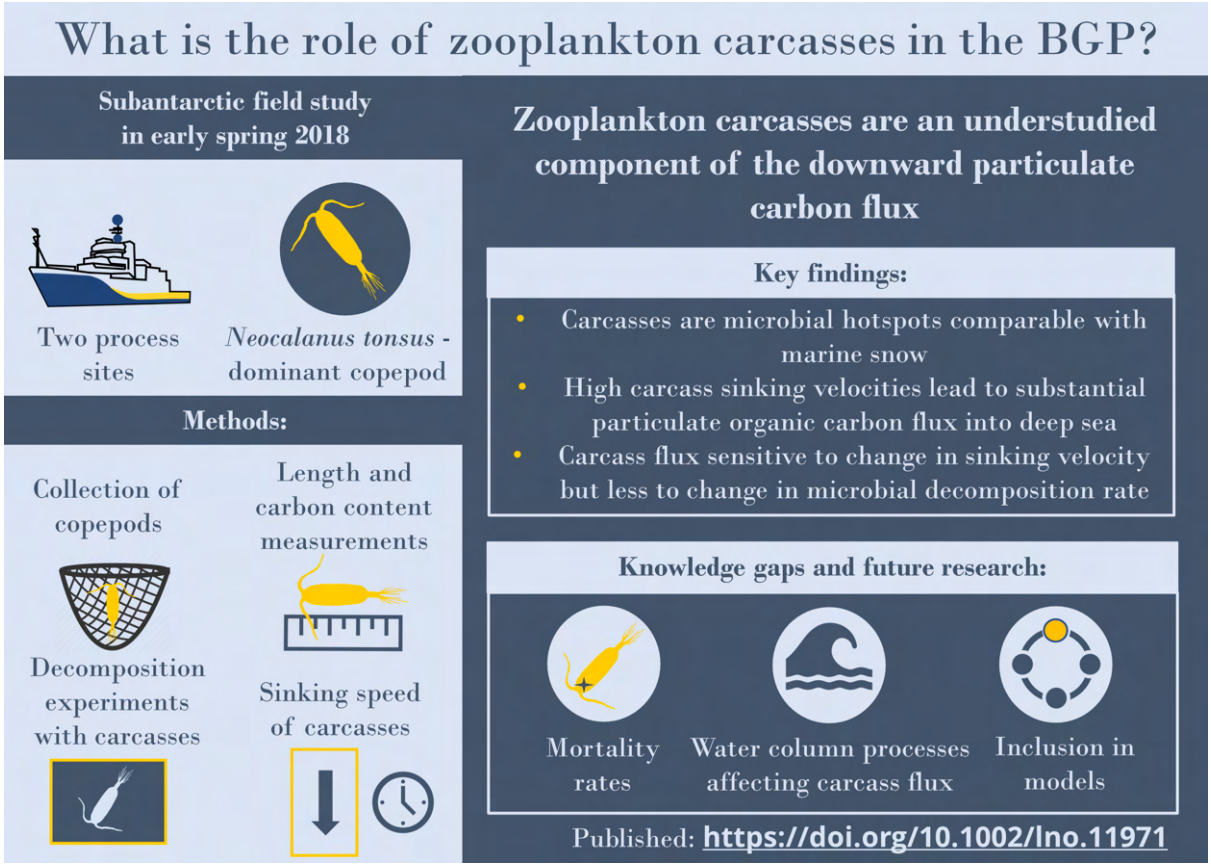

4.1 Abstract

Zooplankton carcasses are an important, yet understudied, pathway of the biological gravitational pump. To understand their contribution to the downward carbon flux in the subantarctic, carcasses of the copepod *Neocalanus tonsus* were analysed for carbon content, microbial remineralisation rates, and sinking velocities. In addition, the sensitivity of carcass flux to varying mortality, microbial turnover, and sinking velocity rates was analysed and compared to carbon flux measurements from sediment traps. Microbial decomposition rates (between 0.02 d^{-1} and 0.16 d^{-1}) were comparable to those of marine snow, highlighting the importance of carcasses as microbial hotspots. High sinking velocities (730 $\pm$ 182 m d^{-1}) suggest that particulate organic carbon flux to the deep ocean is substantial. Carcass flux is sensitive to a change in sinking velocity but appears less sensitive to fluctuations in microbial decomposition rate. More research on zooplankton mortality and the factors that influence carcass sinking through the water column is needed to quantify the carcass-mediated carbon export and enable their inclusion in marine ecosystem and biogeochemical models.

4.2 Introduction

The role of zooplankton in the biological gravitational pump has been intensively studied in recent decades (Boyd et al., 2019; Steinberg and Landry, 2017; Turner, 2002, 2015). In contrast to downward faecal carbon flux, however, zooplankton carcasses as vectors for carbon export have received less attention, despite their importance for marine carbon and nutrient cycles (Daase et al., 2014; Hirst and Kiørboe, 2002; Tang et al., 2014). As carcasses can sink rapidly (>100 m d^{-1}), they sequester carbon as well as supply food for deep-sea detritus feeders (Elliott et al., 2010; Kirillin et al., 2012; Tang et al., 2014). In addition, carcasses enhance nutrient regeneration via bacterial remineralisation within the water column, as they can be degraded quickly while sinking (Daase et al., 2014). Thus, understanding the balance between sinking velocity and microbial remineralisation rates is important to estimate the contribution of carcasses to carbon sequestration and nutrient recycling. Non-consumptive mortality, i.e. mortality not caused by predation, accounts for up to one-third of total mortality in freshwater and marine zooplankton populations (Dubovskaya et al., 2003; Hirst and Kiørboe, 2002; Tang et al., 2014). Mortality

rates, as reviewed by Daase et al. (2014) or Hirst and Kiørboe (2002), vary with temperature (Hirst and Kiørboe, 2002), developmental stage (Yáñez et al., 2019) or season (Sampei et al., 2012). Causes for mortality include food limitation, natural death caused by ageing, or infections (Sampei et al., 2012). Mortality is difficult to measure in the field and most mortality estimates are more readily available for accessible coastal regions or freshwater bodies than for the open ocean.

The subantarctic Southern Ocean is an important region for carbon sequestration due to mode water formation that transports heat, gases and particles to the deep sea (Rintoul and Trull, 2001; Bowie et al., 2011a). One of the most abundant copepods in the region is the neocalanoid copepod species *Neocalanus tonsus* (Bradford-Grieve, 1999; Bradford-Grieve and Jillett, 1998), the size (∼3.5 mm) and role of which in the subantarctic ecosystem are comparable to their northern hemisphere counterparts *Neocalanus cristatus*, *N. plumchrus* or *N. flemingeri* in the subpolar Pacific (Kobari et al., 2008). *N. tonsus* has a seasonal vertical migration pattern: the population lives at the surface in spring and summer and descends to deeper waters (between 500 m and at least 1,300 m depth) as copepodite stage V (CV) or adult (Ohman et al., 1989; Miller et al., 1999). Most of the population reproduces at depth with only the juveniles ascending in spring, however, some females return to the surface in spring to feed on phytoplankton and reproduce (Bradford-Grieve et al., 2001; Jillett, 1968; Miller et al., 1999; Ohman et al., 1989; Saito and Tsuda, 2000).

In this chapter, the zooplankton community in the subantarctic Southern Ocean dominated by *N. tonsus*, was sampled in early spring to explore the role of *N. tonsus* carcasses in downward carbon flux and nutrient recycling. Based on sinking velocity and microbial decomposition, the potential carbon flux by carcasses out of the epipelagic zone was calculated and compared with particulate organic carbon flux collected by sediment traps. In addition, the sensitivity of downward carcass flux estimates to alteration in mortality rate, sinking velocity and microbial decomposition was tested.

4.3 Methods

4.3.1 Study area and environmental conditions

The subantarctic Southern Ocean was sampled during voyage IN2018_V04 on the RV Investigator in September/October 2018 (Figure 4.1). Process Station 1 (PS1; 46°54 S, 141°53 E) in low iron High-Nutrient Low-Chlorophyll (HNLC) waters is also the location of the Southern Ocean Time Series (SOTS) site, with year-round moorings comprising sediment traps and a suite of atmospheric and pelagic sensors (Trull et al., 2010). Process Station 2 (PS2; 45°44 S, 153°31 E) to the east usually exhibits higher surface iron concentrations supplied by the East Australian Current (EAC) (Bowie et al., 2011b). Environmental properties for the upper 200 m zone, including salinity, temperature, pressure, chlorophyll fluorescence, and photosynthetically active radiation, were measured with a Seabird SBE911 CTD 36. The average sea surface chlorophyll *a* concentration, as proxy of phytoplankton biomass, was accessed from the NASA ocean colour server (https://oceancolor.gsfc.nasa.gov/cgi/l3) for September 2018 (Figure 4.1). In addition, seawater samples from the Niskin bottle rosette were collected to determine the in-situ chlorophyll *a* concentration. Seawater was filtered onto 47-mm glass fibre filters (Whatman GF/C) as soon as possible after collection. Chlorophyll *a* was extracted from the phytoplankton cells by placing the filters in 90% acetone in the dark for >24 hours at -20°C, and a Turner Designs model 10-AU fluorometer determined chlorophyll *a* concentration (Axler and Owen, 1994). For the analysis of particulate organic carbon (POC) and particulate organic nitrogen (PON) in the water column, seawater was sampled from 5, 50, 100, 150, and 200 m water depths and filtered through 13 mm QMA quartz filters in a closed system to reduce contamination. 1 L of seawater was filtered from the shallower depths (5 and 50 m) with high concentration of particulate matter, and 2 L from the remaining depths. The filters were dried for 24 hours at 60°C and then stored with desiccant until further analysis. Back on land, the filters plus three blanks (untreated filters) were placed in silver cups, acidified with 20 μL 2N HCl Suprapur to remove inorganic carbon, and fumed overnight. Samples were then dried again for 2 days at 60°C. The cups were pelletised and analysed at the Central Science Laboratory (University of Tasmania), using a Thermo Finnigan EA 1112 Series Flash Elemental Analyser. Combustion of the pellets was achieved in ultra-high purity oxygen at 1000 °C using tungsten oxide on alumina as an oxidising agent, followed by reduced copper wires as a reducing

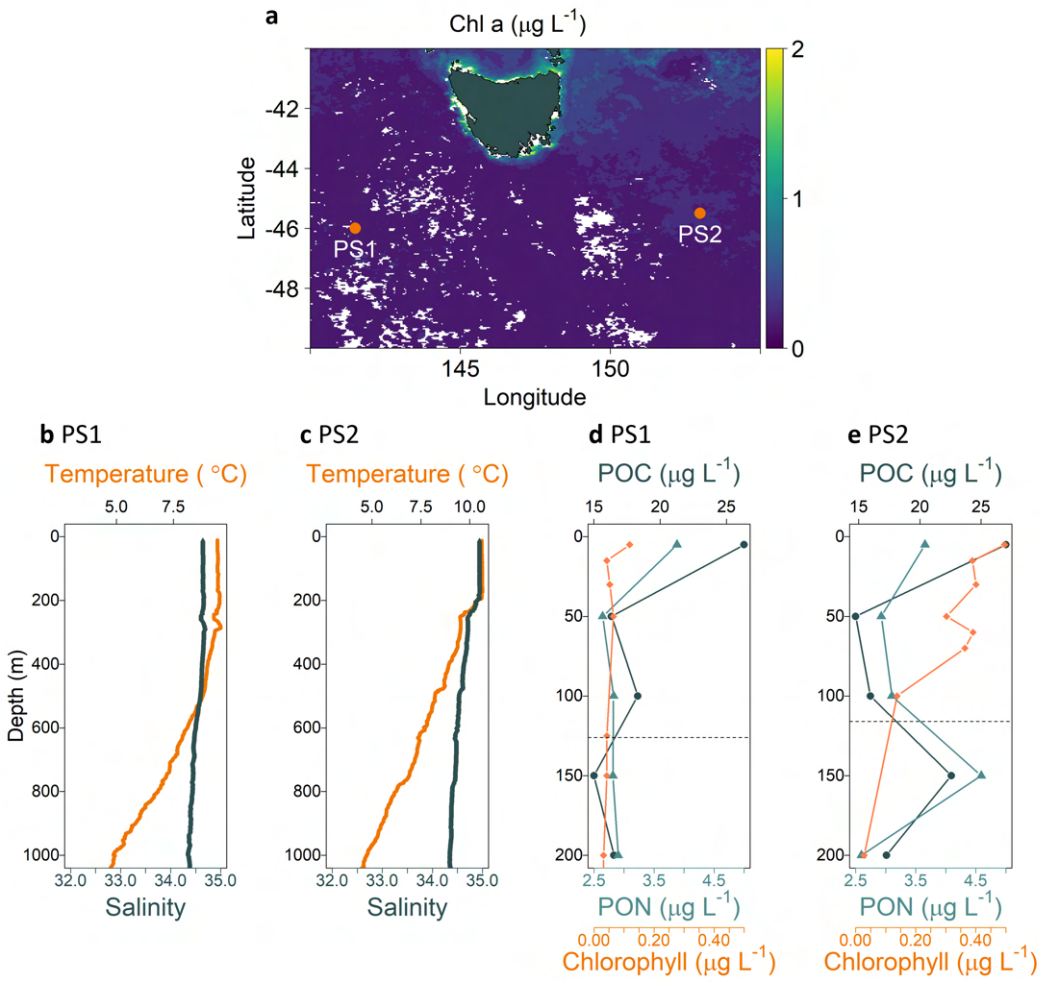

Figure 4.1: (a) Mean chlorophyll *a* (in µg L^{-1}) in the subantarctic Southern Ocean south of Tasmania (green shaded land-mass) in September 2018, derived from MODIS satellite data. White areas indicate cloud cover. The sampling sites are marked in orange. (b) and (c) CTD data of temperature (°C) and salinity in the upper 1000 m at PS1 and PS2, respectively. (d) and (e) Measured particulate organic carbon (dark grey), particulate organic nitrogen (light grey), and chlorophyll *a* concentration (orange) of the upper 200 m at PS1 (left) and PS2 (right). All values are in μg L^{-1}. The lower limit of the euphotic zone is marked at 126 m (PS1) and 116 m (PS2). It was calculated as the depth of 1% of the surface photosynthetically active radiation relative to the surface radiation, measured by the CTD, following Kirk (1994) and Lee et al. (2007). The mixed layer is deeper at both stations (329 m and 199 m at PS1 and PS2, respectively) and is therefore not depicted here.

agent. The results were calibrated using a certified sulphanilamide standard.

4.3.2 Zooplankton sampling and sorting

A Bongo net with a 250 μm mesh size, an opening area of 0.5 m^2 for each net, and an attached flowmeter (General Oceanics) was deployed in vertical tows from 200 m depth to the surface, with a towing speed of less than 15 m min^{-1}. Hard cod ends with small-meshed windows facilitated gentle sampling of zooplankton. Sampling took place at around midday (12:00 - PS2 and 11:00 - PS1, local time) and midnight (1:30 - PS2 and 23:00 - PS1, local time) to account for day and night distribution differences due to diel vertical migration. One net sample was preserved in 4% formaldehyde-seawater solution, and zooplankton were identified to the lowest taxonomic level possible under a WILD stereo microscope (magnification 50×). All specimens of the rarer species (<100 individuals) were counted, while for more abundant species the sample was split and at least 100 individuals were counted. Zooplankton from the second net sample were gently transferred into buckets (40 L) in a constant temperature room set at the in-situ temperature of the surface waters (∼11°C), where they were incubated for at least 12 hours to acclimate to laboratory conditions. All following measurements and experiments were conducted with *N. tonsus* individuals from these incubations.

4.3.3 Carcass carbon and nitrogen analyses

To estimate the POC standing stock of the surface *N. tonsus* population, 37 and 24 copepods at PS1 and PS2, respectively, were randomly selected with a large pipette to avoid body damage from the incubations. The prosome length was measured under the microscope and intact animals were frozen separately in well-plates at -80°C. Back on land, the specimens were gently placed in water baths of filtered freshwater to remove the remaining salt and then dried to constant mass for at least 24 hours at 60°C. Copepods with dry weights above the limits of accuracy (0.1 mg) were weighed into tin capsules using a Sartorius SE2 ultra-microbalance. The cups were pelletised and analysed as described for the POC/PON filters above.

4.3.4 Microbial decomposition and sinking velocities of copepod carcasses

To quantify the attenuation of carcass carbon through the water column, the microbial respiration rate in the water surrounding the carcasses was measured over 24 hours. Twenty-four *N. tonsus* individuals were selected at PS2, placed in approximately 100 mL filtered seawater, and killed by adding 2-4 mL (bottled) soda water. To confirm their mortality, the copepods were analysed under the stereo microscope for movement of appendages and heartbeat; they were physically stimulated with forceps and assumed to be dead if no reaction was shown. Carcasses were then gently removed with forceps and placed in two consecutive seawater baths to remove the remaining soda water. Their prosome length was measured, and two specimens were placed in each of 12 acid-cleaned borosilicate micro-respiration vials of 10 or 20 mL. The vials were filled with seawater from the ship's underway system filtered through a 200-μm mesh to remove larger organisms. The vials were closed with a lid with a capillary hole without introducing air bubbles and then placed in water tanks to prevent gas exchange. Incubations were run in the dark to avoid oxygen production via photosynthesis, or dissolved organic carbon release by phytoplankton, which is light-dependent (Cherrier et al., 2015). Over 24 hours, the dissolved oxygen concentration in μmol L^{-1} of the water was measured every 3 hours with a Presens micro-electrode after gently inverting the vials to homogenise the seawater. We assume that the respiration is carried out by prokaryotes and protists smaller than 200 µm, either free-living in the water or associated with the copepod carcass. The bacterial decomposition of a second batch of *N. tonsus* carcasses was measured for 24 hours following the first experiment to increase the number of replicates. Three controls with seawater without carcasses were conducted in a parallel set-up to determine the respiration rate of free-living bacteria. To determine the POC turnover, dissolved oxygen consumption rates in the vials minus the control runs (µmol L^{-1} h^{-1}) were calculated using linear regression as described in Cavan and Boyd (2018). All vials showed significant dissolved oxygen decrease (linear regression, $p<0.05$) over 24 hours and were therefore included in the analysis. The oxygen consumption rates were then converted from μmol L^{-1} h^{-1} to µmol h^{-1} by multiplying by the volume of the vials (0.01 L or 0.02 L). The POC masses of the copepods in each vial were converted from μg per copepod to μmol to calculate the microbial POC turnover rate (k, h^{-1}). We assumed a respiratory quotient (RQ) of 1 mol O_2 to 1 mol CO_2 (Bach et al., 2012; Ploug and Grossart, 2000;

Trimmer et al., 2012). To enable a comparison to other studies k is expressed as a rate per day.

$$\mathrm{k}\,(d^{-1}) = \frac{\text{oxygen consumption}\,(\mu\,\mathrm{mol}\,h^{-1}) \times \mathrm{RQ}}{\text{POC mass}\,(\mu\,\mathrm{mol})} \times 24\,\mathrm{h} \tag{4.1}$$

In total, 107 and 84 *N. tonsus* from PS1 and 2, respectively, were selected under the microscope, killed with soda water, their mortality confirmed, and prosome length measured (as described above). The carcass sinking velocity was measured in a settling column enclosed in another cylinder connected to the seawater flow-through system to minimise convection. After the carcasses were placed gently into the upper settling column, the time to sink to 20 cm was measured and converted to velocity (m min^{-1}). Carcasses with ruptured carapaces due to handling, or that were slowed artefactually by interactions with the cylinder walls, were excluded from further analysis. The difference in carcass sinking velocity between samples collected from the two stations was tested with a Welch Two Sample t-test. Microbial decomposition and sinking speed could not be calculated for the same *N. tonsus* individuals due to logistical restrictions.

4.3.5 Calculation of the downward carcass flux

Sinking velocity was used together with microbial decomposition to estimate carcass carbon flux at three depths: 1000, 2000, and 3800 m. These depths were chosen to compare potential carcass flux with POC flux estimated from sediment traps at SOTS (see below). First, the remineralisation length scale (RLS, z*), which represents the fractional remineralisation in particles per m settled (Iversen and Ploug, 2010), was calculated by dividing the sinking velocity w (m d^{-1}) by the microbial turnover rate (k, d^{-1}). Due to technical difficulties with the oxygen measurements, k could only be calculated at PS2, which was then applied to PS1. We discuss this potential source of error below.

$$z* = \frac{w}{k} \tag{4.2}$$

To calculate the total downward carbon flux (F_z) at depths (z) 1000, 2000, and 3800 m, we used an exponential function as described in (Boyd and Trull, 2007) with F_z0 as the

reference flux at depth z_{200} calculated as the percentage of carcasses leaving the surface water (in d^{-1}) multiplied by the total carbon stocks of *N. tonsus* in 0-200 m (in mg C m^{-2}). This accounts for the flux attenuation with depth due to microbial decomposition. The carbon stock values were averaged between day and night for each respective station.

$$F_z = F_z0 \times e^{\frac{z-z200}{z*}} \tag{4.3}$$

These estimates provide information about how much carbon is leaving the mesopelagic zone (200-1000 m depth), a region of high microbial remineralisation and particle attenuation (Buesseler and Boyd, 2009). Finally, we calculated the non-consumptive mortality rate to estimate the downward carcass carbon flux by using the relationship between temperature (T, °C) and total mortality rate (β, d^{-1}) for broadcast spawners as established by Hirst and Kiørboe (2002).

$$log_e\beta = 0.0725 \times T – 3.415 \tag{4.4}$$

With surface temperatures of 9.46°C (PS1) and 10.63°C (PS2), total surface mortality is 0.065 d^{-1} and 0.071 d^{-1} at PS1 and 2, respectively. Assuming one-third of the total mortality is due to non-consumptive mortality (see Hirst and Kiørboe, 2002), this results in 0.021 d^{-1} and 0.023 d^{-1} for PS1 and PS2. Using the mortality rates for the two stations, the carcass carbon flux out of the epipelagic can be calculated for the three depths of interest.

4.3.6 Comparison to particulate matter in sediment traps

To compare the estimates for potential carcass flux, the POC flux data from the deep sediment trap mooring at the SOTS site were accessed. SOTS is a sub-facility of the Australian Integrated Marine Observing System (IMOS) and has been serviced regularly since 1997. In 2018, the sediment traps (McLane Parflux, 21-cup) were deployed at 1000, 2000, and 3800 m water depth from 22/03/2018 - 25/02/2019. Details of deployment, sample processing, and quality control are described in detail by Wynn-Edwards et al. (2020). Data is publicly available on the Australian Ocean Data Network (AODN)

(http://thredds.aodn.org.au/thredds/catalog/IMOS/ABOS/SOTS/catalog.html, April 2021).

4.3.7 Sensitivity of downward carbon flux to controlling factors

In addition to temperature, copepod mortality varies with developmental stage and season, among other factors. For example, Yáñez et al. (2019) calculated the mortality of copepod nauplii in the Chilean Humboldt Current to be close to the global rates estimated by Hirst and Kiørboe (2002), but found increased mortality rates at later copepodite stages for the species *Calanus chilensis* (0.14 d^{-1} for copepodite stage IV (CIV) 0.19 d^{-1} for copepodite stage V (CV), calculated from Table 3). Tang et al. (2006) estimated a higher non-consumptive mortality rate for estuarine and oceanic copepods (0.1 d^{-1}), while Sampei et al. (2020) measured a high copepod carcass flux in late winter due to the end of their life cycle. Given that most *N. tonsus* individuals die after reproduction (Bradford-Grieve et al., 2001), the mortality rates are likely higher, which can lead to an underestimation of the carbon flux by copepod carcasses. Therefore, in this study, the average of the two mortality rates given by Yáñez et al. (2019), 0.14 d^{-1} and 0.19 d^{-1} (i.e. 0.17 d^{-1}), was used as the upper limit to analyse the sensitivity of carcass flux to a change in mortality. Parameters such as sinking velocity and microbial decomposition change throughout the water column. To understand the impact of variability in these factors, the following scenarios were tested: first, a lower sinking velocity (107 m d^{-1}) that was calculated for copepod carcasses (CIV-adult) in 15°C and normal dissolved oxygen concentration from Table 3 in Elliott et al. (2010); and second, higher microbial remineralisation (0.17 d^{-1}) and lower remineralisation rate (0.02 d^{-1}), representing the upper and lower range of microbial turnover rates estimated in this study. All data files and R code to perform the calculations and produce the figures of this manuscript are available under https://github.com/SvenjaHalfter/Zoopl_carcass.

4.4 Results

4.4.1 Environmental conditions

Conditions were representative of early spring in the subantarctic zone. Temperatures were on average 9.46°C and 10.63°C in the upper 200 m for PS1 and PS2, respectively, close to the winter temperature of the mixed layer of approximately 9°C (Rintoul and Trull, 2001). A slightly higher salinity was measured at the eastern station PS2 (34.94) than at the western PS1 (34.65), an indicator for a southward extension of the EAC. Low variation in temperature and salinity with depth indicated a well-mixed surface layer at both stations, down to 329 m (PS1) and 199 m (PS2). The euphotic zone was shallower than the mixed layer at both stations (126 at PS1 and 116 m at PS2). The upper water column at station PS2 was more productive compared to PS1 with slightly higher chlorophyll *a* concentrations evident from satellite and in-situ measurements (Figure 4.1). Whereas the chlorophyll *a* concentration at PS1 peaked at the surface (0.15 µg L^{-1}) but was very low throughout the mixed layer, PS2 showed higher values (0.3-0.5 μg L^{-1}) in the upper 150 m. Particulate organic carbon levels were highest at the surface at both stations (26.33 and 27.03 μg L^{-1} for PS1 and PS2, respectively), and decreased below subsurface maxima at 100 m and 150 m for PS1 and PS2. Particulate organic nitrogen followed a similar trend with peak values at the surface (3.88 μg L^{-1} at PS1 and 3.65 μg L^{-1} at PS2) and subsurface maxima at the same depths.

4.4.2 Epipelagic *N. tonsus* abundances

N. tonsus dominated the adult copepod community. Higher abundances were found at PS1 (3.38 ± 0.6 ind. m^{-3}). Here, the majority were collected during the night (4.1 ind. m^{-3}) and consisted of adults and small CIV/large CV copepodite stages, while during the day mostly adults were present (Figure 4.2). By comparison, at PS2, lower abundances were measured on average (2.72 ± 1.0 ind. m^{-3}) and higher numbers of mainly large CIV and small CV and low numbers of adults were encountered during the day (3.7 ind. m^{-3}), while only adults were collected at night (1.7 ind. m^{-3}).

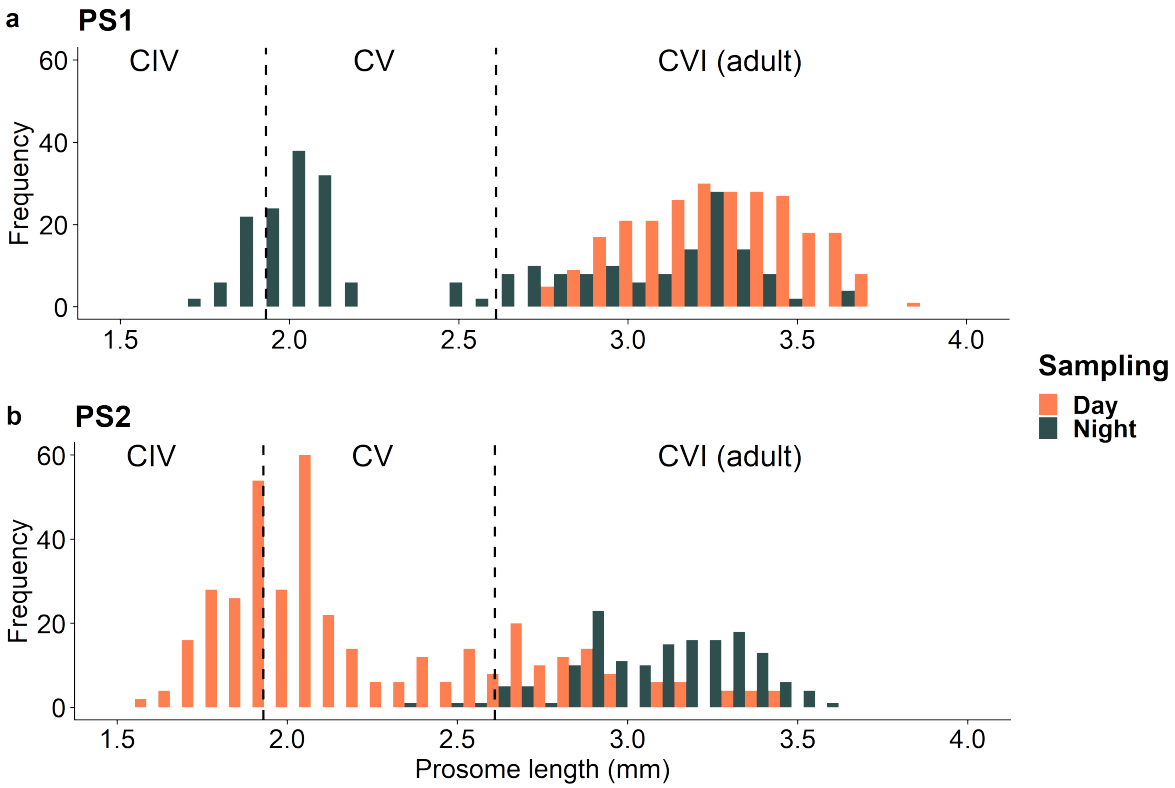

Figure 4.2: Size distribution of *N. tonsus* copepods (copepodites and adults) is displayed for site PS1 (a) and PS2 (b), the orange bars indicate sampling during the day, grey during the night. Dashed lines indicate approximate size boundaries for *N. tonsus* copepodite stage IV (CIV), copepodite stage V (CV) and adult (CVI), as outlined in Bradford et al. (1988).

4.4.3 Carcass carbon content decomposition and sinking velocities

The relationship between prosome length, dry weight, and individual carbon content of the selected stage CV and adult *N. tonsus* carcasses were tested with linear regression models (Figure 4.3). The strongest positive relationship was observed between individual dry weight and carbon content ($p<0.01$, $R^2 = 0.69$, Figure 4.3), followed by prosome length to dry weight ($p<0.01$, $R^2 = 0.59$, data not shown). The weakest relationship was between prosome length and carbon content ($p<0.01$, $R^2 = 0.24$). The following equations were produced from the linear regression analysis:

$$\text{Dry weight } (\mu g) = 469.64 \times \text{prosome length } (mm) - 1123.06 \tag{4.5}$$

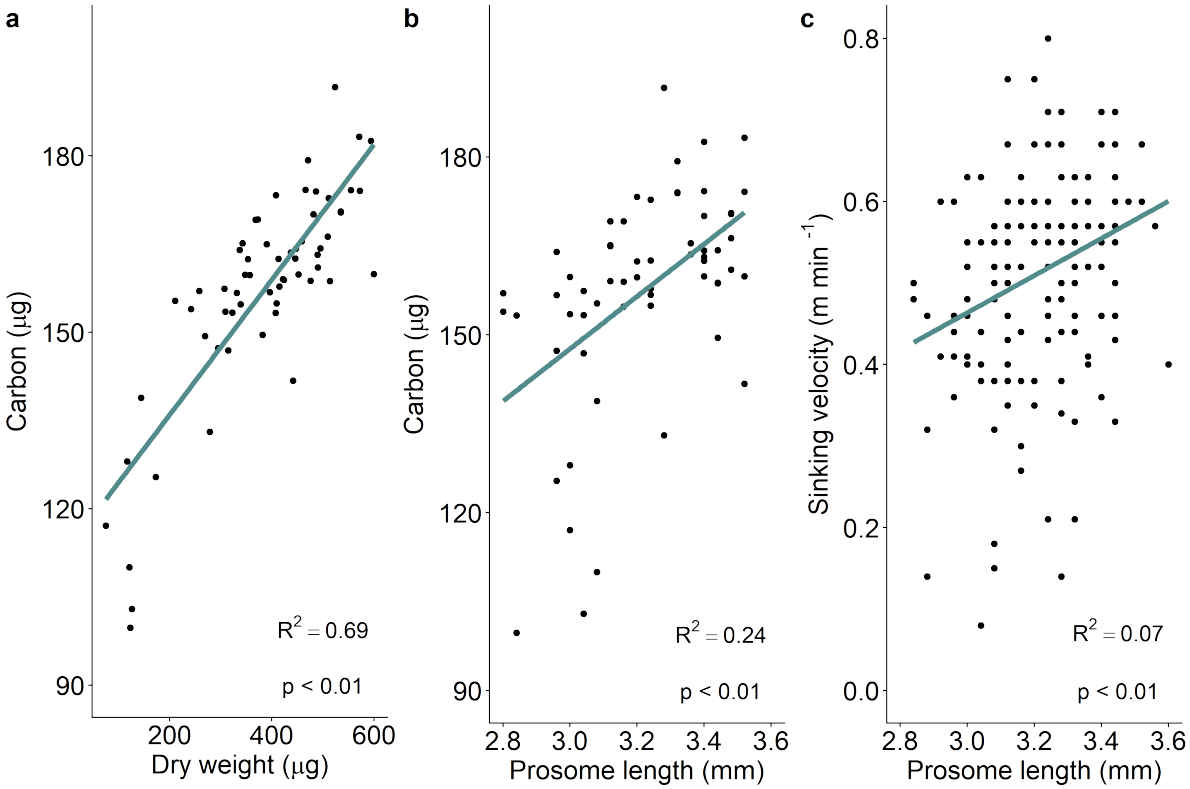

Figure 4.3: Relationship between (a) copepod dry weight (μg) to carbon per individual, (b) prosome length (mm) to carbon per individual and (c) prosome length to sinking velocity (m min^{-1}). The calculated linear trend lines are added and the p and R^2 values are displayed.

$$\text{Carbon } (\mu g \text{ copepod}^{-1}) = 41.64 \times \text{prosome length } (mm) + 23.52 \tag{4.6}$$

$$\text{Carbon } (\mu g \text{ copepod}^{-1}) = 0.12 \times \text{dry weight } (\mu g) + 112.93 \tag{4.7}$$

Exponential models were also fitted for comparison, but were excluded due to a lower R^2. Using the *N. tonsus* abundances and equations above, the standing stock of carbon in the upper water column was calculated. Overall, a higher amount of carbon was stored in the *N. tonsus* community at PS1 compared to PS2 (75.5 mg C m^{-2} and 70.0 mg C m^{-2}), though the concentrations varied between day and night being higher during the day at PS1 (82.3 mg C m^{-2}) and at PS2 (92.2 mg C m^{-2}).

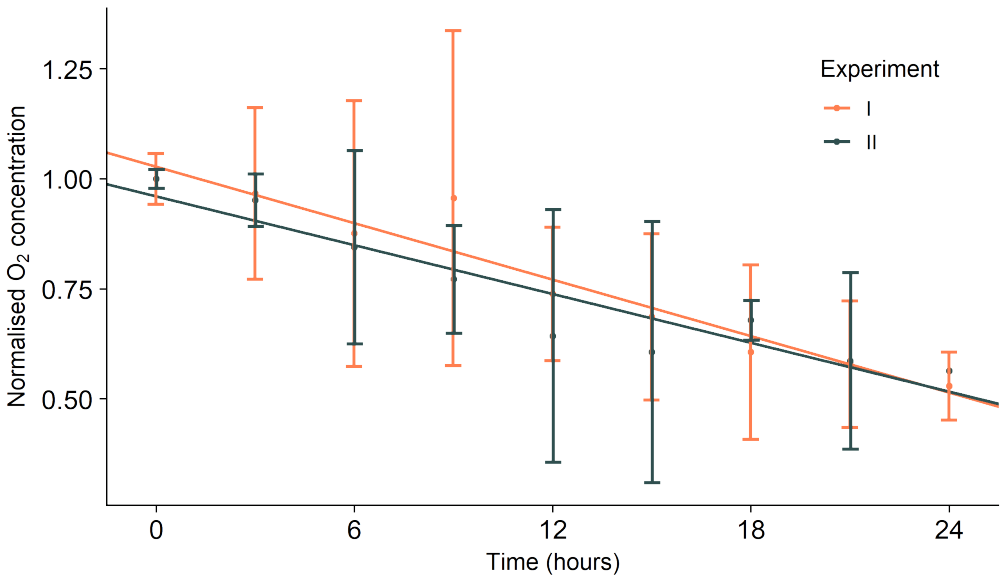

Figure 4.4: The normalised dissolved oxygen decline in two decomposition experiments (replicates) at PS2 over 24 hours. The error bars depict the standard deviation. The linear regressions are displayed for both experiments.

The two batches of replicates of carcass decomposition incubations differed significantly in their oxygen decline (Welch Two Sample t-test, $p<0.05$), between 5.12 ± 1.21 μmol L^{-1} h^{-1} (experiment 1) and 7.62 ± 2.90 μmol L^{-1} h^{-1} (experiment 2) (Figure 4.4). The dissolved oxygen concentrations in the controls remained constant (<5% decline, on average -2.8% over 24 hours) over the measured period (data not shown). To exclude eventual anaerobic respiration, vials with dissolved oxygen concentration <100 μmol were excluded before calculating the dissolved oxygen decline in both experiments. After normalising the oxygen concentration to show the relative decline, the slopes of both curves were very similar (m=0.021% L^{-1} h^{-1} for batch 1 and m= 0.019% L^{-1} h^{-1}, for 2, Figure 4.4). Dissolved oxygen uptake rates were not dependent on individual copepod dry weight or carbon content (linear regression, R^2=0.04, $p>0.05$). The average dissolved oxygen consumption (uptake rates multiplied by the volume of the vials) were 0.09 ± 0.04 μmol h^{-1} in batch 1 and 0.13 ± 0.04 µmol h^{-1} in batch 2. The microbial POC turnover rates k (d^{-1}) differed significantly between the experiments (Welch Two Sample t-test, p¡0.05) and ranged from 0.02 to 0.13 d^{-1} (mean: 0.09 ± 0.03 d^{-1}) in batch 1 and from 0.06 to 0.16 d^{-1} (mean: 0.12 ± 0.03 d^{-1}) in batch 2 (total average: 0.11 ± 0.04 d^{-1}). On average, the selected copepod carcasses sank at 731 ± 182 m d^{-1} (115.2-1152 m d^{-1},

Figure 4.3). The sinking velocity was significantly different between the sites (Welch Two Sample t-test, $p<0.01$), though the prosome lengths showed only minor differences between stations (3.23 at PS1 and 3.18 mm at PS2, $p>0.05$). *N. tonsus* carcasses sank at 797 ± 175 m d^{-1} at PS1 and were slower at PS2 (671 ± 169 m d^{-1}).

4.4.4 Carcass sinking flux relative to downward POC flux

Using the calculated parameters of carbon standing stock in the *N. tonsus* community, mortality rates, carcass decomposition and sinking velocity (defined in Table 4.1), and the derivate remineralisation length scale z*, the estimated carcass flux varied only slightly between stations (Table 4.2). Based on a comparison with the downward POC flux estimated from sediment traps, carcasses export a large amount of carbon to the deep and their importance increases with depth: the carcass carbon flux equals approximately 31-32%, 39-41% and 42-45% of the downward POC flux at 1000, 2000, and 3800 m depths, respectively (Table 4.2). The sensitivity analysis showed that the carcass flux estimations were highly sensitive to uncertainty in mortality rates. When using a higher mortality rate as reported by Yáñez et al. (2019) for the Chilean Humboldt Current region, the flux increased by an order of magnitude, which was three times the amount of POC flux by marine snow. The increase in mortality rate led to a linear increase in carcass flux (i.e. approximately by the factor 8 in this example) compared to the control run. An 84-87% reduction in sinking velocity of carcasses as potentially observed with decreasing body size, decreases the downward carcass flux by ∼54-55% (1000 m), ∼80-81% (2000 m), and ∼95-96% (3800 m), compared with the control run. Similarly, increasing the microbial decomposition rate results in a decrease in carcass flux, though the flux does not appear to be as sensitive to a change in microbial decomposition than to changing mortality rates or sinking speed. An increase in k by ∼45%, translates into a decrease in downward carcass flux by 6%, 11-14%, and 21-24% at 1000 m, 2000 m, and 3800 m, respectively. On the other hand, decreasing the microbial decomposition rate by 83% leads to an increase in flux by 12-15%, 27-32% and 59-73% at 1000 m, 2000 m, 3800 m.

Table 4.1: Parameters used in the sensitivity analysis to estimate carcass downward carbon flux. Numbers in bold indicate the parameter that has been changed relative to the control experiment. The mortality rates were calculated based on an equation by Hirst and Kiørboe (2002) and measurements by Yáñez et al. (2019). The sinking velocity was either measured in this study or calculated from Table 3 in Elliott et al. (2010). The upper and lower rates of microbial decomposition represent the highest and lowest measured k during this study (0.17 and 0.02 d^{-1}).

Parameters	Site	Control	Higher mortality rate	Lower sinking speed	Higher microbial decomposition	Lower microbial decomposition
Carbon standing stock (mg C m^{-2})	PS1	75.5				
	PS2	70.0				
Mortality rate (β)	PS1	0.021	**0.17**	0.021	0.021	0.021
	PS2	0.023	**0.17**	0.023	0.023	0.023
Microbial decomposition (k, d^{-1})		0.11	0.11	0.11	**0.16**	**0.02**
Sinking velocity (w, m d^{-1})	PS1	797	797	**107**	797	797
	PS2	671	671	**107**	671	671

Table 4.2: Sensitivity analysis comparing carcass sinking fluxes in mg C m^{-2} d^{-1} at 1000, 2000, and 3800 m depth in comparison with POC fluxes (mg C m^{-2} d^{-1}) estimated from sediment traps at SOTS in mid-October (midpoint date: 12 October, 2018). Ranges in parentheses consider the variability between day and night biomass and standard deviation in sinking velocity and microbial respiration.

Depth (m)	Site	Control	Higher mortality	Lower sinking velocity	Higher microbial decomposition	Lower microbial decomposition	POC (Sediment trap, SOTS)
1000	PS1	1.40 (1.16-1.62)	11.34 (9.41-13.11)	0.63 (0.41-0.96)	1.32 (1.15-1.49)	1.55 (1.40-1.70)	4.43 ± 0.12
	PS2	1.39 (0.84-1.97)	10.27 (6.21-14.54)	0.64 (0.31-1.17)	1.30 (0.83-1.79)	1.57 (1.06-2.08)	
2000	PS1	1.22 (0.91-1.51)	9.87 (7.40-12.20)	0.22 (0.10-0.50)	1.08 (0.89-1.26)	1.51 (1.36-1.66)	3.00 ± 0.08
	PS2	1.18 (0.62-1.81)	8.72 (4.61-13.38)	0.23 (0.08-0.61)	1.02 (0.60-1.48)	1.52 (1.02-2.03)	
3800	PS1	0.95 (0.59-1.32)	7.70 (4.81-10.71)	0.04 (0.01-0.15)	0.75 (0.56-0.94)	1.44 (1.28-1.60)	2.10 ± 0.06
	PS2	0.88 (0.36-1.56)	6.49 (2.69-11.52)	0.04 (0.01-0.19)	0.67 (0.34-1.05)	1.44 (0.95-1.94)	

4.5 Discussion

4.5.1 Drivers of downward carcass flux

The abundance of *N. tonsus* measured during our study in the upper 200 m in the open ocean of the subantarctic Southern Ocean is two orders of magnitude lower than those reported in the literature, for example, in SE Tasmania in summer max. of 404 ind. m^{-3} (Taw and Ritz, 1979) or off Otago, New Zealand, (mean: 543 ind. m^{-3}, Jillett, 1968). This discrepancy in numbers is likely caused by seasonal differences (summer vs. early spring) and food supply (high in coastal waters vs. low in open ocean). Also, the collected individuals in this study do not represent the entire population, as part of the community would reproduce at depth with only late nauplii and early copepodite stages ascending to surface in November or slightly earlier (Bradford-Grieve et al., 2001; Miller et al., 1999; Ohman et al., 1989; Saito and Tsuda, 2000; Voronina et al., 1988). In comparison, the surface population relies on particulate food to moult and produce eggs (Ohman et al., 1989). For the downward carcass flux, it is important to consider where in the water column the carcasses are produced. Mortality in the deep ocean population increases the carbon flux because it actively injects carbon at the base of the mesopelagic zone (200-1000 m depth), avoiding high microbial remineralisation in this zone (Robinson et al., 2010). Due to insufficient data on deep population biomass in this region, the carcass flux of the deep-water population of *N. tonsus* cannot be calculated in this study. This reiterates the need for understanding a species' ecology to estimate its contribution to the carcass carbon flux. Carcasses are microbial hotspots that are important for the microbial loop and nutrient remineralisation in the water column (Glud et al., 2015; Tang et al., 2019). The microbial decomposition of carcasses was found to be high compared to marine snow from SOTS. For example, Cavan and Boyd (2018) measured a lower average respiration of marine snow aggregates of 3.3 ± 0.3 μmol O_2 L^{-1} h^{-1}. Comparable respiration rates to this study (6-8 µmol O_2 L^{-1} h^{-1}) were only reached at higher temperatures (20-22°C, Cavan and Boyd (2018); compared to ∼11°C in this study). The difference in dissolved oxygen consumption between batch 1 and 2, both from site PS2, can be explained by a different initial microbial community on the surface of and within the carcasses resulting in different successional patterns and, consequently, diverging trends in dissolved oxygen consumption (Moisander et al., 2015). Tang et al. (2019) found a rapid microbial colonisation and utilisation of carcasses, with respiration

increasing over time, and anaerobic taxa were noted towards the end of the incubations, which is an indicator of the formation of micro-anaerobic zones (Glud et al., 2015). The microbial turnover rates (between 0.02 d^{-1} and 0.16 d^{-1}) of carcasses were similar or higher to other studies of fast-sinking particles, e.g. 0.01 - 0.06 d^{-1} for krill faecal pellets in the Scotia Sea (Belcher et al., 2016b), 0.13 ± 0.01 for fast-sinking particles in the Pacific Oxygen Minimum Zone (Cavan et al., 2017b), or 0.08 d^{-1} and 0.20 d^{-1} for phytoplankton aggregates (Iversen and Ploug, 2010). The difference in the microbial decomposition of carcasses compared with other particles is caused by the higher amount of carbon, especially in the lipid-rich subantarctic species *N. tonsus*, and by the protection from decomposition and fragmentation provided by the copepod carapace. As seen in the two batches of decomposition experiments at PS2, microbial respiration varies markedly, even at the same location. As microbial respiration is positively correlated with temperature (Cavan and Boyd, 2018; Kritzberg et al., 2010; Rivkin and Legendre, 2001), using the same microbial turnover rate to calculate the carcass flux at PS1 than at PS2, could therefore lead to underestimation of carbon flux at PS1. However, as downward carcass flux appears to be less sensitive to a change in microbial decomposition rate (Table 4.2) the impact on flux estimations would be only minor. Even with relatively low *N. tonsus* abundance at the surface and high microbial degradation, the high sinking velocity of the carcasses results in a high carbon flux to the deep, representing 31-32% of the POC flux out of the mesopelagic zone in early spring (Figure 4.5). The measured carcass sinking velocity (730 m d^{-1} at 11°C) was more than two-fold higher than for marine snow (globally between 16 – 368 m d^{-1}, Turner (2002)) and higher than other reported sinking velocities of, for example, Mediterranean copepods (107 m d^{-1} at 13 - 19°C; Frangoulis et al. (2011) or copepods in an estuary (90 m d^{-1} at 25°C; Elliott et al. (2010), which is likely due to a smaller size compared with the large and heavy subantarctic species *N. tonsus*. Furthermore, the experiments in an idealised setting do not consider the impact of detritivory, turbulence or decreasing temperature with depth (discussed in detail below). Due to the high sensitivity of downward carcass flux estimates to a change in sinking velocity, it is necessary to understand factors that influence the sinking through the water column.

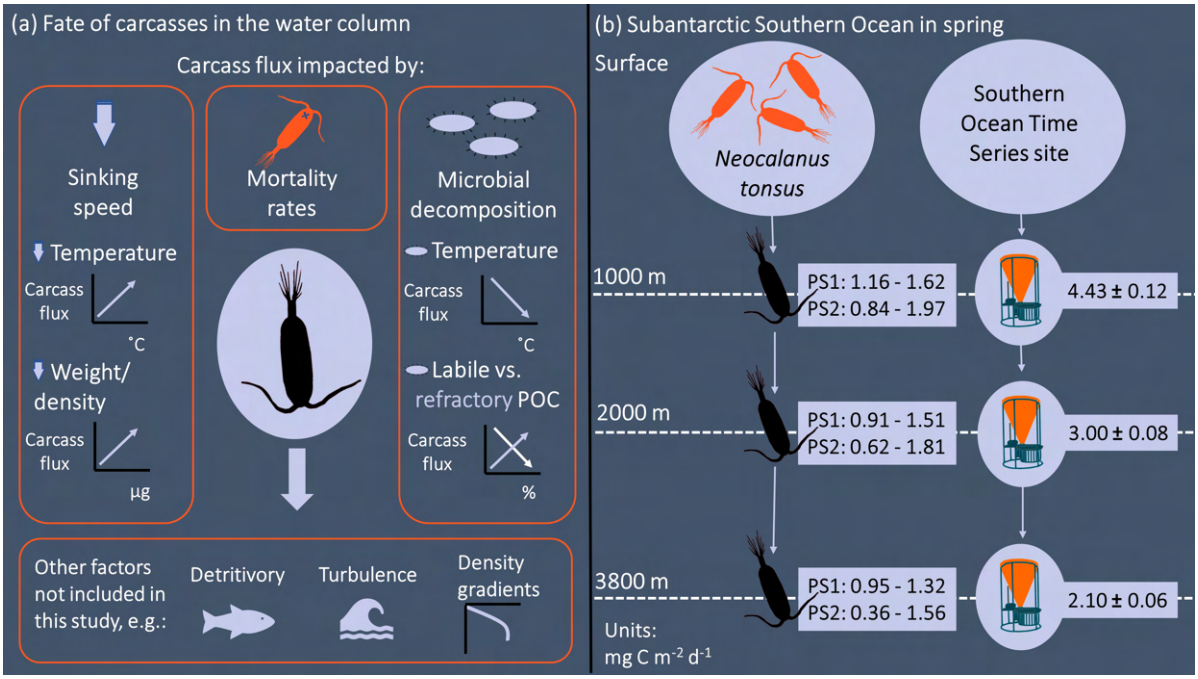

Figure 4.5: (a) The factors that impact the downward carcass flux through the water column: sinking velocity, mortality rates, and microbial decomposition. Other important factors include detritivory, turbulence and seawater density gradients in the water column. (b) The estimated carbon flux by *N. tonsus* carcasses from the surface down to 1000, 2000, and 3800 m depth in comparison to the particulate organic carbon flux in mid-October, estimated with sediment traps at SOTS.

4.5.2 Knowledge gaps and limitations of this study

During the present study, it was not possible to measure copepod mortality rates or carcass flux directly. Conventionally, to distinguish between live and dead zooplankton, either the Neutral Red stain is used (e.g. Elliott et al., 2010; Ivory et al., 2014; Tang et al., 2019) or samples are visually screened for signs such as incomplete consumption (reviewed by Daase et al., 2014). The latter method is less reliable because carcasses cannot be detected when they die of natural causes, for instance infections, and it potentially underestimates the downward carcass flux. Following a copepod population over a longer time to observe the change in abundance and calculate growth and mortality rate is not logistically feasible in the subantarctic Southern Ocean. Consequently, zooplankton mortality rates are not available for this region to date. In addition, POC flux estimates from sediment traps typically exclude carcasses because all larger organisms are

removed before analysis of the particulate fraction (e.g. see Wynn-Edwards et al., 2020), as it is difficult to separate copepod swimmer from carcass. Mortality rates are largely only available for freshwater or coastal environments (Daase et al., 2014). To increase our understanding of oceanic carcass flux, future research needs to focus on zooplankton mortality in the open ocean. The impact of the killing method must be considered when analysing the decomposition rates. Other studies used chemicals (such as ethanol, formaldehyde, HCl, or NaN_3), heat or freezing (Elliott and Tang, 2009; Tang et al., 2006). Most studies focused on the impact of the method on Neutral Red staining, thus, it is unclear how these methods impact the microbiome and decomposition of carcasses in laboratory experiments. Overall, we consider carbon dioxide to be a relatively gentle option compared to the others because the copepod is killed, but the microbiome left relatively intact. The present study does not examine how microbial decomposition and sinking velocity changes when carcasses sink through the water column, caused by the decrease in temperature. First, a decrease in temperature lowers the microbial decomposition and increases the downward carcass flux. At the same time, a lower temperature also leads to a higher sinking velocity of particles, which also increases the downward carbon flux (Bach et al., 2012). Alternatively, the decrease in weight and density of carcasses due to microbial decomposition will decrease the sinking velocity and, hence, downward carbon flux. Therefore, more research is needed to improve our understanding of the interactions between temperature, microbial community, and carcass sinking velocity on the way to the deep sea. Fragmentation of the carcasses by the detritivorous community is currently underestimated due to the lack of information on the subsurface community. Most zooplankton data in the Subantarctic is collected by Continuous Plankton Recorder at the surface (Atkinson et al., 2012; Hunt and Hosie, 2003) and seasonally limited research voyages. For larger-sized zooplankton, we lack knowledge of the diversity and abundance of potential consumers of copepod carcasses in early spring. In addition, water turbulence can lower the sinking velocity and leave carcasses exposed to detritivory (Elliott et al., 2010). However, mixing is patchy on spatial and temporal scales in the global ocean (Whalen et al., 2012), hence, it is difficult to account for in downward carcass flux estimations. In conclusion, the variability and interactions of factors such as microbial decomposition, sinking velocity, detritivory, turbulence, and other environmental conditions throughout the water column affect carcass transport and future research is needed to estimate their importance.

4.5.3 Future research priorities

Given that zooplankton carcasses can be an important contributor to ocean carbon flux, their inclusion in ecosystem models to estimate future changes in carbon sequestration is highly important. However, not all models currently include non-consumptive mortality as a carbon pathway. Zooplankton mortality is calculated from biomass using a linear or quadratic dependency (see Table 4.3 in the supplementary material). Linear terms refer to non-predatory mortality, while quadratic non-linear terms are due to predatory mortality (Anderson et al., 2015). For example, the models REcoM2 (MAREMIP Hauck et al., 2013) and PISCES (CMIP5 Aumont and Bopp, 2006) only include non-consumptive mortality in their carbon flux estimations. In contrast, BEC (MAREMIP Moore et al., 2001) and EMPOWER (Anderson et al., 2015), consider both non-consumptive and predatory mortality. Other models, such as TOPAZ (CMIP5 Dunne et al., 2013), assume all carbon resulting from zooplankton mortality is remineralised immediately and do not include carbon loss from surface waters. Even if non-consumptive mortality is considered, a constant mortality rate and ratio between predatory and non-consumptive mortality is often assumed (e.g. EMPOWER-1.0), while data on total mortality rates, seasonality and the ratio between both mortality components are still insufficient for many regions of the world's oceans, including the subantarctic Southern Ocean.

4.6 Conclusion

This study is the first to estimate the contribution of copepod carcasses to the carbon flux in the subantarctic Southern Ocean. Our results indicate that *N. tonsus* carcasses are characterised by high microbial respiration and carbon turnover rates, but as they sink quickly through the water column, they can significantly increase the POC flux at depth. The performed sensitivity analysis showed that the downward carcass flux is highly sensitive to variations in sinking velocity and mortality rates, but less to a change in microbial decomposition rate. Despite the importance of copepod carcasses, the lack of knowledge on mortality rates and processes that affect sinking in the ocean limit the upscaling and inclusion in ecosystem models.

4.7 Supplementary material

Table 4.3: Parameterisation of zooplankton mortality in the ecosystem models REcoM2, BEC and PISCES. All equations are described in more detail by (Laufkötter et al., 2016). Z is the zooplankton biomass, pzoo the quadratic mortality rate and mzoo the linear mortality rate. PISCES distinguishes between micro- and meso-zooplankton mortality and includes a factor for dissolved oxygen (f (O_2)) and temperature (Tf).

Model	**Calculation of zooplankton mortality**
REcoM2	$$Z\,\frac{mort}{REcoM2} = \text{pzoo} \times Z^2 \quad (4.8)$$
BEC & EMPOWER-1.0	$$Z\,\frac{mort}{BEC/EMPOWER} = mzoo\ \times Z + \ pzoo\ \times Z^2 \quad (4.9)$$
PISCES	$$Z\,\frac{micromort}{PISCES} = mmicro\ \times Tf\ \times \frac{Z\ micro}{Kmicro + Z\ micro} \times Zmicro\ \times f\ (O_2) \quad (4.10)$$
	$$Z\,\frac{mesomort}{PISCES} = mmeso\ \times Tf\ \times \frac{Z\ meso}{Kmeso + Z\ meso} \times Zmeso\ \times f\ (O_2) + p\ meso\ \times Zmeso^2 \quad (4.11)$$

Chapter 5

ZOORESPIRE (ZOOplankton RESPiration In the subsuRface ocEan) - A new tool to measure in-situ zooplankton respiration in the ocean

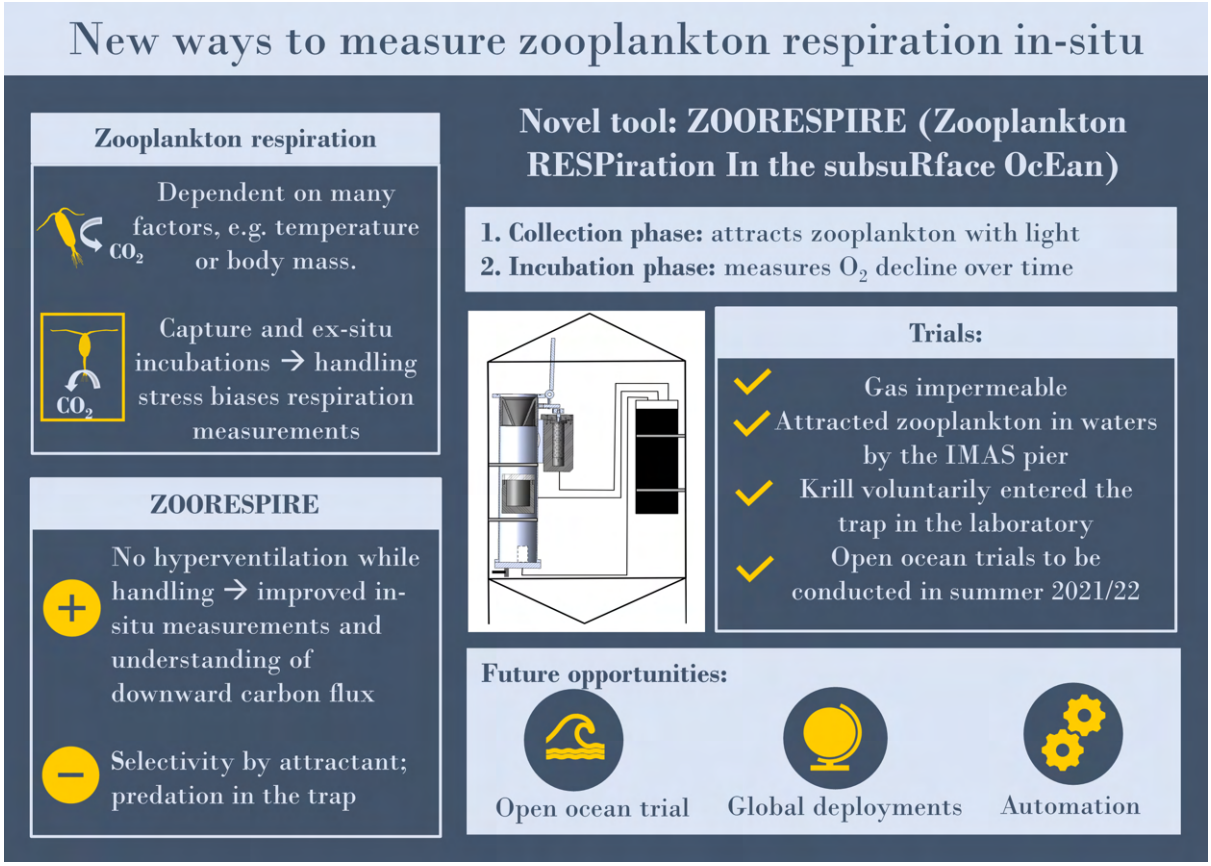

5.1 Abstract

Zooplankton respiration represents an important carbon transformation pathway in the ocean, though it is rarely measured in-situ due to the difficulties of isolating enough individuals while maintaining field conditions and avoiding stressful handling. This chapter presents the development of the ZOOplankton RESPiration in the subsuRface OcEan (ZOORESPIRE), a newly developed research instrument to measure zooplankton respiration in-situ. Initial trials using different zooplankton attractants such as amino acids and a light source were conducted with earlier prototypes and indicated that light was the most successful way to attract zooplankton. During the collection phase, the current prototype of the ZOORESPIRE attracts and traps zooplankton in a sampling chamber, which then closes and functions as an incubation chamber. During the incubation phase, the integrated optode measures dissolved oxygen decline over time. Trials were conducted to analyse the impermeability, trapping efficiency, and sensitivity of the oxygen measurements. The ZOORESPIRE did not allow gas exchange with the surrounding water and is therefore suitable for zooplankton respiration experiments. During the field experiment, the light attracted a significantly higher number of zooplankton (total $\sim$ 1725 ind. L^{-1}), mainly copepods, crustacean larvae, and appendicularians in comparison to the control experiment without light, which resulted in a significant decline in dissolved oxygen concentration within the ZOORESPIRE of 7.3 μM h^{-1}. In addition, it was possible to distinguish a respiration signature between different abundances of zooplankton: differences in oxygen consumption by eight Antarctic krill (*Euphausia superba*) compared to four individuals were measurable. Current biases of the ZOORESPIRE include a change in community composition within the chamber during deployment due to predation, along with the selectivity of the attractant light. Further development of the tool will include an additional field trial in oceanic waters using a neutrally-buoyant float that minimises vertical movement in the water column. The future deployment of ZOORESPIRE arrays will enable improved quantification of zooplankton respiration in the Southern Ocean, including the understudied ocean's twilight zone.

5.2 Introduction

5.2.1 Zooplankton respiration in the oceanic carbon cycle

Zooplankton respiration (hereafter "respiration") is an important pathway for transforming carbon in the ocean. Approximately, 25% of the carbon that zooplankton ingest from primary producers is released again as carbon dioxide, resulting in an annual CO_2 production of 1.4 Gt C yr^{-1} globally (Calbet, 2001). The zooplankton community in the Southern Ocean contributes $\sim$ 0.6 Gt C $year^{-1}$ to oceanic respiration (Mayzaud and Pakhomov, 2014b). Diel and seasonal vertical migrations by zooplankton (mesopelagic migrant pump, MMP, and seasonal lipid pump, SLP), result in carbon injection in the form of respired CO_2 at depth, which is associated with metabolising upper ocean prey, and results in a respiratory flux. This flux is highly variable and can be 2.8-88.3% of the gravitational particle flux, as estimated by Hernández-León et al. (2019) for the Canary Current; the magnitude of the downward flux depends upon the migration depth of zooplankton. Respiration in general varies depending on environmental parameters, such as temperature and dissolved oxygen concentration, as well as zooplankton body mass, feeding rates, and swimming activity (Hernández-León and Ikeda, 2005b; Hernández-León and Gomez, 1996; Ikeda, 1985; Ikeda et al., 2001; Teuber et al., 2013). In addition, species diversity, size distribution and trophic characteristics of zooplankton communities control respiration (Mayzaud and Pakhomov, 2014b, and references therein). Respiration in the epipelagic is estimated to be highest in the water column, as a function of the high biomass, high particulate organic carbon concentration, and warmer temperature in this zone (Hernández-León and Ikeda, 2005b). However, despite less data being available for this layer, the mesopelagic zone (200-1000 m) is estimated to contribute $\sim$ 21% of global zooplankton respiration (Hernández-León and Ikeda, 2005b). Differing estimates in zooplankton community respiration in the mesopelagic zone are the result of large uncertainties and variability in the biomass estimates for the mesopelagic community between regions (Hernández-León and Ikeda, 2005b; Proud et al., 2017; Robinson et al., 2010).

5.2.2 Previous methods to estimate zooplankton respiration

In addition to providing insights into zooplankton physiology, respiration also indicates regions of high zooplankton activity, including particle ingestion and fragmentation (Packard and Christensen, 2004). Sinking particles are ingested to meet part of the carbon demand of the pelagic community, but zooplankton feeding on the particle flux and the associated respiration also result in a decline in downward particulate carbon flux, in particular in the twilight zone (Giering et al., 2014; Steinberg et al., 2008; Burd et al., 2010). Consequently, to estimate the magnitude of the biological gravitational pump and project its future changes, a robust quantification of zooplankton respiration is necessary. Different methods have been used for decades to measure respiration, as reviewed by Hernández-León and Ikeda (2005b). Zooplankton are typically caught with nets and brought to the surface. Many studies have used the "bottle" or "sealed-chamber approach" (Hernández-León and Gomez, 1996; Ikeda, 1985; Ikeda et al., 2001), where selected animals were acclimated to laboratory conditions for a few hours and then placed in an air-tight container. The dissolved oxygen decline is measured over time either continuously or at the start and end of the incubation to infer zooplankton respiration. Another common approach is to determine the enzymatic activity of the Electron Transfer System (ETS), a method developed by Packard (1971) and refined by Owens and King (1975), that works using a conversion factor between respiration and ETS activity. This ratio is not constant, but varies depending on different factors, such as primary production and temperature (Hernández-León and Gomez, 1996).

Although these methods have been commonly used a long time, e.g., to extrapolate respiration estimates for the global ocean (del Giorgio and Duarte, 2002), they have artefacts that could alter the respiration rate estimates. All methods used to date require the collection of undamaged zooplankton from the water column, however, increased handling induces physiological stress leading to a potential over-estimation of respiration rates termed hyperventilation (le Borgne, 1979). Usually, common species are selected for the experiments or, if a community sample is used, larger and rarer species are frequently excluded because of the small volume of the incubation chamber (Hernández-León and Gomez, 1996). In addition, respiration has not been measured over high spatial resolution through the water column or over more than a few hours. Consequently, regions of high zooplankton respiration that lead to particle fragmentation and remineralisation

"hotspots" in the water column are poorly mapped. While zooplankton respiration has been measured in the laboratory for over four decades, in-situ measurements of community respiration have rarely been attempted because it has been difficult to capture sufficient zooplankton biomass under low stress conditions (Hernández-León and Ikeda, 2005b). As one of the few examples of in-situ methods, Collins et al. (2018) developed an autonomous, bottle device to measure community respiration and net production, but their approach focused mainly on phytoplankton.

In contrast to plankton respiration, approaches to measure bacterial respiration associated with of particle remineralisation are further advanced, as their influence on particle attenuation was recognized (Buesseler and Boyd, 2009; Giering et al., 2014; Steinberg et al., 2008; Tamburini et al., 2003). For example, Steinberg et al. (2008) used the incorporation rate of the radio tracer [^{3}H]-thymidine in incubations of water samples to estimate carbon demand by using published conversion factors of bacterial growth efficiency rates. Microsensors that measure dissolved oxygen gradients of particles in a temperature-controlled environment are commonly used as well (Belcher et al., 2016a; Cavan and Boyd, 2018; Ploug and Grossart, 2000). As one of the first in-situ methods, Boyd et al. (2015) developed the RESPIRE dual particle interceptor/incubator, which first intercepts and concentrates marine snow particles for enough time to enable measurement of a respiration signature, and then commences particle incubation by measuring the particle-associated microbial respiration within the inner incubation chamber of the RESPIRE. The RESPIRE has been used successfully in several field campaigns to improve the understanding of microbial physiology and particle biogeochemistry (Boyd et al., 2015; Bressac et al., 2019; McDonnell et al., 2015). Based on the RESPIRE design, which relies on natural gravitational flux of marine snow particles, a similar device was developed for zooplankton, with the difference that zooplankton need to be captured and concentrated prior to incubation.

5.2.3 The development of the ZOORESPIRE

In the following chapter, the ZOOplankton RESPiration in the subsuRface OcEan (ZOORESPIRE), a newly developed tool to measure zooplankton respiration in-situ, is presented. It consists of a titanium chamber (i.e., non oxygen-evolving) with a light source and an inte-

grated oxygen optode (set-up described in detail in the Methods section). During the collection phase, the length of which is programmable, the open device attracts zooplankton that actively swim through the funnel-shaped entranced (similar to a fish trap) and become trapped. After sufficient animals are caught to measure a respiration signal, which is determined by trial and error, the lid closes and the dissolved oxygen decline is measured during the incubation phase. The ZOORESPIRE has the advantage that zooplankton voluntarily swim into the chamber, which significantly reduces the handling stress, avoids hyperventilation, and improves the representativeness of respiration rate measurements. In contrast to previous methods, the tool enables measurement of the respiration rate of a zooplankton community over a long period of time (hours to days) under natural conditions. Throughout the development of the different prototypes (presented in Figure 5.1) two questions needed to be answered: (1) What is the best method to attract sufficient abundance of zooplankton and (2) can sufficient zooplankton biomass be obtained to measure a significant decrease in dissolved oxygen concentration?

Zooplankton occur patchily in the ocean, and patches are formed during diel vertical migration, as a predator avoidance mechanism, searching for prey at high concentration or as mating behaviour (Folt and Burns, 1999). In particular, copepods respond well to chemical stimuli, such as dissolved amino acids released by phytoplankton, and can successfully locate a patch of food (Folt and Burns, 1999; Poulet et al., 1991; Gill and Poulet, 1988). The disadvantage of using amino acids as a chemical attractant in a zooplankton trap is the change in the ambient environmental conditions, which potentially affects respiration rates of the captured zooplankton and in particular the resident heterotrophic bacteria. In addition, amino acids occur in high concentration in shelf waters (Poulet et al., 1991), which impedes their use in a trap in coastal regions (see Prototype 1 in Figure 5.1). Previous zooplankton traps have used a light source to attract zooplankton, mainly in coastal settings. For example, the Doherty trap (Doherty, 1987) deployed to quantify spatial and temporal patchiness in the zooplankton community of Lizard Island, Australia, used a light source to mainly attract larval fish. Further development of the trap design by Hickford and Schiel (1999) and Meekan et al. (2001) enabled a comparison of the zooplankton community between coastal ecosystems. The cost-efficient and robust light trap presented by Chan et al. (2016), who used a 6 L PET mineral bottle as the trap body, served as inspiration for Prototype 2 of the ZOORESPIRE (see Figure 5.1). Despite reports that pelagic organisms largely avoid artificial light (e.g. Geoffroy et al.,

2021), the directed light source (a dive light torch) in Prototype 2 proved to be the most efficient way to attract a diverse array of zooplankton and micronekton (more details in Figure 5.1 and Figure 5.6, 5.7, and 5.8 in the supplementary material). The current version of ZOORESPIRE was developed employing an oxygen optode to detect a decline in dissolved oxygen over time, as used in the RESPIRE by Boyd et al. (2015), a modified light source and a funnel to form a sampling chamber.

5.2.4 Aims for this chapter

The following chapter describes the set-up and trials of the latest prototype of the ZOORESPIRE in the laboratory and field. In particular, I focused on the following questions:

1. Is the chamber **gas-permeable**? Ideally, the dissolved oxygen concentration inside the ZOORESPIRE changes independently of the dissolved oxygen concentration in the water surrounding the chamber.
2. Does the ZOORESPIRE **attract sufficient zooplankton stocks** in the field, i.e., does it attract enough zooplankton to measure a decline in dissolved oxygen?
3. Finally, how **sensitive** is the ZOORESPIRE to minor changes in the number of zooplankton captured?

Additionally, new opportunities for measuring zooplankton respiration in-situ are discussed, as well as biases of the current method and future refinements.

	Prototype	Inspiration	Trials	Question(s)	Results	Issues & improvements
1.	Niskin bottle (2.5 L, horizontal orientation) with dialysis bag of amino acid solution to attract zooplankton	Poulet et al., 1991: amino acids trigger swimming behaviour of copepods Poulet & Gill, 1988: Strongest response with ASP/GLU	IMAS Wharf, Australia	How to attract zooplankton?	Unsuccessful: no zooplankton caught	• Sampling chamber and alteration of closing mechanism required • Unclear if amino acids detected by plankton in the harbour (potential water pollution)
2.	Carboys (30 L) with funnel-shaped holes (three on each side) to create a sampling chamber, dive light torch or dialysis bag with amino acid solution to attract zooplankton Test of different deployment times with light trap: over night, during the day and for 23 hours	Light trap by Doherty, 1987 Simplified by Chan et al., 2016: 	IMAS Wharf, Australia Maria Island, Australia	How to attract zooplankton? What time of deployment is required for light trap?	Light most successful: highest zooplankton diversity and abundance attracted with light compared to control and amino acid solution Highest zooplankton numbers collected during the night. Long opening time = more zooplankton, but also change in species composition	• Loss of water & plankton during trap recovery • More robust design needed for Southern Ocean deployment
3.	Niskin bottle (30 L, horizontal orientation) with external closing mechanism, optode and light More robust to be deployed at sea	Combining light trap by Chan et al., 2016, with optode to measure O_2, e.g. in the RESPIRE trap by Boyd et al., 2015	SOTS voyage 2019 – Southern Ocean	Does the light work in the field?	Optode and program worked, but no zooplankton caught	• Zooplankton needs to be trapped: sampling chamber required • Horizontal orientation not optimal for vertically migrating zooplankton • Light pointing inwards: not strong enough to be perceived? • PVC housing not optimal to measure 0_2 changes

Figure 5.1: Development of the prototypes of the current ZOORESPIRE. Trials were conducted either off the IMAS Wharf (42.88°S, 147.34°E), on the pier on Maria Island (42.58°S, 148.06°E), or at the Southern Ocean Time Series site (47°S, 140°E) during a research voyage in 2019. Images of the prototypes along with zooplankton counts of the successful trial of prototype 2 are displayed in the supplementary materials (Figures 5.6 and 5.7).

5.3 Methods

5.3.1 ZOORESPIRE set-up and development

With the deployment of the ZOORESPIRE, I aimed to attract zooplankton and measure their respiration rate over time. The chamber is a titanium cylinder from a re-purposed RESPIRE trap that is closed with a titanium lid by an attached motor (Figure 5.2). A PVC funnel is inserted into the opening of the chamber to create a zooplankton trap that is difficult to exit for the organisms and tapers the opening diameter down to 5 cm. Approximately mid-way through the cylinder, a light source (Chip LED with Right Angle Lens, 27-21/GHC-YR1S2M/3C, Everlight Electronics) is positioned underneath the funnel opening. Depending on the particle concentration in the water, the light is visible in a radius of approximately 3-4 m. The 3-point attachment of the light ensures that there is water exchange throughout the whole chamber.

At the titanium base plate, an oxygen optode (Andereaa, 4831 series) is mounted before deployment to measure dissolved oxygen concentration within the inner chamber to estimate respiration rate by zooplankton under in-situ pressure and temperature conditions. The accuracy of the measurements is $<\pm$ 8 μM or 5% and a resolution of $<\pm$ 1 μM. A $\frac{1}{4}''$ BSP stainless steel ball valve is attached at the bottom. This enables collection of the zooplankton after recovery of the ZOORESPIRE, which is necessary to estimate the oxygen consumption per zooplankton biomass. Also, the base plate is removable to allow cleaning between deployments. The light, optode and motor are connected via heavy-duty electrical cables to the controller unit, which is programmed with the mission parameters via the Arduino Uno program (version 1.4) prior to deployment (Table 5.1). The controller also logs dissolved oxygen and temperature over time, which are downloaded after recovery of the ZOORESPIRE, and contains the batteries (8 x 4 V) that power the mission. All components are housed within a protective steel frame during deployment.

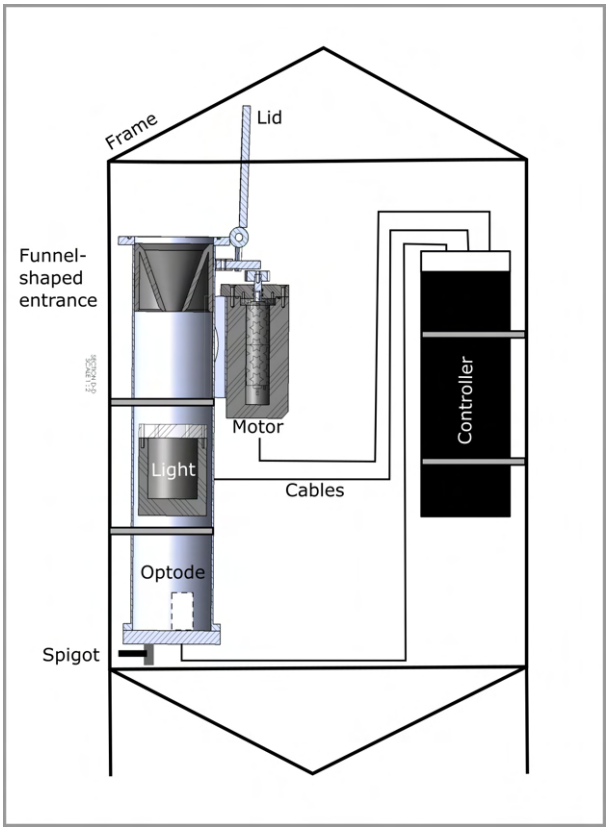

Figure 5.2: Set-up of the ZOORESPIRE within the steel frame during deployment: Construction of the chamber body, including the funnel-shaped trap entrance, lid that closes the chamber, light source, oxygen optode, and sampling tap in the base plate. The sampling component is connected via cables to the controller unit, which is programmed with the mission parameters prior to deployment. The frame is attached to a cable for deployment. The total ZOORESPIRE unit weighs approximately 55 kg.

5.3.2 Software and mission parameters

A typical ZOORESPIRE mission consists of two phases: the collection phase and the incubation phase. During the collection phase, zooplankton are attracted by the light and swim toward and into the open chamber. This zooplankton behaviour can be observed, if a camera is attached to the metal frame pointing at the trap entrance. Once entered, most plankton are unable to exit again because of the funnel-shaped entrance of the ZOORESPIRE. At the end of the pre-set collection phase, the light is turned off and the trap closing is triggered by the motor. The decline in dissolved oxygen caused by zooplankton respiration is measured during the subsequent incubation phase. The

mission parameters, including length of both phases and total mission, are adjusted for the local zooplankton community based on trial and error during some initial pilot deployments. For example, the fewer zooplankton present in the surrounding water the longer the ZOORESPIRE needs to stay open to attract a sufficient number of animals and the longer the total mission to detect any changes in dissolved oxygen. All mission parameters, i.e., speed and time of turning the motor wheel that triggers the closing of the ZOORESPIRE, delayed start of the mission to budget time for deployment, sampling interval of the optode, rotation duration, and overall mission and collection duration, are set with the Arduino interface and a code written for the RESPIRE and adapted for the ZOORESPIRE by Paul Waller (UTAS) (Table 5.1). After each deployment, the collected dissolved oxygen and temperature data that is stored on a SD card inside the controller can be accessed with the Arduino Uno program.

Table 5.1: Mission parameters of the ZOORESPIRE that were set with a software menu in the controller unit during the laboratory and field trials in September- November 2020. (1) Light turned off in the control trial. (2) No collection phase during this trial.

Settings	Range	Explanation	I. Gas permeability (2)	II. Trapping efficiency	III. Sensitivity
Motor speed (s)	0-255	Turning speed of the wheel of the motor	0	100	100
Start delay (h)	0-255	Delayed started of the optode measurement	0	0	0
Sampling interval (min)	0-255	Interval of optode measurements	1	2	2
Rotation duration (s)	0-255	Turning length of the wheel of the motor	0	100	100
Mission duration (h)	0-255	Length of overall mission	72	16	24
Collection duration (min)	0-360	Length of collection phase (trap open and light turned on) (1)	0	150	120

5.3.3 Trials

Gas impermeability & temperature sensitivity

To measure a decline in dissolved oxygen over several hours, the ZOORESPIRE cannot allow an exchange of oxygen with the surrounding water during the incubation phase. Its gas impermeability was tested in a constant temperature laboratory at the Institute for Marine and Antarctic Studies (IMAS), Australia, set to 11°C (lower limit: 9°C, upper limit: 12°C). A water bath of filtered seawater was prepared 24 h before the trial to let the water reach room temperature. The ZOORESPIRE and all the required equipment, i.e., optode, cables and controller, were placed on the same bench to acclimate to temperature. 11°C was chosen as it is within the range of mixed layer temperatures of the subantarctic Southern Ocean (Rintoul and Trull, 2001), the location for further planned field experiments of the ZOORESPIRE. After 24 hours, the ZOORESPIRE was gently submerged in a water bath and nitrogen gas was inserted via a tubing system for 2 hours to artificially lower the dissolved oxygen concentration in the chamber, as oxygen molecules are replaced by nitrogen. After the lid was closed, the dissolved oxygen concentration and saturation were measured over 36 h by the optode inside. Meanwhile, a second optode measured the dissolved oxygen concentration changes in the water bath outside the chamber as a control. The mission parameters for this and the following trials are summarised in Table 5.1. To explore how the light source would influence the temperature within the ZOORESPIRE, I conducted another trial in the constant temperature room. I used the same mission parameters as in the permeability trial above, but only programmed a total mission length of 6 hours. The light was turned on during the collection phase, but the chamber was closed. Although these are not realistic field conditions, I wanted to measure the maximum potential temperature increase by the light.

Trapping efficiency

The ZOORESPIRE was tested in the Derwent Estuary, Australia, off the wharf of IMAS in Hobart (42° 53′S, 147° 20′E). An hour prior to deployment, the ZOORESPIRE was slowly filled with water from off the wharf via a tubing system to avoid the introduction of gas bubbles. A GoPro Hero8 camera was attached to the metal frame to obtain video

material and analyse the animals' behaviour at the trap entrance. The ZOORESPIRE was deployed at around 18:15 local time (sunset 18:00) and lowered down to around 4 m water depth. The ZOORESPIRE closed after 2.25 hours in the water and incubated the captured zooplankton until recovery the next morning at 8:45 (14.5 hours of measurements). In the lab, the chamber was sampled through the tap in the bottom plate. The zooplankton were sieved into size fractions of 50 - 100 μm (small), 100 - 200 μm (medium) and > 200 μm (large) and preserved in 10% ethanol.

A control trial with the light turned off was conducted during the following evening. The ZOORESPIRE was pre-filled with water off the wharf and the same mission parameters were used (Table 5.1). The camera could not be used this time due to the lack of daylight. The ZOORESPIRE was deployed at 18:10 (sunset 18:01) and lowered down to 4 m. The next day, at 8:30, the zooplankton were sampled after recovery, split into size fractions, and preserved. Under ideal conditions, the control trial would be conducted simultaneously with the light trial, however, the availability of only one ZOORESPIRE prototype prevented a direct comparison. The deployment conditions, i.e., wind and waves, were notably calmer during the control trial than during the light trial on the previous day, which could potentially influence the trapping efficiency of zooplankton. This potential source of error will be discussed below.

The collected zooplankton were identified to group level; e.g., copepods, polychaetes, isopods etc. The complete sample was counted for rarer organisms, while it was split for very abundant zooplankton. The number was then calculated per litre (total chamber volume: 5.3 L) and compared to the dissolved oxygen decline in the chamber over time. To test if zooplankton numbers between the trials differed significantly, an Analysis of Variance and a Tukey-HSD post-hoc test were conducted.

Sensitivity trials: zooplankton abundance versus change in dissolved oxygen concentration

To evaluate if the ZOORESPIRE is sensitive enough to detect changes in respiration rates caused by different numbers of trapped zooplankton, experiments were conducted in the krill laboratory at the Australian Antarctic Division in Kingston, Tasmania. The ZOORESPIRE, together with the controller, was gently lowered into a tank (~1 x 1 x

2 m) filled with seawater of approx. 0.3°C and a salinity of 34.5. Instead of using the steel frame, the components were lowered into the tank and suspended from the ceiling. The ZOORESPIRE was programmed with a collection time of 2 hours. Between 35 and 50 individuals of Antarctic krill *Euphausia superba* were added to the tank water surrounding the ZOORESPIRE. The behaviour of the krill was recorded, again using the GoPro Hero 8 camera mounted in front of the trap opening. Throughout the trial, the tank was covered with a black cloth to avoid light pollution from the laboratory. During the incubation phase, the dissolved oxygen decline was measured for a minimum of 20 hours. After the trial, the krill were sampled and frozen at -80°C. The total length (rostrum to urosome) was recorded and wet weight was measured with a balance (AND GR-200, accuracy of 0.1 mg). The dry weight was obtained by multiplying the wet weight by 0.2278 following Ericson et al. (2018) to account for 77.2% body water content. The respiration rate in each trial was calculated as dissolved oxygen decline per gram dry weight per hour to enable a comparison with other methods. In total, two trials were conducted to attract different numbers of krill. Additionally, a third trial with the light turned off was used as a control. Another light trial was excluded from the analysis, as the water temperature fluctuated due a technical issue. The water had to be changed regularly between trials to avoid algal growth within the tank.

5.4 Results

5.4.1 Gas impermeability & temperature stability

During the bubbling of nitrogen gas, the dissolved oxygen inside the ZOORESPIRE decreased sharply by approximately 200 μM (from 300 μM to around 100 μM, Figure 5.4a), while the optode outside recorded only a minor decrease of 26 μM. After closing the lid, the dissolved oxygen levels in the chamber fluctuated slightly, likely due to diffusion within, but remained relatively constant. Similarly, the dissolved oxygen concentration in the water bath outside the chamber remained constant at around 265 μM. Therefore, no gas exchange between the surrounding water bath and ZOORESPIRE, which would be conspicuous as an increase in dissolved oxygen concentration inside the chamber, was detected over 72 hours. The temperature remained constant at approximately 10.5°C (Figure 5.4b). During the trial testing the temperature increase of the light source there

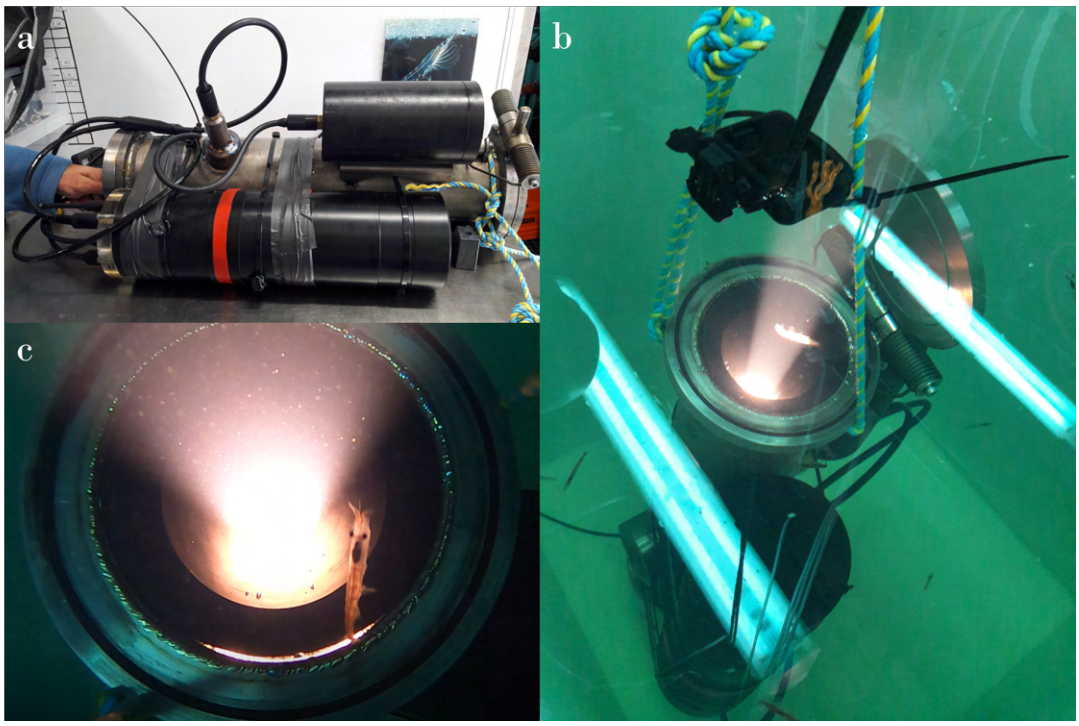

Figure 5.3: The ZOORESPIRE trial at the Australian Antarctic Division. (a) The ZOORESPIRE was deployed without the metal frame due to a lack of space in the krill tank. Instead, the controller and the ZOORESPIRE were suspended from the ceiling. (b) The ZOORESPIRE in the krill tank with an attached GoPro camera to document the krill behaviour. (c) An Antarctic krill during the first trial that was attracted by the light and entered the chamber afterwards.

was a slight decrease in temperature during the test rather than an increase caused by the lamp (11.5 to 11.3°, results not shown). Hence, I assume the impact of the lamp on the water temperature to be negligible.

5.4.2 Attraction and capture efficiency

The light source trial of the ZOORESPIRE off the IMAS Wharf attracted a 2.5-fold higher number of zooplankton compared to the control without light (total 1725 and 682 ind. L^{-1} in light trial and control, respectively, Figure 5.5). The highest numbers ($\sim$ 1600 ind. L^{-1} in total) were counted in the largest size fraction (>200 μm) of the light trial, containing mostly copepods, porcelain crab larvae, appendicularians, and crustacean larvae (cyprid and unidentified). In contrast, the control was dominated by dinoflagellates

in the smallest size fraction (50-100 μm) with ~640 ind. L^{-1}. In the light trial, dinoflagellates were also caught, however, their concentration was only minor (20 ind. L^{-1}). The numbers of the other size fractions (small and medium in the light trial and large and medium in the control) were negligible.

The abundance of large zooplankton during the light source trial led to a decrease in dissolved oxygen concentration even before the chamber was closed (Figure 5.4c). After an initial slight increase in dissolved oxygen concentration, likely due to the mixing of water in the ZOORESPIRE with the seawater off the wharf, concentration declined from 300 μM to 194 μM within 14.5 hours (oxygen consumption 7.3 μM h−1). In contrast, the dissolved oxygen concentration of the control that was dominated by small zooplankton with lower numbers, decreased only slightly from 290 to 283 μM during the deployment (oxygen consumption ~0.5 μM h−1). Temperature in the chamber decreased from 12.4 to 11.8°C, similar for both trials, within the first hour of deployment, caused by a mixing of the water as described above (Figure 5.4d). Afterwards, the temperature remained constant for approximately 6 hours and then decreased further to 11.4°C (control) or fluctuated around 11.6°C. The temperature fluctuations were likely caused by tidal inflow within the harbour.

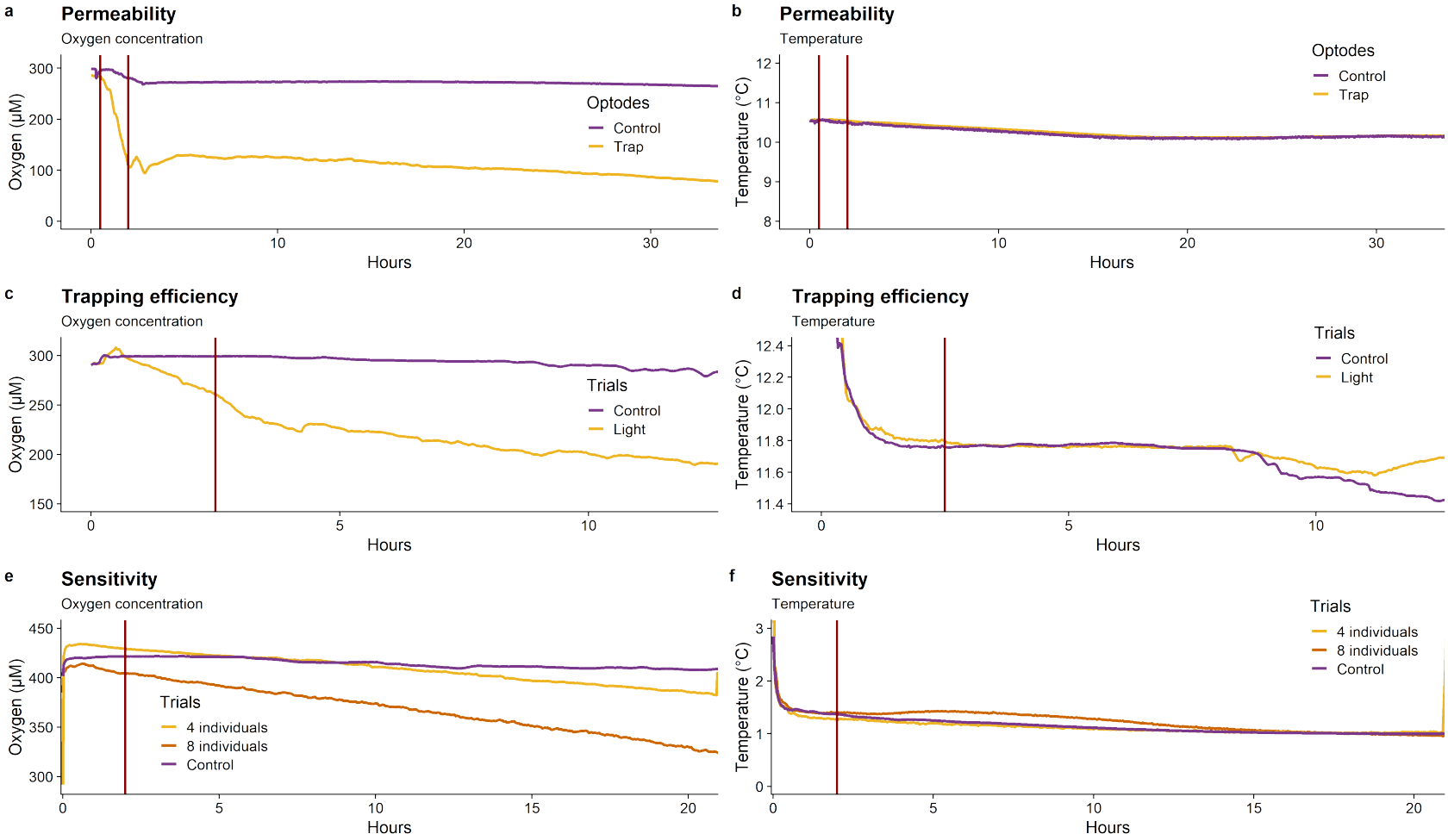

Figure 5.4: The change in dissolved oxygen concentration (left panel) and temperature (right panel) during the ZOORESPIRE trials. The control outside the chamber (permeability trial) and without light (trapping efficiency trial and sensitivity trial) is depicted in purple, while the test inside the chamber or with a light source are yellow or orange. (a)-(b) The red line indicates the start and finish of the introduction of nitrogen gas into the chamber to artificially lower the dissolved oxygen concentration during the permeability trial in the IMAS laboratory. (c)-(d) and (e)-(f): The red line indicates the closing of the ZOORESPIRE after the collection phase, commencing the incubation phase. Note that the scale on the x-axis varies between trials.

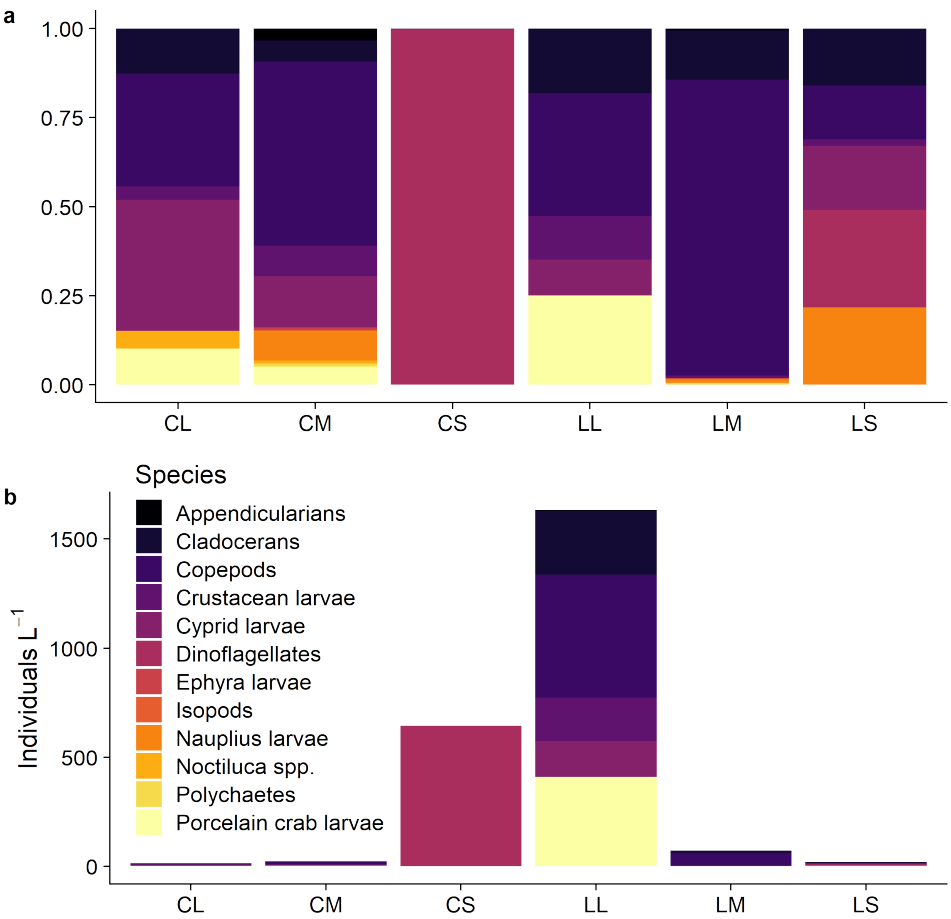

Figure 5.5: Zooplankton abundance in the trapping efficiency trial of the ZOORESPIRE. The upper panel (a) depicts the fractions of each taxonomic group in the community, while the lower panel (b) shows the total concentration in individuals L^{-1}. The bars represent the large, medium and small zooplankton size fraction in the control trial without light (CL= control large, CM = control medium, CS= control small, respectively) and the large, medium, and small fraction in the trial with light (LL= light large, LM= light medium, LS= light small, respectively).

5.4.3 Sensitivity of respiration measurements to varying zooplankton abundances

Eight krill were attracted into the ZOORESPIRE during the first experiment, four during the second and none in the control trial without light. Consequently, the decrease in dissolved oxygen due to eight krill was almost double the oxygen consumption by four in-

dividuals (48 μM compared to 26 μM over 12 hours, respectively, Figure 5.4). In contrast, the dissolved oxygen concentration declined by 7 μM in the control experiment. After an initial decline in temperature to ~1.5°C within the first 0.5 h of the sensitivity experiment, temperature remained constant throughout the deployment, though temperatures in the trial with eight krill were approximately 0.2°C higher than the other two (Figure 5.4). Assuming the control represents the background respiration by phytoplankton and bacteria in the water, the total individual oxygen consumption per krill is 2.21 μM O_2 h^{-1} on average (2.26 and 2.10 μM h^{-1} in experiment 1 and 2, respectively, Table 5.2). This equals to a respiration rate of 19.87 and 21.61 μmol O_2 g DW^{-1} h^{-1} in experiments 1 and 2, respectively.

5.5 Discussion

5.5.1 Trial results

The results of the trials indicate that changes in dissolved oxygen concentration were detected by the ZOORESPIRE independently of the dissolved oxygen concentration outside, a requirement for respiration measurements. In addition, the light source did not cause a significant increase in temperature, hence, I conclude that the environmental conditions inside the chamber represent in-situ conditions. The ZOORESPIRE also successfully attracted a sufficient number of zooplankton to record a significant decrease in dissolved oxygen concentration over the duration of the experiment. Though the wet weight of zooplankton in the trapping efficiency trial was not evaluated, which limits the estimation of respiration rates, the significant difference between control and light treatment in species abundance showed the high efficiency in attracting crustacean and tunicate plankton. The calculated respiration rates of krill are comparable to similar laboratory experiments in the literature. For example, Saborowski et al. (2002) determined the respiration rates by the Northern krill *Meganyctiphanes norvegica* during incubations in flow chambers of between 19.9 and 89.9 μmol O_2 g DW^{-1} h^{-1}, with temperatures ranging from 4 to 16°C. This is in the same range as the respiration rates in the sensitivity trial with the Antarctic krill of 19.8-21.61 μmol O_2 g DW^{-1} h^{-1}. The lower water temperature during the experiments with the ZOORESPIRE and the larger size of Antarctic krill likely resulted in lower metabolic rates and hence, caused low respiration rates by the

Antarctic krill compared to the Northern krill. Similarly, Ericson et al. (2018) measured oxygen consumption by Antarctic krill of 0.13-0.50 μL O_2 mg DW^{-1} h^{-1} at 0.5°C, using respirometry vessels in water baths, which is comparable to the estimated rates in the ZOORESPIRE (0.45-0.48 μL O_2 mg DW^{-1} h^{-1}, converted μmol to μL).

5.5.2 Challenges and biases

Using light to attract zooplankton seems counter-intuitive at first. It is widely assumed that zooplankton exhibit a light-escape response to avoid predation during daytime, causing diel vertical migrations (Lampert, 1993; Zaret and Suffern, 1976). In addition, zooplankton avoid artificial lights from ships and other sampling platforms (Geoffroy et al., 2021; Ludvigsen et al., 2018; Berge et al., 2020; Benoit-Bird et al., 2010). The successes of the ZOORESPIRE and other zooplankton traps (e.g. by Doherty, 1987; De Leon-Casasola and Stevens, 2001; Hickford and Schiel, 1999; Meekan et al., 2001) confirm that responses to light by the diverse group of zooplankton are more complex, which is also reflected by the contradictory literature. For example, while krill are known to be attracted by light in laboratory experiments (Utne-Palm et al., 2018), copepods are reported to avoid artificial light (Ludvigsen et al., 2018), which stands in contrast to our findings. Light has lethal effects on the jellyfish *Periphylla periphylla* (Jarms et al., 2002), but is used for collection of the jellyfish *Copula sivickisi* (Schlaefer et al., 2020). Nothing is known about the response to light by amphipods and pteropods (Geoffroy et al., 2021), or tunicates. Given the diversity of taxonomic groups under the umbrella term of zooplankton, it is unlikely to find a "one-size-fits-all" solution when building a device to attract zooplankton. Understanding the phototactic behaviour of zooplankton remains an important requirement when estimating respiration rates in the ZOORESPIRE, as not all organisms will be attracted by light equally.

In addition, the potential changes in the zooplankton community in the chamber during the incubation period might bias the results. Deployment results of prototype 4 indicate a change in community relative to the control, probably caused by predation inside the chamber. Dinoflagellates of the small size fraction (50-100 μm), which dominated the control, were likely ingested by the caught copepods and crustacean larvae. Appendicularians produce gelatinous houses to catch pico- and nanoplankton and particles (Gorsky

et al., 1999), which excludes them as active consumers of dinoflagellates, which were mostly microplankton in our study. The longer the duration of the incubation period in the ZOORESPIRE the more the community will change due to predation. Similarly, the accumulation of faecal pellets and molts, if the ZOORESPIRE is to be deployed over days, has to be considered when estimating oxygen consumption rates. To circumvent this issue, a short duration of field deployments (hours rather than days) as well as installing camera systems that record entering zooplankton will assist in assessing the bias.

One of the issues during the field experiments was the absence of a control to measure background respiration of heterotrophic bacteria in the water column and on particles. The high numbers of dinoflagellates in the control trial in the Derwent, restricted the distinction between bacterial and protist respiration. Consequently, as predation decreased the dinoflagellate fraction in the light experiment, as discussed above, the measured respiration rate was not directly comparable to the control. Due to overall lower plankton concentrations offshore relative to coastal regions, the bias will be less significant for respiration rate measurements in the open ocean. However, going forward, I recommend complementary measurements of microbial respiration rates in the water column, for example by deploying the ZOORESPIRE in conjunction with RESPIRE traps or by laboratory-based incubations.

In addition, the growing phytoplankton (used as feedstock) in the tank of the krill experiments biases the results. Due to the high food supply, krill will focus on feeding outside the ZOORESPIRE rather than swimming into the chamber. In addition, the total oxygen consumption by phytoplankton increases with abundance and was therefore higher in the control trial after two days than in the first experiment at day 1. These effects are likely minor in the field, but were a significant influence during the laboratory trials.

Additional trials of the ZOORESPIRE were conducted on the SOLACE voyage in December 2020 in the subantarctic Southern Ocean (43.5-58°S, 134-148°E) However, no zooplankton were caught, despite deployment of varying times (1-3 hours) and at different depths (100, 150, and 200 m in the scattering layer). As the trap was tested successfully off the wharf in the harbour, three factors could have caused the unsuccessful trial: (1) the dominant zooplankton were not attracted by light, (2) the concentration of zooplankton was too low in surface waters, or (3) the vertical movement of the ZOORESPIRE

in the water (1-2 m in <1 min due to wave and swell motions) was too high for weak swimmers such as zooplankton to swim into the chamber. The zooplankton community in the subantarctic zone is dominated by small and large copepods (Hunt, 2005; Hunt and Hosie, 2005; Halfter et al., 2020), and during SOLACE, I caught high numbers of copepodite and adult calanoid copepods (Halfter, pers.comm). This zooplankton group was attracted by light, as seen in trials of Prototype 2 (see supplementary material) and 4. Hence, it is likely that the vertical movement of the ship caused a relatively abrupt movement of the ZOORESPIRE, which deterred the zooplankton.

5.5.3 Opportunities for future deployments & Outlook

Despite the biases in the method and challenges in developing an instrument to attract a broad range of zooplankton, the ZOORESPIRE is the first tool to efficiently measure zooplankton respiration in-situ. It avoids stressful handling of zooplankton and hyperventilation, as animals voluntarily swim into the chamber. If deployed at different water depths, it can provide insight into both local zooplankton physiology and community composition and improve our knowledge on oceanic processes such as attenuation of downward particle flux by zooplankton, in particular in under-sampled zones such as the mesopelagic zone. Another advantage of the ZOORESPIRE is its potential combination with other methods as an integrative approach to study subantarctic zooplankton and downward carbon flux. In addition to monitoring programs, e.g., Continuous Plankton Recorder and net trawls, the ZOORESPIRE advances our knowledge on ecology and biodiversity of oceanic zooplankton communities. If deployed together with the RESPIRE traps, it closes existing gaps in the oceanic carbon budget by mapping carbon remineralisation "hotspots". Furthermore, it will help predict the effects of a future ocean warming and other environmental changes for both zooplankton physiology and particle flux attenuation.

Development of the ZOORESPIRE, occurring in the near future, will focus on the improvement of deployment offshore, with planned trials in 2021/2022 in conjunction with neutrally buoyant floats in Storm Bay, Tasmania, and the subantarctic Southern Ocean. The floats will reduce the vertical movement of the ZOORESPIRE in the water column, which increases the chances of zooplankton intercepting the trap. If these deployments are

successful, further prototypes will be produced for simultaneous deployment at different water depths and in different regions. This enables a quantification of zooplankton respiration between regions in the global oceans and a comparison with particle-associated microbial respiration in the same provinces. Also, deployments during different times of the day, e.g., dusk and dawn, enable the comparison between starving zooplankton migrating up to surface and satiated zooplankton that migrate back down to the mesopelagic. Consequently, this can measure the amount of carbon that is transported downward as part of the respiratory flux.

The future vision for the ZOORESPIRE is two-fold: First, deployments from research vessels in different regions of the global oceans will increase our knowledge of in-situ zooplankton respiration and map particle fragmentation and -remineralisation "hotspots". Oxygen consumption rates by the ZOORESPIRE can be used to evaluate and adjust estimated rates by previous methods (as mentioned in 5.2.2) and either confirm respiration rates or offer correction factors. Second, continued development that will culminate in the automation of the ZOORESPIRE. A global array of ZOORESPIREs that are deployed together with sediment traps and other sensors will significantly enhance our understanding of temporal variability of zooplankton respiration in the water column. For the automation of the approach to sample more than one data point over a longer time period, the design needs to be adjusted. This includes, e.g., the removal and preservation of the zooplankton from the incubation chamber after the incubation period, increased battery size and life, and automated cleaning or replacement of the incubation chamber.

5.6 Conclusion

This chapter presents the development of the ZOORESPIRE, a new research instrument to measure zooplankton respiration in-situ. Using a light source to concentrate zooplankton and krill in field and laboratory experiments, respectively, the ZOORESPIRE successfully measured their oxygen consumption over time. In addition, the approach avoided handling stress and resulting hyperventilation of the organisms, which will largely improve estimated respiration rates. Despite mentioned biases of sampling selectivity and difficulty to distinguish microbial from zooplankton respiration, the ZOORESPIRE will provide insight into local species diversity and enable a comparison of in-situ respiration

rates with traditionally-measured rates. Future plans include deployment in conjunction with neutrally buoyant floats, deployment in different regions of the world's ocean, and automation of measurements, to quantify oceanic particle attenuation mediated by zooplankton and close gaps in the marine carbon budgets.

5.7 Supplementary material

5.7.1 Prototype 2 - Images and results

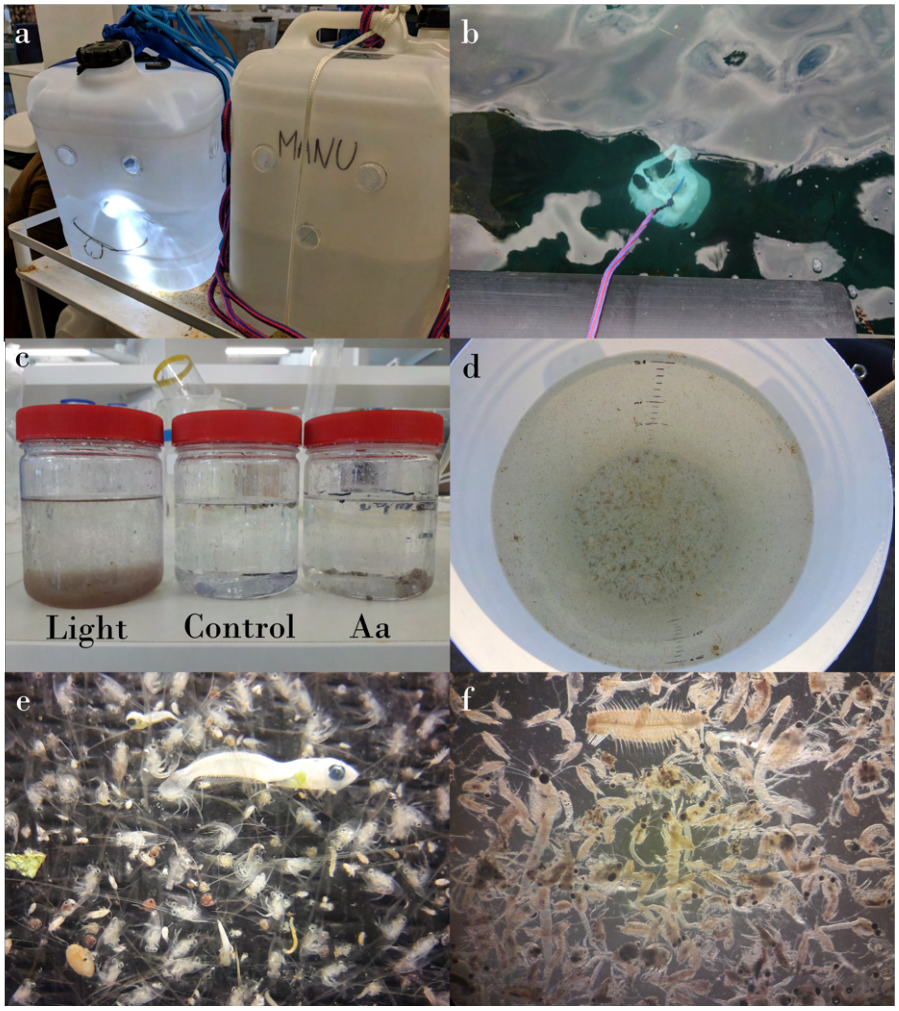

Figure 5.6: Images of the second prototype: set-up, deployment and results. The first trial was conducted off the IMAS wharf to test a light source versus an amino acid solution (Aa) in a dialysis bag to attract zooplankton (left panel): (a) Two of the three carboys, one with the dive light torch (left) and one control (right); (c) Results of the trials: light trap is visibly most successful; (e) Qualitative picture of the light sample, containing a fish larvae and many porcelain crab larvae. The second trial was conducted off the pier on Maria Island to find the best deployment time of day and duration (right panel): (b) Deployment in approximately 1.5 m water depth; (d) Zooplankton sample caught overnight; (f) Qualitative picture of the overnight sample, containing krill, polychaetes and copepods.

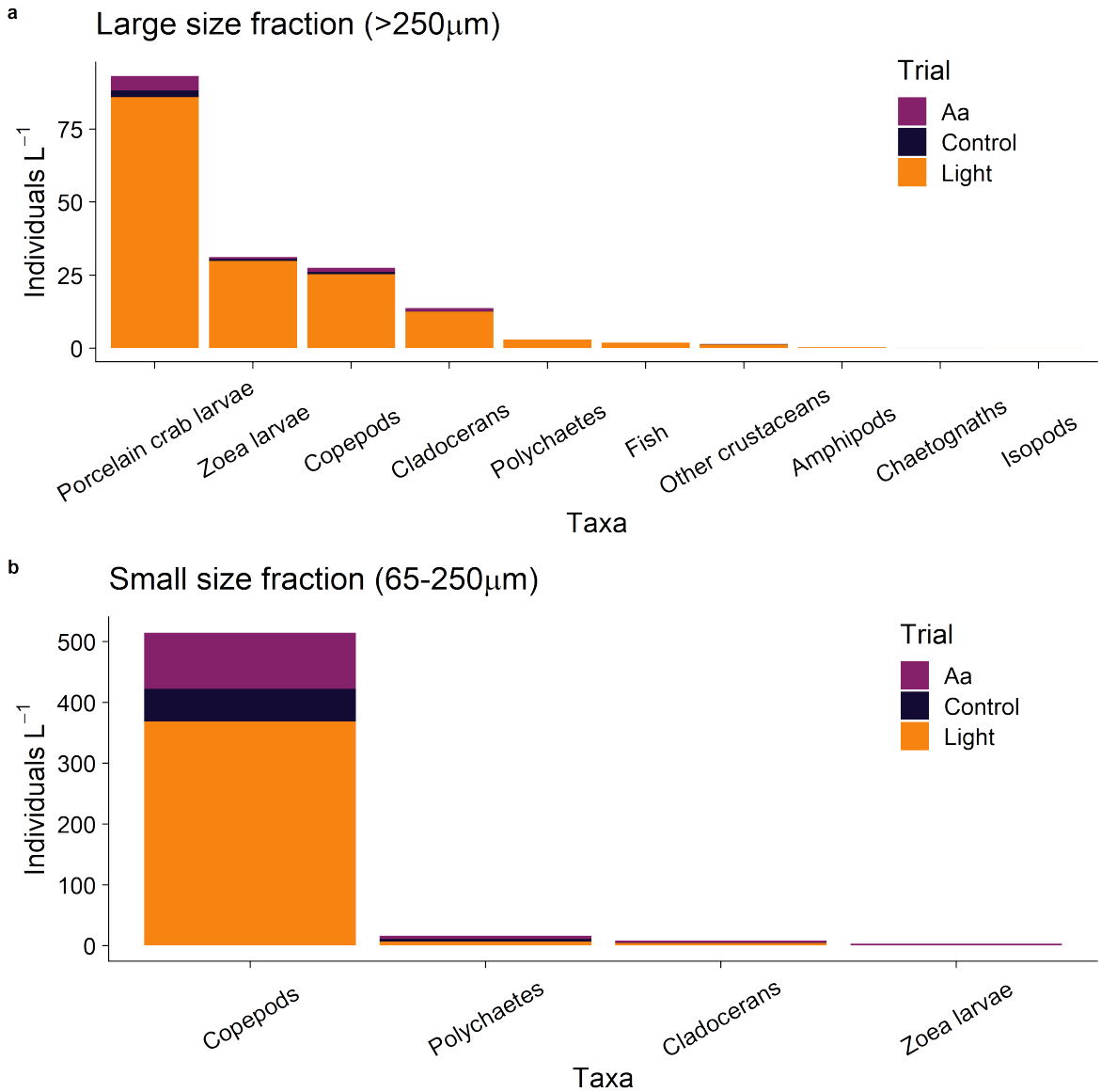

Figure 5.7: Zooplankton of the two size fractions (a) >250 μm and (b) 65-250 μm, caught overnight in prototype 2 off the IMAS Wharf. Trials were conducted with a light source (yellow), an amino acid solution in a dialysis bag (Aa, purple) and a control (dark blue).

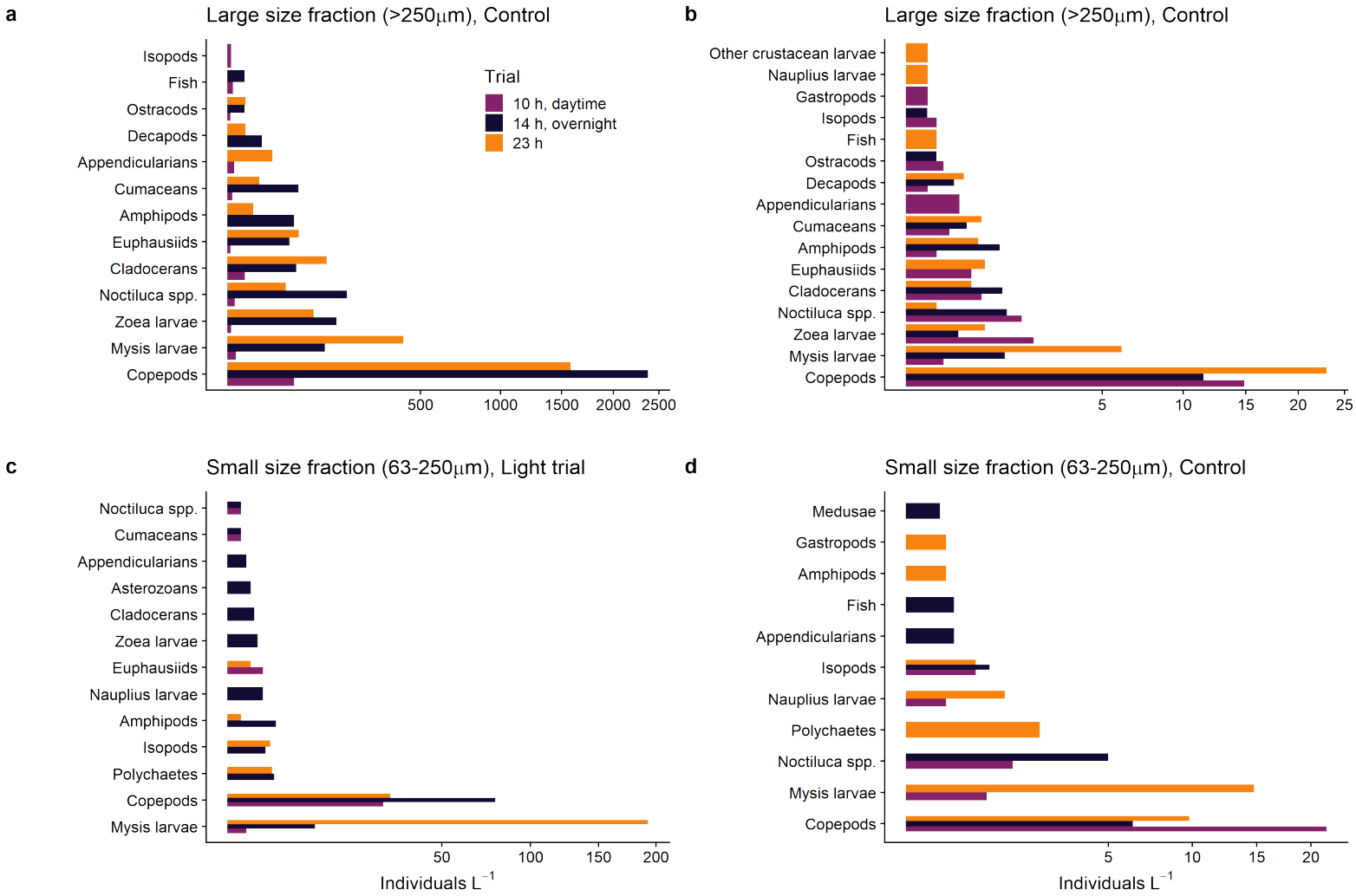

Figure 5.8: Zooplankton of the two size fractions (a) - (b) >250 μm and (c)-(d) 65-250 μm, caught in prototype 2 off the pier on Maria Island, Australia, in the light treatment (left side) and control without a light source (right side). Trials were conducted over 10 hours during the day (purple), 14 hours overnight (dark blue) and over 23 hours. Note the different scales of the x-axis between the trials and size fractions.

5.7.2 Prototype 1 & 3

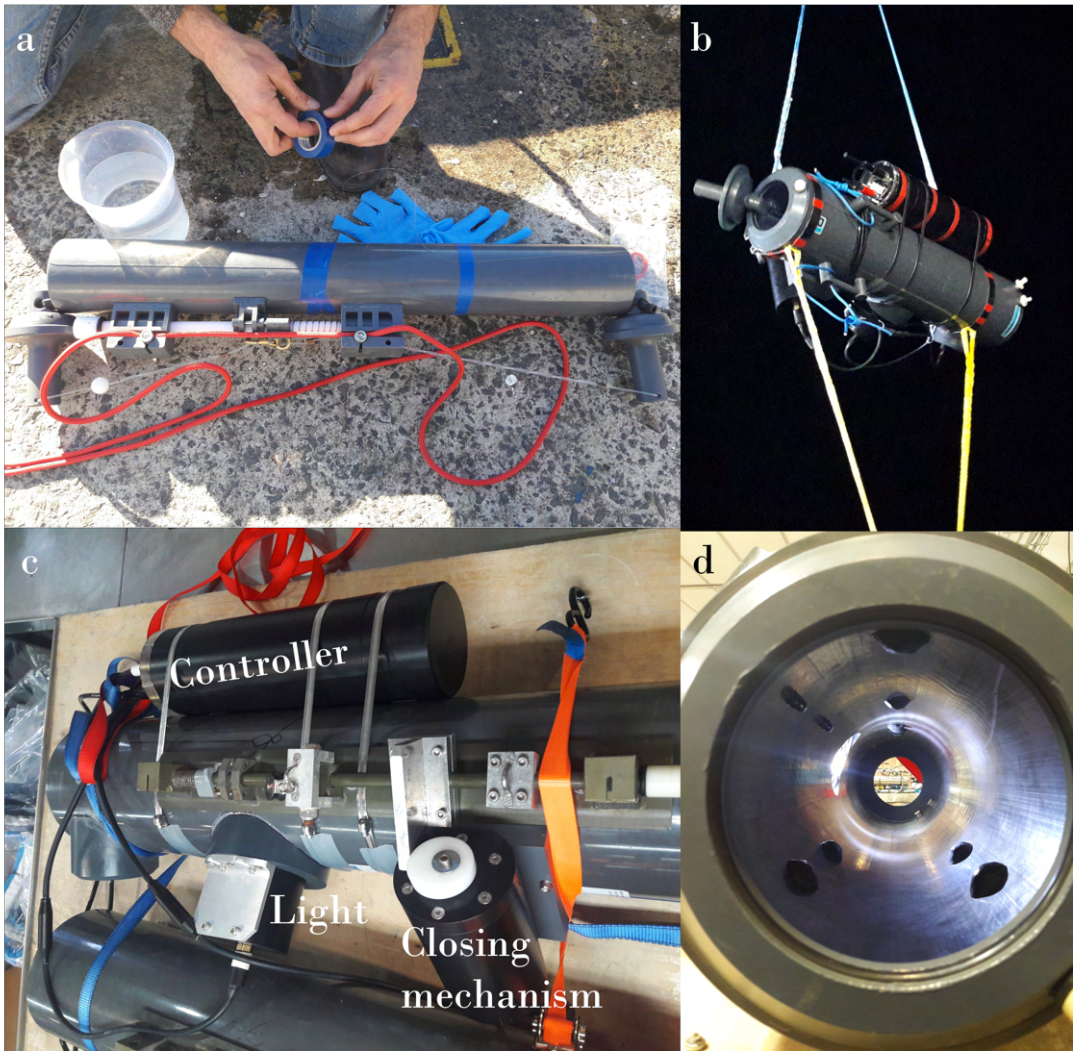

Figure 5.9: (a) Images of the first prototype, a small Niskin bottle (2.5 L) that was deployed in horizontal orientation from the IMAS Wharf. A solution of amino acids was used, however, no zooplankton were caught. (b)-(d) Images of the third prototype, a large Niskin bottle (30 L) that included a light (pointing inward, d), a controller, closing mechanism and an optode (latter not pictured in c). This prototype was deployed over the side off the RV Investigator in the subantarctic Southern Ocean but did not collect any zooplankton.

5.7.3 Prototype 4 - Results of krill attraction, capture and respiration trials

Table 5.2: Measured lengths (TL: Total length, distance from rostrum to urosome) and wet weights of the tested krill (*Euphausia superba*).

Trial	**Date**	**TL (mm)**	**Wet weight (g)**	**Oxygen consumption (μmol ind.$^{-1}$ h^{-1})**
1	10/11/2020	47	0.4973	2.2506
1	10/11/2020	47	0.4738	2.1443
1	10/11/2020	46	0.7392	3.3454
1	10/11/2020	41	0.4658	2.1081
1	10/11/2020	41	0.4245	1.9212
1	10/11/2020	37	0.3952	1.7886
1	10/11/2020	40	0.5411	2.4489
1	10/11/2020	41	0.4643	2.1013
2	11/11/2020	42	0.4821	2.3735
2	11/11/2020	41	0.4444	2.1879
2	11/11/2020	37	0.3484	1.7153
2	11/11/2020	40	0.4296	2.1150

Chapter 6

Synthesis and future directions

Climate change will affect the environmental conditions, particulate and dissolved carbon flux, and marine ecosystems in the subantarctic zone of the Southern Ocean, although its impact is not yet well quantified (Meredith et al., 2019; Deppeler and Davidson, 2017). Both warming and higher wind speeds are projected for the Southern Ocean, with consequences for physical and biogeochemical parameters, such as density stratification, underwater light levels and (micro-)nutrient distributions (Matear and Hirst, 1999; Boyd et al., 2008; Deppeler and Davidson, 2017; Poloczanska et al., 2016; Strzepek et al., 2012). The projected intensification of the East Australian Current extension into the subantarctic will influence all trophic levels, including zooplankton, and may lead to a more subtropical environmental conditions in the subantarctic zone (Herraiz-Borreguero and Rintoul, 2011). With zooplankton playing an important role in shaping particulate carbon export regimes (Laurenceau-Cornec et al., 2015; Ebersbach and Trull, 2008), it is necessary to fill remaining knowledge gaps in the zooplankton-mediated carbon pathways to improve forecasts for the carbon cycle in the future Southern Ocean.

Therefore, I have focused on three major research themes throughout the thesis, using a range of field and laboratory methods, as well as covering a variety of zooplankton-mediated carbon pathways:

1. **Understanding the importance of zooplankton for the carbon cycle of the subantarctic Southern Ocean**
   The zooplankton community produces, fragments, and transports organic particles within the water column and, hence, must be considered when estimating carbon sequestration potential of the global ocean. In this theme, I summarised current knowledge on how zooplankton shape particulate carbon export regimes, with a focus on the subantarctic zone, and explored an important, yet understudied aspect of the Biological Gravitational Pump.

2. **Characterising meso- and bathy-pelagic zooplankton communities and their relationship to the passive downward particle flux through the water column**
   While the seasonality and distribution of zooplankton communities in surface waters of the subantarctic zone (0-200 m depth) are relatively well studied, research has not focused on meso- and bathy-pelagic plankton despite their equal importance for downward particulate carbon flux and attenuation. In this theme, I have focused on characterising seasonal and inter-annual changes in the deep-sea zooplankton community, along with exploring potential drivers for their community composition and diversity, e.g. downward POC flux.

3. **Evaluation of opportunistic sampling methods and development of new technologies**
   Sampling zooplankton in the Southern Ocean is logistically challenging and often restricted to the summer season. In this theme, I have evaluated methods beyond the traditional net sampling to close knowledge gaps in the zooplankton community composition and its temporal dynamics. In addition, I discuss a newly-designed research tool that will allow an improved quantification of the attenuation of the downward POC flux by zooplankton respiration.

In the following Table (6.1, 6.2, and 6.3) summarised the main findings of this thesis and suggestions for addressing the above knowledge gaps. In addition, I present recommendations for future research priorities to further increase our understanding of the role of zooplankton in particulate and dissolved carbon flux in the Southern Ocean.

Table 6.1: Synthesis of thesis results and future research priorities.

Theme 1: Understanding the importance of zooplankton in the carbon cycle of the subantarctic Southern Ocean	
Synthesis	Future research priorities
✓ Revealed that zooplankton play an important role in establishing particulate carbon export regimes in the subantarctic zone by grazing on sinking marine particles (Chapter 2). ✓ Determined that zooplankton act as gate-keepers of the mesopelagic particulate carbon flux, which leads to low carbon export on the highly productive Kerguelen Plateau (Chapter 2). ✓ Found that zooplankton in the HNLC region south of Australia mainly feed on small particles, which results in a relatively high export of large particles out of the epipelagic zone (Chapter 2). ✓ Conducted the first study in the subantarctic Southern Ocean to estimate zooplankton carcass transport (Chapter 4). ✓ Showed that carcasses contribute significantly to the POC flux out of the epipelagic, due to their high reported sinking velocities (Chapter 4). ✓ Found that estimations of zooplankton carcass flux through the water column are sensitive to a change in mortality and sinking rates, but less to a change in microbial decomposition rate (Chapter 4).	➢ Methodology used to study zooplankton-mediated carbon flux are rarely comparable between oceanic sites: future efforts must focus on development of best practices and standardized sampling/analysis. ➢ Seasonal coverage needs to be expanded as zooplankton and particulate and dissolved carbon flux data from the winter season are often missing. ➢ Future research needs to focus on small-sized (> 200 µm) zooplankton, as their role in carbon export is vastly under-studied. ➢ Almost no data on diel and seasonal vertical migration by zooplankton are available for the subantarctic Southern Ocean. For an estimation of the magnitude of mesopelagic migrant abundance and biomass and the seasonal lipid pump as well as carcass flux, this knowledge gap needs to be closed. ➢ Non-consumptive zooplankton mortality rates from the Southern Ocean are currently not available but need to be estimated to quantify the contribution of carcasses to the BGP. ➢ Sinking of carcasses and other particles through the water column is affected by several factors, e.g. turbulence, detrivory, impact of temperature and density gradients. Future research needs to focus on these factors to quantify carbon sequestration in the Southern Ocean.

Table 6.2: Cont.

Theme 2: Characterising meso- and bathy-pelagic zooplankton communities and their relationship to the passive particle flux through the water column	
Synthesis	Future research priorities
✓ Analysed one of the longest zooplankton time-series in the southern hemisphere, collected as "swimmers" in deep-sea sediment traps between 1997-2020 (Chapter 3). ✓ Revealed that the zooplankton deep-sea community is dominated by copepods, amphipods and pteropods, with decreasing abundance and diversity with increasing depth (Chapter 3). ✓ Found that abundances of the dominating groups do not follow a distinct seasonal cycle, nor a prominent decadal trend (Chapter 3). ✓ Found that the relationship between swimmer community and flux parameters are mostly non-linar and complex (Chapter 3).	➢ Drivers of changes in the deep-sea community other than particulate flux parameters at depth need to be explored in future. ➢ Inter-calibration of methods is required: Zooplankton community collected by sediment traps needs to be compared to net trawls to understand selectivity and bias of the traps. ➢ Despite the wide use of sediment traps for sinking flux studies, the zooplankton swimmer material is rarely analysed. The increased identification of archived swimmer samples will be beneficial to compare qualitative changes between regions of the global ocean. ➢ Swarms of amphipods and other swimmers have the potential to negatively affect carbon estimates from sediment traps by scavenging on incoming particles. Integrated camera systems in "visual" sediment traps will increase knowledge of animal behaviour around the traps.

Table 6.3: Cont.

Theme 3: Evaluation of opportunistic sampling methods and development of new technologies	
Synthesis	Future research priorities
✓ Revealed that opportunistic sampling of the zooplankton community by sediment traps provides important information on temporal dynamics (Chapter 3). ✓ Discovered that biases are introduced into swimmer composition studies by interruption of time-series, mechanical handling, lack of taxonomic knowledge, and long time duration between sampling and analysis (Chapter 3). ✓ Describes the development process of a new research tool to quantify zooplankton respiration and its impact on particle attenuation in the water column, including field and laboratory trials of the final prototype (Chapter 5). ✓ Presents opportunities, challenges, and biases of a zooplankton respiration trap using light as an attractant (Chapter 5).	➢ Continuation of the present time-series at SOTS will allow for improved understanding of the impact of environmental changes, e.g. further extension of the EAC into the subantarctic zone. ➢ Future research needs to aim for minimising biases, e.g. timely analysis of zooplankton swimmers from sediment traps (within 1-2 years after recovery) and minimised mechanical handling. ➢ Deploying the ZOORESPIRE in conjunction with neutrally buoyant floats will minimise the movement of the trap in the water column and extend its use beyond coastal regions. ➢ Using arrays of the refined ZOORESPIRE prototype will allow (1) an improved comparison of zooplankton communities between sites and (2) better quantification of zooplankton respiration, especially in the understudied mesopelagic zone.

LIST OF ACRONYMS

AAIW Antarctic Intermediate Water

ACC Antarctic Circumpolar Current

ANOSIM Analysis of Similarities

AODN Australian Ocean Data Network

ASH aragonite saturation horizon

BATS Bermuda Atlantic Time Series

BCP biological carbon pump

BGP biological gravitational pump

BSi Biogenic Silica

CAP Canonical Analysis of Principal coordinates

CIV copepodite stage IV

CV copepodite stage V

CDW Circumpolar Deep Water

CPR Continuous Plankton Recorder

DIC dissolved inorganic carbon

DVM diel vertical migration

EAC East Australian Current

ENSO El Niño–Southern Oscillation

ETS Electron Transfer System

FP faecal pellets

GAM General Additive Models

GLM Generalised Linear Models

HBLE High-Biomass Low-Export

HNLC High-Nutrient Low-Chlorophyll

IMOS Integrated Marine Observing System

MMP mesopelagic-migrant pump

nMDS non-metric multi-dimensional scaling

NPP Net Primary Productivity

PC particulate carbon

PERMANOVA Permutational Multivariate Analysis of Variance

PF Polar Front

PFZ Polar Frontal Zone

PIC particulate inorganic carbon

POC particulate organic carbon

PN particulate nitrogen

PON particulate organic nitrogen

RQ respiratory quotient

sACCF southern Antarctic Circumpolar Front

SAMW Subantarctic Mode Water

SAZ Subantarctic Zone

SAZ-Sense Sensitivity of the sub-Antarctic zone to environmental change

SAF Subantarctic Front

SBdy Southern Boundary front

SLP seasonal lipid pump

SOLACE Southern Ocean Large Scale Carbon Export

SOTS Southern Ocean Time Series

STF Subtropical Front

tf total flux

ZOORESPIRE ZOOplankton RESPiration in the subsuRface OcEan

Chapter 7

Glossary

Bathypelagic zone: Also known as "midnight zone" or bathyal, the bathypelagic zone is the part of the ocean between 1,000 and 4,000 m below the the surface. It lies below the mesopelagic zone ("twilight zone") and above the abyssopelagic zone.

Biological carbon pump: Term established by Volk and Hoffert (1985) for the fixation of inorganic carbon through photosynthesis by phytoplankton, and subsequent export and sequestration to deeper waters.

Biological gravitational pump: Passive sinking of biogenic produced particles from surface waters. Zooplankton are part of the BGP by feeding and modifying the sinking particles, and producing faecal pellets and carcasses (Steinberg and Landry, 2017).

Carbon export vs. sequestration: Carbon export describes the amount of carbon transported out of the euphotic zone (defined as water depth of 1% photosynthetically active radiation) (Buesseler and Boyd, 2009), while carbon sequestration is the long-term carbon storage in carbon sinks and typically refers to the transport of carbon below 1,000 m.

Epipelagic zone: Surface zone of the ocean, where enough sunlight is available to perform photosynthesis. The epipelagic reaches from the sea surface to approximately 200 m depth and overlies the mesopelagic zone.

Mesopelagic zone: The mesopelagic zone or "twilight zone" reaches from 200 m down to 1,000 m water depth and is characterised by dysphotic conditions (<1% photosyn-

thetically active radiation). Characterised by high bacterial remineralisation rates and organism biomass, the mesopelagic zone plays an important role in the global biogeochemical cycles (Costello and Breyer, 2017; Proud et al., 2017; Robinson et al., 2010).

Mesopelagic-migrant pump: The injection of particles, e.g. faecal pellets, by migrating organisms such as zooplankton and fish, into deep-waters, before further fragmentation by detritivores and remineralisation by bacteria can occur (Boyd et al., 2019). The MMP is based on the diel vertical migration movement of organisms that typically migrate to the surface during dusk to feed and back down to depth during dawn, as predator avoidance mechanism (Bollens et al., 2011; Boyd et al., 2019; Lampert, 1993).

Mesozooplankton, micronnekton and microzooplankton: The terms refer to different size classes for organisms. Mesozooplankton are organisms between 0.2 and 20 mm, micronekton are 2-20 cm, and microzooplankton are between 20-200 μm.

Zooplankton swimmers: Zooplankton organisms that actively enter the sediment trap and are, if the trap is poisoned) subsequently killed by the preservative. They represent a bias to the carbon flux estimates, in particular, when they disintegrate over time ("Cryptic swimmers") and are not distinguishable from the sinking particles (Buesseler et al., 2007b; Lee et al., 1988; Michaels et al., 1990).

Appendix A

Chevreuxiopsis franki n. gen. n. sp. (Crustacea, Amphipoda, Thoriellidae) from the deep sea southwest of Tasmania

A.1 Abstract

A new amphipod species and genus *Chevreuxiopsis franki* found in a pelagic sediment trap southwest of Tasmania is subsequently described. The new species can be recognized by its unique antenna 2, which consists of a narrow peduncle and a 4-articulate flagellum, which has a massively developed, article 1, large, posteriorly drawn out articles 2 and 3 and an elongate lanceolate 4th article. The pereopod 1 basis surrounds large maxillipedal plates. Pereopod 3 to 6 are equipped with subchelate propodus dactylus arrangements. The bases of pereopods 5–7 are narrow.

A.2 Introduction

An unusual amphipod was found in a pelagic sediment trap deployed at 1000 m depth in the Indian sector of the Southern Ocean, southwest of Tasmania, Australia. Careful examination allowed us to identify it as a member of the family Thoriellidae. The Thoriellidae Lowry et al. (2011) consists of 4 genera: *Chevreuxiella* Stephensen (1915); *Danaella* Stephensen (1925); *Parachevreuxiella* Andres (1987) and *Thoriella* Stephensen

(1915). The morphological diversity in this family is very high. The two *Danaella* species, *Danaella mimonectes* Stephensen (1925) and *Danaella obensis* Birstein and Vinogradov (1962) (initially described as *Chevreuxiella obensis*) have inflated bodies that remind more of hyperiid amphipods than of other Aristioidea Lowry and Stoddart (1997). In contrast to *Danaella*, the genus *Thoriella*, represented by the slender *Thoriella islandica* Stephensen (1915), has rather small coxal plates. *Chevreuxiella* and *Parachevreuxiella* are very similar, only differing by the length of uropods 1 and 2, their shape and the presence/absence of an inner ramus on both appendages. As the new species, we are proposing in the following, does not fit in any of the thoriellid genera we are erecting the new genus *Chevreuxiopsis* herein.

A.3 Methods

The material was collected by a McLane 21-cup sediment trap at 1,000 m depth in the subantarctic Southern Ocean, southwest of Tasmania. The conical sediment trap has a surface of 0.5 m^2 and is filled with unfiltered water from the region (49°S/153°E at 1,200 m), which was treated with sodium chloride (5 g L^{-1}) to increase the solution density, sodium tetracarborate (1 g L^{-1}) as a pH buffer and mercuric chloride (3 g L^{-1}) for preservation (Roberts et al. 2008). The sample was filtered through a 1 mm screen and the specimen was found in the fraction >1 mm, which contains plankton and micronekton organisms Roberts et al. (2008). For taxonomic study, we transferred the material in a graded series of ethanol-glycerol mixes into pure glycerol and then mounted the specimen or dissected parts on slides for the preparation of the drawings. Pencil drawings of the habitus were made with on a Leica M 205c dissecting microscope and details of the appendages and mouthparts on a Leica DMLB compound microscope. Both microscopes were equipped with a camera lucida. The line drawings were made following the technique described in Coleman (2003, 2009). Measurements were made along the dorsal outline of the animals, from the rostrum to the end of the urosome. The material is held in the collections of the Leibniz Institute for Evolution and Biodiversity Science, Museum für Naturkunde Berlin (ZMB).

A.4 Systematics

Thoriellidae Lowry and Stoddart, 2011

Species List
Chevreuxiella metopoides Stephensen, 1915
Chevreuxiopsis franki n. gen. n. sp.
Danaella mimonectes Stephensen, 1925
Danaella obensis (Birstein & Vinogradov, 1962)
Parachevreuxiella justi Lowry & Stoddart, 2011
Parachevreuxiella lobata Andres, 1987
Thoriella islandica Stephensen, 1915

Key to the species of the Thoriellidae

1. Coxae small and separate from each other, in uropods 1 and 2 both rami subequal in length ..... ***Thoriella islandica***

1. Coxae large and overlapping each other, uropods 1 and 2 inner ramus short, vestigial or absent

    2. Pereonites 3–6 grossly swollen

        3. Posterior margin of urosome straight ..... ***Danaella mimonectes***

        3. Posterior margin of urosome incised ..... ***Danaella obensis***

    2. Pereonites 3–6 ordinary

        4. Antenna 2 flagellum consisting of 4 massive articles, article 1 expanded, articles 2–3 drawn out posteriorly, article 4 lanceolate .... ***Chevreuxiopsis franki n. gen. n. sp.***

        4. Antenna 2 with flagellum consisting of subequal articles

            5. Uropods 1 and 2 with spine-like inner rami .... ***Chevreuxiella metopoides***

5. Uropods 1 and 2 without inner rami

6. Uropods 1 and 2 rami much longer than peduncle .... ***Parachevreuxiella lobata***

6. Uropods 1 and 2 rami subequal or shorter than peduncle .... ***Parachevreuxiella justi***

***Chevreuxiopsis* n. gen.**

Diagnosis *Body* slender, pereon not inflated. *Antenna 1* slender, with normal flagellum. *Antenna 2* flagellum 4-articulate, much wider than peduncle, massively developed; article 1 enlarged, weakly drawn out posteriorly; articles 2 and 3 strongly drawn out posteriorly; article 4 lanceolate. *Maxilla 1* inner plate with 2 terminal plumose setae; outer plate with 6+1 apical spine-like setae; palp 2–articulate; article 2 inflated, lanceolate. *Maxilla 2* ordinary. *Pereopod 1* basis ovoid, expanded, with anteromarginal nose-like process; dactylus knob-like. *Pereopods 3–6* propodus subchelate; dactylus falcate (probably prehensile). Pereopod 3 coxa slightly longer than that of peropod 2. *Pereopod 4* coxa enlarged, posteromarginally straight. *Pereopods 5–7* basis slender. *Urosome* segments 2 and 3 fused; uropods 2 pairs, each with lanceolate outer ramus and spine-like inner ramus. *Telson* absent.

Type species. *Chevreuxiopsis franki* n. sp., monotypic

***Chevreuxiopsis franki* n. sp.** (A.1 - A.5)

Material examined. Holotype: female (the specimen appears to have unsetose oostegites), 12 mm.

Type locality. The specimen was collected with a McLane 21-cup sediment trap at 1,000 m depth between the 11 and 26 August 1998 at the Southern Ocean Time Series site (SOTS, 46°45.52′S, 142°5.38′E), southwest of Tasmania, Australia; (ZMB Crust 31700).

Etymology The species is named for Frank Halfter, the father of the first author.

Diagnosis. As for generic diagnosis.

Description, based on holotype, 12 mm. **Body** (A.1c). Head deeper than long, shorter than pereonite 1. Pereonite 2 slightly longer than 1. Pereonites 3 and 4 subequal in length. Pereonite 5 as long as pereonite 2. Pleonites subequal in length, posteroventrally rounded. Urosomite 1 longer than the fused urosomites 2 and 3. Telson absent.

Head (A.1c) with anterior rounded lobe between insertion of antenna 1 and 2. Eyes present, dark pigments visible in alcohol; weakly reniform, extended dorsoventrally. *Antenna 1* (A.1a, c) about 2 x as long as antenna 2; peduncular article ratios 1 : 0.4 : 0.6, width successively smaller; 15 flagellum articles, slender, with very few slender setae. *Antenna 2* (A.1b, 6) peduncle articles slender, with 2 minute basal articles (which were damaged during dissection), article 3 short; article 4 about 2 x as long as article 3; article 5 as long as article 1–4 combined; flagellum article 1 distally expanded, about 3 x as wide as basal articles, posterodistally lobate; article 2–3 proximally as wide as peduncular article 3 and posterodistally drawn out into long narrow lobes; article 4 lanceolate, distally pointed and inside with a dense mass of tissue. *Mouthparts* (A.1c, 2f) extended ventrally, all covered by large outer plates of maxilliped, which leave an anteriorly and ventrally slit-like opening and additionally surrounded posteriorly by wide bases of pereopods 1. Mandibles to maxilla 2 directed anteriorly; ventrally of these mouthparts is a dense tissue mass (dashed in A.2f; A.3a), that might represent the inner maxillipedal plates. Both mandibles slender without molar, setal rows or palp (A.2a, b). *Labrum* without pronounced epistome, rounded from lateral view (A.1d). *Lower lip* (A.2e) with rather long rounded apices with few setae in the hypopharyngeal gap and with slender mandibular lobes. *Maxilla 1* (A.2c, d) inner plate with 2 plumose apical setae; outer plate with 6 plus 1 apical robust setae; palp 2-articulate, line between both articles barely visible, distal article lanceolate, with 1 short seta on tapering tip. *Maxilla 2* (A.2g) inner plate with some medial setae; outer plate with 4 distolateral plumose setae.

Pereon. *Pereopod 1* (A.3b) dark purple/black pigmented in ethanol; coxa subquadrate;

basis anteromarginally expanded with short nose-shaped protrusion; ischium and merus subequal; carpus weakly expanded distally 2.2 x as long as wide; propodus slightly tapering distally with distal knob-like dactylus. *Pereopod 2* (A.3d, e) basis elongate and slender; ischium 2.7 x as long as wide; merus short, distally pointed; carpus longer than propodus with cushions of slender, hair-like setae on anterior and posterior margins; propodus anteromarginally rounded with similar setation as carpus; dactylus subapically, accompanied with long several long setulated setae and with few setae on the inner curvature. *Pereopod 3* (A.3c) coxa subrectangular, slightly directed anteriorly; basis as long as coxa; ischium 0.6 x the width of basis; merus relatively short, distally expanded; carpus wider than long, distally expanded; carpus curved posteriorly, distally oblique; dactylus with proximal rounded joint, weakly curved, slender; propodus and dactylus form subchelate complex. *Pereopod 4* (A.4a) coxa largest, about 4 x as long as coxa 1, surpassing basis, ischium and part of merus, anteriorly convex, posteriorly straight; basis to dactylus subequal to pereopod 3, except for the slightly longer carpus. *Pereopod 5* (A.4b) coxa bilobed; basis to merus subequal to pereopod 4; carpus shorter than wide, with anterior process; propodus curved anteriorly with oblique distal margin; carpus and long, slender, weakly curved dactylus form a very large subchela. *Pereopod 6* (A.5a, d) coxa wide, weakly bilobate, posterior lobe slightly longer than anterior one; basis about half as long as coxa width; ischium longer than wide; merus expanded posterodistally; carpus short, distally expanded, with some small teeth anteromarginally; propodus, relatively slender, convex posteromarginally, anteromarginally straight, with marginal small teeth, especially on the medial face; dactylus falcate. *Pereopod 7* (A.4c) coxa shorter than wide, subrectangular; basis posteroproximally weakly expanded, somewhat tapering distally; ischium subquadrate; merus weakly expanded posterodistally; carpus subquadrate; propodus convex posteromarginally, straight anteromarginally; dactylus much shorter than preceding appendages.

Pleon. *Pleopod 1* (A.5b, c) peduncle 2 x as long as wide; coupling hooks (A.5c) long with rows of protrusions ventrally; both rami slightly longer than peduncle, inner ramus somewhat shorter than outer ramus; swimming setae moderately long with dense setulation (A.5f).

Urosome. First urosomite longer than the fused second and third segment; urosomite

2 expanded midlaterally and weakly incised posteromarginally forming 2 short rounded lobes; peduncle of uropod 1 2.5 x as long as wide; outer ramus lanceolate; inner ramus spine-like, 25 % of outer ramus length; uropod 2 peduncle shorter than that of uropod 1 and weakly expanded distally; outer ramus slightly wider compared to that of uropod 1; inner ramus 23 % of outer ramus. *Telson* absent.

Distribution. The species is so far only known from the type locality.

A.5 Discussion

We classified the new species in a new genus *Chevreuxiopsis*. This genus is related to *Chevreuxiella* (represented by the only species *C. metopoides*) and both genera share the following: - pereon not inflated (cf. *Danaella*); - coxa 4 enlarged; - similarities in the mouthparts: rather underived maxilla 1 and 2 and the morphology of the maxilliped; - urosome and both uropods are very similar in the lanceolate shape of the rami and the dimensions of the inner rami.

However, there are also strong differences between the new species and *C. metopoides*. *Chevreuxiopsis franki* n. gen. n. sp. has a differently shaped, slender antenna 1 (vs expanded and elongate first flagellar article. This is perhaps a sexually dimorphic character, as *C. metopoides* was described on a male specimen) and especially antenna 2 flagellum, which has an enlarged article 1, large, posteriorly drawn out articles 2 and 3 and a lanceolate article 4 (vs normally shaped and multiarticulate); maxilla 1 with inflated palp article 2 (vs normal), inner plate with 2 plumose setae (vs 4 setae); basis of pereopod 1 ovoid expanded with anteromarginal nose-like process (vs weakly expanded and without nose-like process); coxa 3 slightly longer than coxa 2 (vs much longer and wider); coxa 4 posteromarginally straight (vs posteroventally lobate); basis of pereopods 5–7 slender (vs expanded); pereopod 3–6 probably prehensile due to their subchelate arrangement of propodus and falcate dactylus (vs simple).

The maxilliped is of a unique shape in thoriellids. Large plates surround the mouthparts and leave a small slit anteriorly and ventrally. However, due to its derived morphology

it is very difficult to homologize the parts. For example, Stephensen (1915, p. 41, Fig. 24) labelled the massive maxillipedal plates, that surround the mouthparts, as the first palp articles, but we think they are the outer plates of the maxilliped. These plates are overlapped by the huge bases of the first pereopod, which has dark purple/black pigmentation and may act as a shutter (see below).

Due to the low number of records in literature, knowledge about the biology of the Thoriellidae is limited (Lowry et al., 2011). Stephensen (1915) suggested a semiparasitic lifestyle for *Chevreuxiella* and *Thoriella* and Andres (1987) found *Parachevreuxiella lobata* attached to a wound of a bathypelagic fish. However, it is difficult to draw conclusions about the lifestyle of *Chevreuxiopsis franki* n. sp. Due to the relatively good preservation of the body, an active entering of the specimen into the sediment trap is assumed. The long-term deployment of the sediment trap prevents analyses of potential differences in day versus night distribution due to diurnal vertical migration. Hence, no additional information on the vertical distribution of this species can be concluded.

The specimen is of transparent appearance apart from the dark purple gnathopod 1, which covers the maxilliped (A.6). Herring (1981) already noted a blue-green bioluminescence in the genera *Chevreuxiella* and *Danaella* in the thoriellid family while handling, which "almost extinguished when the maxilliped plate was withdrawn between the two densely pigmented expanded basal articles of the first pair of gnathopods". Also, Parker (1999) studied the luminescence of an unidentified thoriellid juvenile and found the expanded fifth articles of the second antennae to act as reflectors of the luminescent maxilliped. He assumed that rather than having a communication or defensive function, light flashes could be used to catch prey. Similarly, this could be the case in our specimen. Additional to the dark purple/black shutter, we also note enlarged articles of the second antenna, which could function as reflector of the emitted bioluminescence and lead potential prey towards the maxillipeds. However, this has to be further investigated in behavioural studies.

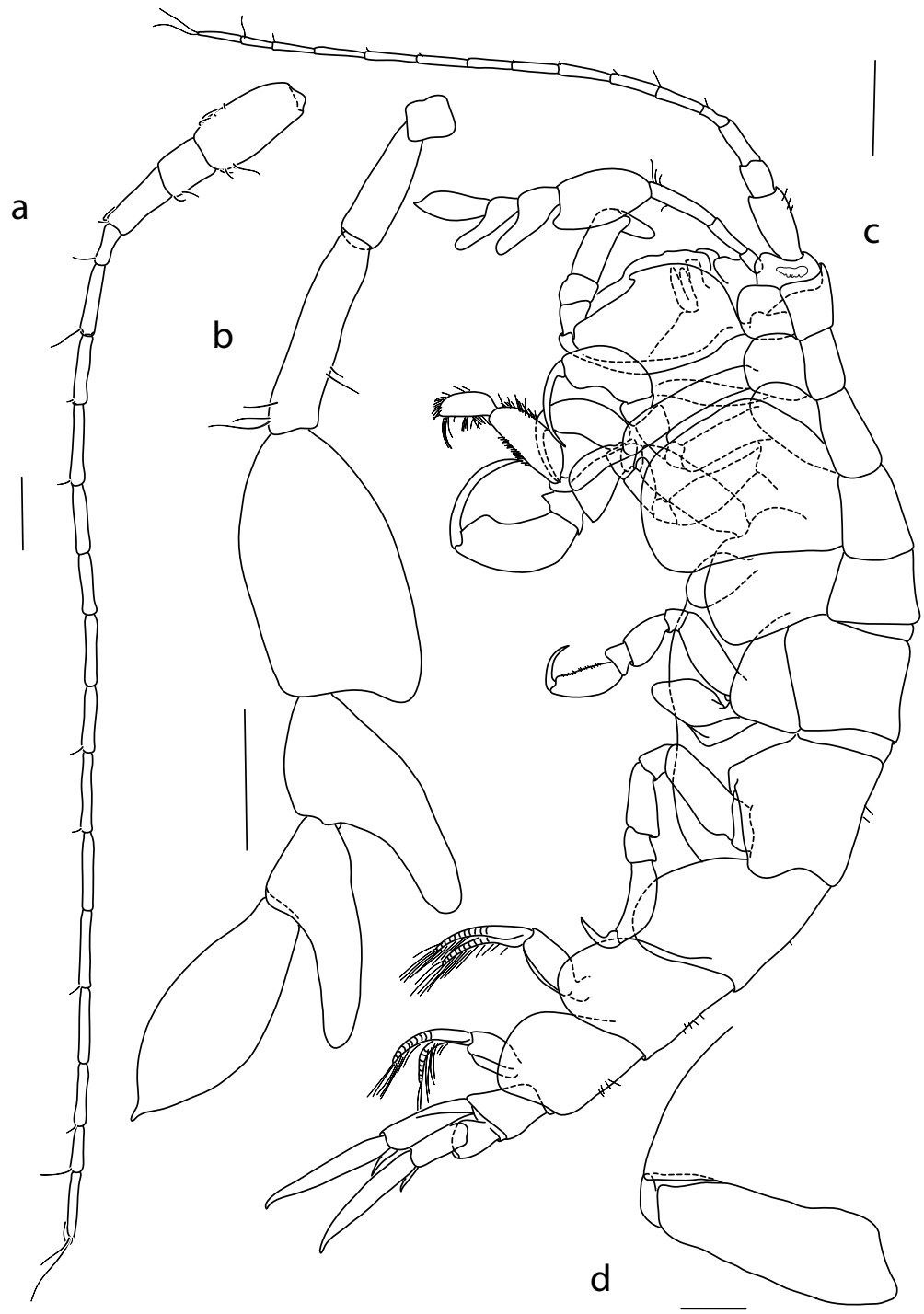

Figure A.1: a–d. *Chevreuxiopsis franki* n. gen. n. sp., holotype 12 mm. a) antenna 1; b) antenna 2, peduncular articles 1–2 missing; c) habitus; d) labrum and mandible, lateral view. Scale bars: a, b = 500 μm; c = 1 mm; d = 100 μm.

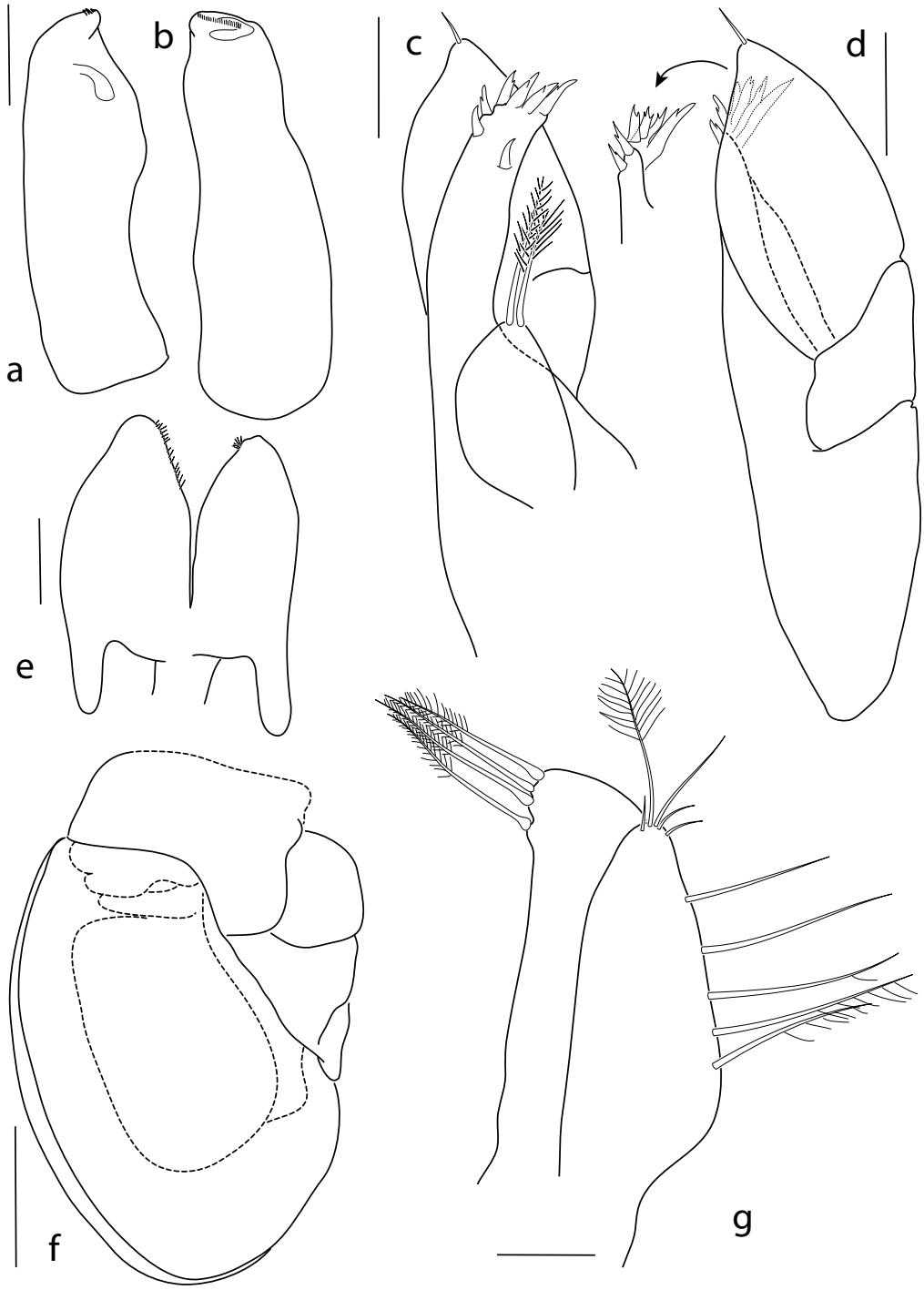

Figure A.2: a–g. *Chevreuxiopsis franki* n. gen. n. sp., holotype 12 mm. a) right mandible; b) left mandible; c, d) maxilla 1; e) lower lip; f) mouthparts, left aspect; g) maxilla 2. Scale bars: a–e = 100 μm; f = 500 μm.

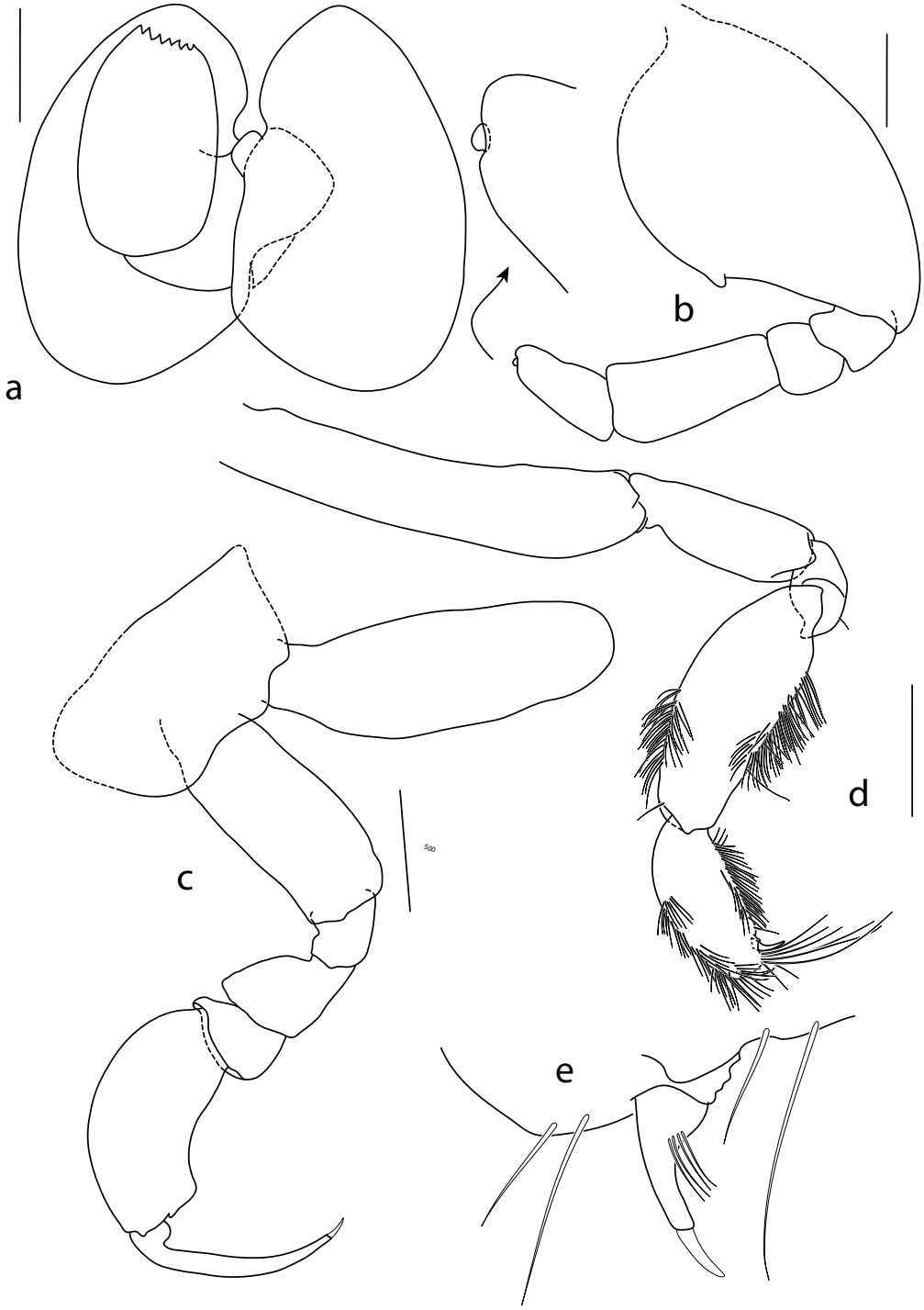

Figure A.3: a–e. *Chevreuxiopsis franki* n. gen. n. sp., holotype 12 mm. a) maxilliped, opened up; b) pereopod 1, basis to dactylus; detail shows knob-like dactylus; c) pereopod 3; d) pereopod 2, without coxa; e) dactylus of pereopod 2. Scale bars: a–d = 500 μm.

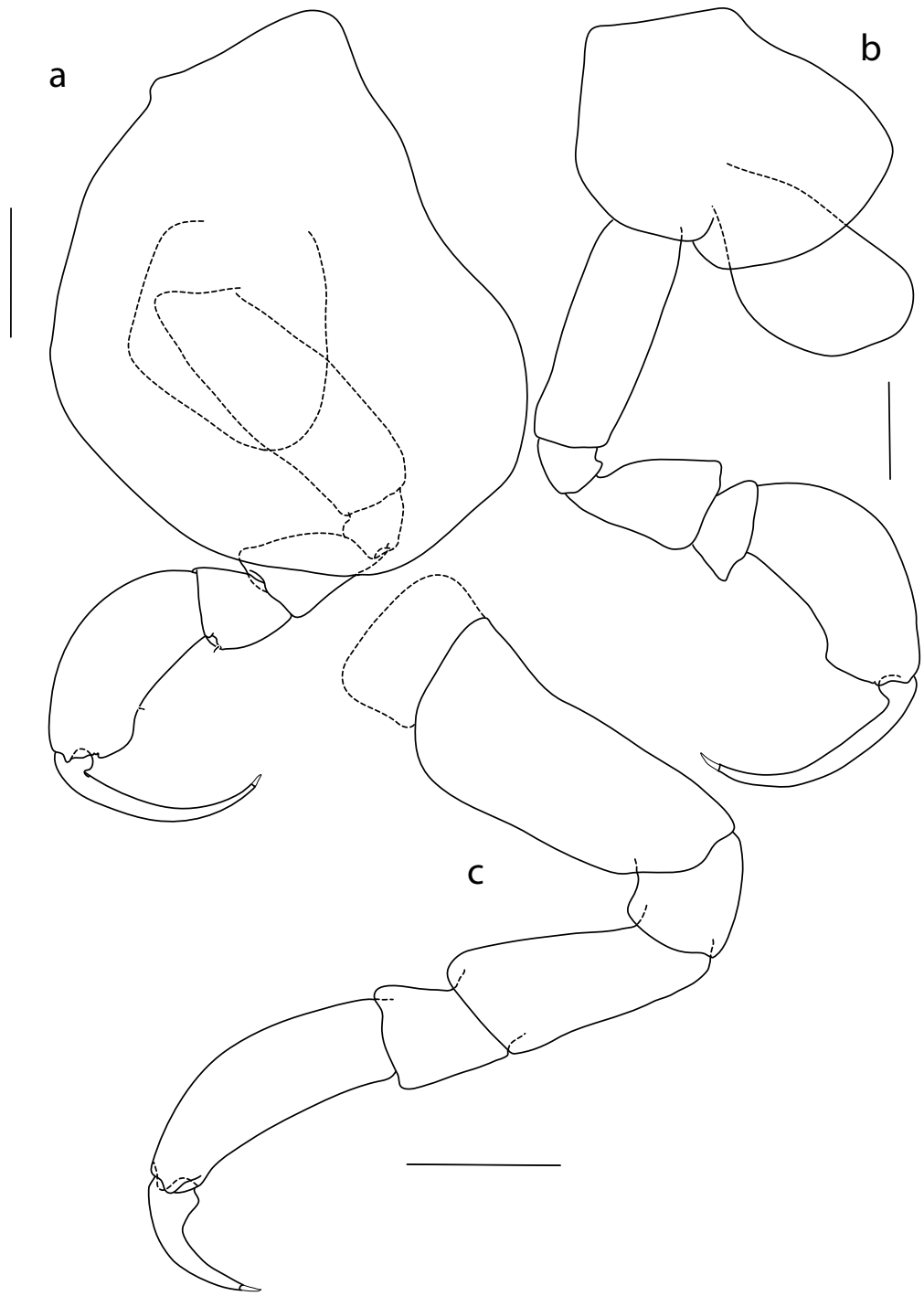

Figure A.4: a–c. *Chevreuxiopsis franki* n. gen. n. sp., holotype 12 mm. a) pereopod 4; b) pereopod 5; c) pereopod 7, medial aspect. Scale bars: a–c = 500 μm.

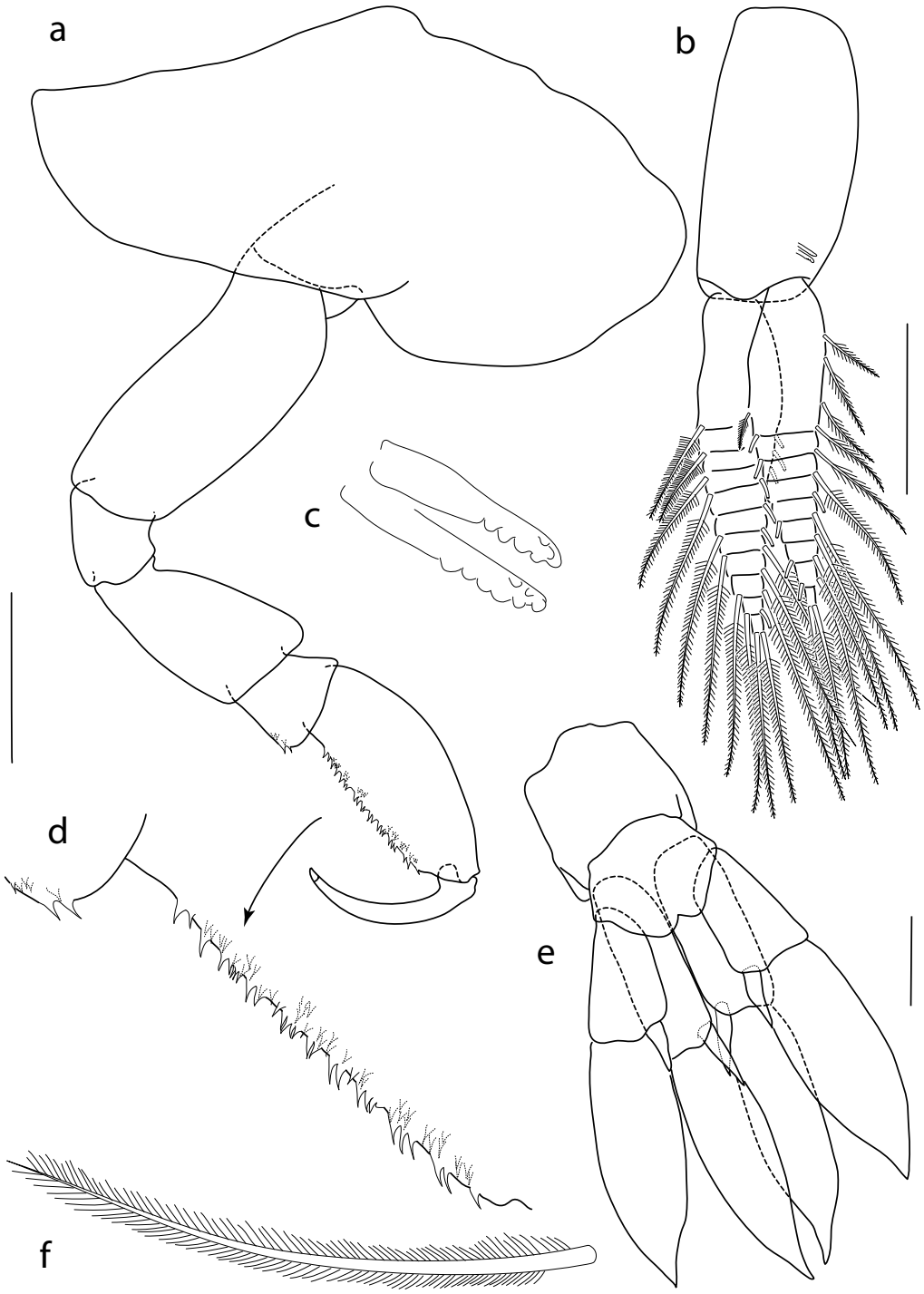

Figure A.5: *Chevreuxiopsis franki* n. gen. n. sp., holotype 12 mm. a) pereopod 6; b) pleopod 1; c) coupling hooks of pleopod; d) anterior margin of propodus; e) urosome, dorsal view; f) setulated seta of pleopod. Scale bars: a, b, e = 500 μm.

Figure A.6: *Chevreuxiopsis franki* n. gen. n. sp., holotype 12 mm. Photo of head, antennae, maxillipeds and anterior pereopods. Note the dark purple/black colour of the 1st pereopods. Scale bar = 500 μm.

REFERENCES

Anderson, T. R., Gentleman, W. C., and Yool, A. (2015). EMPOWER-1 . 0 : an Efficient Model of Planktonic ecOsystems. *Geoscientific Model Development*, 8:2231–2262.

Andres, H. G. (1987). Die Gammaridea der 76. Reise von FFS" Walther Herwig mit Beschreibung von Parachevreuxiella lobata gen. n. und sp. n.(Crustacea: Amphipoda). *Mitteilungen aus dem Hamburgischen Zoologischen Museum und Institut*, 84:95–103.

Armand, L. K., Cornet-Barthaux, V., Mosseri, J., and Quéguiner, B. (2008). Late summer diatom biomass and community structure on and around the naturally iron-fertilised Kerguelen Plateau in the Southern Ocean. *Deep Sea Research Part II: Topical Studies in Oceanography*, 55(5-7):653–676.

Armstrong, R. A., Peterson, M. L., Lee, C., and Wakeham, S. G. (2009). Settling velocity spectra and the ballast ratio hypothesis. *Deep Sea Research Part II: Topical Studies in Oceanography*, 56(18):1470–1478.

Arteaga, L., Haëntjens, N., Boss, E., Johnson, K. S., and Sarmiento, J. L. (2018). Assessment of export efficiency equations in the Southern Ocean applied to satellite-based net primary production. *Journal of Geophysical Research: Oceans*, 123(4):2945–2964.

Atkinson, A. (1998). Life cycle strategies of epipelagic copepods in the Southern Ocean. *Journal of Marine Systems*, 15(1-4):289–311.

Atkinson, A., Siegel, V., Pakhomov, E., and Rothery, P. (2004). Long-term decline in krill stock and increase in salps within the Southern Ocean. *Nature*, 432(7013):100–103.

Atkinson, A. and Sinclair, J. D. (2000). Zonal distribution and seasonal vertical migration of copepod assemblages in the Scotia Sea. *Polar Biology*, 23(1):46–58.

Atkinson, A., Ward, P., Hunt, B. P. V., Pakhomov, E. A., and Hosie, G. W. (2012). An overview of Southern Ocean zooplankton data: Abundance, biomass, feeding and functional relationships. *CCAMLR Science*, 19:171–218.

Auguie, B. (2017). gridExtra: Miscellaneous Functions for "Grid" Graphics. R package version 2.3.

REFERENCES

Aumont, O. and Bopp, L. (2006). Globalizing results from ocean in situ iron fertilization studies. *Global Biogeochemical Cycles*, 20(GB2017):1–15.

Axler, R. P. and Owen, C. J. (1994). Measuring chlorophyll and phaeophytin: Whom should you believe? *Lake and Reservoir Management*, 8(2):143–151.

Bach, L. T., Riebesell, U., Sett, S., Febiri, S., Rzepka, P., and Schulz, K. G. (2012). An approach for particle sinking velocity measurements in the 3-400 µm size range and considerations on the effect of temperature on sinking rates. *Marine Biology*, 159(8):1853–1864.

Baumgartner, M. F. and Tarrant, A. M. (2017). The physiology and ecology of diapause in marine copepods. *Annual Review of Marine Science*, 9(1):387–411.

Belcher, A., Iversen, M., Giering, S., Riou, V., Henson, S., and Sanders, R. (2016a). Depth-resolved particle associated microbial respiration in the northeast Atlantic. *Biogeosciences Discussions*, 13(17):4927–4943.

Belcher, A., Iversen, M., Manno, C., Henson, S. A., Tarling, G. A., and Sanders, R. (2016b). The role of particle associated microbes in remineralization of fecal pellets in the upper mesopelagic of the Scotia Sea, Antarctica. *Limnology and Oceanography*, 61(3):1049–1064.

Benoit-Bird, K. J., Moline, M. A., Schofield, O. M., Robbins, I. C., and Waluk, C. M. (2010). Zooplankton avoidance of a profiled open-path fluorometer. *Journal of Plankton Research*, 32(10):1413–1419.

Berge, J., Geoffroy, M., Daase, M., Cottier, F., Priou, P., Cohen, J. H., Johnsen, G., McKee, D., Kostakis, I., Renaud, P. E., Vogedes, D., Anderson, P., Last, K. S., and Gauthier, S. (2020). Artificial light during the polar night disrupts Arctic fish and zooplankton behaviour down to 200 m depth. *Communications Biology*, 3(1):102.

Birstein, J. A. and Vinogradov, M. E. (1962). Pelagic Gammaridea (Amphipoda, Gammaridea) collected by the Soviet Antarctic Expedition on the M/V "Ob", south of 40°S. *Akademiya Nauk SSSR, Issledovaniya Fauny Morei*, 1(10):33–56.

Blain, S., Quéguiner, B., Armand, L., Belviso, S., Bombled, B., Bopp, L., Bowie, A. R., Brunet, C., Brussaard, C. P. D., and Carlotti, F. (2007). Effect of natural iron fertilization on carbon sequestration in the Southern Ocean. *Nature*, 446(7139):1070–1074.

Blain, S., Renaut, S., Xing, X., Claustre, H., and Guinet, C. (2013). Instrumented elephant seals reveal the seasonality in chlorophyll and light-mixing regime in the iron-fertilized Southern Ocean. *Geophysical Research Letters*, 40(24):6368–6372.

Blain, S., Sarthou, G., and Laan, P. (2008). Distribution of dissolved iron during the natural iron-fertilization experiment KEOPS (Kerguelen Plateau, Southern Ocean). *Deep Sea Research Part II: Topical Studies in Oceanography*, 55(5):594–605.

REFERENCES

Blain, S., Tréguer, P., Belviso, S., Bucciarelli, E., Denis, M., Desabre, S., Fiala, M., Martin Jézéquel, V., Le Fèvre, J., Mayzaud, P., Marty, J.-C., and Razouls, S. (2001). A biogeochemical study of the island mass effect in the context of the iron hypothesis: Kerguelen Islands, Southern Ocean. *Deep Sea Research Part I: Oceanographic Research Papers*, 48(1):163–187.

Bollens, S. M., Rollwagen-Bollens, G., Quenette, J. A., and Bochdansky, A. B. (2011). Cascading migrations and implications for vertical fluxes in pelagic ecosystems. *Journal of Plankton Research*, 33(3):349–355.

Bowie, A. R., Griffiths, B. F., Dehairs, F., and Trull, T. W. (2011a). Oceanography of the subantarctic and Polar Frontal Zones south of Australia during summer: Setting for the SAZ-Sense study. *Deep-Sea Research Part II: Topical Studies in Oceanography*, 58(21-22):2059–2070.

Bowie, A. R., Trull, T. W., and Dehairs, F. (2011b). Estimating the sensitivity of the subantarctic zone to environmental change: The SAZ-Sense project. *Deep Sea Research Part II: Topical Studies in Oceanography*, 58(21-22):2051–2058.

Boyd, P. W., Claustre, H., Levy, M., Siegel, D. A., and Weber, T. (2019). Multi-faceted particle pumps drive carbon sequestration in the ocean. *Nature*, 568(7752):327–335.

Boyd, P. W., Doney, S. C., Strzepek, R., Dusenberry, J., Lindsay, K., and Fung, I. (2008). Climate-mediated changes to mixed-layer properties in the Southern Ocean: assessing the phytoplankton response. *Biogeosciences*, 5(3):847–864.

Boyd, P. W., McDonnell, A., Valdez, J., LeFevre, D., and Gall, M. P. (2015). RESPIRE: An in situ particle interceptor to conduct particle remineralization and microbial dynamics studies in the oceans' Twilight Zone. *Limnology and Oceanography: Methods*, 13(9):494–508.

Boyd, P. W. and Trull, T. W. (2007). Understanding the export of biogenic particles in oceanic waters: Is there consensus? *Progress in Oceanography*, 72(4):276–312.

Bradford, J. M., Ohman, M. D., and Jillett, J. B. (1988). Larval morphology and development of Neocalanus tonsus, Calanoides macrocarinatus, and Calanus australis (Copepoda: Calanoida) in the laboratory. *New Zealand Journal of Marine and Freshwater Research*, 22(3):301–320.

Bradford-Grieve, J. (1999). Pelagic ecosystem structure and functioning in the subtropical front region east of New Zealand in austral winter and spring 1993. *Journal of Plankton Research*, 21(3):405–428.

Bradford-Grieve, J. M. and Jillett, J. B. (1998). Ecological constraints on horizontal patterns - with special reference to the copepod Neocalanus tonsus (Brady, 1883). In *Pelagic Biogeography ICoPB II. Proceedings of the second International Conference. IOC/UNESCO. Intergov. Oceanogr. Comm., Workshop Rep.*, pages 65–77.

REFERENCES

Bradford-Grieve, J. M., Nodder, S. D., Jillett, J. B., Currie, K., and Lassey, K. R. (2001). Potential contribution that the copepod Neocalanus tonsus makes to downward carbon flux in the Southern Ocean. *Journal of Plankton Research*, 23(9):963–975.

Bray, J. R. and Curtis, J. T. (1957). An Ordination of the Upland Forest Communities of Southern Wisconsin. *Ecological Monographs*, 27(4):325–349.

Bressac, M., Guieu, C., Ellwood, M. J., Tagliabue, A., Wagener, T., Laurenceau-Cornec, E. C., Whitby, H., Sarthou, G., and Boyd, P. W. (2019). Resupply of mesopelagic dissolved iron controlled by particulate iron composition. *Nature Geoscience*, 12(12):995–1000.

Britten, G. L., Wakamatsu, L., and Primeau, F. W. (2017). The temperature-ballast hypothesis explains carbon export efficiency observations in the Southern Ocean. *Geophysical Research Letters*, 44(4):1831–1838.

Bucciarelli, E., Blain, S., and Tréguer, P. (2001). Iron and manganese in the wake of the Kerguelen Islands (Southern Ocean). *Marine Chemistry*, 73(1):21–36.

Buesseler, K. O. (1998). The decoupling of production and particulate export in the surface ocean. *Global Biogeochemical Cycles*, 12(2):297–310.

Buesseler, K. O., Antia, A. N., Chen, M., Fowler, S. W., Gardner, W. D., Gustafsson, O., Harada, K., Michaels, A. F., Loeff, M. R. v. d., Sarin, M., Steinberg, D. K., and Trull, T. (2007a). An assessment of the use of sediment traps for estimating upper ocean particle fluxes. *Journal ofMarine Research*, 65(3):345–416.

Buesseler, K. O. and Boyd, P. W. (2009). Shedding light on processes that control particle export and flux attenuation in the twilight zone of the open ocean. *Limnology and Oceanography*, 54(4):1210–1232.

Buesseler, K. O., Lamborg, C. H., Boyd, P. W., Lam, P. J., Trull, T. W., Bidigare, R. R., Bishop, J. K. B., Casciotti, K. L., Dehairs, F., Elskens, M., Honda, M., Karl, D. M., Siegel, D. A., Silver, M. W., Steinberg, D. K., Valdes, J., Van Mooy, B., and Wilson, S. (2007b). Revisiting Carbon Flux Through the Ocean's Twilight Zone. *Science*, 316(5824):567–570.

Burd, A. B., Hansell, D. A., Steinberg, D. K., Anderson, T. R., Arístegui, J., Baltar, F., Beaupré, S. R., Buesseler, K. O., DeHairs, F., Jackson, G. A., Kadko, D. C., Koppelmann, R., Lampitt, R. S., Nagata, T., Reinthaler, T., Robinson, C., Robison, B. H., Tamburini, C., and Tanaka, T. (2010). Assessing the apparent imbalance between geochemical and biochemical indicators of meso- and bathypelagic biological activity: What the @$#! is wrong with present calculations of carbon budgets? *Deep Sea Research Part II: Topical Studies in Oceanography*, 57(16):1557–1571.

Calbet, A. (2001). Mesozooplankton grazing effect on primary production: A global comparative analysis in marine ecosystems. *Limnology and Oceanography*, 46(7):1824–1830.

Calbet, A. (2008). The trophic roles of microzooplankton in marine systems. *ICES Journal of Marine Science*, 65(3):325–331.

REFERENCES

Calbet, A. and Landry, M. R. (2004). Phytoplankton growth, microzooplankton grazing, and carbon cycling in marine systems. *Limnology and Oceanography*, 49(1):51–57.

Carlotti, F., Jouandet, M. P., Nowaczyk, A., Harmelin-Vivien, M., Lefèvre, D., Richard, P., Zhu, Y., and Zhou, M. (2015). Mesozooplankton structure and functioning during the onset of the Kerguelen phytoplankton bloom during the KEOPS2 survey. *Biogeosciences*, 12(14):4543–4563.

Carlotti, F., Thibault-Botha, D., Nowaczyk, A., and Lefe, D. (2008). Zooplankton community structure , biomass and role in carbon fluxes during the second half of a phytoplankton bloom in the eastern sector of the Kerguelen Shelf (January – February 2005). *Deep Sea Research Part II*, 55(5-7):720–733.

Cassar, N., DiFiore, P. J., Barnett, B. A., Bender, M. L., Bowie, A. R., Tilbrook, B., Petrou, K., Westwood, K. J., Wright, S. W., and Lefevre, D. (2011). The influence of iron and light on net community production in the Subantarctic and Polar Frontal Zones. *Biogeosciences*, 8(2):227–237.

Cavagna, A. J., Fripiat, F., Elskens, M., Mangion, P., Chirurgien, L., Closset, I., Lasbleiz, M., Florez-Leiva, L., Cardinal, D., Leblanc, K., Fernandez, C., Lefèvre, D., Oriol, L., Blain, S., Quéguiner, B., and Dehairs, F. (2015). Production regime and associated N cycling in the vicinity of Kerguelen Island, Southern Ocean. *Biogeosciences*, 12(21):6515–6528.

Cavan, E., Henson, S., Belcher, A., and Sanders, R. (2017a). Role of zooplankton in determining the efficiency of the biological carbon pump. *Biogeosciences*, 14(1):177–186.

Cavan, E. L., Belcher, A., Atkinson, A., Hill, S. L., Kawaguchi, S., McCormack, S., Meyer, B., Nicol, S., Ratnarajah, L., Schmidt, K., Steinberg, D. K., Tarling, G. A., and Boyd, P. W. (2019a). The importance of Antarctic krill in biogeochemical cycles. *Nature Communications*, 10(1):1–13.

Cavan, E. L. and Boyd, P. W. (2018). Effect of anthropogenic warming on microbial respiration and particulate organic carbon export rates in the sub-Antarctic Southern Ocean. *Aquatic Microbial Ecology*, 82(2):111–127.

Cavan, E. L., Laurenceau-Cornec, E. C., Bressac, M., and Boyd, P. W. (2019b). Exploring the ecology of the mesopelagic biological pump. *Progress in Oceanography*, 176(102125):1–15.

Cavan, E. L., Le Moigne, F. A. C., Poulton, A. J., Tarling, G. A., Ward, P., Daniels, C. J., Fragoso, G. M., and Sanders, R. J. (2015). Zooplankton fecal pellets control the attenuation of particulate organic carbon flux in the Scotia Sea, Southern Ocean. *Geophysical Research Letters*, 42(3):821–830.

Cavan, E. L., Trimmer, M., Shelley, F., and Sanders, R. (2017b). Remineralization of particulate organic carbon in an ocean oxygen minimum zone. *Nat Commun*, 8(14847):1–9.

Chan, B. K. K., Shao, K.-T., Shao, Y.-T., and Chang, Y.-W. (2016). A simplified, economical, and robust light trap for capturing benthic and pelagic zooplankton. *Journal of Experimental Marine Biology and Ecology*, 482:25–32.

REFERENCES

Chapman, C. C., Lea, M.-A., Meyer, A., Sallée, J.-B., and Hindell, M. (2020). Defining Southern Ocean fronts and their influence on biological and physical processes in a changing climate. *Nature Climate Change*, 10(3):209–219.

Cherrier, J., Valentine, S., Hamill, B., Jeffrey, W. H., and Marra, J. F. (2015). Light-mediated release of dissolved organic carbon by phytoplankton. *Journal of Marine Systems*, 147:45–51.

Christaki, U., Georges, C., Genitsaris, S., and Monchy, S. (2015). Microzooplankton community associated with phytoplankton blooms in the naturally iron-fertilized Kerguelen area (Southern Ocean). *FEMS Microbiology Ecology*, 91(June):1–15.

Christaki, U., Obernosterer, I., Van Wambeke, F., Veldhuis, M., Garcia, N., and Catala, P. (2008). Microbial food web structure in a naturally iron-fertilized area in the Southern Ocean (Kerguelen Plateau). *Deep Sea Research Part II: Topical Studies in Oceanography*, 55(5-7):706–719.

Clarke, K. R. (1993). Non-parametric multivariate analyses of changes in community structure. *Australian Journal of Ecology*, 18(1):117–143.

Coleman, C. O. (2003). "Digital inking": How to make perfect line drawings on computers. *Organisms Diversity and Evolution*, 3(4):303.

Coleman, C. O. (2009). Drawing setae the digital way. *Zoosystematics and Evolution*, 85(2):305–310.

Collins, J. R., Fucile, P. D., McDonald, G., Ossolinski, J. E., Keil, R. G., Valdes, J. R., Doney, S. C., and Van Mooy, B. A. S. (2018). An autonomous, in situ light-dark bottle device for determining community respiration and net community production. *Limnology and Oceanography: Methods*, 16(6):323–338.

Conte, M. H., Ralph, N., and Ross, E. H. (2001). Seasonal and interannual variability in deep ocean particle fluxes at the Oceanic Flux Program (OFP)/Bermuda Atlantic Time Series (BATS) site in the western Sargasso Sea near Bermuda. *Deep Sea Research Part II: Topical Studies in Oceanography*, 48(8):1471–1505.

Costello, M. J. and Breyer, S. (2017). Ocean Depths: The Mesopelagic and Implications for Global Warming. *Current Biology*, 27(1):R36–R38.

Daase, M., Varpe, O., and Falk-Petersen, S. (2014). Non-consumptive mortality in copepods: occurrence of Calanus spp. carcasses in the Arctic Ocean during winter. *Journal of Plankton Research*, 36(1):129–144.

Dagg, M. J., Frost, B. W., and Newton, J. A. (1997). Vertical migration and feeding behavior of Calanus pacificus females during a phytoplankton bloom in Dabob Bay, U.S. *Limnology and Oceanography*, 42(5):974–980.

Dagg, M. J., Jackson, G. A., and Checkley, D. M. (2014). The distribution and vertical flux of fecal pellets from large zooplankton in Monterey bay and coastal California. *Deep Sea Research Part I: Oceanographic Research Papers*, 94:72–86.

REFERENCES

Danovaro, R., Carugati, L., Boldrin, A., Calafat, A., Canals, M., Fabres, J., Finlay, K., Heussner, S., Miserocchi, S., and Sanchez-Vidal, A. (2017). Deep-water zooplankton in the Mediterranean Sea: Results from a continuous, synchronous sampling over different regions using sediment traps. *Deep Sea Research Part I: Oceanographic Research Papers*, 126:103–114.

Danovaro, R., Dinet, A., Duineveld, G., and Tselepides, A. (1999). Benthic response to particulate fluxes in different trophic environments: A comparison between the Gulf of Lions–Catalan Sea (western-Mediterranean) and the Cretan Sea (Eastern-Mediterranean). *Progress in Oceanography*, 44(1):287–312.

Dauby, P., Nyssen, F., and de Broyer, C. (2003). Amphipods as food sources for higher trophic levels in the Southern Ocean: A synthesis. In Huiskes, A., Giesekes, W., Rozema, J., Schorno, R., van der Vries, S., and Wolff, W., editors, *Antarctic Biology in a Global Context*, pages 129–134. Backhuys, Leiden.

Davis, C. O., Hollibaugh, J. T., Seibert, D. L. R., Thomas, W. H., and Harrison, P. J. (1980). Formation of resting spores by Leptocylindrus danicus (Bacillariophyceae) in a controlled experimental ecosystem. *Journal of Phycology*, 16(2):296–302.

Davison, P. C., Checkley Jr, D. M., Koslow, J. A., and Barlow, J. (2013). Carbon export mediated by mesopelagic fishes in the northeast Pacific Ocean. *Progress in Oceanography*, 116:14–30.

De Broyer, C. and Jazdzewski, K. (1996). Biodiversity of the Soutern Ocean: Towards a new synthesis for the Amphipoda (Crustacea). *Bollettino del Museo Civico Storia naturale di Verona*, 20:547–568.

De Leon-Casasola, O. and Stevens, R. A. (2001). A comparison of catches of fishes and invertebrates by two light trap designs, in tropical NW Australia. *Marine Biology*, 139(2):373–381.

de Salas, M. F., Eriksen, R., Davidson, A. T., and Wright, S. W. (2011). Protistan communities in the Australian sector of the Sub-Antarctic Zone during SAZ-Sense. *Deep Sea Research Part II: Topical Studies in Oceanography*, 58(21-22):2135–2149.

del Giorgio, P. A. and Duarte, C. M. (2002). Respiration in the open ocean. *Nature*, 420:379–384.

Deppeler, S. L. and Davidson, A. T. (2017). Southern Ocean phytoplankton in a changing climate. *Frontiers in Marine Science*, 4(40):1–28.

Dippner, J. W. and Krause, M. (2013). Continuous plankton recorder underestimates zooplankton abundance. *Journal of Marine Systems*, 111-112:263–268.

Doherty, P. J. (1987). Light-Traps: Selective but useful devices for quantifying the distributions and abundances of larval fishes. *Bulletin of Marine Science*, 41(2):423–431.

Dubovskaya, O. P., Gladyshev, M. I., Gubanov, V. G., and Makhutova, O. N. (2003). Study of non-consumptive mortality of Crustacean zooplankton in a Siberian reservoir using staining for live/dead sorting and sediment traps. *Hydrobiologia*, 504(1):223–227.

Duffy, G. A., Horton, T., and Billett, D. S. M. (2012). Deep-sea scavenging amphipod assemblages from the submarine canyons of the Iberian Peninsula. *Biogeosciences Discussions*, 9(6):7831–7851.

Dunne, J. P., Armstrong, R. A., Gnanadesikan, A., and Sarmiento, J. L. (2005). Empirical and mechanistic models for the particle export ratio. *Global Biogeochemical Cycles*, 19(GB4026):1–16.

Dunne, J. P., John, J. G., Shevliakova, E., Stouffer, R. J., Krasting, J. P., Malyshev, S. L., Milly, P. C. D., Sentman, L. T., Adcroft, A. J., Cooke, W., Dunne, K. A., Griffies, S. M., Hallberg, R. W., Harrison, M. J., Levy, H., Wittenberg, A. T., Phillips, P. J., and Zadeh, N. (2013). GFDL's ESM2 Global Coupled Climate–Carbon Earth System Models. Part II: Carbon System Formulation and Baseline Simulation Characteristics. *Journal of Climate*, 26(7):2247–2267.

Ebersbach, F. and Trull, T. W. (2008). Sinking particle properties from polyacrylamide gels during the KErguelen Ocean and Plateau compared Study (KEOPS): Zooplankton control of carbon export in an area of persistent natural iron inputs in the Southern Ocean. *Limnol. Oceanogr.*, 53(1):212–224.

Ebersbach, F., Trull, T. W., Davies, D. M., and Bray, S. G. (2011). Controls on mesopelagic particle fluxes in the Sub-Antarctic and Polar Frontal Zones in the Southern Ocean south of Australia in summer — Perspectives from free-drifting sediment traps. *Deep-Sea Research Part II*, 58(21-22):2260–2276.

Elliott, D. T., Harris, C. K., and Tang, K. W. (2010). Dead in the water: The fate of copepod carcasses in the York River estuary, Virginia. *Limnology and Oceanography*, 55(5):1821–1834.

Elliott, D. T. and Tang, K. W. (2009). Simple staining method for differentiating live and dead marine zooplankton in field samples. *Limnology and Oceanography: Methods*, 7(8):585–594.

Ericson, J. A., Hellessey, N., Kawaguchi, S., Nicol, S., Nichols, P. D., Hoem, N., and Virtue, P. (2018). Adult Antarctic krill proves resilient in a simulated high CO2 ocean. *Communications Biology*, 1(190):1–9.

Eriksen, R., Trull, T. W., Davies, D., Jansen, P., Davidson, A. T., Westwood, K., and van den Enden, R. (2018). Seasonal succession of phytoplankton community structure from autonomous sampling at the Australian Southern Ocean Time Series (SOTS) observatory. *Marine Ecology Progress Series*, 589:13–31.

Falkowski, P. G., Barber, R. T., and Smetacek, V. (1998). Biogeochemical controls and feedbacks on ocean primary production. *Science*, 281(5374):200–206.

Folt, C. L. and Burns, C. W. (1999). Biological drivers of zooplankton patchiness. *Trends in Ecology & Evolution*, 14(8):300–305.

Forest, A., Sampei, M., Hattori, H., Makabe, R., Sasaki, H., Fukuchi, M., Wassmann, P., and Fortier, L. (2007). Particulate organic carbon fluxes on the slope of the Mackenzie Shelf

(Beaufort Sea): Physical and biological forcing of shelf-basin exchanges. *Journal of Marine Systems*, 68(1-2):39–54.

Forest, A., Sampei, M., Makabe, R., Sasaki, H., Barber, D. G., Gratton, Y., Wassmann, P., and Fortier, L. (2008). The annual cycle of particulate organic carbon export in Franklin Bay (Canadian Arctic): Environmental control and food web implications. *Journal of Geophysical Research: Oceans*, 113(C3):1–13.

Francois, R., Honjo, S., Krishfield, R., and Manganini, S. (2002). Factors controlling the flux of organic carbon to the bathypelagic zone of the ocean. *Global Biogeochemical Cycles*, 16(4):20–34.

Frangoulis, C., Skliris, N., Lepoint, G., Elkalay, K., Goffart, A., Pinnegar, J. K., and Hecq, J.-H. (2011). Importance of copepod carcasses versus faecal pellets in the upper water column of an oligotrophic area. *Estuarine, Coastal and Shelf Science*, 92(3):456–463.

Friedlingstein, P., Jones, M. W., O'Sullivan, M., Andrew, R. M., Hauck, J., Peters, G. P., Peters, W., Pongratz, J., Sitch, S., Le Quéré, C., Bakker, D. C. E., Canadel, J. G., Ciais, P., Jackson, R. B., Anthoni, P., Barbero, L., Bastos, A., Bastrikov, V., Becker, M., Bopp, L., Buitenhuis, E., Chandra, N., Chevallier, F., Chini, L. P., Currie, K. I., Feely, R. A., Gehlen, M., Gilfillan, D., Gkritzalis, T., Goll, D. S., Gruber, N., Gutekunst, S., Harris, I., Haverd, V., Houghton, R. A., Hurtt, G., Jain, A. K., Joetzjer, E., Kaplan, J. O., Kato, E., Goldewijk, K. K., Korsbakken, J. I., Landschützer, P., Lauvset, S. K., Lefèvre, N., Lenton, A., Lienert, S., Lombardozzi, D., Marland, G., McGuire, P. C., Melton, J. R., Metzl, N., Munro, D. R., Nabel, J. E. M. S., Nakaoka, S.-I., Neill, C., Omar, A. M., Ono, T., Peregon, A., Pierrot, D., Poulter, B., Rehder, G., Resplandy, L., Robertson, E., Rödenbeck, C., Séférian, R., Schwinger, J., Smith, N., Tans, P. P., Tian, H., Tilbrook, B., Tubiello, F. N., Werf, G. R. v. d., Wiltshire, A. J., and Zaehle, S. (2019). Global carbon budget 2019. *Earth System Science Data*, 11(4):1783–1838.

Frölicher, T. L., Sarmiento, J. L., Paynter, D. J., Dunne, J. P., Krasting, J. P., and Winton, M. (2015). Dominance of the Southern Ocean in anthropogenic carbon and heat uptake in CMIP5 models. *Journal of Climate*, 28(2):862–886.

Gallienne, C. P. and Robins, D. B. (2001). Is Oithona the most important copepod in the world's oceans? *Journal of Plankton Research*, 23(12):1421–1432.

Gambi, C. and Danovaro, R. (2006). A multiple-scale analysis of metazoan meiofaunal distribution in the deep Mediterranean Sea. *Deep Sea Research Part I: Oceanographic Research Papers*, 53(7):1117–1134.

Garza, A. G. d. l., Vandekar, S., Roalf, D., Ruparel, K., Gur, R., Gur, R., Satterthwaite, T., and Shinohara, R. T. (2018). voxel: Mass-univariate voxelwise analysis of medical imaging data. R package version 1.3.5.

Geoffroy, M., Langbehn, T., Priou, P., Varpe, O., Johnsen, G., Le Bris, A., Fisher, J. A., Daase, M., McKee, D., Cohen, J., and Berge, J. (2021). Pelagic organisms avoid white, blue, and red artificial light from scientific instruments. *Scientific Reports*, 11(1):1–13.

Giering, S. L., Sanders, R., Lampitt, R. S., Anderson, T. R., Tamburini, C., Boutrif, M., Zubkov, M. V., Marsay, C. M., Henson, S. A., Saw, K., Cook, K., and Mayor, D. J. (2014). Reconciliation of the carbon budget in the ocean's twilight zone. *Nature*, 507(7493):480–483.

Gill, C. W. and Poulet, S. A. (1988). Responses of copepods to dissolved free amino acids. *Marine Ecology Progress Series*, 43(3):269–276.

Glud, R. N., Grossart, H.-P., Larsen, M., Tang, K. W., Arendt, K. E., Rysgaard, S., Thamdrup, B., and Gissel Nielsen, T. (2015). Copepod carcasses as microbial hot spots for pelagic denitrification. *Limnology and Oceanography*, 60(6):2026–2036.

Gorsky, G., Chrétiennot-Dinet, M. J., Blanchot, J., and Palazzoli, I. (1999). Picoplankton and nanoplankton aggregation by appendicularians: Fecal pellet contents of Megalocercus huxleyi in the equatorial Pacific. *Journal of Geophysical Research: Oceans*, 104(C2):3381–3390.

Graeve, M., Hagen, W., and Kattner, G. (1994). Herbivorous or omnivorous? On the significance of lipid compositions as trophic markers in Antarctic copepods. *Deep Sea Research Part I: Oceanographic Research Papers*, 41(5-6):915–924.

Grolemund, G. and Wickham, H. (2011). Dates and times made easy with lubridate. *Journal of Statistical Software*, 40(3):1–25.

Halfter, S., Cavan, E. L., Swadling, K. M., Eriksen, R. S., and Boyd, P. W. (2020). The role of zooplankton in establishing carbon export regimes in the Southern Ocean – A comparison of two representative case studies in the subantarctic region. *Frontiers in Marine Science*, 7:837.

Hansen, B., Fotel, F. L., Jensen, N. J., and Madsen, S. D. (1996). Bacteria associated with a marine planktonic copepod in culture. II. Degradation of fecal pellets produced on a diatom, a nanoflagellate or a dinoflagellate diet. *Journal of Plankton Research*, 18(2):275–288.

Harbison, G. R. and Gilmer, R. W. (1986). Effects of animal behavior on sediment trap collections: implications for the calculation of aragonite fluxes. *Deep Sea Research Part A. Oceanographic Research Papers*, 33(8):1017–1024.

Hauck, J., Völker, C., Wang, T., Hoppema, M., Losch, M., and Wolf-Gladrow, D. A. (2013). Seasonally different carbon flux changes in the Southern Ocean inresponse to the southern annular mode. *Global Biogeochemical Cycles*, 27(4):1236–1245.

Hays, G. C. (2003). A review of the adaptive significance and ecosystem consequences of zooplankton diel vertical migrations. In Jones, M. B., Ingólfsson, A., Ólafsson, E., Helgason, G. V., Gunnarsson, K., and Svavarsson, J., editors, *Migrations and Dispersal of Marine Organisms*, pages 163–170. Springer Netherlands, Dordrecht.

Henjes, J., Assmy, P., Klaas, C., Verity, P., and Smetacek, V. (2007). Response of microzooplankton (protists and small copepods) to an iron-induced phytoplankton bloom in the Southern Ocean (EisenEx). *Deep Sea Research Part I: Oceanographic Research Papers*, 54(3):363–384.

Henschke, N., Bowden, D. A., Everett, J. D., Holmes, S. P., Kloser, R. J., Lee, R. W., and Suthers, I. M. (2013). Salp-falls in the Tasman Sea: a major food input to deep-sea benthos. *Marine Ecology Progress Series*, 491:165–175.

Henson, S., Le Moigne, F., and Giering, S. (2019). Drivers of Carbon Export Efficiency in the Global Ocean. *Global Biogeochemical Cycles*, 33:1–13.

Henson, S. A., Sanders, R., Madsen, E., Morris, P. J., Le Moigne, F., and Quartly, G. D. (2011). A reduced estimate of the strength of the ocean's biological carbon pump. *Geophysical Research Letters*, 38(L04606):1–5.

Hernández-León, S. and Gomez, M. (1996). Factors affecting the respiration/ETS ratio in marine zooplankton. *Journal of Plankton Research*, 18(2):239–255.

Hernández-León, S. and Ikeda, T. (2005a). A global assessment of mesozooplankton respiration in the ocean. *Journal of Plankton Research*, 27(2):153–158.

Hernández-León, S. and Ikeda, T. (2005b). Zooplankton respiration. In *Respiration in Aquatic Systems*, pages 57–82. Oxford University Press, New York.

Hernández-León, S., Putzeys, S., Almeida, C., Bécognée, P., Marrero-Díaz, A., Arístegui, J., and Yebra, L. (2019). Carbon export through zooplankton active flux in the Canary Current. *Journal of Marine Systems*, 189:12–21.

Herraiz-Borreguero, L. and Rintoul, S. R. (2011). Regional circulation and its impact on upper ocean variability south of Tasmania. *Deep Sea Research Part II: Topical Studies in Oceanography*, 58(21-22):2071–2081.

Herring, P. J. (1981). Studies on bioluminescent marine amphipods. *Journal of the Marine Biological Association of the United Kingdom*, 61(1):161–176.

Hickford, M. J. H. and Schiel, D. R. (1999). Evaluation of the performance of light traps for sampling fish larvae in inshore temperate waters. *Marine Ecology Progress Series*, 186:293–302.

Hirst, A. G. and Kiørboe, T. (2002). Mortality of marine planktonic copepods: Global rates and patterns. *Marine Ecology Progress Series*, 230:195–209.

Horton, T., Thurston, M. H., and Duffy, G. A. (2013). Community composition of scavenging amphipods at bathyal depths on the Mid-Atlantic Ridge. *Deep Sea Research Part II: Topical Studies in Oceanography*, 98:352–359.

Hosie, G. W., Fukuchi, M., and Kawaguchi, S. (2003). Development of the Southern Ocean Continuous Plankton Recorder survey. *Progress in Oceanography*, 58(2-4):263–283.

Howard, W. R., Roberts, D., Moy, A. D., Lindsay, M. C., Hopcroft, R. R., Trull, T. W., and Bray, S. G. (2011). Distribution, abundance and seasonal flux of pteropods in the Sub-Antarctic Zone. *Deep-Sea Research Part II: Topical Studies in Oceanography*, 58(21-22):2293–2300.

Hunt, B. (2005). *The spatio-temporal distribution of zooplankton communities in the Southern Ocean south of Australia: high resolution sampling by the Continuous Plankton.* PhD thesis, University of Tasmania.

Hunt, B. and Hosie, G. (2006). The seasonal succession of zooplankton in the Southern Ocean south of Australia, part II: The Sub-Antarctic to Polar Frontal Zones. *Deep Sea Research Part I: Oceanographic Research Papers*, 53(7):1203–1223.

Hunt, B. P. and Hosie, G. W. (2005). Zonal structure of zooplankton communities in the Southern Ocean South of Australia: Results from a 2150 km continuous plankton recorder transect. *Deep-Sea Research Part I: Oceanographic Research Papers*, 52(7):1241–1271.

Hunt, B. P. V. and Hosie, G. W. (2003). The Continuous Plankton Recorder in the Southern Ocean: a comparative analysis of zooplankton communities sampled by the CPR and vertical net hauls along 140 E. *Journal of Plankton Research*, 25(12):1561–1579.

Ikeda, T. (1985). Metabolic rates of epipelagic marine zooplankton as a function of body mass and temperature. *Marine Biology*, 85:1–11.

Ikeda, T., Kanno, Y., Ozaki, K., and Shinada, A. (2001). Metabolic rates of epipelagic marine copepods as a function of body mass and temperature. *Marine Biology*, 139(3):587–596.

Ikeda, T., Sano, F., Yamaguchi, A., and Matsuishi, T. (2006). Metabolism of mesopelagic and bathypelagic copepods in the western North Pacific Ocean. *Marine Ecology Progress Series*, 322:199–211.

Iversen, M. H. and Ploug, H. (2010). Ballast minerals and the sinking carbon flux in the ocean: Carbon-specific respiration rates and sinking velocity of marine snow aggregates. *Biogeosciences*, 7(9):2613–2624.

Iversen, M. H. and Poulsen, L. K. (2007). Coprorhexy, coprophagy, and coprochaly in the copepods Calanus helgolandicus, Pseudocalanus elongatus, and Oithona similis. *Marine Ecology Progress Series*, 350:79–89.

Ivory, J. A., Tang, K. W., and Takahashi, K. (2014). Use of Neutral Red in short-term sediment traps to distinguish between zooplankton swimmers and carcasses. *Marine Ecology Progress Series*, 505:107–117.

Jacquet, S. H. M., Dehairs, F., Dumont, I., Becquevort, S., Cavagna, A. J., and Cardinal, D. (2011). Twilight zone organic carbon remineralization in the Polar Front Zone and Subantarctic Zone south of Tasmania. *Deep Sea Research Part II: Topical Studies in Oceanography*, 58(21-22):2222–2234.

Jansen, P., Weeding, B., Shadwick, E. H., and Trull, T. W. (2020). Southern Ocean Time Series (SOTS) Quality Assessment and Control Report-Sediment Trap Particle Fluxes Records Version 1.0. Technical Report April, CSIRO, Australia.

Jarms, G., Tiemann, H., and Båmstedt, U. (2002). Development and biology of Periphylla periphylla (Scyphozoa: Coronatae) in a Norwegian fjord. *Marine Biology*, 141(4):647–657.

Jillett, J. B. (1968). Calanus tonsus (Copepoda, Calanoida) in southern New Zealand waters with notes on the male. *Marine and Freshwater Research*, 19(1):19–30.

Jónasdóttir, S. H., Visser, A. W., Richardson, K., and Heath, M. R. (2015). Seasonal copepod lipid pump promotes carbon sequestration in the deep North Atlantic. *Proceedings of the National Academy of Sciences*, 112(39):12122–12126.

Karl, D. M. and Knauer, G. A. (1989). Swimmers: a recapitulation of the problem and a potential solution. *Oceanography*, 2(1):32–35.

Khatiwala, S., Primeau, F., and Hall, T. (2009). Reconstruction of the history of anthropogenic CO2 concentrations in the ocean. *Nature*, 462(7271):346–349.

Kirillin, G., Grossart, H. P., and Tang, K. W. (2012). Modeling sinking rate of zooplankton carcasses: Effects of stratification and mixing. *Limnology and Oceanography*, 57(3):881–894.

Kirk, J. T. O. (1994). Photosynthesis in the aquatic environment. In Kirk, J. T. O., editor, *Light and photosynthesis in aquatic ecosystems*. Cambridge University Press, 2nd ed. edition.

Klaas, C. and Archer, D. E. (2002). Association of sinking organic matter with various types of mineral ballast in the deep sea: Implications for the rain ratio. *Global Biogeochemical Cycles*, 16(4):14–63.

Klevjer, T. A., Irigoien, X., Rostad, A., Fraile-Nuez, E., Benitez-Barrios, V. M., and Kaartvedt, S. (2016). Large scale patterns in vertical distribution and behaviour of mesopelagic scattering layers. *Sci Rep*, 6:19873.

Knauer, G. A., Martin, J. H., and Bruland, K. W. (1979). Fluxes of particulate carbon, nitrogen, and phosphorus in the upper water column of the northeast Pacific. *Deep Sea Research Part A. Oceanographic Research Papers*, 26(1):97–108.

Kobari, T., Steinberg, D. K., Ueda, A., Tsuda, A., Silver, M. W., and Kitamura, M. (2008). Impacts of ontogenetically migrating copepods on downward carbon flux in the western subarctic Pacific Ocean. *Deep-Sea Research Part II: Topical Studies in Oceanography*, 55(14-15):1648–1660.

Kopczynska, E. E., Dehairs, F., Elskens, M., and Wright, S. (2001). Phytoplankton and microzooplankton variability between the Subtropical and Polar Fronts south of Australia: Thriving under regenerative and new production in late summer. *Journal of Geophysical Research: Oceans*, 106(C12):31597–31609.

Koski, M., Valencia, B., Newstead, R., and Thiele, C. (2020). The missing piece of the upper mesopelagic carbon budget? Biomass, vertical distribution and feeding of aggregate-associated copepods at the PAP site. *Progress in Oceanography*, 181(102243):1–9.

Koubbi, P., Guinet, C., Alloncle, N., Ameziane, N., Azam, C. S., Baudena, A., Bost, C. A., Causse, R., Chazeau, C., Coste, G., Cotté, C., Ovidio, D. F., Delord, K., Duhamel, G., Forget, A., Gasco, N., Hautecœur, M., Lehodey, P., Marteau, C., Martin, A., Mignard, C., Pruvost,

P., Sinegre, R., Thellier, T., Verdier, A. G., and Weimerskirch, H. (2016). Ecoregionalisation of the Kerguelen and Crozet islands oceanic zone Part I : Introduction and Kerguelen oceanic zone. Technical report, CCAMLR Report WG-EMM- 16/43.

Kraft, A., Bauerfeind, E., and Nöthig, E.-M. (2010). Amphipod abundance in sediment trap samples at the long-term observatory HAUSGARTEN (Fram Strait, ∼79°N/4°E). Variability in species community patterns. *Marine Biodiversity*, 41(3):353–364.

Kraft, A., Bauerfeind, E., Nöthig, E. M., and Bathmann, U. V. (2012). Size structure and life cycle patterns of dominant pelagic amphipods collected as swimmers in sediment traps in the eastern Fram Strait. *Journal of Marine Systems*, 95:1–15.

Kritzberg, E. S., Duarte, C. M., and Wassmann, P. (2010). Changes in Arctic marine bacterial carbon metabolism in response to increasing temperature. *Polar Biology*, 33(12):1673–1682.

Lam, P. J. and Bishop, J. K. (2007). High biomass, low export regimes in the Southern Ocean. *Deep-Sea Research Part II: Topical Studies in Oceanography*, 54(5-7):601–638.

Lam, P. J., Doney, S. C., and Bishop, J. K. (2011). The dynamic ocean biological pump: Insights from a global compilation of particulate organic carbon, CaCO3, and opal concentration profiles from the mesopelagic. *Global Biogeochemical Cycles*, 25(3):1–14.

Lampert, W. (1993). Ultimate causes of diel vertical migration of zooplankton: New evidence for the predator-avoidance hypothesis. *Arch. Hydrobiol. Beih. Ergebn. Limnol.*, 39:79–88.

Lampitt, R. S., Noji, T., and von Bodungen, B. (1990). What happens to zooplankton faecal pellets? Implications for material flux. *Marine Biology*, 104(1):15–23.

Landry, M. R., Selph, K. E., Brown, S. L., Abbott, M. R., Measures, C. I., Vink, S., Allen, C. B., Calbet, A., Christensen, S., and Nolla, H. (2002). Seasonal dynamics of phytoplankton in the Antarctic Polar Front region at 170° W. *Deep Sea Research Part II: Topical Studies in Oceanography*, 49(9-10):1843–1865.

Lasbleiz, M., Leblanc, K., Armand, L. K., Christaki, U., Georges, C., Obernosterer, I., and Queguiner, B. (2016). Composition of diatom communities and their contribution to plankton biomass in the naturally iron-fertilized region of Kerguelen in the Southern Ocean. *FEMS microbiology ecology*, 92(11 (fiw171)):1–16.

Laufkötter, C., Vogt, M., Gruber, N., Aumont, O., Bopp, L., Doney, S. C., Dunne, J. P., Hauck, J., John, J. G., Lima, I. D., Seferian, R., and Völker, C. (2016). Projected decreases in future marine export production: The role of the carbon flux through the upper ocean ecosystem. *Biogeosciences*, 13(13):4023–4047.

Laurenceau-Cornec, E. C., Trull, T. W., Davies, D. M., Bray, S. G., Doran, J., Planchon, F., Carlotti, F., Jouandet, M., Cavagna, A., and Waite, A. M. (2015). The relative importance of phytoplankton aggregates and zooplankton fecal pellets to carbon export: insights from free-drifting sediment trap deployments in naturally iron-fertilised waters near the Kerguelen Plateau. *Biogeosciences*, 12(4):1007–1027.

Laws, E. A., D'Sa, E., and Naik, P. (2011). Simple equations to estimate ratios of new or export production to total production from satellite-derived estimates of sea surface temperature and primary production. *Limnology and Oceanography: Methods*, 9(12):593–601.

le Borgne, R. P. (1979). Influence of duration of incubation on zooplankton respiration and excretion results. *Journal of Experimental Marine Biology and Ecology*, 37(2):127–137.

Le Moigne, F. A., Henson, S. A., Cavan, E., Georges, C., Pabortsava, K., Achterberg, E. P., Ceballos-Romero, E., Zubkov, M., and Sanders, R. J. (2016). What causes the inverse relationship between primary production and export efficiency in the Southern Ocean? *Geophysical Research Letters*, 43(9):4457–4466.

Le Quéré, C., Rödenbeck, C., Buitenhuis, E. T., Conway, T. J., Langenfelds, R., Gomez, A., Labuschagne, C., Ramonet, M., Nakazawa, T., Metzl, N., Gillett, N. P., and Heimann, M. (2008). Response to comments on "Saturation of the Southern Ocean CO2 sink due to recent climate change". *Science*, 319(5863):570.

Lee, C., Hedges, J. I., Wakeham, S. G., and Zhu, N. (1992). Effectiveness of various treatments in retarding microbial activity in sediment trap material and their effects on the collection of swimmers. *Limnology and Oceanography*, 37(1):117–130.

Lee, C., Wakeham, S. G., and Hedges, J. I. (1988). The measurement of oceanic particle flux-are" swimmers" a problem? *Oceanography*, 1(2):34–36.

Lee, Z. P., Weidemann, A., Kindle, J., Arnone, R., Carder, K. L., and Davis, C. (2007). Euphotic zone depth: Its derivation and implication to ocean-color remote sensing. *Journal of Geophysical Research: Oceans*, 112(C03009):1–11.

Lindsey, R. (2020). Climate Change: Atmospheric Carbon Dioxide. *https://www.climate.gov/news-features/understanding-climate/climate-change-atmospheric-carbon-dioxide*.

Liszka, C. M., Manno, C., Stowasser, G., Robinson, C., and Tarling, G. A. (2019). Mesozooplankton community composition controls fecal pellet flux and remineralization depth in the Southern Ocean. *Frontiers in Marine Science*, 6(230):1–14.

Loeb, V. J., Hofmann, E. E., Klinck, J. M., Holm-Hansen, O., and White, W. B. (2009). ENSO and variability of the Antarctic Peninsula pelagic marine ecosystem. *Antarctic Science*, 21(2):135–148.

Lowry, J. K. and Stoddart, H. E. (1997). Amphipoda Crustacea IV. Families Aristiidae, Cyphocarididae, Endevouridae, Lysianassidae, Scopelocheiridae, Uristidae. *Memoirs of the Hourglass Cruises*, 10(1):1–148.

Lowry, J. K., Stoddart, H. E., Sciences, O., Parker, A. R., and Tabelle, I. D. (2011). The new deep-sea families Cebocaridae fam. nov., Cyclocaridae fam. nov. and Thoriellidae fam. nov. (Crustacea: Amphipoda: Lysianassoidea). *Zootaxa*, 68(2747):53–68.

Ludvigsen, M., Berge, J., Geoffroy, M., Cohen, J. H., De La Torre, P. R., Nornes, S. M., Singh, H., Sørensen, A. J., Daase, M., and Johnsen, G. (2018). Use of an Autonomous Surface Vehicle reveals small-scale diel vertical migrations of zooplankton and susceptibility to light pollution under low solar irradiance. *Science Advances*, 4(1 (eaap9887)):1–8.

Lumpkin, R. and Speer, K. (2007). Global ocean meridional overturning. *Journal of Physical Oceanography*, 37(10):2550–2562.

Maiti, K., Charette, M. A., Buesseler, K. O., and Kahru, M. (2013). An inverse relationship between production and export efficiency in the Southern Ocean. *Geophysical Research Letters*, 40(8):1557–1561.

Makabe, R., Hattori, H., Sampei, M., Darnis, G., Fortier, L., and Sasaki, H. (2016). Can sediment trap-collected zooplankton be used for ecological studies? *Polar Biology*, 39(12):2335–2346.

Manno, C., Stowasser, G., Enderlein, P., Fielding, S., and Tarling, G. A. (2015). The contribution of zooplankton faecal pellets to deep carbon transport in the Scotia Sea (Southern Ocean). *Biogeosciences*, 12:1955–1965.

Marinov, I., Gnanadesikan, A., Toggweiler, J. R., and Sarmiento, J. L. (2006). The Southern Ocean biogeochemical divide. *Nature*, 441:964–967.

Marsay, C. M., Sanders, R. J., Henson, S. A., Pabortsava, K., Achterberg, E. P., and Lampitt, R. S. (2015). Attenuation of sinking particulate organic carbon flux through the mesopelagic ocean. *Proceedings of the National Academy of Sciences*, 112(4):1089–1094.

Matear, R. J. and Hirst, A. C. (1999). Climate change feedback on the future oceanic CO2 uptake. *Tellus B: Chemical and Physical Meteorology*, 51(3):722–733.

Matsuno, K., Yamaguchi, A., Fujiwara, A., Onodera, J., Watanabe, E., Harada, N., and Kikuchi, T. (2015). Seasonal changes in the population structure of dominant planktonic copepods collected using a sediment trap moored in the western Arctic Ocean. *Journal of Natural History*, 49(45-48):2711–2726.

Matsuno, K., Yamaguchi, A., Fujiwara, A., Onodera, J., Watanabe, E., Imai, I., Chiba, S., Harada, N., and Kikuchi, T. (2014). Seasonal changes in mesozooplankton swimmers collected by sediment trap moored at a single station on the Northwind Abyssal Plain in the western Arctic Ocean. *Journal of Plankton Research*, 36(2):490–502.

Mayewski, P. A., Meredith, M. P., Summerhayes, C. P., Turner, J., Worby, A., Barrett, P. J., Casassa, G., Bertler, N. A. N., Bracegirdle, T., and Naveira Garabato, A. C. (2009). State of the Antarctic and Southern Ocean climate system. *Reviews of Geophysics*, 47(1):1–38.

Mayor, D. J., Sanders, R., Giering, S. L., and Anderson, T. R. (2014). Microbial gardening in the ocean's twilight zone: detritivorous metazoans benefit from fragmenting, rather than ingesting, sinking detritus: fragmentation of refractory detritus by zooplankton beneath the euphotic zone stimulates the harvestable productio. *Bioessays*, 36(12):1132–1137.

Mayzaud, P. and Pakhomov, E. A. (2014a). The role of zooplankton communities in carbon recycling in the Ocean: the case of the Southern Ocean. *Journal of Plankton Research*, 36(6):1543–1556.

Mayzaud, P. and Pakhomov, E. A. (2014b). The role of zooplankton communities in carbon recycling in the Ocean: The case of the Southern Ocean. *Journal of Plankton Research*, 36(6):1543–1556.

Mayzaud, P., Tirelli, V., Errhif, A., Labat, J. P., Razouls, S., and Perissinotto, R. (2002). Carbon intake by zooplankton. Importance and role of zooplankton grazing in the Indian sector of the Southern Ocean. *Deep Sea Research Part II: Topical Studies in Oceanography*, 49(16):3169–3187.

McDonnell, A., Boyd, P. W., and Buesseler, K. O. (2015). Effects of sinking velocities andmicrobial respiration rates on the attenuation of particulate carbon fluxes through the mesopelagic zone. *Global biogeochemical cycles*, 29:175–193.

McLeod, D. J., Hosie, G. W., Kitchener, J. A., Takahashi, K. T., and Hunt, B. P. V. (2010). Zooplankton Atlas of the Southern Ocean: The SCAR SO-CPR Survey (1991–2008). *Polar Science*, 4(2):353–385.

MEA (2005). Ecosystems and human wellbeing: current state and trends. In *Millennium Ecosystem Assessment*, page 948p. Island Press, Washington, DC.

Meekan, M., Wilson, S., Halford, A., and Retzel, A. (2001). A comparison of catches of fishes and invertebrates by two light trap designs, in tropical NW Australia. *Marine Biology*, 139(2):373–381.

Meredith, M., Sommerkorn, M., Cassotta, S., Derksen, C., Ekaykin, A., Hollowed, A., Kofinas, G., Mackintosh, A., Melbourn-Thomas, J., Muelbert, M. M. C., Ottersen, G., Pritchard, H., and Schuur, E. (2019). Chapter 3: Polar Regions. In Poörtner, H.-O., Roberts, D., Masson-Delmotte, V., Zhai, P., Tignor, M., Poloczanska, E., Mintenbeck, K., Alegriía, A., Nicolai, M., Okem, A., Petzold, J., Rama, B., and Weyer, N., editors, *IPCC Special Report on the Oceans and Cryosphere in a changing climate*, pages 203–320. Intergovernmental Panel on Climate Change.

Michaels, A. F., Caron, D. A., Swanberg, N. R., Howse, F. A., and Michaels, C. M. (1995). Planktonic sarcodines (Acantharia, Radiolaria, Foraminifera) in surface waters near Bermuda: abundance, biomass and vertical flux. *Journal of Plankton Research*, 17(1):131–163.

Michaels, A. F., Silver, M. W., Gowing, M. M., and Knauer, G. A. (1990). Cryptic zooplankton swimmers in upper ocean sediment traps. *Deep Sea Research*, 37(8):1285–1296.

Miller, K. J., Bradford-Grieve, J. M., and Jillett, J. B. (1999). Genetic relationship between winter deep-dwelling and spring surface-dwelling female Neocalanus tonsus in the Southern Ocean. *Marine Biology*, 134(1):99–106.

Minutoli, R., Granata, A., Brugnano, C., Zagami, G., and Guglielmo, L. (2014). Mesozooplankton carbon requirement in the southern Adriatic Sea: Vertical distribution, diel and seasonal variability, relation to particle flux. *Marine Ecology Progress Series*, 495:91–104.

Moisander, P. H., Sexton, A. D., and Daley, M. C. (2015). Stable associations masked by temporal variability in the marine copepod microbiome. *PLoS One*, 10(9):e0138967.

Moore, J., Doney, S. C., Kleypas, J. A., Glover, D. M., and Fung, I. Y. (2001). An intermediate complexity marine ecosystem model for the global domain. *Deep Sea Research Part II: Topical Studies in Oceanography*, 49(1):403–462.

Mosseri, J., Queguiner, B., Armand, L., and Cornet-Barthaux, V. (2008). Impact of iron on silicon utilization by diatoms in the Southern Ocean: A case study of Si/N cycle decoupling in a naturally iron-enriched area. *Deep Sea Research Part II: Topical Studies in Oceanography*, 55(5-7):801–819.

Nishibe, Y. and Ikeda, T. (2008). Metabolism and elemental composition of four oncaeid copepods in the western subarctic Pacific. *Marine Biology*, 153(3):397–404.

Odate, T. and Fukuchi, M. (1995). Distribution and community structure of picophytoplankton in the Southern Ocean during late austral summer of 1992. *Proc. NIPR Symp. Polar Biol., Nat. Inst. Polar Res.*, 8:86–100.

Ohman, M. D., Bradford, J. M., and Jillett, J. B. (1989). Seasonal growth and lipid storage of the circumglobal, subantarctic copepod, Neocalanus tonsus (Brady). *Deep Sea Research Part A. Oceanographic Research Papers*, 36(9):1309–1326.

Oksanen, J., Blanchet, F. G., Friendly, M., Kindt, R., Legendre, P., McGlinn, D., Minchin, P. R., O'Hara, R. B., Simpson, G. L., Solymos, P., Henry, M., Stevens, H., Szoecs, E., and Wagner, H. (2020). vegan: Community ecology rackage. R version 2.5-7.

Orr, J. C., Fabry, V. J., Aumont, O., Bopp, L., Doney, S. C., Feely, R. A., Gnanadesikan, A., Gruber, N., Ishida, A., and Joos, F. (2005). Anthropogenic ocean acidification over the twenty-first century and its impact on calcifying organisms. *Nature*, 437(7059):681–686.

Orsi, A. H., Whitworth, T., and Nowlin, W. D. (1995). On the meridional extent and fronts of the Antarctic Circumpolar Current. *Deep Sea Research Part I: Oceanographic Research Papers*, 42(5):641–673.

Owens, T. G. and King, F. D. (1975). The measurement of respiratory electron-transport-system activity in marine zooplankton. *Marine Biology*, 30:27–36.

Packard, T. T. (1971). The measurement of respiratory electron-transport activity in marine phytoplankton. *Journal of Marine Research*, 29(3):235–244.

Packard, T. T. and Christensen, J. P. (2004). Respiration and vertical carbon flux in the Gulf of Maine water column. *Journal of Marine Research*, 62(1):93–115.

Pakhomov, E. A., Froneman, P. W., and Perissinotto, R. (2002). Salp/krill interactions in the Southern Ocean: spatial segregation and implications for the carbon flux. *Deep Sea Research Part II: Topical Studies in Oceanography*, 49(9-10):1881–1907.

Parekh, P., Dutkiewicz, S., Follows, M., and Ito, T. (2006). Atmospheric carbon dioxide in a less dusty world. *Geophysical Research Letters*, 33(L03610):1–4.

Park, Y.-H., Durand, I., Kestenare, E., Rougier, G., Zhou, M., d'Ovidio, F., Cotté, C., and Lee, J.-H. (2014). Polar Front around the Kerguelen Islands: An up-to-date determination and associated circulation of surface/subsurface waters. *Journal of Geophysical Research: Oceans*, 119(10):6575–6592.

Parker, A. R. (1999). An unusually isolated reflector for host bioluminescence on the second antenna of a lysianassoid (Amphipoda: Gammaridea). In Schram, F. and von Vaupel Klein, J., editors, *Crustaceans and the biodiversity crisis (Crustaceana)*, pages 879–887. Brill, Leiden.

Pasternak, A., Hagen, W., Kattner, G., Michels, J., Graeve, M., and Schnack-Schiel, S. B. (2009). Lipid dynamics and feeding of dominant Antarctic calanoid copepods in the eastern Weddell Sea in December. *Polar biology*, 32(11):1597–1606.

Pearce, I., Davidson, A. T., Thomson, P. G., Wright, S., and van den Enden, R. (2011). Marine microbial ecology in the sub-Antarctic Zone: Rates of bacterial and phytoplankton growth and grazing by heterotrophic protists. *Deep Sea Research Part II: Topical Studies in Oceanography*, 58(21-22):2248–2259.

Peloquin, J., Hall, J., Safi, K., Ellwood, M., Law, C. S., Thompson, K., Kuparinen, J., Harvey, M., and Pickmere, S. (2011). Control of the phytoplankton response during the SAGE experiment: A synthesis. *Deep Sea Research Part II: Topical Studies in Oceanography*, 58(6):824–838.

Peterson, W. and Dam, H. G. (1990). The influence of copepod "swimmers" on pigment fluxes in brine-filled vs. ambient seawater-filled sediment traps. *Limnology and Oceanography*, 35(2):448–455.

Pielou, F. C. (1975). *Ecological Diversity.* John Wiley & Sons, Ltd, New York.

Pierce, D. (2019). ncdf4: Interface to Unidata netCDF (Version 4 or Earlier) Format Data Files.

Ploug, H. and Grossart, H. P. (2000). Bacterial growth and grazing on diatom aggregates: Respiratory carbon turnover as a function of aggregate size and sinking velocity. *Limnology and Oceanography*, 45(7):1467–1475.

Poloczanska, E. S., Burrows, M. T., Brown, C. J., García Molinos, J., Halpern, B. S., Hoegh-Guldberg, O., Kappel, C. V., Moore, P. J., Richardson, A. J., Schoeman, D. S., and Sydeman, W. J. (2016). Responses of marine organisms to climate change across oceans. *Frontiers in Marine Science*, 3(62):1–23.

Pondaven, P., Gallinari, M., Chollet, S., Bucciarelli, E., Sarthou, G., Schultes, S., and Jean, F. (2007). Grazing-induced changes in cell wall silicification in a marine diatom. *Protist*, 158(1):21–28.

Poulet, S. A., Williams, R., Conway, D. V. P., and Videau, C. (1991). Co-occurrence of copepods and dissolved free amino acids in shelf sea waters. *Marine Biology*, 108(3):373–385.

Proud, R., Cox, M. J., and Brierley, A. S. (2017). Biogeography of the Global Ocean's mesopelagic zone. *Current Biology*, 27(1):113–119.

Quéguiner, B. (2013). Iron fertilization and the structure of planktonic communities in high nutrient regions of the Southern Ocean. *Deep-Sea Research Part II: Topical Studies in Oceanography*, 90:43–54.

Razouls, S., Koubbi, P., and Mayzaud, P. (1996). Spatio-temporal distribution of mesozooplankton in a sub-Antarctic coastal basin of the Kerguelen Archipelago (southern Indian Ocean). *Polar Biology*, 16:581–587.

Record, N. R., Ji, R., Maps, F., Varpe, O., Runge, J. A., Petrik, C. M., and Johns, D. (2018). Copepod diapause and the biogeography of the marine lipidscape. *Journal of Biogeography*, 45(10):2238–2251.

Rembauville, M., Blain, S., Armand, L., Queguiner, B., and Salter, I. (2014). Export fluxes in a naturally fertilized area of the Southern Ocean , the Kerguelen Plateau: Ecological vectors of carbon and biogenic silica to depth (Part 2). *Biogeosciences Discussions*, 11:17089–17150.

Rembauville, M., Blain, S., Armand, L., Quéguiner, B., and Salter, I. (2015a). Export fluxes in a naturally iron-fertilized area of the Southern Ocean - Part 2: Importance of diatom resting spores and faecal pellets for export. *Biogeosciences*, 12(11):3171–3195.

Rembauville, M., Briggs, N., Ardyna, M., Uitz, J., Catala, P., Penkerc'h, C., Poteau, A., Claustre, H., and Blain, S. (2017). Plankton Assemblage Estimated with BGC-Argo Floats in the Southern Ocean: Implications for Seasonal Successions and Particle Export. *Journal of Geophysical Research: Oceans*, 122(10):8278–8292.

Rembauville, M., Salter, I., Leblond, N., Gueneugues, A., and Blain, S. (2015b). Export fluxes in a naturally iron-fertilized area of the Southern Ocean - Part 1: Seasonal dynamics of particulate organic carbon export from a moored sediment trap. *Biogeosciences*, 12(11):3153–3170.

Rintoul, S. R. and Trull, T. W. (2001). Seasonal evolution of the mixed layer in the Subantarctic Zone south of Australia. *Journal of Geophysical Research: Oceans*, 106(C12):31447–31462.

Rivkin, R. B. and Legendre, L. (2001). Biogenic carbon cycling in the upper ocean: Effects of microbial respiration. *Science*, 291(5512):2398–2400.

Roberts, D., Howard, W. R., Moy, A. D., Roberts, J. L., Trull, T. W., Bray, S. G., and Hopcroft, R. R. (2008). Interannual variability of pteropod shell weights in the high-CO 2 Southern Ocean. *Biogeosciences Discussions*, Preprint(6):4453–4480.

Robinson, C., Steinberg, D. K., Anderson, T. R., Arístegui, J., Carlson, C. A., Frost, J. R., Ghiglione, J.-F., Hernández-León, S., Jackson, G. A., Koppelmann, R., Quéguiner, B., Ragueneau, O., Rassoulzadegan, F., Robison, B. H., Tamburini, C., Tanaka, T., Wishner, K. F., and Zhang, J. (2010). Mesopelagic zone ecology and biogeochemistry – a synthesis. *Deep Sea Research Part II: Topical Studies in Oceanography*, 57(16):1504–1518.

Romano, C., Flexas, M. M., Segura, M., Román, S., Bahamon, N., Gili, J. M., Sanchez-Vidal, A., and Martin, D. (2017). Canyon effect and seasonal variability of deep-sea organisms in the NW Mediterranean: Synchronous, year-long captures of "swimmers" from near-bottom sediment traps in a submarine canyon and its adjacent open slope. *Deep Sea Research Part I: Oceanographic Research Papers*, 129:99–115.

Sabine, C., Feely, R., Gruber, N., Key, R., Lee, K., Bullister, J., Wanninkhof, R., Wong, C., Wallace, D., Tilbrook, B., Millero, F., Peng, T., Kozyr, A., Ono, T., and Rios, A. (2004). The Oceanic Sink for Anthropogenic CO2. *Science*, 305(5682):367–371.

Saborowski, R., Bröhl, S., Tarling, G., and Buchholz, F. (2002). Metabolic properties of Northern krill, Meganyctiphanes norvegica, from different climatic zones. I. Respiration and excretion. *Marine Biology*, 140(3):547–556.

Saito, H. and Tsuda, A. (2000). Egg production and early development of the subarctic copepods Neocalanus cristatus, N. plumchrus and N. flemingeri. *Deep-Sea Research Part I: Oceanographic Research Papers*, 47(11):2141–2158.

Salter, I., Kemp, A. E. S., Moore, C. M., Lampitt, R. S., Wolff, G. A., and Holtvoeth, J. (2012). Diatom resting spore ecology drives enhanced carbon export from a naturally iron-fertilized bloom in the Southern Ocean. *Global Biogeochemical Cycles*, 26(GB1014):1–17.

Sampei, M., Forest, A., Fortier, L., Yamamoto, T., Hattori, H., and Sasaki, H. (2020). Variations in contributions of dead copepods to vertical fluxes of particulate organic carbon in the Beaufort Sea. *Marine Ecology Progress Series*, 642:67–81.

Sampei, M., Sasaki, H., Forest, A., and Fortier, L. (2012). A substantial export flux of particulate organic carbon linked to sinking dead copepods during winter 2007–2008 in the Amundsen Gulf (southeastern Beaufort Sea, Arctic Ocean). *Limnology and Oceanography*, 57(1):90–96.

Sampei, M., Sasaki, H., Hattori, H., Forest, A., and Fortier, L. (2009). Significant contribution of passively sinking copepods to the downward export flux in Arctic Waters. *Limnology and Oceanography*, 54(6):1894–1900.

Sanders, R., Henson, S. A., Koski, M., De La Rocha, C. L., Painter, S. C., Poulton, A. J., Riley, J., Salihoglu, B., Visser, A., Yool, A., Bellerby, R., and Martin, A. P. (2014). The Biological Carbon Pump in the North Atlantic. *Progress in Oceanography*, 129:200–218.

Sarmiento, J. L. and Gruber, N. (2006). *Ocean Biogeochemical Dynamics*. Princeton University Press, Princeton.

Sarthou, G., Vincent, D., Christaki, U., Obernosterer, I., Timmermans, K. R., and Brussaard, C. P. (2008). The fate of biogenic iron during a phytoplankton bloom induced by natural fertilisation: Impact of copepod grazing. *Deep-Sea Research Part II: Topical Studies in Oceanography*, 55(5-7):734–751.

Schallenberg, C., Bestley, S., Klocker, A., Trull, T. W., Davies, D. M., Gault-Ringold, M., Eriksen, R., Roden, N. P., Sander, S. G., Sumner, M., Townsend, A. T., van der Merwe, P., Westwood, K., Wuttig, K., and Bowie, A. (2018). Sustained upwelling of subsurface iron supplies seasonally persistent phytoplankton blooms around the southern Kerguelen Plateau, Southern Ocean. *Journal of Geophysical Research: Oceans*, 123(8):5986–6003.

Schlaefer, J. A., Wolanski, E., Yadav, S., and Kingsford, M. J. (2020). Behavioural maintenance of highly localised jellyfish (Copula sivickisi, class Cubozoa) populations. *Marine Biology*, 167(4):1–18.

Schnack-Schiel, S. B. (2001). Aspects of the study of the life cycles of Antarctic copepods. In Lopes, R. M., Reid, J. W., and Rocha, C. E. F., editors, *Copepoda: Developments in Ecology, Biology and Systematics*, pages 9–24. Springer.

Schnack-Schiel, S. B. and Isla, E. (2005). The role of zooplankton in the pelagic-benthic coupling of the Southern Ocean. *Scientia Marina*, 69(Suppl. 2):39–55.

Sedwick, P. N., DiTullio, G. R., Hutchins, D. A., Boyd, W., Brian, F., Crossley, A. C., and Trull, W. (1999). Limitation of algal growth by iron deficiency in the Australian Subantarctic region. *Geophysical Research Letters*, 26(18):2865–2868.

Semelkina, A. (1993). Development of the zooplankton in the Kerguelen Island region in the years 1987–88. In Duhamel, G., editor, *Campagnes SKALP 1987 et 1988 aux Iles Kerguelen a bord des navires 'SKIF' et 'KALPER'*, page 90–104. Institut Francais pour la recherche.

Shadwick, E. H., Trull, T. W., Tilbrook, B., Sutton, A. J., Schulz, E., and Sabine, C. L. (2015). Seasonality of biological and physical controls on surface ocean CO2 from hourly observations at the Southern Ocean Time Series site south of Australia. *Global Biogeochemical Cycles*, 29(2):223–238.

Shannon, C. E. and Weaver, W. (1949). *The mathematical theory of communication.* University of illinois Press, Urbana.

Silver, M. (1991). The biologist's view of sediment trap collections: Problems of marine snow and living organisms. In Wassmann, P., Heiskanen, A., and Lindahl, O., editors, *Sediment trap studies in the Nordic Countries, Vol. 2*, pages 76–93. Nurmi Print Oy.

Slowikowski, K. (2021). ggrepel: Automatically Position Non-Overlapping Text Labels with 'ggplot2'. R package version 0.9.1.

Smetacek, V. S. (1985). Role of sinking in diatom life-history cycles: ecological, evolutionary and geological significance. *Marine Biology*, 84(3):239–251.

Steinberg, D. K. and Landry, M. R. (2017). Zooplankton and the Ocean Carbon Cycle. *Annual Review of Marine Science*, 9:413–444.

Steinberg, D. K., Pilskaln, C. H., and Silver, M. W. (1998). Contribution of zooplankton associated with detritus to sediment trap 'swimmer' carbon in Monterey Bay, California, USA. *Marine Ecology Progress Series*, 164:157–166.

Steinberg, D. K., Van Mooy, B. A. S., Buesseler, K. O., Boyd, P. W., Kobari, T., and Karl, D. M. (2008). Bacterial vs. zooplankton control of sinking particle flux in the ocean's twilight zone. *Limnology and Oceanography*, 53(4):1327–1338.

Stephensen, K. (1915). Isopoda, Cumacea, Amphipoda,(excl. Hyperiidea). *Rep. Danish oceanogr. Exped. Mediterranean*, 2(D1):1–53.

Stephensen, K. (1925). Danaella mimonectes (n. gen., n. sp.), a new bathypelagic gammarid (Fam. Lysianassidae) from South Greenland waters. *Videnskabelige Meddelelser fra Dansk Naturhistorisk Forening i Kjöbenhavn*, 80:423–428.

Stich, H.-B. and Lampert, W. (1981). Predator evasion as an explanation of diurnal vertical migration by zooplankton. *Nature*, 293(5831):396–398.

Strzepek, R. F., Hunter, K. A., Frew, R. D., Harrison, P. J., and Boyd, P. W. (2012). Iron-light interactions differ in Southern Ocean phytoplankton. *Limnology and Oceanography*, 57(4):1182–1200.

Stukel, M. R., Ohman, M. D., Kelly, T. B., and Biard, T. (2019). The roles of suspension-feeding and flux-feeding zooplankton as gatekeepers of particle flux into the mesopelagic ocean in the Northeast Pacific. *Frontiers in Marine Science*, 6(397):1–16.

Takahashi, K. T., Hosie, G. W., Cowen, T., Hunt, B., Kitchener, J. A., McLeod, D. J., Meilland, J., Pinkerton, M., Raymond, B., Robinson, K. V., and Swadling, K. M. (2020). Report on the status and trends of Southern Ocean Zooplankton based on the SCAR Southern Ocean Continuous Plankton Recorder (SO-CPR) Survey. Technical report, SCAR.

Takahashi, K. T., Hosie, G. W., Kitchener, J. A., McLeod, D. J., Odate, T., and Fukuchi, M. (2010). Comparison of zooplankton distribution patterns between four seasons in the Indian Ocean sector of the Southern Ocean. *Polar Science*, 4(2):317–331.

Tamburini, C., Garcin, J., and Bianchi, A. (2003). Role of deep-sea bacteria in organic matter mineralization and adaptation to hydrostatic pressure conditions in the NW Mediterranean Sea. *Aquatic Microbial Ecology*, 32(3):209–218.

Tang, K. W., Backhaus, L., Riemann, L., Koski, M., Grossart, H.-P., Munk, P., and Nielsen, T. G. (2019). Copepod carcasses in the Subtropical Convergence Zone of the Sargasso Sea: Implications for microbial community composition, system respiration and carbon flux. *Journal of Plankton Research*, 00(00):1–12.

Tang, K. W. and Elliott, D. T. (2014). Copepod carcasses: Occurrence, fate and ecological importance. In Seuront, L., editor, *Copepods: Diversity, Habitat and Behavior*, pages 255–278. Nova.

Tang, K. W., Freund, C. S., and Schweitzer, C. L. (2006). Occurrence of copepod carcasses in the lower Chesapeake Bay and their decomposition by ambient microbes. *Estuarine, Coastal and Shelf Science*, 68(3-4):499–508.

Tang, K. W., Gladyshev, M. I., Dubovskaya, O. P., Kirillin, G., and Grossart, H. P. (2014). Zooplankton carcasses and non-predatory mortality in freshwater and inland sea environments. *Journal of Plankton Research*, 36(3):597–612.

Taw, N. and Ritz, D. A. (1979). Influence of subantartic and subtropical oceanic water on the zooplankton and hydrology of waters adjacent to the Derwent River Estuary, south-eastern Tasmania. *Marine and Freshwater Research*, 30(2):179–202.

Teuber, L., Kiko, R., Séguin, F., and Auel, H. (2013). Respiration rates of tropical Atlantic copepods in relation to the oxygen minimum zone. *Journal of Experimental Marine Biology and Ecology*, 448:28–36.

Trimmer, M., Grey, J., Heppell, C. M., Hildrew, A. G., Lansdown, K., Stahl, H., and Yvon-Durocher, G. (2012). River bed carbon and nitrogen cycling: state of play and some new directions. *Science of the total environment*, 434:143–158.

Trull, T. W., Bray, S. G., Manganini, S. J., Honjo, S., and Francois, R. (2001). Moored sediment trap measurements of carbon export in the Subantarctic and Polar Frontal Zones of the Southern Ocean, south of Australia. *Journal of Geophysical Research: Oceans*, 106(C12):31489–31509.

Trull, T. W., Jansen, P., Schulz, E., Weeding, B., Davies, D. M., Bray, S. G., and Robinson, C. (2019). Autonomous multi-trophic observations of productivity and export at the Australian Southern Ocean Time Series (SOTS) reveal sequential mechanisms of physical-biological coupling. *Frontiers in Marine Science*, 6(525):1–17.

Trull, T. W., Schulz, E., Bray, S. G., Pender, L., McLaughlan, D., Tilbrook, B., Rosenberg, M., and Lynch, T. (2010). The Australian Integrated Marine Observing System Southern Ocean Time Series facility. In *OCEANS'10 IEEE SYDNEY*, pages 1–7.

Turner, J. T. (2002). Zooplankton fecal pellets, marine snow and sinking phytoplankton blooms. *Aquatic Microbial Ecology*, 27:57–102.

Turner, J. T. (2015). Zooplankton fecal pellets, marine snow, phytodetritus and the ocean's biological pump. *Progress in Oceanography*, 130:205–248.

Urbin-Rich, J., Nordby, E., Andreassen, I. J., and Wassmann, P. (1999). Contribution by mesozooplankton fecal pellets to the carbon flux on Nordvestbanken,north Norwegian shelf in 1994. *Sarsia*, 84:253–264.

Utne-Palm, A. C., Breen, M., Løkkeborg, S., and Humborstad, O.-B. (2018). Behavioural responses of krill and cod to artificial light in laboratory experiments. *PLOS ONE*, 13(1 (e0190918)):1–17.

Van der Spoel, S. and Dadon, J. (1999). Pteropoda. In Boltovskoy, D., editor, *South Atlantic zooplankton*, pages 649–706. Backhuys, Leiden.

Volk, T. and Hoffert, M. I. (1985). Ocean carbon pumps: Analysis of relative strengths and efficiencies in ocean-driven atmospheric CO2 changes. In Sundquist, E. and Broecker, W., editors, *The carbon cycle and atmospheric CO2: natural variations Archean to present*, volume 32, pages 99–110. Wiley Online Library.

Voronina, N. M., Kolosova, E. G., and Flint, M. V. (1988). Distribution and biology of mass species of mesoplankton. In *Ecosystem of Subarctic Zone of the Pacific Ocean*, pages 197–209. Nauka, Moscow.

Whalen, C. B., Talley, L. D., and MacKinnon, J. A. (2012). Spatial and temporal variability of global ocean mixing inferred from Argo profiles. *Geophysical Research Letters*, 39(L18612):1–6.

Wickham, H. (2007). Reshaping Data with the reshape Package. *Journal of Statistical Software*, 21(12):1–20.

Wickham, H. (2017). tidyverse: Easily install and load the 'Tidyverse'. R package version 1.2.1.

Wilke, C. O. (2019). cowplot: Streamlined Plot Theme and Plot Annotations for 'ggplot2'. R package version 1.0.0.

Wilks, J. V., Rigual-Hernández, A. S., Trull, T. W., Bray, S. G., Flores, J.-A., and Armand, L. K. (2017). Biogeochemical flux and phytoplankton succession: A year-long sediment trap record in the Australian sector of the Subantarctic Zone. *Deep Sea Research Part I: Oceanographic Research Papers*, 121:143–159.

Wood, S. N. (2011). Fast stable restricted maximum likelihood and marginal likelihood estimation of semiparametric generalized linear models. *Journal of the Royal Statistical Society (B)*, 73(1):3–36.

Wright, K. (2019). pals: Color palettes, colormaps, and tools to evaluate them. R package version 1.6.

Wynn-Edwards, C. A., Shadwick, E. H., Davies, D. M., Bray, S. G., Jansen, P., Trinh, R., and Trull, T. W. (2020). Particle fluxes at the Australian Southern Ocean Time Series. *Frontiers in Earth Science*, 8(329):1–20.

Yáñez, S., Hidalgo, P., and Tang, K. W. (2019). Relative importance of predatory versus non-predatory mortality for dominant copepod species in the northern Chilean (23° S) Humboldt Current Ecosystem. *Marine Ecology Progress Series*, 630:13–23.

Zaret, T. M. and Suffern, J. S. (1976). Vertical migration in zooplankton as a predator avoidance mechanism. *Limnology and Oceanography*, 21(6):804–813.

Zeidler, W. and De Broyer, C. (2009). Catalogue of the Hyperiidean Amphipoda (Crustacea) of the Southern Ocean with distribution and ecological data. In Broyer, C. d., editor, *Census of Antarctic Marine Life, Synopsis of the Amphipoda of the Southern Ocean.*, volume 3, pages 1–96. Institut royal des sciences naturelles de Belgique, Koninklijk Belgisch institutt voor natuurwetenschappen, Brussel.